



**US Army Corps
of Engineers®**
Engineer Research and
Development Center

Strategic Environmental Research and Development Program ER-1481

Characterization and Fate of Gun and Rocket Propellant Residues on Testing and Training Ranges

Final Report

Michael R. Walsh, Sonia Thiboutot, Marianne E. Walsh,
Guy Ampleman, Richard Martel, Isabelle Poulin, and Susan Taylor

August 2011



COVER: Field expedient disposal of 65 kg of M1 single-base propellant in the CRREL mobile burn pan at FP Neibar, Ft. Richardson, Alaska, 10 March 2011. (Photo by Michael Walsh.)

Characterization and Fate of Gun and Rocket Propellant Residues on Testing and Training Ranges

Final Report

Michael R. Walsh, Marianne E. Walsh, Susan Taylor, Alan D. Hewitt, Susan R. Bigl,
Kathleen Jones, Kelsey Gagnon, Charles M. Collins, Nancy M. Perron, Arthur B. Gelvin,
Karen L. Foley, Ronald N. Bailey, and Anna M. Wagner

*Cold Regions Research and Engineering Laboratory
U.S. Army Engineer Research and Development Center
72 Lyme Road
Hanover, NH 03755*

Sonia Thiboutot, Guy Ampleman, Isabelle Poulin, Michel Kervarec, Firmin Boucher,
André Marois, Annie Gagnon, and Pierre Archambeault

*Defence R&D Canada-Valcartier
2459 Pie-XI Blvd North
Québec, Québec G3J 1X5 CANADA*

Richard Martel, Sébastien Lange, and Sébastien Côté

*Institut National de la Recherche Scientifique
Centre Eau, Terre, et Environnement
290, de la Couronne
Québec, Québec G1K 9A9 CANADA*

James W. Hug

*USACE, Los Angeles District, AZ/NV Area Office
3636 N. Central
Phoenix, AZ 85012*

Jeffrey N. Bryant

*Bering Sea Eccotech LLC
4300 B Street, Suite 402
Anchorage, AK 99503*

Charles A. Ramsey

*EnviroStat, Inc.
PO Box 636
Fort Collins, CO 80522*

Thomas F. Jenkins

*Bowhead Science and Technology, LLC
3530 Manor Drive, Suite 4
Vicksburg, MS 39180*

Final report

Approved for public release; distribution is unlimited.

Abstract: The Cold Regions Research and Engineering Laboratory and the Defence Research and Development Canada–Valcartier have partnered to improve the understanding of the distribution and fate of propellant residues on military training ranges. Field studies were conducted to estimate the propellant residue mass deposited per round fired from various munitions as well as residues from the field disposal of excess propellants. Experiments were conducted to measure the rate of release of energetic compounds after deposition. Training ranges were examined to determine the mass and distribution of residue accumulation. Profile sampling was conducted to document the depth to which these residues had penetrated the ground. Column studies were conducted with propellants to document transport rates for solution-phase propellant constituents and to develop process descriptors for use in models to enable prediction of fate and transport for constituents of concern. Gaps were filled in other areas of energetics residues impacts in an effort to describe all aspects of energetics impacts on range environments. Testing of propellant burn structures was begun, and we continue to promote and refine the multi-increment sampling protocol for energetics. Major accomplishments are presented for the final year and the total of Environmental Restoration Project 1481, Phase II.

DISCLAIMER: The contents of this report are not to be used for advertising, publication, or promotional purposes. Citation of trade names does not constitute an official endorsement or approval of the use of such commercial products. All product names and trademarks cited are the property of their respective owners. The findings of this report are not to be construed as an official Department of the Army position unless so designated by other authorized documents.

DESTROY THIS REPORT WHEN NO LONGER NEEDED. DO NOT RETURN IT TO THE ORIGINATOR.

Table of Contents

Preface	xv
Unit Conversion Factors.....	xviii
Nomenclature.....	xix
1 Introduction.....	1
1.1 Background.....	1
1.2 Propellants.....	2
1.3 Project scope	4
1.4 Objectives.....	4
1.5 Previous research	5
1.5.1 Propellant residues deposition.....	5
1.5.2 Fate and transport	8
1.5.3 Disposal of propellants	10
1.5.4 Explosives residues.....	13
1.6 FY10 Research.....	14
2 Propellant Residues Deposition from Firing of 40-mm Grenades.....	15
2.1 Summary.....	15
2.2 Introduction.....	16
2.2.1 Background	16
2.2.2 Objectives	17
2.2.3 Approach.....	17
2.3 Field sampling methodology	18
2.3.1 Field site and conditions	18
2.3.2 Munitions tested.....	20
2.3.3 Firing of munitions	21
2.3.4 Sampling method.....	22
2.4 Sample processing and analysis	24
2.4.1 Snow samples	24
2.4.2 Quality Control Procedures	28
2.5 Results: Deposition rate	29
2.6 Discussion.....	32
2.7 Conclusions.....	37
3 Propellant Residues Emitted by Triple Base Ammunition Live Firing using a British 155-mm Howitzer Gun at CFB Suffield, Canada	39
3.1 Summary.....	39
3.2 Introduction.....	40
3.3 Background.....	44

3.3.1	<i>Logistics</i>	44
3.3.2	<i>Equipment and munitions</i>	44
3.4	Experimental.....	50
3.4.1	<i>Test setup</i>	50
3.4.2	<i>Sampling strategy and nomenclature</i>	51
3.4.3	<i>Sample treatment and analytical methods</i>	60
3.5	Results and discussion	68
3.5.1	<i>Soil samples</i>	68
3.5.2	<i>Propellant residues in particle traps</i>	68
3.5.3	<i>Samples from the burn tests</i>	71
3.6	Conclusion	72
4	Fixed and Mobile Burn Pans for the Burning of Excess Artillery Propellant Charge Bags	77
4.1	Summary.....	77
4.2	Introduction.....	78
4.3	Artillery propellants and environmental and health considerations.....	83
4.3.1	<i>105-mm Artillery propellant</i>	83
4.3.2	<i>155-mm Artillery propellant</i>	85
4.3.3	<i>Environmental and health impacts</i>	86
4.4	Design, construction, and safety aspects	88
4.4.1	<i>Design and construction of the fixed Canadian burn pan</i>	88
4.4.2	<i>Design and construction of the mobile burn pan</i>	92
4.4.3	<i>Safety considerations</i>	93
4.5	Test trials.....	97
4.5.1	<i>February 2009 trial</i>	97
4.5.2	<i>November 2009 trial</i>	100
4.5.3	<i>March 2010 trial</i>	104
4.6	Sample analysis.....	108
4.6.1	<i>Energetic materials</i>	108
4.6.2	<i>Hazardous materials analysis</i>	109
4.7	Results	109
4.7.1	<i>February 2009 trial</i>	109
4.7.2	<i>November 2009 trial</i>	118
4.7.3	<i>March 2010 trial: Canadian trial results</i>	123
4.7.4	<i>March 2010 trial: U.S. results</i>	125
4.8	Conclusion and future implementation.....	126
5	Fate and Behavior of Energetic Material Residues in the Unsaturated Zone: Sand Columns and Dissolution Tests	129
5.1	Summary.....	129
5.2	Sand columns.....	130
5.2.1	<i>Introduction</i>	130
5.2.2	<i>Methodology</i>	131
5.2.3	<i>Results</i>	137
5.3	Dissolution tests.....	150
5.3.1	<i>Introduction</i>	150

5.3.2 Methodology.....	150
5.3.3 List of dissolution tests with water drops	152
5.3.4 Results.....	153
5.4 Conclusion	179
6 A Simple Device for Initiating High-Order Detonations.....	183
6.1 Introduction and background	183
6.2 Objective	183
6.3 Materials and methods	184
6.4 Testing	184
6.4.1 Testing of the device	186
6.4.2 Test of the total system.....	186
6.5 Results	190
6.5.1 Test of the device	190
6.5.2 Test of the system.....	190
6.6 Discussion.....	193
6.7 Conclusions.....	194
7 Close-Proximity Detonations: a Study of the Damage to 81-mm Mortar Projectiles.....	195
7.1 Summary.....	195
7.2 Introduction.....	196
7.3 Experimental design.....	199
7.3.1 Munitions used.....	199
7.3.2 Test locations	199
7.3.3 Tests sequence and setup.....	199
7.3.4 Detonating the rounds	203
7.3.5 Data collected on UXO rounds.....	203
7.4 Results	204
7.4.1 Damage to the UXO.....	204
7.4.2 Detailed patterns of damage from vertical detonating rounds	210
7.4.3 Detailed patterns of damage from horizontal detonating round: 0.50 m.....	229
7.5 Discussion.....	232
7.5.1 Damage to UXO seen in the field.....	232
7.5.2 Surface versus buried UXO.....	234
7.6 Conclusion	234
8 Particle Mass Distribution of High Explosives from Sympathetic Partial Detonations.....	235
8.1 Summary.....	235
8.2 Introduction.....	235
8.3 Experimental Methods	237
8.4 Results and Discussion	239
8.4.1 Samples studied.....	239
8.4.2 Mass distributions.....	246
8.4.3 Mass of the largest HE piece.....	251
8.4.4 Changes in mass distributions caused by weathering.....	251
8.4.5 Implications for explosive particles in training range soils	252

8.5 Conclusions.....	253
9 Sampling for Comp B Residues using Shallow Wells at Two Low-order Detonation Sites	255
9.1 Introduction and background	255
9.2 Objective	256
9.3 Materials and methods	256
9.3.1 Shallow wells	256
9.3.2 Water sampling	260
9.3.3 Piezometer well	261
9.3.4 Analysis of water samples	261
9.4 Results	263
9.4.1 Water levels	263
9.4.2 Comp B residues	264
9.5 Discussion.....	265
9.6 Conclusions.....	266
10 Subsampling of Soils Containing Energetics Residues.....	267
10.1 Introduction and background	267
10.2 Objective	268
10.3 Materials and methods	268
10.3.1 Phase I Study.....	269
10.3.2 Phase II study	270
10.4 Results.....	271
10.4.1 Phase I study	271
10.4.2 Phase II Study.....	274
10.5 Discussion.....	278
10.6 Conclusions.....	279
11 Report Summary.....	281
11.1 Introduction.....	281
11.2 Characterization of residues deposition and accumulation	281
11.2.1 Deposition rate studies	281
11.2.2 Fate and behavior of energetic material residues in the unsaturated zone: sand columns and dissolution tests	283
11.3 Open burning of excess propellants: Fixed and mobile burn pans.....	284
11.4 Simulation of live-fire breaching of UXO	286
11.4.1 A simple device for initiating high-order detonations.....	286
11.4.2 Physical damage to UXO from a close-proximity high-order detonation.....	286
11.4.3 Particle mass of high explosives from sympathetic partial detonations.....	287
11.5 Explosives residues deposition rates: Sampling for Comp B residues using shallow wells at two low-order detonation sites	288
11.6 Multi-increment sampling strategy and EPA Method 8330B	289
12 Project Summary.....	291
12.1 Introduction.....	291
12.2 Research Summaries	292

12.2.1 Small arms.....	292
12.2.2 Medium caliber weapon system.....	295
12.2.3 Mortars and howitzers	296
12.2.4 Tanks.....	306
12.2.5 Rockets	308
12.2.6 EPA 8330B Dissemination	310
12.3 Future work	311
References.....	315
Appendix A: Munitions Data	329
Appendix B: Analytical Results	331
Appendix C: DRDC Soil Samples and Results	335
Appendix D: Data Processing for the Dissolution Tests.....	337
Appendix E: Munitions Data	341
Appendix F: Analytical Data and Results	343
Appendix G: Results of prior Canadian study	345
Appendix H: STANAG Definitions of Sympathetic Detonation Reactions.....	347
Bibliography.....	349
Report Documentation Page	

List of Figures and Tables

Figures

Figure 2-1. 40/90 Range firing point parking area prior to pad construction.	19
Figure 2-2. Test pad for first firing from down range. Gun is to left of image.	19
Figure 2-3. Test pad layout.	20
Figure 2-4. Firing of M430 HE grenades over test pad.	22
Figure 2-5. Propellant debris on test pad surfaces after tests.	23
Figure 2-6. Location of trays used to collect propellant debris.	24
Figure 2-7. Samples in tubs at thaw location.	25
Figure 2-8. Images of propellant residue during initial processing of 0-5m SU samples.	25
Figure 2-9. Sample filtration setup at the processing laboratory on post.	27
Figure 2-10. Cross-section of an EI pro-pellant grain.	34
Figure 3-1. British L131 (AS90) Braveheart 39-caliber 155-mm howitzer.	44
Figure 3-2. 155-mm Howitzer L131 setup at firing position.	45
Figure 3-3. Shell of the 155-mm HE L15.	46
Figure 3-4. Shell of the 155-mm Practice Inert L17.	46
Figure 3-5. Propellant charge L8 A1.	47
Figure 3-6. Propellant charge L10 A1.	47
Figure 3-7. Schematic of the L8A1 propellant charge.	48
Figure 3-8. Schematic of the L10A1 propellant charge.	49
Figure 3-9. Half-circle setup of trays in front of the gun.	51
Figure 3-10. Particles traps setup in front of the gun.	52
Figure 3-11. Particles traps beside the gun.	52
Figure 3-12. Gunside particles traps.	53
Figure 3-13. Particles trap in holder.	53
Figure 3-14. Gun setup at firing position.	55
Figure 3-15. Firing point sampling decision unit configuration.	55
Figure 3-16. View of decision unit from downrange towards gun emplacement.	56
Figure 3-17. Sampling of firing point following the firing of the final projectiles.	56
Figure 3-18. Setup of four charge 7 propellant bags on sand.	58
Figure 3-19. Ignition of four charge 7 propellant bags on sand.	58
Figure 3-20. Setup of six charge 4 propellant bags on sand.	59
Figure 3-21. Sampling test pads following burning of propellants.	59
Figure 3-22. Test sites after completion of sampling.	60
Figure 4-1. Ignition train material.	79
Figure 4-2. Burning setup on snow.	79
Figure 4-3. Burning on snow.	79

Figure 4-4. Left over residues after burning on snow.....	80
Figure 4-5. Left over residues after burning on concrete pads in Gagetown RTA.....	80
Figure 4-6. M67 Propelling charges.....	84
Figure 4-7. M1 propellant grains in bags 6 and 7	85
Figure 4-8. Bags of 155-mm charge 4 and 5 and the flash reducer pad.....	86
Figure 4-9. Initial table design with removable cover and integrated ignition tool.	89
Figure 4-10. Inverted view of the aluminium table cover.	90
Figure 4-11. CRREL mobile propellant burn pan: first prototype.....	93
Figure 4-12. Transition from burning to detonation in GD-OTS experiments	95
Figure 4-13. Transfer of propellant bags for burning test.....	98
Figure 4-14. Prior to burning with 150 kg of M67 propellant load.....	98
Figure 4-15. Prior to burning with 75 kg M67 propellant load.	99
Figure 4-16. Prior to burning with 104 kg of M4 propellant load.	99
Figure 4-17. Table on concrete blocks and prior to burning 75 kg of M67 propellant.	100
Figure 4-21. Table with new reinforced shields.....	106
Figure 4-22. Table loaded with charge bags 4, 6 and 7	107
Figure 4-23. Grip to hold the conductive strap to the table.	107
Figure 4-24. Conductive bracelets tested in the trial.....	107
Figure 4-25. U.S. table prototype.....	108
Figure 4-26. U.S. table prototype prior to ignition.	108
Figure 4-27. Ignition of the propellant bed.....	110
Figure 4-28. Three seconds after ignition.....	110
Figure 4-29. Maximum intensity of burning 10 s after ignition.	111
Figure 4-30. Residues projected outside the table, trial 1.....	112
Figure 4-31. Residues projected outside the table, trial 3.....	112
Figure 4-32. Burning residues collection.	113
Figure 4-33. Burning residues from trial 3.	113
Figure 4-34. Inorganic, organic and flares residues segregated, trial 1.....	114
Figure 4-35. Close-up of the lead deposited in the burn table.	114
Figure 4-36. Close-up view of the organic matter deposited in the burn table.....	115
Figure 4-37. Trial 3 using shield e, after burn.	120
Figure 4-38. Full burning using the model d shields.	120
Figure 4-39. Thermocouples in the flame and 5 m away for radiation measurement.	122
Figure 4-40. Temperatures monitored during trial 2.	122
Figure 4-41. Representative large particle collected near the burning location.	125
Figure 5-1. Fiberglass wicks positioned on the bottom of each column.	132
Figure 5-2. Soil compaction in the sand column.....	134
Figure 5-3. Laboratory temperature recorded by the CR10X.....	138
Figure 5-4. Cumulative measured inflow for each column.	138
Figure 5-5. Cumulative measured outflow for each column.....	139

Figure 5-6. Volumetric water content as a function of time for columns A and D, B, E, C, F	140
Figure 5-7. Perchlorate concentration vs. total pore volume for columns A, B, and C.....	143
Figure 5-8. Perchlorate concentration vs. total pore volume for columns D, E, and F.....	143
Figure 5-9. Concentrations of 2,4-DNT and 4-A-2,6-DNT in column A effluent.	144
Figure 5-10. Concentrations of 2,4-DNT and 4-A-2,6-DNT in column D effluent.....	145
Figure 5-11. HMX and TNT effluent concentrations in Column B.	147
Figure 5-12. HMX and TNT effluent concentrations in Column E.	147
Figure 5-13. Profile of the bulk density and the volumetric water content of column F.....	150
Figure 5-14. Dissolution experiment: the entire setup	151
Figure 5-15. Cumulative NG mass lost on residues from Wellington firing position	155
Figure 5-16. Cumulative mass lost of 1,2-dinitroglycerine at CFB Gagetown.	156
Figure 5-17. Cumulative mass lost of 1,3-dinitroglycerine related at CFB Gagetown.....	156
Figure 5-18. NG concentration in eluted water from drop test at CFB Gagetown	157
Figure 5-19. NG, DNG, MNG leachate concentration vs. transport pore volumes, C-Valcartier	158
Figure 5-20. Cumulative EM mass lost in sample	159
Figure 5-21. Cumulative EM mass lost in sample H a during 2 years of simulation.....	159
Figure 5-22. Cumulative EM mass lost in sample I during the first year of simulation.....	160
Figure 5-23. Cumulative EM mass lost in sample I during 2 years of simulation.....	160
Figure 5-24. Cumulative EM mass lost in sample G during the first year of simulation.	161
Figure 5-25. Cumulative EM mass lost in sample G during 2 years of simulation.....	161
Figure 5-26. Conceptual model of dissolution of Composition B as a function of time.....	163
Figure 5-27. Percentage of total EM mass lost from three samples, the first year of simulation...163	
Figure 5-28. Percentage of total EM mass lost from three samples during 2 years simulation.165	
Figure 5-29. Concentration of each EM in test H during 1 year of simulation.....	168
Figure 5-30. Concentration of each EM in test I during 2 years of simulation.....	169
Figure 5-31. Concentration of each EM in test G during 2 years of simulation.....	169
Figure 5-32. Cumulative EM mass lost test D during 2 years of simulation.	171
Figure 5-33. Cumulative EM mass lost in test E 2 years of simulation.	171
Figure 5-34. Cumulative EM mass lost in test F during 2 years of simulation.....	172
Figure 5-35. Cumulative EM mass lost in test G during 2 years of simulation.	172
Figure 5-36. Cumulative EM mass lost in test H during 2 years of simulation.	173
Figure 5-37. Cumulative EM mass lost in test I during 2 years of simulation.....	173
Figure 5-38. Total EM mass lost in six Octol water drop tests during 2 years of simulation.....	176
Figure 5-39. Dissolution of Octol on fritted glass funnel during water drop test vs. time.	177
Figure 6-1. Device with C4 booster installed.	186
Figure 6-2. Test setup for the initiation system.	187
Figure 6-3. Detonation plume following first system test.	188
Figure 6-4. Initiator device after blast.	191
Figure 6-5. Initiator test detonation plumes.	192
Figure 7-1. Lewis' work.	197

Figure 7-2. Typical setup for arena tests. The munition is placed in the center stand.....	198
Figure 7-3. Setup 1, vertical incoming round, one UXO on the side.....	201
Figure 7-4. Setup 2, vertical incoming round, two UXOs on the side.....	201
Figure 7-5. Setup 3, horizontal incoming round, two UXOs on the side.....	202
Figure 7-6. Setup 4, vertical incoming round, five UXOs on the side.....	203
Figure 7-7. Regions used when identifying damage to an 81-mm mortar.....	204
Figure 7-8. Typical dings to an 81-mm mortar	204
Figure 7-9. Typical holes to an 81-mm mortar	205
Figure 7-10. Typical breaches/cracks to an 81-mm mortar.....	205
Figure 7-11. Typical 81-mm mortar metal pieces after a partial detonation of a simulated UXO..	206
Figure 7-12. Typical craters from high-order detonations of 81-mm mortars.....	207
Figure 7-13. Overall results of damage types observed on the simulated UXOs.....	209
Figure 7-14. Damages on the UXO when the detonating mortar is 0.50 m from simulated UXO..	210
Figure 7-15. Damage recorded and HE chunks collected in test 4, round 4b.....	211
Figure 7-16. Damages recorded for test 11, round 11a	212
Figure 7-17. Damages recorded for the test1 round	213
Figure 7-18. Damages recorded to the test 2 round	214
Figure 7-19. Damages recorded for test 3, round 3a.....	215
Figure 7-20. Damages recorded for test 3, round 3b.....	217
Figure 7-21. Damages recorded for test 5, round 5a.....	218
Figure 7-22. Damages recorded for test 5, round 5b	219
Figure 7-23. Damages recorded for test 6, round 6b.....	220
Figure 7-24. Damages recorded for test 6, round 6b.....	221
Figure 7-25. Damages recorded for test 7, round 7a.....	223
Figure 7-26. Damages recorded for test 7, round 7b.....	224
Figure 7-27. Damages recorded for test 8, round 8a	224
Figure 7-28. Damages recorded for test 8, round 8b.....	225
Figure 7-29. Damages recorded for test 11, round 11b	226
Figure 7-30. Damages recorded for test 11, round 11c	227
Figure 7-31. Damages recorded for test 11, round 11d	228
Figure 7-32. Damages recorded for test 11, round 11e	229
Figure 7-33. Damages recorded for test 9, round 9a.....	230
Figure 7-34. Tail recovered after sympathetic detonation of a UXO in test 9, round 9b	231
Figure 7-35. Damages recorded for test 10, round 10a	232
Figure 7-36. Damaged howitzer projectile UXOs observed in the field.....	232
Figure 7-37. Damaged mortar UXOs observed in the field.....	233
Figure 8-1. Damage caused by high velocity fragments from nearby high-order detonation.....	240
Figure 8-2. Cross-section of round 4b next to an undetonated 81-mm mortar projectile.	241
Figure 8-3. Test 4, vertical “incoming” round to be set off high-order and two “UXO”	242
Figure 8-4. Location of the crater, centimeter-sized HE strewn field, individual larger pieces	242

Figure 8-5. Sub-centimeter-sized HE pieces deposited close to detonation 4b.	243
Figure 8-6. Comp B left after the partial detonation of round 4b.....	243
Figure 8-7. Residues recovered from round 8a (left) and round 8b.....	244
Figure 8-8. Residues recovered from round 9a (left) and round 10a.	244
Figure 8-9. Crater and centimeter-sized HE scatter area for test 10a.	245
Figure 8-10. Piece size distribution for round 4b plotted	246
Figure 8-11. Same data shown in Figure 8-10 fitted using cumulative distributions.....	248
Figure 8-12. Pieces collected from rounds 8a, 9a, and 10a, and 8b	248
Figure 8-13. Particle masses plotted versus probability of not exceeding that mass	250
Figure 8-14. Change in particle distributions after 22 months of outdoor dissolution.....	252
Figure 9-1. Aerial image of six shallow groundwater monitoring wells on a salt marsh.....	257
Figure 9-2. Image showing the crater at L03 in 2006.....	257
Figure 9-3. Images of well screen and foam bridge used for the monitoring well.....	258
Figure 9-4. Well installation.....	258
Figure 9-5. Instrumentation for collecting piezometer water depth readings.	261
Figure 9-6. Water levels in 2009 and 2010 within a piezometer well near the monitoring wells ..	263
Figure 9-7. Mouth of the drainage channel located between the two low-order detonation sites.	264
Figure 10-1. Subsampling of a ground large sample.....	270
Figure 12-1. Propellant burn test, FP Neibar, Ft. Richardson, AK, March 2011.	313

Tables

Table 2-1. Propellant constituents analyzed for firing point test.	21
Table 2-2. Sampling unit areas, February 2010.....	23
Table 2-3. NG Residue mass for test sampling units.....	31
Table 2-4. Filter mass components.	31
Table 2-5. Comparison of various firing point analyte loads.	36
Table 3-1. Technical data for 155 mm charge propelling L8A1 and L10A1.....	49
Table 3-2. Total masses of NG and NQ fired during the trial.....	50
Table 3-3. Mass of NG and NQ detected in particle traps.....	69
Table 3-4. Mass and percentages of NG and NQ deposited in front of the gun	70
Table 3-5. Percentages of NG/NQ deposited by the open burning tests.....	72
Table 4-1. Chemical composition of M1 propellant.	84
Table 4-2. Mass of propellant in the M67 propelling charges.	84
Table 4-3. Mass of propelling charge M1 in the M3A1.	86
Table 4-4. Soil standards from U.S. EPA, Quebec, and Ontario.	88
Table 4-5. Specification of the sheets selected for the screens.	92
Table 4-6. February 2009 burn trial.	100
Table 4-7. November 2009 Nicolet burn trial.	104
Table 4-8. March 2010 burn trial.....	106
Table 4-9. February 2009 burn trial results.....	115

Table 4-10. November 2009 Nicolet burn trial results.....	118
Table 5-1. Arnhem sand physico-chemicals properties.....	131
Table 5-2. Mass of Arnhem sand for each 5-cm layer	133
Table 5-3. Initial EM content of the residues put on the large sand columns.....	135
Table 5-4. Parameters for the large sand column test.	136
Table 5-5. Ion chromatography conditions for the analysis of perchlorate.....	142
Table 5-6. Transport pore volume for each column and recovery of perchlorates.	142
Table 5-7. Dissolved EM mass for columns A and D and for single-base propellant residues.	146
Table 5-8. Dissolved EM mass for columns B and E and 1 m ² contaminated soil CFB Gagetown.	148
Table 5-9. Description of all dissolution tests that were done and in progress.	152
Table 5-10. Physico-chemical parameters of contaminated soils from anti-tank ranges	154
Table 5-11. Initial NG content in residues from anti-tank range firing position at CFB Gagetown.	154
Table 5-12. Initial and final residues from anti tank range firing position at CFB Gagetown.	157
Table 5-13. Initial contents of the EM in the Composition B residues	158
Table 5-14. EM contents in Composition B residues at end of dissolution experiment.....	165
Table 5-15. Initial EM content in Octol powder and in Octol flakes.....	170
Table 5-16. EM contents in Octol at the end of the dissolution experiment	175
Table 5-17. Parameters of the third dissolution tests	179
Table 6-1. Munitions used for the detonation system tests.....	185
Table 6-2. Mass of energetic compounds recovered in detonation plumes.	193
Table 7-1. Summary of the setups used in the close-proximity trials.....	200
Table 7-2. Damage types observed for the different setups and replicates.	208
Table 7-3. Damages description for test 1 round.....	213
Table 7-4. Damages description for test 2 round.....	214
Table 7-5. Damage description for test 3, round 3a.....	216
Table 7-6. Damage description for Test 3, round 3b.	216
Table 7-7. Damage description for test 5, round 5a.	217
Table 7-8. Damage description for test 5, round 5b.....	218
Table 7-9. Damage description for test 6, round 6a.....	220
Table 7-10. Damage description for Test 6, round 6b.	222
Table 7-11. Damage description for test 7, round 7a.....	222
Table 7-12. Damage description for test 8, round 8b.	225
Table 7-13. Damage description for test 11, round 11c.	227
Table 7-14. Damage description for test 11, round 11d.	228
Table 7-15. Damage description for test 11, round 11e.	229
Table 7-16. Damage description for test 9, round 9a.....	230
Table 8-1 Fate of the unfuzed rounds.	240
Table 8-2. Total mass and number of HE pieces recovered.....	245
Table 8-3. Parameters of a cumulative lognormal distribution.....	249
Table 9-1. Aqueous concentrations of RDX and HMX in water samples from shallow wells	265

Table 10-1. Sample and subsample data for Phase I study	270
Table 10-2. Sample and subsample data for Phase II study.....	271
Table 10-3. Results for Phase I study: large firing point sample.....	272
Table 10-4. Results for Phase I study: large urban range sample.....	272
Table 10-5. Results for Phase I study: small firing point sample.....	273
Table 10-6. Results for Phase II study: worst-case for the small firing point sample.....	273
Table 10-7. Results for Phase II study: firing point—low concentration sample.....	275
Table 10-8. Results for Phase II study: impact point—worst-case for the low concentrations.....	276
Table 10-9. Results for Phase II study: firing point—worst-case for the low-concentrations.....	277
Table 12-1. Small arms firing points: propellant residues deposition rates.....	293
Table 12-2. Small arms firing points: propellant residues soil concentrations.....	294
Table 12-3. Medium Caliber weapon firing points: propellant residues deposition rates	295
Table 12-4. Expedient propellant disposal: environmental influence tests.....	297
Table 12-5. Artillery systems firing points: propellant residues deposition rates.....	299
Table 12-6. Artillery systems impact points: high explosives residues deposition rates.....	300
Table 12-7. Artillery systems UXO BIP tests: High explosives residues deposition rates.....	303
Table 12-8. Close-proximity detonation tests: damage assessment.....	305
Table 12-9. Close-proximity detonation tests.	306
Table 12-10. Tank firing point test: DNT mass deposition.	307
Table 12-11. Shoulder-fired rockets firing points: propellant residues deposition rates.	309
Table 12-12. Shoulder-fired rockets firing points: firing point characterizations.	309

Preface

This report was prepared by the U.S. Army Engineer Research and Development Center's Cold Regions Research and Engineering Laboratory (ERDC-CRREL) and represents the collaboration of researchers from ERDC-CRREL in Hanover, New Hampshire, and Defence Research and Development Canada-Valcartier (DRDC) of Québec, Canada. This research was sponsored by the Strategic Environmental Research and Development Program (SERDP) of Arlington, Virginia, under Environmental Restoration Project Number ER-1481 (extension). Bradley P. Smith was Executive Director for SERDP, Dr. Jeff Marqusee Technical Director, and Dr. Andrea Leeson Project Monitor.

The principal investigator was Michael R. Walsh, Engineering Resources Branch (ERB) at ERDC-CRREL with Dr. Sonia Thiboutot of DRDC co-principal investigator. Major contributors included Marianne Walsh, Dr. Susan Taylor, and Alan Hewitt of CRREL, Dr. Guy Ampleman and Dr. Isabelle Poulin of DRDC, and Dr. Richard Martel and Dr. Auriél Bellavance-Godin of the Institut National de la Recherche Scientifique, Centre—Eau Terre, et Environnement, Université du Québec.

Various chapters of this report were reviewed by Dr. Clarence L. Grant, Professor Emeritus, University of New Hampshire; Marianne E. Walsh, Michael R. Walsh, Dr. Susan Taylor, and Susan R. Bigl from ERDC-CRREL; Dr. Sonia Thiboutot from DRDC-Valcartier; and Charles A. Ramsey from Envirostat.

The manuscripts for this report were edited, organized, and assembled by Susan R. Bigl, Biogeochemical Branch (BCB), ERDC-CRREL. Final editing was performed by Mr. Mark Hardenberg of ERDC-ITL.

At the time of publication, Colonel Kevin J. Wilson was Commander and Executive Director of ERDC, and Dr. Jeffery Holland was Director. Dr. Robert E. Davis was Director of CRREL.

This report may be cited as one document or by chapters as follows.

Whole document:

Characterization and Fate of Gun and Rocket Propellant Residues on Testing and Training Ranges: Final Report
M.R. Walsh, S. Thiboutot, M.E. Walsh, G. Ampleman, R. Martel, I. Poulin, and S. Taylor.

Chapter 1: *Introduction*

M.R. Walsh

Chapter 2: *Propellant Residues Deposition from Firing of 40-mm Grenades*

M.R. Walsh, M.E. Walsh, J.W. Hug, S.R. Bigl, K.L. Foley, A.B. Gelvin, and N.M. Perron

Chapter 3: *Study of the Propellant Residues Emitted by Triple Base Ammunition Live Firing Using a British 155-mm Howitzer Gun at CFB Suffield, Canada*

G. Ampleman, S. Thiboutot, A. Marois, A. Gagnon, M.R. Walsh, M.E. Walsh, C.A. Ramsey, and P. Archambeault

Chapter 4: *Fixed and Mobile Burn Pans for the Burning of Excess Artillery Propellant Charge Bags*

S. Thiboutot, G. Ampleman, M. Kervarec, A. Gagnon, A. Marois, F. Boucher, and M.R. Walsh

Chapter 5: *Fate and Behavior of Energetic Material Residues in the Unsaturated Zone: Sand Columns and Dissolution Tests*
R. Martel, S. Lange, S. Côté, S. Thiboutot, and G. Ampleman

Chapter 6: *A Simple Device for Initiating High-Order Detonations*

M.R. Walsh, M.E. Walsh, and J.W. Hug

Chapter 7: *Close-Proximity Detonations: A Study of the Damage to 81-mm Mortar Projectiles*

I. Poulin, S. Taylor, M.R. Walsh, S. Bigl, M.E. Walsh, A. Wagner, and J. Hug

Chapter 8: *Particle Mass Distribution of High Explosives from Sympathetic Partial Detonations*
S. Taylor, S. Bigl, K. Jones, I. Poulin, M.R. Walsh, M.E. Walsh,
A. Wagner, and J. Hug

Chapter 9: *Sampling for Comp B Residues using Shallow Wells at Two Low-order Detonation Sites*
M.E. Walsh, A.D. Hewitt, M.R. Walsh, C.M. Collins, R.N. Bailey,
S.R. Bigl, and J.N. Bryant

Chapter 10: *Subsampling of Soils Containing Energetics Residues*
M.R. Walsh, M.E. Walsh, A.D. Hewitt, T.F. Jenkins, and K. Gagnon

Chapter 11: *Report Summary*
M.R. Walsh

Chapter 12: *Project Summary*
M.R. Walsh

Unit Conversion Factors

Multiply	By	To Obtain
acres	4,046.873	square meters
cubic feet	0.02831685	cubic meters
cubic yards	0.7645549	cubic meters
degrees Fahrenheit	(F-32)/1.8	degrees Celsius
fathoms	1.8288	meters
feet	0.3048	meters
inches	0.0254	meters
microns	1.0 E-06	meters
miles (U.S. statute)	1,609.347	meters
pints (U.S. liquid)	0.473176	liters
pounds (mass)	0.45359237	kilograms
quarts (U.S. liquid)	9.463529 E-04	cubic meters
square feet	0.09290304	square meters
square inches	6.4516 E-04	square meters
square miles	2.589998 E+06	square meters
square yards	0.8361274	square meters

Nomenclature

2,4-DNT	2,4-Dinitrotoluene, an explosive compound
2,6-DNT	2,6-Dinitrotoluene, an explosive compound
AcN	Acetonitrile
AT	Anti-Tank
BATUS	British Army Training Unit Suffield
BIP	Blow In Place
BRI	Biotechnology Research Institute
C4	Explosive material composed of 91% RDX, 9% oil
CCME	Canadian Council of Ministers of the Environment
CEC	Cation Exchange Capacity
CF	Canadian Forces
CFB	Canadian Forces Base
CFB/ASU	Canadian Forces Bases/Area Support Unit
CH	Critical Height
Comp B	Explosive material composed of 60% RDX, 39% TNT, 1% wax
CRIQ	Centre de Recherche Industriel du Québec
CRREL	Cold Regions Research Engineering Laboratory
DAEME	Director Ammunitions Explosive Management and Engineering
DAER	Director Ammunitions & Explosives Regulations
DGLEPM	Director General Land Equipment and Program Management
dl	Detection Limit
DLE	Director Land Environment
DNB	Dinitrobenzene
DND	Department of National Defence

DNG	Dinitroglycerol, a breakdown product for NG
DNT	Dinitrotoluene (2,4-dinitrotoluene), an explosive compound
DoD	U.S. Department of Defense
DODIC	Department of Defense Identification Code
DRDC-Valcartier	Defence Research and Development Canada—Valcartier
DRDC	Defence Research and Development Canada
DRDKIM	Director Research and Development Knowledge and Information Management
DREV	Defence Research Establishment Valcartier
DTA	Donnelly Training Area (formerly Fort Greely), Alaska
DU	Decision Unit
EC	Ethyl Centralite (diethyl diphenyl urea), a propellant additive
EI [®]	Extruded–Impregnated
EM	Energetic Material
EOD	Explosive Ordnance Disposal
EPA	U.S. Environmental Protection Agency
ER	Environmental Restoration
ERDC	Engineer Research and Development Center
ERF	Eagle River Flats
ESTCP	Environmental Security Technology Certification Program
FP	Firing Point or Firing Position
FT-IR	Fourier Transformed Infrared spectroscopy
GC	Gas Chromatography
GC/ECD	Gas Chromatography/Electron Capture Detector
GC/MS	Gas Chromatography coupled to Mass Spectrometry
GD-OTS	General Dynamics–Ordnance and Tactical Systems Canada
GMG	Grenade Machine Gun

GPS	Global Positioning System
HE	High Explosive
HEDP	High-Explosive / Dual-Purpose
HMX	High Melting Explosive, an explosive compound cyclotetramethylene-tetranitramine or 1,3,5,7-tetrahydro-1,3,5,7-tetranitrotetrazocine or octahydro-1,3,5,7-tetranitro-1,3,5-tetrazocine, or Octogen
HPLC	High Performance Liquid Chromatography
IARC	International Agency for Research on Cancer
ICP-MS	Inductively Coupled Plasma coupled to Mass Spectrometry
ICP-OES	Inductively Coupled Plasma coupled to Optical Emission Spectroscopy
INRS	Institut National de la Recherche Scientifique
INRS-ETE	Institut National de la Recherche Scientifique—Eau, Terre et, Environnement
IRSST	Institut de Recherche en Santé et Sécurité au Travail
KClO ₄	Potassium Perchlorate
LAW	Light Anti-Tank Weapon
LCS	Laboratory Control Spike; Laboratory Control Sample
LFCA TC	Land Force Central Area Training Camp
MACS	Modular Army Charge Systems
METC	Munitions Experimental Test Center
MG	Maching Gun
MI	Multi-Increment®
MIDAS	Munitions Items Disposition Action System
MIS	Multi-Increment Sample(ing)
MMR	Massachusetts Military Reservation
MMRP	Military Munitions Response Program
MNG	Mononitroglycerol
MOD	Ministry of Defense

MS	Matrix Spike
MSD	Matrix Spike Duplicate
MSIAC	Munitions Safety Information Center
MWO	Master Warrant Officer
N.A.	Not Available
n/a	Not Applicable
NATO	North Atlantic Treaty Organization
NB	Nitrobenzene
NC	Nitrocellulose, an energetic compound
nd	Not Detected
NG	Nitroglycerin, an energetic compound, 1,2,3-propanetriol trinitrate glycerol trinitrate
NQ	Nitroguanidine, an energetic compound, Picrite Guanylnitramine
NRC	National Research Council
NSN	NATO Stock Number
NT	Nitrotoluene
Ø	Diameter
OB	Open Burning
OESS	Ordnance and Explosive Safety Specialist
OSHA	Occupational Safety and Health Administration
OTP	Outside the Plume
PE	Polyethylene
PTFE	Polytetrafluoroethylene
PVDF	Polyvinylidene fluoride
QA	Quality Assurance
QC	Quality Control
R&D	Research & Development
RALC	Régiment d'Artillerie Légère du Canada

RDDC	Recherche et Développement pour la Défense Canada
RDX	RDX or Cyclonite, and explosive compound, Cyclotrimethylenetrinitramine, or hexahydro-1,3,5-trinitro-1,3,5-triazine, or 1,3,5-trinitro-1,3,5-triazacyclohexane, or hexogen
RPD	Relative Percent Differences
RP-HPLC	Reverse Phase High Pressure Liquid Chromatography
RSD	Relative Standard Deviation
RTA	Range and Training Area
SERDP	Strategic Environmental Research and Development Program
SOP	Standard Operating Procedure
SPE	Solid-Phase Extraction
SS	Stainless Steel
SU	Sampling Unit
TDR	Time Domain Reflectometry
TNB	Trinitrobenzene, an explosive compound
TNT	2,4,6-Trinitrotoluene, an explosive compound
TP	Training and Practice
UN	United Nations
USACE	U.S. Army Corps of Engineers
USEPA	U.S. Environmental Protection Agency
UV	Ultraviolet
UXO	Unexploded ordnance

1 Introduction

Michael R. Walsh

1.1 Background

Live-fire training is an essential element in maintaining the readiness of our armed forces. This training is conducted on a limited number of ranges located within military installations or exclusion zones. The size, power, and performance of modern weapon systems have made many legacy ranges obsolete, narrowing the training options for the modern military. It is thus of paramount importance that these ranges be functional and available when needed. To ensure the sustained use of these critical resources, our armed forces must comply with regulations that protect not only human health but the environment. The failure to do so will lead to detrimental consequences.

Awareness of the environmental impacts of live-fire training on military ranges was brought to the forefront in the 1990s with the closure of Camp Edwards on the Massachusetts Military Reservation (MMR) and Eagle River Flats impact area on Fort Richardson, Alaska (ERF). Groundwater contamination at MMR was migrating offsite, affecting a critical drinking water aquifer with the munition compound RDX (1,3,5-hexahydro-1,3,5-trinitrotriazine), a possible carcinogen that has exhibited adverse teratogenic effects in animal studies (Clausen et al. 2004). At ERF, the contaminant was white phosphorus, an obscurant, which was killing large numbers of waterfowl that dabbled in the soft mud of shallow ponded areas, picking up unreacted particles and dying of a degeneration of liver and loss of motor control (Coburn et al. 1950; Racine et al. 1992a). Use of MMR is still severely restricted, and ERF is now available for live-fire training with high-explosive (HE) rounds only during the winter months when the rounds will not penetrate the ice cover.

At both sites, propellant residues at firing points have also been found. The propellant component 2,4-DNT (2,4-Dinitrotoluene) is a suspected carcinogen (IARC 1997). Artillery propellants used in the U.S. include 2,4-DNT in many of their formulations, so the potential for contamination is

significant. In 2005, the U.S. Department of Defense Strategic Environmental Research and Development Program (SERDP) funded project ER-1481 to develop the environmental data to characterize potential releases and fate of gun and rocket propellants as they occur on training and testing ranges and to characterize residues from gun propellants and leaching rates of contaminants bound in these materials. Based on the results from the project, in 2008 a 3-year extension was granted to further investigate gun and rocket propellants and their fate and impact on the environment.

This the final report for project ER-1481. It includes detailed reports from research completed since the interim report (Walsh, M.R., et al. 2010b) as well as a summary of the research conducted since the inception of the extension. A bibliography of all publications since the extension is included.

1.2 Propellants

The main thrust of this project is directly related to propellants, so a brief review of the types of military propellants available, their chemical components, and their physical characteristics will be useful. These attributes are critical to their functioning as well as to their behavior after their use. A more detailed discussion of propellants and their attributes can be found in Jenkins et al. (2008).

Propellants are known as low explosives because of their reaction speed. Unlike high explosives, which detonate, propellants deflagrate, or burn rapidly. This rapid burning produces large quantities of gas that propels the projectile out of the barrel of the weapon system. Propellants are a formulation of different compounds, combined to produce the desired characteristics necessary for the delivery of the projectile.

The most common propellants used by the U.S. and Canadian military are nitrocellulose (NC) based. Nitrocellulose is a polymeric material that has a very low solubility in water. Energetic compounds typically alloyed to NC include DNT, nitroglycerin (NG), and nitroguanidine (NQ). Ballistic modifiers, decoppering agents, flash and smoke suppressors, and binders are also added to the formulations, but it is the energetic compounds that are of the most interest in this research.

Propellants are classified by the major energetic constituents. For the NC-based propellants, NC alloyed with or without DNT is known as single-base propellant. These are typically used with howitzer and tank munitions. Double-base propellants contain NG and may contain DNT. These are used with mortar, small arms, and rocket munitions. They burn faster than single-based propellants. Triple-base propellants contain nitroguanidine, which burns cooler than other propellant compounds while delivering comparable barrel pressures. Other energetic components in triple-base propellants include NG and in some cases DNT. These propellants tend to be used with long-barreled, large-caliber weapons systems. Finally, some NC-based propellants are formulated with other energetic compounds, such as RDX. These compounds do not figure into the three basic classifications of propellants, but may be an additional source of contamination from firing point residues.

The physical size, shape, and configuration of propellants are tailored to the function to be performed. For rapid combustion, the surface area to mass of the propellant must be high. Thus, the grains for small arms and mortar propellants, used in short-barreled weapon systems, tend to be small (<1 mm). For longer barreled weapon systems, a controlled combustion rate is desired. The size of propellant grains increases and the shape takes on many different forms, from solid cylinders or strands to perforated cylinders to extruded shapes, which modifies the burn rate. Shoulder-fired rockets, which also require a rapid propellant burn rate, have long, thin strands or thin, narrow strips for propellant with high surface area to mass ratios.

When a gun or rocket is fired, the combustion of the propellant is never complete. Energetic residues will be deposited on the ground from the end of a gun barrel or behind a rocket launcher. These residues will contain the constituents of the original propellant formulation, typically (but not always) in the ratios of the unburned propellants. Combustion efficiency is influenced by barrel length, combustion temperature and pressure, the propellant formulation, and propellant age. The NC matrix within which most of the propellant components are embedded does not dissolve readily in water, trapping the components within the matrix after an initial leaching from the edges and faces of the residues. This characteristic will have a profound effect on the fate and transport of energetics from the residues.

1.3 Project scope

The research conducted under this project was designed to acquire data for estimating mass and concentration of propellant residues in the source zone as well as to derive process descriptors for mass transportation from the surface to groundwater, all data required for use in risk assessments.

In addition, some data gaps were addressed from previous SERDP projects (CP-1155, ER-1155) with the completion of deposition studies of BIP operations and the effect of close-proximity detonations on unexploded ordnance (UXO). Solutions to propellant burn contamination are included in the extension scope as well as an effort to disseminate and promote related sampling and sample processing methods developed through earlier SERDP- and ESTCP-funded research.

1.4 Objectives

The research conducted under the ER-1481 extension had several objectives. These are:

1. Develop mass deposition rate and distribution pattern data for propellant residues resulting from live-fire training with several propellant types and weapon systems.
2. Characterize active and legacy firing positions.
3. Derive fate and transport characteristics of propellants using physical models and propellant residues from firing positions.
4. Develop a safe, effective method of disposal for excess propellant charges resulting from live-fire training exercises.
5. Conduct experiments to determine the effects of close-proximity detonations of high-explosive rounds of unexploded HE rounds.
6. Complete blow-in-place detonation tests to obtain mass and distribution data for explosives.
7. Disseminate the multi-increment sampling protocol and sample preparation methods as outlined in EPA Method 8330B.

Although ambitious, the objectives are closely related, enabling the leveraging of work both within SERDP and the ESTCP programs as well as with then-current outside projects being conducted by members of our research team. Some of these objectives were driven by work in progress at the end of the original ER-1481, and with leveraged funds, there was a seamless transition to the extension.

1.5 Previous research

Previous research conducted under the ER-1481 Extension is reported in Walsh, M.R., et al. (2010b). This work covered the first 2 years of the project and will not be covered in detail in this report. The objectives were the same as stated above. A quick synopsis of the research follows.

1.5.1 Propellant residues deposition

1.5.1.1 AT4 rockets (U.S.)

In March 2009, tests were conducted by CRREL with assistance from DRDC at Fort Richardson, Alaska, to determine the residues related to the firing of AT4 anti-armor shoulder-fired rockets. Six rockets were fired from the same firing position over the snow-covered range. Each rocket had an initial propellant load of 355 g of AKB 204 propellant, a double-base propellant containing 133 g (37.5%) nitroglycerin in a 61% nitrocellulose matrix. Replicate multi-increment samples were collected from the snow surface behind and downrange of the firing position. Sampling decision units (DUs) included the main plume areas in front of and behind the firing position, two concentric 3-m deep decision units surrounding the main plumes, and two 3- × 10-m transects located 40- and 50-m downrange. All sampled areas and the firing position were recorded using a geographical positioning system. Samples were analyzed and results composited to derive an estimate of the mass of unreacted energetic materials. Total estimated per-round deposition rate of nitroglycerin (NG) for the M136 AT4 rocket is 95 g/round, or 73% of the original NG load. This indicates that the propellant burn efficiency for the AT4 is poor, with much propellant not consumed during firing. These results are comparable to tests run by DRDC-Valcartier in Canada for which an estimated deposition rate of 14% was derived from residues collected in water-filled pans (Thiboutot et al. 2007b).

Follow-up sampling was conducted in May 2009. A 30- × 30-m DU was created in the backblast plume region behind the AT4 firing position. A set of three systematic-random multi-increment samples were taken from this area to determine residue loads. Because no background samples of the soils in the area were taken prior to our test in March, this sampling characterized the site rather than providing us with rigorous depositional information. Soil samples were obtained using a coring device or scoops, depending on the cohesiveness of the soils. Sample collection and processing

followed EPA Method 8330B. Maximum sampling depth was 2.5 cm. In these samples, we found through analytical analyses that approximately one-third of the NG had leached out of the propellant fragments since March. Large propellant strip segments collected in May contained 67% of the nominal NG of the original propellant, and we hypothesize that even more had leached from the more numerous, smaller segments. The soil concentration of NG was 13 µg/g, which gives an estimated mass loading of the 900-m² DU of 250 g (Walsh, M.R., et al. 2009b).

1.5.1.2 M72 rockets (Canada)

DRDC Valcartier participated in a live-firing exercise of the Royal 22e Régiment to determine the residues generated by the firing of 98 M72 66-mm rounds. Each rocket contained 122 g of M7 Type I double-base propellant, composed in part of 43 g (35.5%) NG and 9.5 g (7.8%) potassium perchlorate (KClO₄) in a 54.6% NC matrix. Residue samples were collected in 0.17-m², rectangular, thin-walled, aluminum pans filled to a depth of about 1 cm with ethanol. These pans or traps were anchored to the ground with specially designed steel holders and located in rows up to 10 m in front and 30 m behind the weapons at 5-m intervals, with 2-m spacing between the traps. Following the completion of firing, the traps were immediately collected and the contents composited by row to derive the residue loading.

Analysis of the samples indicates that the unreacted propellant residue mass from each round contained 42 mg of NG (0.1 % by weight), with 92% of the residues being deposited within the first 20 m behind the firing positions. Although this trial demonstrated that the burning of propellant was incomplete, the burn efficiency is much higher (99.9%) than that for similar rocket propellant that does not contain perchlorates (14–73%). The residues were not analyzed for perchlorates. The results demonstrate that these weapons lead to the accumulation of propellant residues in the environment and that the propellant formulation has a significant impact on combustion efficiency (Thiboutot et al. 2009).

1.5.1.3 105-mm Tank (Canada– U.S.)

DRDC-Valcartier coordinated a test firing of a Canadian 105-mm 51-caliber gunned Leopard main battle tank at their facility in February 2009. Their SERDP partners, CRREL, were invited to participate in the live-fire exercise. The main objective was to determine the mass and distribution of

propellant residues resulting from firing of 90 C109A1 practice rounds having 3 kg of M1 single-base propellant with a nominal formulation containing 300 g (10%) 2,4-DNT in an 85% NC matrix. Residue samples were collected using two methods: snow collection (CRREL) and particle trap collection (DRDC).

DRDC placed a total of 57 traps in a series of nine rows downrange of the tank. The heavy aluminum traps, measuring 53- × 48-cm × 8-cm deep, were weighted down with stainless steel anchor plates. Placement of the traps was centered on the direction of fire. Three traps were positioned 3 m from the muzzle, five traps at 5 m, and seven traps per row at 10, 15, 20, 25, 30, 40, and 45 m in front of the gun muzzle. This resulted in a rectangular pattern with its longest axis in the firing direction. At the end of the trial, the contents of the traps were collected by row for analysis. Most of the traps contained snow that was recovered and put in plastic containers for further analyses in the laboratory. Any traps that were displaced by the blast were combined with the closest row for analysis.

The snow sample analysis was conducted by CRREL with assistance from DRDC. Prior to the commencement of firing, a multi-increment background sample was taken downrange from the tank. Following the cessation of firing, the outline of the residues plume was visually determined and demarcated by packing a path in the snow. The main plume area was a polygon, 6 m across at the gun, 26 m across at a distance of 27 m downrange, with the side lengths being 28 and 30 m. Two 3-m deep areas outside the main plume were demarcated along the sides of the main decision unit for additional sampling. An area 26 m wide and 19 m downrange from the downrange end of the main plume was also demarcated for sampling. A 3-m-deep zone along the edges and far end of this DU was the final area demarcated for sampling. Triplicate samples were taken in the two large decision units with a 20- × 20-cm scoop to a depth of 2.5 cm. Duplicate samples taken outside the main DUs were collected with 10- × 10-cm scoops to a depth of 2.5 cm.

Results from both collection methods were compared. The residue analyses from the particle traps indicated that 710 mg of DNT was deposited over the 930-m² area in which the traps were placed. Dividing these results by the number of rounds fired results in an estimated 7.9 mg (0.0026%) of the original DNT load deposited for each round, most of which occurred within the 20- to 25-m zone downrange of the gun. For the snow samples,

92% of the DNT residues were found in the main downrange plume, with an estimated 390 mg on the surface, 160 mg in the subsurface, and 9 mg in the side DUs. The large DU beyond the main plume contained an estimated 36 mg of DNT with 1 mg estimated in the area surrounding the DU. A total of 92% of the residues occur within the main downrange plume while only 6% occurs in the secondary downrange plume. The remaining 2% lies in the 3-m zone surrounding these plumes. The total estimated mass of DNT in the DUs is 600 mg, or 6.7 mg (0.0022%) of the original DNT load per round. Similar results were thus obtained with both methods (Ampleman et al. 2009a).

1.5.2 Fate and transport

1.5.2.1 Site characterization (DRDC-INRS)

The long-term fate of double-base propellant residues in the environment has been poorly studied in the past. To fill this data gap, DRDC and the Institut National de la Recherche Scientifique—Eau, Terre, et Environnement (INRS-ETE), QC, Canada, initiated a study in 2008 at the former Carpiquet anti-tank shoulder-fired rocket range, which was decommissioned in 1975. The range is located southeast of the Valcartier training area in Quebec, Canada, and was chosen because antitank rockets are propelled by double-base propellants. The range spanned the Jacques-Cartier River with the firing point on the south bank and the target impact area on the north bank. A fence is located 5 m behind and parallel to the former concrete firing wall. The old firing wall is 16 m long with one firing position at each end.

With multi-increment sampling, five replicate soil samples were collected over a 16- × 5-m rectangular region located behind the firing wall, between the wall and the fence. Samples were also collected in parallel 2- × 16-m decision units (transects) up to 30 m from the fence. Subsurface soils were collected from pits dug with a shovel up to 1 m deep to measure the vertical migration of NG with time. The soil samples were sieved to determine which fractions held the highest concentrations of NG.

The surface concentrations of NG are still at 4000 mg/kg after more than 25 years of inactivity. Vadose zone monitoring equipment was installed by INRS-ETE. Four lysimeters were used for the sampling of interstitial water (depths: 10, 30, 60 cm, and background). Their installation provided further information on the subsoil stratigraphy. A trench was also dug for the

installation of other water monitoring equipment. High concentrations of NG were detected in the soils at the surface and colloidal penetration in the soil profile was observed, although neither NG nor NG degradation products were detected in the interstitial water of the soil column or underlying groundwater. This work indicates that high concentrations of NC-based propellants can persist in the environment for many years after a site is closed, but the risk to groundwater from this legacy contamination is low because of the entrapment of the NG in the insoluble NC matrix. These sites should be monitored for propellant residues, even after many years of inactivity, and will need to be cleaned up prior to being used for other purposes (Thiboutot et al. 2010).

1.5.2.2 Column studies (INRS)

Knowledge of the fate and transport of propellant residues is critical to determining the impact to the environment of these substances. This study focused on characterizing the impact on soil and groundwater of propellant residues from antitank firing points. The munitions utilize double-base propellants containing nitrocellulose (NC) and nitroglycerin (NG), with some munitions containing up to 7.8% potassium perchlorate (KClO₄). The compounds of interest were NG and its metabolites as well as perchlorate. Soils contaminated with propellant residues were collected from two firing positions, one from a rocket range on the Canadian Forces Base (CFB) Petawawa in Ontario and the other from a similar range on CFB Gagetown in New Brunswick, Canada, for the study. The Petawawa column was constructed entirely from soils collected at that firing position, while the contaminated surface soils from Gagetown were placed on a column consisting of soils from CFB Valcartier. Both columns were 60-cm tall and 62 cm in diameter. Time-domain reflectometry ports were located at 10-, 30-, 50-, and 60-cm from the surface to monitor pore water in the soil column. Six drain holes on a 21-cm radius and one in the center were located on the bottom of the column enclosure to monitor effluent. Water was applied to the columns following the recharge patterns of their respective locations. Effluent of the columns was sampled to evaluate the contaminants transport through the unsaturated zone.

A solid-phase extraction method, coupled with high-pressure liquid chromatography-ultraviolet (HPLC-UV) analysis, was developed to monitor both NG and its degradation products in the water samples (Martel et al. 2010). Initial concentrations of NG and perchlorate were 3145 mg/kg and 3.52 ug/kg for the Gagetown–Valcartier columns and 5652 mg/kg and

53.5 µg/kg for the Petawawa columns. Nitrite and nitrate initial concentrations were 307 and 296/mg/kg and 483 and 634 mg/kg for the two columns respectively. In the Gagetown column effluent, high concentrations of NG, dinitroglycerol (DNG), mononitroglycerol (MNG), nitrites, and nitrates were detected. All the mobile fractions of these compounds were flushed out of the soil column within 1 year of infiltration. In the Petawawa columns, no nitrite, NG, DNG, nor MNG was detected in the effluent of the columns. Only perchlorate and nitrate, mainly from oxidation of nitrite through degradation of NC, NG, MNG, and DNG, were detected in that effluent.

This study demonstrates that groundwater in the unsaturated zone under antitank firing positions may be contaminated by dissolved NG, NG metabolites, nitrites, nitrates, and perchlorate. However, in the saturated zone, the concentrations of these pollutants are diluted by the flowing groundwater. Dissolution and diffusion of non-NC components of the propellant residues occurred during the first year cycle but was greatly attenuated after that, indicating a stabilization of the residues through the inability of constituent to leach out of the NC matrix.

1.5.3 Disposal of propellants

1.5.3.1 Propellant residues from expedient disposal (CRREL)

Military live-fire training missions utilizing mortars and howitzers frequently generate excess propellant charges. This propellant is often disposed of on-site and is called expedient disposal. Investigations into energetics residues resulting from expedient disposal of propellants began in 2002, with the collection of residues inside and outside a propellant burn structure at Fort Richardson, AK (Walsh, M.E., et al. 2005). These residues contained very high concentrations of 2,4-Dinitrotoluene, an indication that the burning process was not complete. Other informal tests were conducted, indicating the same results. In 2006 and 2008, a series of tests were conducted on snow using propellants from various mortar cartridges. In 2006, a small amount of mortar propellant was burned on snow and the residues collected and analyzed. In 2008, two series of tests were conducted, one involving winter disposal of mortar propellants, the other summer disposal of howitzer propellants. These tests were conducted under controlled conditions to determine if the environmental setting and climatic conditions can influence the efficiency of expedient propellant disposal (Walsh, M.R., et al. 2010b).

In 2006, following a mortar training exercise, 10 charges of M9 double-base propellant from 81-mm mortar cartridges were burned on the surface of the snow adjacent to the firing position. All the residues were collected and analyzed. In 2008, two sets of tests were conducted. In the winter, 32 charges of M45 double-base propellant from 120-mm mortar cartridges were burned, 11 on a 40-cm deep snowpack, one on the frozen ground from an area from which the snow was removed, and 10 in a stainless steel bowl placed on the snow surface. Residues from the bowl and surrounding snow pack were collected and analyzed. Residues from the other two tests were collected in May and July of 2008. In addition, soil profiles were created and propellant grains collected and analyzed. In July of 2008, two burn tests were conducted on a clean bed of sand with M1 single-base propellant from 105-mm howitzer projectiles. One bed was dry, the other thoroughly wetted with water. All residues from both burns were collected for analysis.

Results varied significantly among the tests. For the first test, conducted in 2006, over 1.6% (870 mg) of the original NG content was recovered from the 10 mortar propellant charges (Walsh et al. 2006a). In 2008, the 10 mortar charges burned in the bowl resulted in the generation of 270 mg of NG residues, of which 73% was found outside the bowl on the snow surface. This represents 0.21% of the original NG load. In May, the remaining two burn sites had significantly higher amounts of residues. The frozen soil burn site yielded 7300 mg of NG, 5.2% of the initial load, and the snowpack burn site yielded 25,000 mg NG, 18% of the initial load. Unburned propellant grains collected in June, 4 months after the initial test, contained only 5.6% NG, around 55% of the initial NG load. The remainder had leached out into the soil. Soil profiles indicated a steep attenuation of NG concentration in the peaty soil with depth. Surface contamination (0–2 cm) was dominant, 52 mg/kg at the frozen-soil test site, where the surface residues had been removed in June, 23 mg/kg at the snow test sites, where the grains had been previously removed, and 180 mg/kg for the snow test site below an area where the surface grains were removed in July. Only the July site had detectable concentrations below 2 cm: 46 mg/kg in the 2- to 4-cm zone and 9 mg/kg in the 4- to 6-cm zone. These results show that leaching of NG from the unburned grains continued at least through July, but that the surface 2 cm continued to dominate the contamination profile. The M1 burn tests in July indicated that surface wetness was not a significant factor in burn efficiency, with less than 1% of the original DNT load remaining in the residues.

An interesting test was conducted on the residues of the 120-mm propellant residues. Three 3-cm diameter cores were taken at the snow and frozen ground test sites prior to removal of the unburned propellant grains. NG concentrations averaged 5400 mg/kg for the six cores. The implication of this result is that a single increment of a multi-increment sample can greatly influence the outcome, indicating that replicates are advisable when using this sampling method.

1.5.3.2 Dioxin and furan contamination at propellant burn sites (DRDC)

Burning bags of excess gun propellant left after an artillery exercise is a common practice on Canadian Forces Bases ranges and training areas. When expedient field disposal of excess propellant is carried out, the charge bags are aligned and burned on the ground. This operation is known to leave significant quantities of energetic residues. It was also suspected to produce dioxins and furans, two structurally and chemically related chlorinated compounds that are known to be toxic and persistent in the environment. At CFB Petawawa, ON, Canada, dioxins and furans were detected in soil and water samples at disposal areas. Railroad fuses, used to initiate propellant burns by the Canadian military, were the suspected source. The objective of this research was to determine if these devices were the source of these highly toxic contaminants.

Howitzer propellants containing no chlorinated compounds were used in a series of trials on dry land to investigate the source of the dioxins and furans. In each series, the trials were set up to test if the initiation fuses are the source of the dioxins and furans when propellants are burned. In some tests, propellants were initiated with a fuse; in others, propellants were initiated without a fuse; and in some tests, only a fuse was burned. Residues were collected from different parts of each burn to test for the contaminants.

In the first trial, burning of propellants, the dioxin and furan levels in the propellant residues were lower than background levels, indicating that the propellants are not the source of the contaminants. When the propellant was initiated with a fuse, the elevated presence of dioxins and furans became evident. For the trials on sand, elevated levels of the contaminants ($\times 10^3$) appeared adjacent to the fuse, although the level, measured in toxic equivalent quantities (TEQs), was low (0.04 max). When burned on a stainless steel disposal pan, the same test yielded TEQs of 0.07 for the propellant residues approximately 2 m from the flare, 5.2 in the propellant

residues at the fuse, and 0.33 in the fuse residues. Samples were analyzed by gas chromatography mass spectrometry at a private lab not associated with DRDC. These results demonstrate that the production of dioxins and furans was not related to the combustion patterns, chemical composition, or mass of gun propellant but to the presence of the igniter, a railroad fuse containing perchlorates. The accepted procedure published by the Canadian Forces previously required the use of a railroad fuse as the ignition source of the gun propellant. As this device has been shown to be the source of dioxins and furans in propellant burns, the disposal procedure for excess gun propellant by open burning has now been modified and a new standard operating procedure is in place (Poulin et al. 2009).

1.5.4 Explosives residues

1.5.4.1 Blow-in-place tests (CRREL)

SERDP Projects CP-1155 and ER-155 had as their main focus the fate and transport of explosives residues resulting from military training activities. Many source terms were examined, including high-order detonations, low-order detonations, and residues from blow-in-place (BIP) operations. All major army weapon systems that could be tested safely for high-order and BIP residues had been tested with the exception of BIP residues for 60- and 120-mm mortar projectiles. The tests to fill this gap were carried out on the snow-covered ice of the Eagle River Flats impact area on Fort Richardson, AK.

Seven of each type of fuzed round were detonated using a 0.57-kg unconfined block of Composition 4 (C4) explosive (91% RDX, 9% plasticizer) applied to the body of the projectile and initiated by a blasting cap. Initiation points were located far enough apart to minimize cross contamination between residue plumes. Following the detonation of a series of projectiles, the main residue plume areas were demarcated by walking along the edge of the visible residues. These plumes were then sampled using a random multi-increment sampling method with 10- × 10- × 2.5-cm scoops to construct an approximately 100-increment sample. Samples were then process in a nearby field lab and analyzed back at the main lab in Hanover, NH. Results from the analyses show that, for the 60-mm projectile, the seven BIP operations resulted in 200 mg/round ($2.3 \times 10^{-2}\%$) of the total explosive load, including the donor charge, and for the 120-mm test, the seven detonations resulted in 25 mg/round ($7.7 \times 10^{-4}\%$) of the total explosive load. Only RDX and HMX were detected in the residues; these per-

centages become $2.7 \times 10^{-2}\%$ and $1.1 \times 10^{-3}\%$, respectively. Results were as expected from previous research (Walsh, M.R., 2007). Smaller rounds with a higher donor charge to projectile load have higher residues rates because of the unconfined charge. Although residues rates are low for BIP operations, donor charge size can be refined to lower contamination from these actions (Walsh, M.R., et al. 2008).

1.6 FY10 Research

The following chapters describe in detail the research completed during FY10 under SERDP ER1481. They will be followed by a concluding chapter tying the many tasks of the project together and summarizing the results. In addition, a description of the progress on the dissemination of EPA Method 8330B will be given.

2 Propellant Residues Deposition from Firing of 40-mm Grenades

Michael R. Walsh, Marianne E. Walsh, James W. Hug, Susan R. Bigl, Karen L. Foley, Arthur B. Gelvin, and Nancy M. Perron

2.1 Summary

Military live-fire training utilizes energetic materials that are never completely consumed. In February 2010, tests were conducted at Fort Richardson, AK, to determine the propellant residues deposition rates related to the firing of 40-mm grenades from a Mk19 machine gun. Two test pads were constructed, with 127 Mk-281 (BA12) training rounds containing F15080 propellant (9.1% nitroglycerin-NG) fired over one and 144 M430 (B542) high-explosive rounds containing M2 propellant (19.5% NG) fired over the other. Replicate multi-increment samples were collected from the snow surface downrange of the firing positions in three sampling units on each pad. Samples were analyzed and results composited to derive an estimate of the unreacted energetics mass. The total estimated per-round deposition rate for the M430 high-explosive cartridge is 76 mg/round, 8.4% of the original NG load. The deposition rate for the Mk-281 cartridge is 2.2 mg/round, 0.59% of the original NG load. Energetics deposition rates for the M430 rounds were between those for mortar projectiles and shoulder-fired rockets, which also utilize double-based propellants, are medium-velocity projectiles, and are fired from short-barreled guns. The Mk-281 cartridges, with their NG-impregnated propellant grains, had a much lower NG deposition rate but a greater mass of unconsumed propellant.

This study was conducted for the Department of Defense (DoD) Strategic Environmental Research and Development Program (SERDP) under Environmental Restoration Program Project ER-1481. Dr. Andrea Leeson was the program manager.

2.2 Introduction

2.2.1 Background

The use of munitions during live-fire training is a necessary component for a well-trained military. The environmental impacts caused by the energetics associated with these munitions were not fully known until relatively recently. That knowledge was accelerated with the closure of ranges in Alaska (Eagle River Flats on Fort Richardson) and Massachusetts (Massachusetts Military Reservation) and subsequent research into the characterization of contaminants on those ranges (Racine et al. 1992; Clausen et al. 2004).

Initially, the emphasis was on the impact areas, where detonation of the projectiles had the potential to introduce large quantities of energetics into the environment. Characterization and deposition studies indicated that a properly functioning munition does not deposit appreciable amounts of energetics during training (Hewitt et al. 2005; Jenkins et al. 2006a; Walsh, M.R., 2007a,b). In the process of examining impact areas, the focus expanded to include the characterization of firing points (Walsh, M.E., et al. 2001, 2007; Walsh, M.R. et al. 2005a, 2005b, 2007a)

The examination of firing points (FPs) as a source of energetic residues is a recent thrust in range sustainability research. Starting in 2000, studies funded by U.S. Army Alaska at Fort Wainwright's Donnelly Training Area (DTA) (Walsh, M.E., et al. 2001) indicated propellant-related energetic compounds were persisting at heavily used indirect-fire and direct-fire FPs. Further research in 2001 and 2002 (Walsh, M.E., et al. 2004) reinforced the original indications, with the propellant constituents nitroglycerin (NG) and 2,4-dinitrotoluene (DNT) recovered at several FPs. The state of Alaska lists DNT as a hazardous substance.

In 2002, the U.S. Department of Defense (DoD) Strategic Environmental Research and Development Program (SERDP) funded research at Fort Richardson, AK, to estimate high-explosives (HE) residue deposition (RDX, HMX, and TNT) from the live-fire detonation of 105- and 81-mm HE projectiles. Following the firing of the 105-mm howitzers, propellant residues containing DNT were collected from the snow-covered area in front of one of the guns (Walsh, M.E., et al. 2004). Results indicated concentrations of energetic residues that were four orders of magnitude higher for the firing points than found at the impact areas (Hewitt et al. 2003;

Walsh, M.R., et al. 2005c; Walsh, M.E., et al. 2007). When firing positions for shoulder-fired rockets were characterized, high concentrations of propellant residues were found in the surface soils (Thiboutot et al. 1998; Jenkins et al. 2006a; Wingfors et al. 2006).

The ease of sample collection on snow and the straightforward processing of these samples led us to consider further investigations at winter firing points as an adjunct to the impact area research we were then conducting for SERDP. The methodology for the collection of samples on snow originally developed by Jenkins et al. (2000a, 2000b, 2002) was optimized by M.R. Walsh et al. (2005a, 2007b), making sampling much more efficient and repeatable.

Trials have been conducted on several common weapon systems including howitzers (Walsh, M.R., et al. 2005b; Diaz et al. 2008), mortars (M.R. Walsh et al. 2005c, 2006a), small arms (Walsh, M.R., et al. 2007a; Brochu et al. 2009), rockets (Walsh, 2009), and tanks (Ampleman in review). One common weapon system class for which no data had been collected is the medium caliber class, which includes 14.5- to 40-mm weapon systems. This report describes testing and results for one of these weapon systems, the Mk-19 40-mm machine gun.

2.2.2 Objectives

The objectives of these tests were to derive an estimate of propellant residues generated as a result of live-fire training with the Mk-19 40-mm machine gun with two different cartridges. Tests were conducted firing both high-explosive rounds and training rounds. Propellants for these two types of cartridges differed in composition. The ultimate objective of this work is to provide data and results that can be used by the range community to assess the environmental impact of training with the Mk-19. This information then can be used to develop an integrated training lands management plan.

2.2.3 Approach

Tests were conducted 22–23 February 2010 on the 40/90 range located on Fort Richardson, AK. Tests were conducted in winter to enable us to collect samples from an uncontaminated surface (snow) at an active range. During the test, propellant residues from the firing of the weapon system are deposited on the snow surface downrange from the gun. These

residues are visible, allowing demarcation of the area of deposition. The residues and underlying snow are collected using multi-increment sampling to estimate the total mass of energetic residues. The samples are then easily processed and analyzed. As two tests were run, two areas within the firing point were required to prevent cross contamination. These firing positions were constructed on snow pads built for this purpose on the parking area of the range. No down range sampling beyond the constructed pads was conducted because of the danger presented by the probable presence of unexploded ordnance below the snow cover and the sensitive nature of the fuzing on the 40-mm HE projectiles. As each round contains only about 4 g of propellant, a large number of cartridges (>100) were fired to ensure adequate residues for the analyses.

2.3 Field sampling methodology

2.3.1 Field site and conditions

No live-fire training had occurred at the Fort Richardson 40/90 Range during the winter immediately prior to our test. The parking area at the firing point had been plowed, leaving little snow cover in the areas where the firing positions were to be set up (Fig. 2-1). We delineated test areas and transferred snow from the area behind the firing positions to construct snow pads to be used for our tests (Fig. 2-2). Forward of the firing positions, the area was flat for 15 m before the opposite edge of the parking area was encountered. The snow bank on the downrange side was removed by Range Control to facilitate the firing of the weapon system. The temperature at the time of testing was around -4°C with winds out of the north, variable at around 1 m/s. The sky was partially overcast under a weak sun at the start of the testing, clearing as the day progressed. Undisturbed snow depth was less than 60 cm on either side of the parking area.

The two snow pads measured approximately 11.5-m long and 7.5-m wide for the first test and 13.5-m long by 8.2-m wide for the second test (Fig. 2-3). Depths of the pads were variable, with a target depth of 20 cm. A 5-cm top layer was added to a 15-cm base layer to serve as a sampling surface. The pads were separated by about 4 m. The second pad was built following the conclusion of the first test to prevent cross-contamination between the tests.



Figure 2-1. 40/90 Range firing point parking area prior to pad construction.



Figure 2-2. Test pad for first firing from down range. Gun is to left of image.

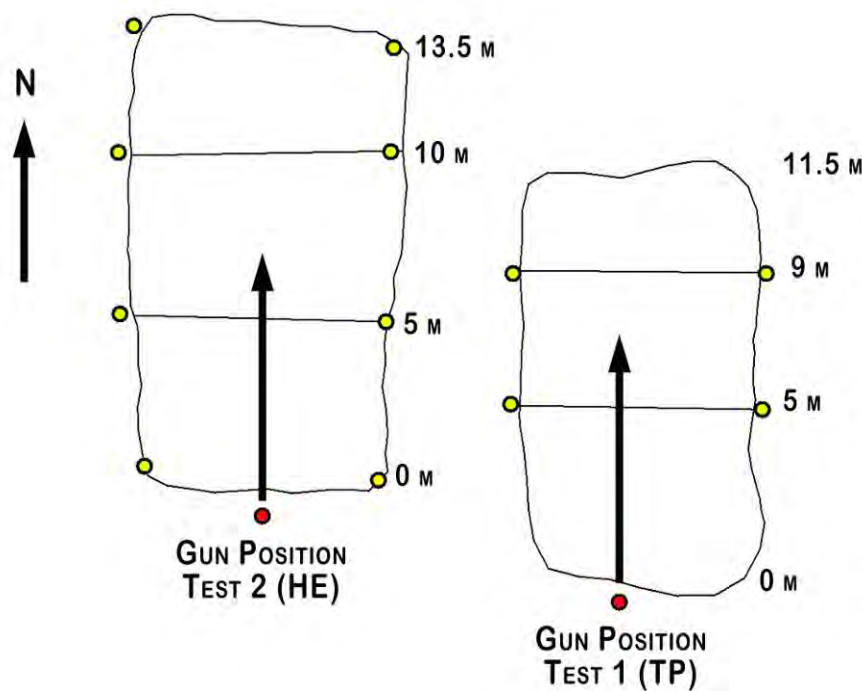


Figure 2-3. Test pad layout.

To determine if any pre-existing residues occurred in the area, baseline samples were taken from both the snow mine used to construct the pads as well as areas adjacent to the range. The snow mine samples were taken at mid-snow depth, the source of the pad base layers, and the surface, from which we obtained the topping layer for the pads. Baseline samples were obtained at three locations away from the firing pads on 22 and 23 February. The unusually mild weather allowed efficient operations, and there were no delays in site preparation. The pads, snow mines, and baseline sample locations were recorded using a Trimble GPS Pathfinder Pro XR system (± 1 m) supplemented with hand measurements taken with a tape measure.

2.3.2 Munitions tested

The munitions tested were the Mk281 MOD 0 training and practice (TP) round and the M430 high explosive (HE) round (Table 2-1). The M430 HE round contains 4000 mg of M2 double-based propellant, a standard U.S. military propellant formulation, with nitrocellulose (NC) and nitroglycerin (NG) as the energetic constituents (U.S. Army 1994). The Mk281 TP round can contain any one of several types of propellants, depending on the lot. For the lot used in our tests, the propellant specified was 4040 mg of

F15080, a European-manufactured¹ NG-impregnated double-based propellant with NC, NG, EC (Ethyl Centralite), and Akardite II as the major constituents. The F15080 propellant is quite different from previously tested propellants in that the NG resides on the surface of the propellant grains rather than as a component of the NC matrix that makes up the bulk of the propellant grain. We hypothesize that these physical and chemical characteristics had a major effect on the resulting NG deposition rate for our test utilizing this propellant compound. Detailed information on the munitions and propellant constituents can be found in Appendix A.

Table 2-1. Propellant constituents analyzed for firing point test.

Weapon system	Munition (Mil-DODIC)	Propellant	Constituent	Constituent load (mg/% of total load)
40 mm Mk19 MOD 3 Grenade Machine Gun	Mk281 MOD 0 / BA12 (TP)	F15080*	NG	370/9.1
	M430 / B542 (High Explosive)	M2	NG	900/19.44

*From ammunition data card for a different lot number. Data for both munitions from MIDAS.

2.3.3 Firing of munitions

Live-fire testing of the 40-mm weapon system was done in two stages (Fig. 2-4). On 22 February, 127 Mk281 TP rounds were fired from the first firing position. One round jammed on loading and was not fired. On 23 February, 144 M430 HE rounds were fired from the second firing position. The cartridges, which were assembled onto a metal belt for automatic fire, were fired in up to 5-round bursts until all ammunition was expended. Sampling commenced after the area was cleared by our unexploded ordnance technician.

¹ Manufacturer is Nitrochemie of Wimmis, Switzerland.



Figure 2-4. Firing of M430 HE grenades over test pad.

2.3.4 Sampling method

The post-firing propellant sampling of residues was done from the surface of the two test pads following the multi-increment sampling (MIS) protocol established by M.R. Walsh et al. (2007b). Briefly, a representative sample composed of 40–48 increments of surface snow and residues was collected with a flat-bottomed hand scoop to make up a single sample within a sampling unit (SU). MIS allowed us to test and compensate for uncertainty derived from the small total area collected from within each SU, typically less than 1 m².

The pads were divided into three SUs along the downrange axis (Table 2-2, Fig. 2-3). In each SU, three MI samples were taken with a 10- × 10- × 2.5-cm polytetraflouoroethylene-(PTFE)-coated scoop. Increments were placed in a laboratory-grade, clean polyethylene (PE) bag. When sampling was done, the bag was labeled, a tag labeled and attached to the bag, the bag sealed with a tie-wrap, the sample recorded in a log book, and the sample placed in a shaded location until transportation back to the processing laboratory located nearby on post.

Table 2-2. Sampling unit areas, February 2010.

Sampling Unit	Area (m ²)	Percent of pad area
Pad 1 (TP Rounds) 0–5 m	36	42
Pad 1 (TP Rounds) 5–9 m	29	34
Pad 1 (TP Rounds) 9–11.5 m	21	24
Pad 2 (HE Rounds) 0–5 m	38	34
Pad 2 (HE Rounds) 5–10 m	41	37
Pad 2 (HE Rounds) 10–13.5 m	32	29

In addition, we obtained one surface MI sample in the 0- to 5-m sampling unit of each pad using a 20- × 20- × 2-cm scoop. These samples were difficult to obtain because of the traffic in the area that took place during the taking of the triplicate samples. Very little area was available for sampling, that area was not evenly distributed throughout the SU. No subsurface samples were obtained because the muzzle blast of the weapon was insufficient to cause mixing of the surface snow. A visual inspection of propellant debris on the pad surfaces (Fig. 2-5) showed that the debris was contained on the pads, obviating the need to sample off the pads.



a. F15080 Propellant debris (TP).

b. M2 Propellant debris (HE).

Figure 2-5. Propellant debris on test pad surfaces after tests.

Trays were placed in front of the muzzle of the gun for both tests to collect a small amount of residues for microscopic analysis for another project as well as chemical analyses for this project (Fig. 2-6). These trays were removed partway through both tests to minimize the impact on the mass deposition tests covered in this report.



Figure 2-6. Location of trays used to collect propellant debris.

2.4 Sample processing and analysis

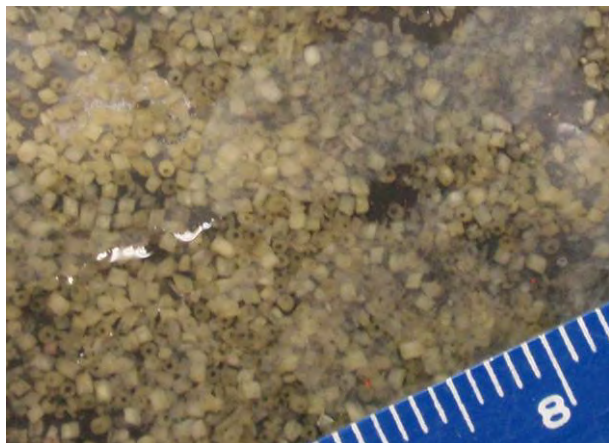
2.4.1 Snow samples

The samples of snow were transferred to a laboratory at the Fort Richardson cantonment area for processing. Upon arrival, the samples were transferred from the field bags to clean bags, double-bagged, and placed in clean polyethylene tubs for thawing (Fig. 2-7). Placing the samples in clean bags reduces the chances of cross-contamination from contact with adjoining bags and residues on the exterior of the sample bags. Double-bagging and the tubs were necessary because of the inclusion of sharp pieces of debris collected with the snow samples. Otherwise, debris from the firing of the rounds could pierce the sample bags, allowing the thawed samples to leak.

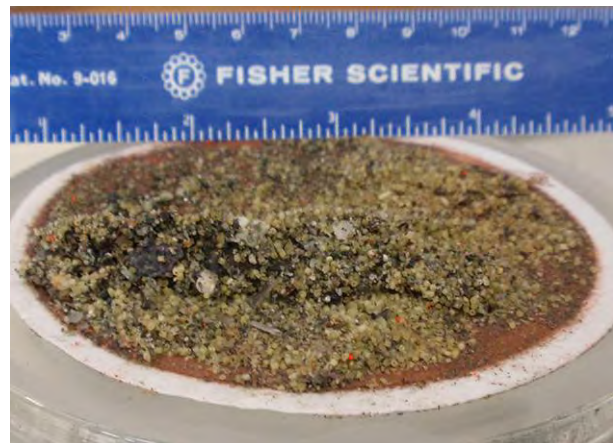


Figure 2-7. Samples in tubs at thaw location.

Samples were shifted from warmer to cooler areas of the lab's logistics bay to prevent over-warming (temperatures $>4^{\circ}\text{C}$) after melting. The samples were then processed based on completion of melting and the sampled area from which they were taken. Samples anticipated to have the least residues were processed first and those anticipated to be more contaminated were done last to reduce the possibility of cross-contamination (Fig. 2-8).



a. Close-up of F15080 propellant in sample bag.



b. F15080 propellant on filter.

Figure 2-8. Images of propellant residue during initial processing of 0-5m SU samples.



c. M2 propellant on filter.

d. Close-up of M2 propellant.

Figure 2-8 (cont'd). Images of propellant residue during initial processing of 0-5m SU samples.

Processing involved filtering the melted samples using a vacuum system to separate the solid fraction from the aqueous fraction (Fig. 2-9). The solid fraction was collected on filter papers.¹ Following filtering, the papers were placed in a clean amber jar, air dried, and stored in a refrigerator at <4°C. The volume of the aqueous fraction was recorded prior to mixing and decanting of two or four 500-mL aliquots into glass amber bottles. (Two bottles were the normal number collected for analyses; four were collected for a laboratory quality assurance procedure.)

One (or three) 500-mL aliquot of the filtrate was pre-concentrated by passing it through a Waters Porpak RDX² solid-phase extraction (SPE) cartridge and eluted with 5 mL of acetonitrile (AcN), resulting in a 100:1 concentration of the analytes (Walsh, M.E., and Ranney 1998). The concentrate was split into two aliquots, 3.5 mL for analysis and 1.5 mL for archiving. When processing was completed, the 3.5-mL splits and the filters were shipped to the CRREL's analytical chemistry laboratory in Hanover, NH, for final processing and analysis.

Prior to final processing, the air-dried filters were weighed. Subtracting out the weight of the filter gives us the weight of the firing point debris. This debris consists of whole and partial propellant grains, propellant residues, debris from the firing of the cartridges (metal fragments from the rotating bands, parts of the obturator rings, etc.), and whatever other solid contaminants may be in the sampling snow matrix. Separation and analy-

¹ Whatman glass microfiber 90 mm Ø grade GF/A.

² Sep-Pak, 6-cm³, 500-mg.

sis of these components will give us a good estimate of the total propellant components resulting from the firing of the rounds.

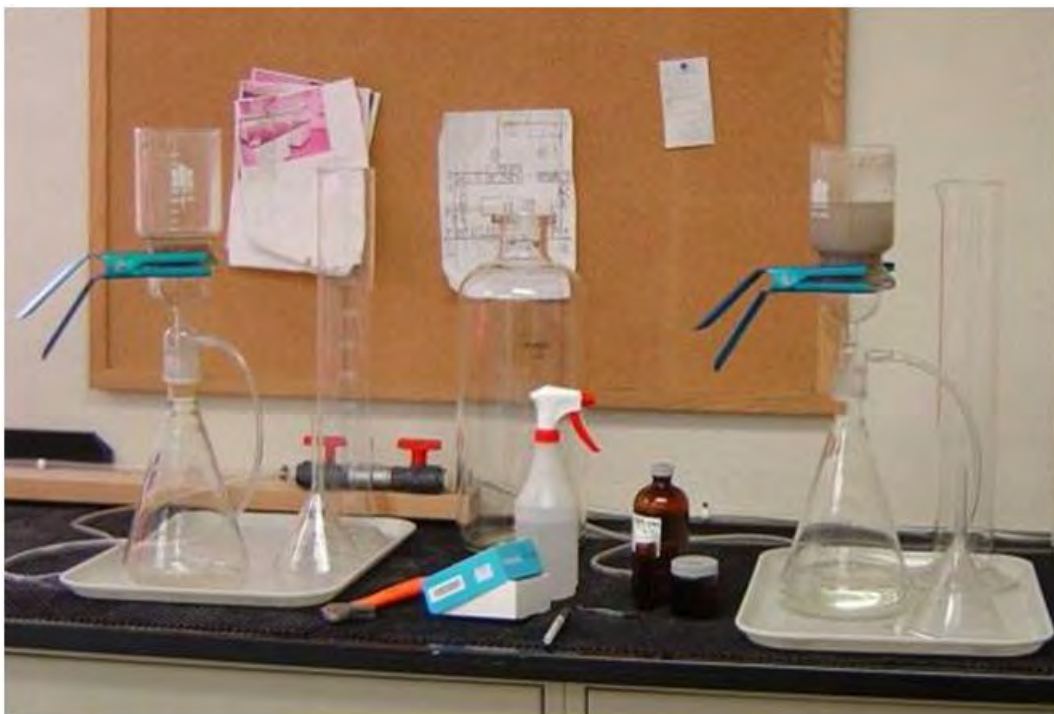


Figure 2-9. Sample filtration setup at the processing laboratory on post.

The NG was extracted from the solids on the filters by shaking for 18 hours with AcN. The AcN extracts from the solid phase extraction of the melted snow and of the solid residue on the filters were analyzed by high-performance liquid chromatography (HPLC). Analyte concentrations were determined following the general procedures of SW 846 Method 8330B to determine nitroaromatics, nitrate esters, and nitramines by HPLC (USEPA 2006). The HPLC method has an analytical error that is very small, about 2% relative standard deviation (RSD) for replicate injections.

Prior to analysis, each extract was diluted with AcN based on the intensity of the color from the EXPRAY test (Walsh, M.R., et al. 2010a) so that the injected concentration would be less than 10 mg/L. The AcN was then mixed with reagent-grade water (1:3 v/v) and filtered through a Millex-FH filter unit¹. Determinations were made on a modular system² composed of a Finnigan SpectraSYSTEM Model P4000 pump, a Finnigan SpectraSYSTEM UV2000 dual wavelength ultraviolet/visible absorbance detector set

¹ Millipore, PTFE, 0.45 µm.

² Thermo Electron Corporation of Waltham, MA.

at 210 and 254 nm (cell path 1 cm), and a Finnigan SpectraSYSTEM AS300 autosampler. Samples were introduced with a 100- μ L sample loop. Separations were achieved on a 15- \times 3.9-mm (4- μ m) NovaPak C8 column¹ at 28°C and eluted with 1.4 mL/min of 15:85 isopropanol/water (v/v). Under these conditions, NG eluted at 8.7 minutes and Akardite II[®] eluted at 9.7 minutes.

Energetics calibration standards were prepared from analytical reference materials obtained from Restek Corporation (Bellefonte, PA). The analytical reference materials were 8095 Calibration Mix A (1 mg/mL) and a single-component solution of NG (1 mg/mL). A spike solution at 1 mg/L was prepared from 8095A Calibration Mix and the single-component solution of NG. Spiked water samples at 0.002 mg/L were prepared by mixing 1.0 mL of the spike solution into 500 mL of water in a volumetric flask. Following SPE, the extract target concentration was 0.20 mg/L for each analyte. Reference material for Akardite II (3-methyl-1,1-diphenylurea) was obtained² and used to prepare a calibration standard at 20 mg/L in AcN.

To calculate the mass of unreacted energetic compounds in the residues deposited on the snow, we first had to derive an estimate of the mass in the soot and aqueous fractions. For the soot fraction, the extract concentration (mg/L) is multiplied by the volume of AcN used in the extraction (L). For the aqueous fraction, the extract concentration is multiplied by the volume of water from the snow melt. These masses were then divided by the actual area sampled with the scoops (m^2) to derive the surface concentrations in mg/m². This value was multiplied by the measured area of the SU to derive our estimates of the mass within the area sampled (mg) (Jenkins et al. 2002; Hewitt et al. 2003). For the HPLC, the detection limit was 0.05 mg/L for NG in the AcN extract. Values below this limit are labeled as “ND” in the data, indicating “no detectable” analyte.

2.4.2 Quality Control Procedures

Quality control (QC) procedures were conducted both in the field and in the laboratory. Field QC, noted previously, included replicate sampling within the residue plumes, background samples, and snow mine samples. In the processing laboratory, blank samples, consisting of filtered water from a reagent water filtration system, were periodically run through a fil-

¹ Waters Chromatography Division, Milford, MA.

² Sigma-Aldrich.

ter assembly and SPE setup for later analysis at the laboratory. This procedure was designed to determine whether there was cross-contamination from the sample filtering apparatus. Water fractions for several samples were divided into three aliquots and run through the SPE to determine whether recovery rates from the SPE procedure were consistent. SPE spikes were run to determine cartridge filter retention and recovery. These processes are described in greater detail in M.R. Walsh (2007). Two samples were taken in February to determine the background concentration of the analyte in the areas to be sampled prior to the test. Two baseline samples were taken from the snow mine areas used as sources for the test pads. These mines were adjacent to the test pads and thus more likely to contain energetics from training at this site. Surface and subsurface samples were taken and analyzed for NG.

Initially, we did not know the composition or chemical compound distribution of the TP propellant grains. Analyses of the results for these rounds indicated a need to further investigate the propellant residues captured on the filters during processing. The normal procedure for processing of the filters, which we followed, is to weigh the filters and solids after drying and prior to dissolution of the propellant. Following propellant dissolution and sampling for the analytical chemistry, the filters and remaining debris are returned to refrigerated storage.

The filters for the most heavily loaded sampling units were taken out of refrigerated storage and washed with acetone in a glass dish. The solids were gathered in a pre-weighed weight boat, allowed to dry in a fume hood for 1 hour, and reweighed to derive the mass of solid non-propellant debris. These data enabled a more accurate estimate of the original propellant and propellant residues on the filters, allowing us to refine our NG recovery estimates. We also determined the NG content of several propellant grains recovered from sample trays placed in front of the gun firing the TP rounds. The results for these tests still looked low in comparison to the amount of solids on the filters for the TP rounds, leading to the need to further investigate the propellant (refer to *Discussion*, Section 2-7).

2.5 Results: Deposition rate

The background samples collected from the area surrounding the firing position and the baseline samples collected from the snow mines contained no detectable nitroglycerin, indicating a clean test area.

A total of 20 MI samples, composed of 833 increments over a combined area of 200 m² in six sampling units, was taken to determine the deposition and distribution of NG from the firing of 127 TP and 144 HE 40-mm rounds during the two tests conducted. The test pads over which the firing occurred were divided into three SUs each, ranging in size from 21 to 41 m² (Fig. 2-3). No subsurface samples were obtained and there was no sampling outside the pad areas, except for background samples and baseline samples at the snow mines used to construct the test pads.

A summary of the analytical data averaged for the replicate samples is given below in Table 2-3 (see also Appendix B). The estimated average mass values do not include the 20-cm scoop samples in the 0–5 m areas (refer to *Discussion*, Section 2-7). The average mass of NG per TP round is 270 mg/127 rounds or 2.1 mg/round and for the HE rounds 11,000 mg/144 rounds or 76 mg/round. The largest estimated average mass of NG lies within the first 5 m downrange of the firing position, with the remaining areas containing an order of magnitude less additional NG. For Pad 1 (TP), 92% of the estimated total NG was in the 0- to 5-m SU (42% of total pad area), 7.8% in the 5- to 9-m SU (34% of pad area), and 0.058% in the 9- to 11.5-m SU (24% of pad area). For Pad 2 (HE), 98% of the estimated total NG was in the first 5 m (34% of pad area), 1.7% in the 5- to 10-m SU (37% of pad area), and 0.04% in the downrange transect (29% of pad area). Although the SUs are not equal in area, looking at the NG deposition rates based on mass per unit area shows that, in the 0- to 5-m SU, deposition rates are 7.2 and 260 mg/m² for the TP and HE pads respectively, 0.76 and 4.1 mg/m² for the center SU, and 7.6×10^{-3} and 0.13 mg/m² for the downrange SU. Three points are not sufficient to derive a formula for the gradient, but the data indicate a power relationship with distance from the firing position.

The solids masses on the filters from the 0- to 5-m sampling units were substantial, so we weighed them (Table 2-4). The mass of solids recovered from the 0- to 5-m SUs of the two pads differed substantially. The following masses are normalized to a sampled area of 0.40 m². For the TP rounds, 1.6 g of residues on average was filtered from each sample. For the HE rounds, 0.77 g of solid residues was filtered from each sample. Thus, Pad 2 (HE) yielded 44% as much solid residues as Pad 1 (TP). We weighed the remaining debris on the filters, following solvent extraction of the filters, to obtain the mass of the insoluble debris. For the three filters from the triplicate samples taken from Pad 1 (TP), the insoluble debris weighed

0.78, 0.55 and 0.55 g. There was very little insoluble debris remaining on the Pad 2 filters. We weighed only the debris from the median-weight filter. This filter contained only 0.12 g of material.

Table 2-3. NG Residue mass for test sampling units.

Sampling unit (SU)*	SU area (m ²)	Sampled area [†] (m ²)	Replicates	Est. avg. mass NG (mg)	NG mass in SU
<i>Pad 1 (40-mm TP Rounds)</i>					
0 to 5 m*	36	0.40 (1.1%)	3	250	92%
0 to 5 m**	36	1.5 (4.2%)	1	290	—
5 to 9 m	29	0.40 (1.4%)	3	22	7.9%
9 to 11.5 m	21	0.40 (1.9%)	3	0.16	0.06%
Total for Pad 1	87	5.1 (5.9%)		270	—
<i>Pad 2 (40-mm HE Rounds)</i>					
0 to 5 m	38	0.41 (1.1%)	3	11,000	98%
0 to 5 m**	38	1.9 (5.0%)	1	7000	—
5 to 10 m	41	0.48 (1.2%)	3	170	1.5%
10 to 13.5 m	32	0.40 (1.2%)	3	4.1	0.04%
Total for Pad 2	110	5.8 (5.3%)		11,000	—

*Distance from Firing Position.
** Taken with 20-cm scoop. Not counted in averages.
† Average sampled area of replicates. Percentage is of sampling unit area sampled.

Table 2-4. Filter mass components.

Sample	Total mass on filter (g)	Mass of debris* on filter (g)	Propellant mass on filter (g)	Percentage propellant on filter	Percentage debris on filter
<i>Pad 1 (40-mm TP Rounds)</i>					
0 to 5 m Rep 1	1.9	0.78	1.1	58	42
0 to 5 m Rep 2	1.5	0.55	0.94	63	37
0 to 5 m Rep 3	1.5	0.55	0.98	64	36
Average Values	1.6	0.63	1.0	62	38
<i>Pad 2 (40-mm HE Rounds)</i>					
0 to 5 m Rep 2	0.77	0.12	0.65	84	16

*Insoluble debris remaining after solvent extraction process.

The original NG loads for the TP and HE munitions are 370 and 900 mg respectively. The calculated propellant residue deposition rate for NG is 8.4% (76/900) of the original propellant NG load for the HE rounds (M2

propellant) and 0.59% (2.2/370) of the original NG load for the propellant for the TP rounds (F15080 propellant). The NG percentage value for the TP rounds was very low compared to the results of past experience and the results of analysis of the HE round residues, but it agrees well with the NG analyses of propellant grains recovered from trays placed in front of the gun muzzle for the TP firing test. We also analyzed the TP firing point residues for Akardite II, a component of the F15080 propellant, to verify the mass quantities we were estimating. Approximately 950 mg of Akardite II were estimated to have been deposited from the residues recovered from the 0- to 5-m section of the test pad and 80 mg from the 5- to 9-m section of the pad (Appendix B). These values correspond to a concentration of 9.1%, within range of the propellant formulation. From this, we can conclude that the masses of residues estimated for the tests are valid (see Section 2–7).

Quality control procedures were conducted to verify the procedures and supplies used to obtain the results of our analyses. Laboratory and process control spikes and blanks were analyzed and the data indicates that these processes did not contribute significant error to the results. Neither of the filtered water blanks processed at the field lab contained detectable levels of NG. Four solid phase extraction blanks were run using fresh Waters Porpak RDX cartridges and filtered water. When eluted, no NG was detected in the filtrate, indicating no analyte contamination in the process. Lab control spikes (0.002 mg/L) indicated a recover rate of 90–95% for three runs.

2.6 Discussion

The estimated NG deposition rates for the TP and HE rounds tested were 0.59 and 8.4% of the original propellant loads, respectively. In developing these estimates, we did not use the 20-cm scoop samples from the 0- to 5-m SUs because of the difficulty in sampling in a systematic way in the areas. The triplicate samples taken with the 10-cm scoops had very good agreement in the 0- to 5-m SUs, where 92 to 98% of the residual NG was recovered (Tables 2–3 and Appendix Table B-2). In these areas, the RSD for the replicate MIS data are 2.0% for the TP rounds and 5.4% for the HE rounds. In other areas where the deposition rate is not as high, the RSD varies from 2.7 to 54%, the highest being in the furthest downrange SU for the TP test. This area contained less than 0.1% of the total residues for that test.

The disparity between the NG deposition masses of the TP and the HE rounds warranted further investigation. Although the firing of the TP rounds generated more solid residues, the NG deposition rate estimate was significantly lower. Our experience has been that residues typically reflect the chemical composition of the original propellants. A significant difference in NG concentration of the residues thus indicated two different propellants. This is in conflict with the U.S. Army training manual (TM), which states that the propellants for the two different rounds are both the same—M2 (U.S. Army 1994). This TM was our original source of information on propellant types for the rounds.

The first indication that the propellants for the two munitions actually differed was the physical appearance of the unconsumed grains recovered from the samples. The size, color, and quantities of the residues were all clearly different. The solid residues on the filters from the three samples taken in the 0- to 5-m SUs with the 10-cm scoops were analyzed for NG (Table 2-4). Initially, we hypothesized that the solids on the filters were composed of 85% propellant residues and 15% insoluble debris. Much less NG was recovered from the residues of the TP rounds than from the residues from the HE rounds. The initial results from the analyses of the HE propellant residues were within the range of the published specification on M2 propellant if the mass of solid residues is around 85% propellant. The analytical method seemed to be functioning, so we continued to look into the TP propellant because it did not appear to be the M2 propellant specified in the TM.

A check of the ammunition lot numbers and ammunition data cards showed that the propellants were not the same for the two types of cartridges. The HE rounds contained the standard M2 propellant, while the TP rounds contained the Swiss-manufactured F15080 propellant (Haeselich et al. 2006). The specifications for the F15080 propellant, given in the European Community Safety Data Sheet (Moor 2006), indicated an NG content of 8–12%, about half that of M2 propellant’s 18.5–20.5% NG content (U.S. Army 2005). Even after taking the lower NG content into account, the estimated residual mass of NG for the TP propellant was still much lower than expected.

Being unfamiliar with this propellant formulation, we felt it was necessary to analyze some of the propellant grains to determine their actual NG content. Ten mostly intact grains were recovered from one of the trays placed

in front of the firing position for the TP test. These grains were weighed collectively (5.2 mg), dissolved in 10 mL of acetonitrile, and two replicates analyzed for NG. A total of 0.025 mg was recovered, corresponding to approximately 0.6% of the original propellant mass. There still existed a discrepancy between what we were seeing in the laboratory ($\approx 0.6\%$) and what the specification for the propellant stated (9.1%). As a result of our observations, we looked further into the propellant formulation and manufacture.

The F18050 propellant is classified as a double-base propellant in some literature and as a single-base extruded propellant with NG impregnation (EI[®] propellant) in others. The NG resides on the surfaces of the grains, penetrating part way into the grains at the outside surfaces and along the perforations (Fig. 2-10). The propellant burns at around 3000 K (2700°C). We hypothesize that the presence of most of the NG on the surface of the grains, the high burning temperature of the propellant, and the highly labile nature of NG will result in more complete consumption of NG than if it were thoroughly embedded within the NC matrix of the grains, as with M2 propellant. In other words, it behaves like a single-base propellant with a surface matrix diffused with readily available NG.

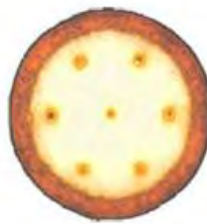


Figure 2-10. Cross-section of an EI propellant grain (Elmasri et al. 2008).

Our test data indicate that a much lower percentage of the original NG remains in the residues of the 40-mm TP round than in the residues of the HE rounds. However, from our analysis of the mass of propellant and propellant residues following firing, much more of the propellant remains after firing TP rounds than HE rounds. Based on our investigations into the physical characteristics of the propellant grains, this is expected, as the TP propellant consists of multi-perforated grains that are known to be inefficiently consumed (U.S. Army 1984). However, the TP residue is mostly NC, which has not been found to be a problem in the environment. We have little information on the Akardite II, a stabilizer component of the

propellant (<2%), other than it has very low water solubility. This low solubility combined with the stability of the NC matrix within which it is embedded, and the low mass present within the propellant, leads us to hypothesize that it will not be a concern to the environment. The toxicity of the compound is not known, however, and a final determination of its impact on training ranges cannot be known at this time.

We used the 0- to 5-m SU results to estimate the amount of propellant residue deposited from firing the two munitions. For the HE rounds, an average of 0.65 g of propellant was contained in the 0.42-m² samples. Extrapolated over the 38-m² SU, we estimated about 60 g of propellant after firing 144 rounds. This correlates well with the 8.4% recovered NG for the M2 propellant. For the TP rounds, the corresponding estimate was over 90 g of propellant from firing 127 rounds. Extrapolated over the whole test pad, this is over 19% of the original F15080 propellant load for the round, which does not correlate well with the NG residues for this round. Because the NG resides on the surface, the single-base core of the propellant grain is what mostly remains in the residues. A better confirmatory indicator for the F15080 residue mass is the stabilizing compound Akardite II, found throughout the propellant. The mass of Akardite found in the propellant grains recovered from the tray in front of the gun was 0.060 mg, 1.1% of the total mass (5.2 g) of the grains. The specification calls for 0.9 to 1.2%. For the 0- to 5-m area for the TP tests, a mean of 9.1 mg of Akardite II was recovered from a mean of 1 g of unconsumed propellant, corresponding to a concentration of 9.1% in the propellant residues, again within specifications. The total estimated mass of Akardite II deposited on the test pad was a little over 1 g, which corresponds to 19% of the initial mass contained in the cartridges fired for the test. This agrees well with the rate derived from the sample mass calculations above.

We have found in the past that weapon systems that have longer barrels, rifled barrels, or larger propellant loads, generally have a lower percentage of their propellant deposited as residues. This is likely attributable to the higher temperatures and pressures generated in these types of armaments. By contrast, short-barreled guns, such as mortars and the Mk19, are likely to have higher residues mass deposition rates. The Mk19 machine gun firing the 40-mm HE grenade cartridge is not a clean firing weapon system. Table 2-5 summarizes the results of testing we have done with the Mk19, man-portable rockets, mortars, howitzers, a tank, and small arms. The da-

ta are presented in rough order of the percentage of the analyte not consumed per round fired. The 40-mm HE grenades rank near the top.

Table 2-5. Comparison of various firing point analyte loads.

Weapon System	Propellant	Analyte	Analyte / round (g)	Residues*/ round (mg)	Residues*/ original load (%)
Shoulder-fired Rockets					
84-mm Carl Gustav ³	AKB 204	NG	140	20,000	14
66-mm LAW ⁴	M7	NG	22	42	0.1
84-mm AT	AKB 204	NG	130	95,000	73
Medium-caliber Weapon Systems					
40-mm (HEDP)	M2	NG	0.90	76	8.4
40-mm (TP)	F15080	NG	0.37	2.2	0.59
Mortars					
81-mm	M9	NG	30	1000	3.5
120-mm	M45	NG	26	350	1.4
Small Arms					
5.56-mm Rifle	WC844	NG	0.16	1.8	1.10
5.56-mm MG ¹	WC844	NG	0.16	1.3	0.79
7.62-mm MG	WC846	NG & DNT	0.27	1.5	0.56
9-mm Pistol	WPR289	NG	0.040	2.1	5.44
12.7-mm MG ¹	WC860 & WC857	NG	1.5	11.	0.73
Leopard Tank²					
105-mm (MIS)	M1	DNT	300	6.7	2.2×10^{-3}
105-mm (Trays)	M1	DNT	300	7.8	$2.7 \times 10^{-3}\%$
Howitzers					
105-mm	M1-I & II	DNT	42	34	$8 \times 10^{-2}\%$
155-mm	M1	DNT	275	1.2	$5 \times 10^{-4}\%$

* Analyte residues (Estimated).

¹ Average loads and residues from ball and tracer rounds in linked ammunition.

² Preliminary results. (Ampleman et al. in prep).

³ Thiboutot et al. (2008a).

⁴ Thiboutot et al. (2008b).

What are the implications of this research for the range manager or the soldier on the training range? For every 100 TP rounds fired, over 60 g of NC will be deposited less than 5 m from the barrel of the gun. This is more propellant than is contained in 17 live rounds. For a vehicle-mounted weapon system, this may become a serious fire hazard. On a heavily used, fixed-position firing range, the same hazard may be present.

A laboratory test conducted by Dr. Susan Taylor is underway at CRREL to determine the environmental leaching rate of NG from propellant residues as collected from the trays in front of the gun positions during the firing point tests for the study reported here. Past experience indicates that NG leaches readily from surfaces and from the edges of NC-based propellant residues. When these surfaces are depleted, the leaching rate slows significantly, and NG may remain within the NC propellant matrix for over 30 years. For small-volume propellant residues such as from the 40-mm tests, most NG will likely leach out quickly because of the high surface-to-volume ratio and the presence of many edges. If the NG remains stable within the residues, there will eventually be a range hazard. If it leaches out, there will be a groundwater contamination problem. Either case warrants attention from the range community.

2.7 Conclusions

Training with the Mk19 machine gun using the M430 40-mm HE cartridge will result in moderate deposition and accumulation of nitroglycerin-containing residues in the first 5 m in front of the firing position. Our tests indicated that about 8% of the propellant and NG are not consumed during firing of the weapon. The Mk281 40-mm TP cartridge leaves more unconsumed propellant, but significantly less NG (0.59% of the bulk mass) at the firing position owing to the presence of the NG on the propellant grain surface. On 40-mm ranges with fixed firing positions, the propellant residues from both types of rounds may build up to hazardous levels over time, an issue that will have to be addressed by range managers. Furthermore, leaching of NG from the unburned propellant may cause a groundwater contamination problem. For mounted weapon systems, the presence of the propellant residues may constitute a fire hazard.

3 Propellant Residues Emitted by Triple Base Ammunition Live Firing using a British 155-mm Howitzer Gun at CFB Suffield, Canada

Guy Ampleman, Sonia Thiboutot, André Marois, Annie Gagnon, Michael Walsh, Marianne Walsh, Charles Ramsey, and Pierre Archambeault

3.1 Summary

Current research indicates that propellant residues accumulate at firing positions and represent a concern for the environment and human health. To better understand the impacts of live-fire training on firing positions, a series of tests was conducted to measure the deposition of propellant residues from many sources. Most of these studies were done to look at the deposition of 2,4-DNT from single-base M1 propellant or nitroglycerin (NG) from double-base propellants. The study described in this chapter is the first conducted with ammunition utilizing triple-base propellant containing nitroguanidine (NQ). Before this work, nothing was known about the deposition of triple-base propellant residues resulting from training activities; because NQ is water soluble (4.4 g/L at 25°C, 8.2 g/L at 100°C), it may represent an environmental issue. This trial was carried out at Canadian Forces base (CFB) Suffield by Defence Research and Development Canada–Valcartier (DRDC Valcartier) with the help of the British Army Training Unit Suffield (BATUS), who supplied materials and military personnel, in collaboration with Cold Regions Research Engineering Laboratory (CRREL) and Envirostat, who sampled soils between firings and conducted the propellant burn tests.

This study was conducted in June 2009 with ammunition fired from a 155-mm British howitzer artillery gun using three different triple-base propellant loads. At the firing position, the DRDC setup consisted of half-circles of particle traps distributed 5, 10, 15, 20, 30, 40, 50 and 60 m in front of the muzzle of the gun. Eleven particle traps were also placed around the dug-in gun position. This allowed collection of the residues deposited directly in front and beside the gun. Distilled water was poured inside the

traps to contain the particles emitted during firings. A total of 79 rounds were fired in three series. The first series consisted of 30 L8 high-explosive (HE) rounds fired at charge 5, followed by a second series of 30 L8 HE rounds at charge 3. The last series consisted of firing 19 L10 inert rounds at full charge. After each series of firings, all particle traps of each row were combined and the water was poured into separate pails. From each of these pails, 1 L of water was collected and poured into separate jars to verify if NG was adsorbed in the plastic of the pails. Results indicated that NG was not adsorbed on plastic. In addition, five replicate, multi-increment soil samples were collected between the DRDC traps by CRREL in a 30- × 40-m area in front of the gun before and after each series. Furthermore, multi-increment soil samples were collected before and after each series of firing between the DRDC Traps to represent the areas between 0–30 m and 30–60 m. Results from the DRDC sampling indicate that firing 155-mm howitzer gun triple-base ammunition leads to the accumulation of solid propellant residues in the vicinity of the gun at $0.59\text{--}3.1 \times 10^{-5}\%$ by weight of unburned NG and $0.62\text{--}4.4 \times 10^{-5}\%$ of NQ, most of which are deposited within 10 m of the gun. CRREL samples indicated no detectable NG ($<0.4 \text{ mg/m}^2$) or NQ ($<40 \text{ mg/m}^2$) deposition within a 30- × 40-m area for any of the trials. No detectable NG or NQ were detected in any of the 0–30 and 0–60 m samples.

At the end of the firing trials, field-expedient disposal of excess propellant trials were conducted. Four burnings were conducted using two sets of four charge 7 bags and two sets of six charge 4 bags. Results from these open burning experiments indicate that NG and NQ were found in all samples. NG was found at levels varying from 0.006–0.0027% while NQ levels varied from 0.008–0.002%. The most efficient burns were obtained with charge 7.

3.2 Introduction

For many years, Defence Research and Development Canada—Valcartier (DRDC Valcartier) has been evaluating the environmental impacts of the live-fire training to characterize and mitigate adverse effects on training ranges and thereby sustain ongoing military activities (Jenkins et al. 2007; Pennington et al. 2006a, b, c; Jenkins et al. 2006b; Pennington et al. 2005). Over the years, many efforts were made to assess the environmental loading of explosives at most of the Canadian Forces bases (CFB). To date, these efforts have addressed mainly heavily used target areas (Ampleman et al. 2009c; Brochu et al. 2008; Diaz et al. 2007; Thiboutot et al.

2007a; Ampleman et al. 2004; Thiboutot et al. 2004; Marois et al. 2004; Pennington et al 2004; Ampleman et al. 2003; Thiboutot et al. 2000; Ampleman et al. 2000).

Many of these studies were conducted in collaboration with the U.S. Army Engineer Research and Development Center's Cold Regions Research and Engineering Laboratory (CRREL) in Hanover, NH, and Environmental Laboratory (EL) in Vicksburg, MS (Jenkins et al. 2006b; Pennington et al. 2006b; Pennington et al. 2005; Pennington et al. 2004; Jenkins et al. 2005a; Pennington et al. 2003; Pennington et al. 2002; Pennington et al. 2001). Walsh, M.E., et al. (2001) observed that firing points were also experiencing a build-up of energetic residues, and, since then, many studies have been dedicated to characterizing firing points and positions (Pennington et al. 2002; Jenkins et al. 2001; Ampleman et al. 2007; Ampleman et al. 2008; Thiboutot et al. 2007b; Jenkins et al. 2006a).

This research determined that nitroglycerin (NG) or 2,4-dinitrotoluene (2,4-DNT), or both, embedded in the nitrocellulose-based propellant fibers are deposited in front and around firing positions (Ampleman et al. 2004; Walsh, M.E., et al. 2001; Jenkins et al. 2001; Ampleman et al. 2007; Ampleman et al. 2008; Thiboutot et al. 2007b; Jenkins et al. 2006a).

Moreover, it is a common practice in the U.S. and in Canada to burn, directly on the ground, excess (unused) propellant bags that are removed from the munitions to adjust the ballistic parameters. Burning on the ground leads to incomplete combustion of the propellants, resulting in high concentrations of propellant compounds on the soils. This burning practice was assessed by DRDC Valcartier tasked by Director Land Environment and a burning table has been constructed and tested under the Strategic Environmental R&D Program. The burning table will be implemented in 2011 based on the good results obtained with it.

Four years ago, DRDC Valcartier assessed the dispersion of propellant residues following 105-mm artillery and tank gun firings at CFB Valcartier by placing aluminum witness plates in front of the muzzles of the guns (Dubé et al. 2006). At CRREL, similar trials were conducted using snow as a collection media (Walsh, M.R, et al. 2005b; Walsh, M.E., et al. 2004). These studies demonstrated that propellant residues composed of nitrocellulose fibers containing 2,4-DNT were deposited in front of the muzzle of artillery guns, but in a similar test, no residues were found after firing tank ammunition in Valcartier (Dubé et al. 2006). The conditions being not

ideal in Valcartier, the trial was repeated in CFB Gagetown (Ampleman et al. 2007). During the trial in Gagetown, no residues were detected in any of the particle traps in front of the tank, but we realized that our setup was not adequate. We concluded that the experiment would have to be repeated. This was done and the study indicated that 2,4-DNT is deposited 20–25 m in front of the tank (Ampleman et al. 2009a). Particle traps and snow cover collection were used in this study and results from both collection methods were compared (Walsh, M.R. et al. 2007b). It was found that firing 105-mm tank gun ammunition leads to the accumulation of solid propellant residues in the vicinity of the gun at 0.0026% by weight of unburned 2,4-DNT. Similar results were obtained by both methods, confirming the validity of these results. Finally, Walsh, M.R. et al. (2006a) studied residues at mortar firing positions and found NG at elevated concentrations for 81-mm mortars.

Although extensive research has been done and indicated that propellant residues accumulate at firing positions and represent a concern for the environment and human health, the deposition of triple-base propellant residues during live fire events had not been studied. Triple-base propellants are composed of nitrocellulose, nitroglycerin and nitroguanidine (NQ). Nitroguanidine is a colorless crystalline solid that melts at 232°C and decomposes at 250°C. It is not flammable and is an extremely low sensitivity explosive; however, its detonation velocity is high. Nitroguanidine is manufactured from guanine that is oxidized to guanidine (Strecker 1861). Guanidine is then nitrated to form nitroguanidine.

Another laboratory synthesis involves preparing guanidine nitrate by reacting dicyanodiamide with ammonium nitrate. The guanidine nitrate is then dehydrated to nitroguanidine (Gilman and Blatt 1941). Nitroguanidine is used in smokeless propellants to reduce the propellant's flash and flame temperature without sacrificing chamber pressure. Nowadays, the interest in nitroguanidine as an insensitive explosive ingredient is growing. Considering that nitroguanidine and its derivatives are also used as insecticides and considering that it is water soluble (4.4 g/L at 25°C, 82.2 g/L at 100°C) (McBride et al. 1951) and may travel long distances in groundwater, NQ is a potential environmental issue in our training areas. Nitroguanidine derivatives classified as nitroguanidine nicotinoid insecticides include clothianidin, dinotefuran, imidaclothiz, imidacloprid and thiamethoxam. These derivatives raise questions as to the environmental impact of this compound, especially owing to their potential groundwater

mobility, which is why it became important to get data on the deposition of triple base propellant residues.

Because triple-base propellants are more powerful, they are typically used in large-bore guns such as the 155-mm howitzer, the 120-mm gun of the British Challenger tank, and larger gun propellant charges where barrel erosion and flash are particularly important. Triple-base propellants are also found in 105-mm Armor Piercing Fin Stabilised Discarding Sabot (APFSDS) tank ammunition. For large caliber guns using triple-base propellants, a large safety template (fan) must be put in place in ranges to allow the use of these weapon platforms. The main problem encountered in our search for a location to conduct triple-base propellants trials was that most the Canadian Forces bases are not large enough to contain such a large template. The only suitable training area for these weapons in Canada is CFB Suffield. The British Army is training in CFB Suffield and upon negotiations and collaboration between Canada and United Kingdom, it was agreed that Canada would help UK to characterize the Otterburn training area in the UK, and, in exchange, the British army supplied DRDC Valcartier with the 155-mm howitzer gun, gun crew and ammo to conduct a study with the triple-base propellants.

This is the first firing point deposition study conducted using triple-base propellant ammunition fired from an artillery gun. Before this work, nothing was known about the deposition rate of triple-base propellant residues resulting from live firing training. Moreover, it is known that excess bags are burned following artillery exercises. Following the firings, we conducted open burning of some excess bags to analyze the residues generated by the burning of triple base propellants. This was never done before and also brought interesting data.

This chapter describes the June 2009 trial conducted at CFB Suffield, the sampling strategy, the laboratory procedure, and the results obtained from the deposition of triple-base propellant residues during a complete live-fire training activity. This work was co-funded by the Thrust Sustain from Defence Research and Development Canada and by the Strategic Environmental Research and Development Program of the U.S. through project ER-1481.

3.3 Background

3.3.1 Logistics

The trial was conducted in June 2009 at CFB Suffield by DRDC Valcartier and CRREL in collaboration with the BATUS. After months of preparation and negotiations, the UK MOD agreed to supply a 155-mm artillery self-propelled howitzer (SPHz) with a gun crew and 80 rounds of ammunition to study the deposition of triple-base propellant emitted during a firing exercise designed by DRDC. Particle traps used in the DRDC study were shipped to CFB Suffield by DRDC Valcartier, the distilled water necessary for the study was supplied by DRDC Suffield, and the rest of the sampling material was brought on-site by the respective scientists. The self-propelled howitzer was used to fire 60 rounds with L8 propellant and 19 rounds with L10 propellant. It was not possible to fire all the 20 rounds at full charge as we experienced a gun breach during the firing of round 19 and it was decided to end the trial there.

3.3.2 Equipment and munitions

The current British in-service 155-mm SPHz is the L131 (Fig. 3-1) developed by the Artillery System for the 90s (AS 90) program. It is a fully tracked, self-propelled gun carrying a crew of five, consisting of the commander, a driver, a gun layer and two loaders. The gun is turret mounted with a 360° arc of fire and may be elevated from -5° to +70° (Fig. 3-2).



Figure 3-1. British L131 (AS90) Braveheart 39-caliber 155-mm howitzer self propelled gun.



Figure 3-2. 155-mm Howitzer L131 setup at firing position.

A 7.62-mm L7A2 GPMG may be mounted on the air sentry cupola and the vehicle is fitted with multi-barrel smoke dischargers. A total of 48 projectiles and propelling charges are carried in the vehicle, of which 31 projectiles are held in the magazine module located in the turret bustle. The remaining 17 projectiles are stowed in brackets within the confines of the fighting compartment. The bag charges are stowed in containers located in the turret and fighting compartment. A transfer arm is used to move projectiles from the magazine module to the hydraulically operated loading tray, which incorporates a power rammer. The AS 90 is fitted with a 39 caliber barrel giving a maximum range of 24.7 km. When equipped with a 52 caliber barrel, the maximum range is 30 km with standard charges.

The L131 (AS 90) is capable of firing both the M107 and L15 systems of ammunition; the older M107 system is retained primarily for training. Our study utilized the L15 system of ammunition that uses different projectiles and propellant charges: 60 rounds were equipped with HE L15 projectiles (Fig. 3-3) and 20 were equipped with the L17 inert/practice projectile (Fig. 3-4).



Figure 3-3. Shell of the 155-mm HE L15.



Figure 3-4. Shell of the 155-mm Practice Inert L17.

To fire these projectiles, different propelling charges are available, mainly Charge Propelling 155-mm L2A1 (charge 1–2), L8A1 (charge 3–7), L8A2 (charge 3–7), L10A1 (charge 8), and Charge Blank 155-mm 3 lb Mk1. Our trial used only propellant charges L8A1 and L10A1 in conjunction with HE L15 and inert L17 projectiles respectively (Fig. 3-3 to 3-6). The Charge

Propelling 155-mm L8A1 (charge 3-7) (Fig. 3-5 and 3-7) is a bag charge with a maximum length of 780 mm and a maximum diameter of 152 mm. It is made up of a Base Charge in the form of a closed, cylindrical bag that contains several additional charge bags that form the base charge bag (Fig. 3-7). There are up to seven charge increments in the L8A1, and different loading can be done to achieve specific firing distances by removing specific increments, starting with the highest numbered charge (charge 7). Once the increments are completely removed, only the main bag (charge 3) remains, which is made of the combustible case tube that contains 1.39 kg of N M06 gun propellant.



Figure 3-5. Propellant charge L8 A1.



Figure 3-6. Propellant charge L10 A1.

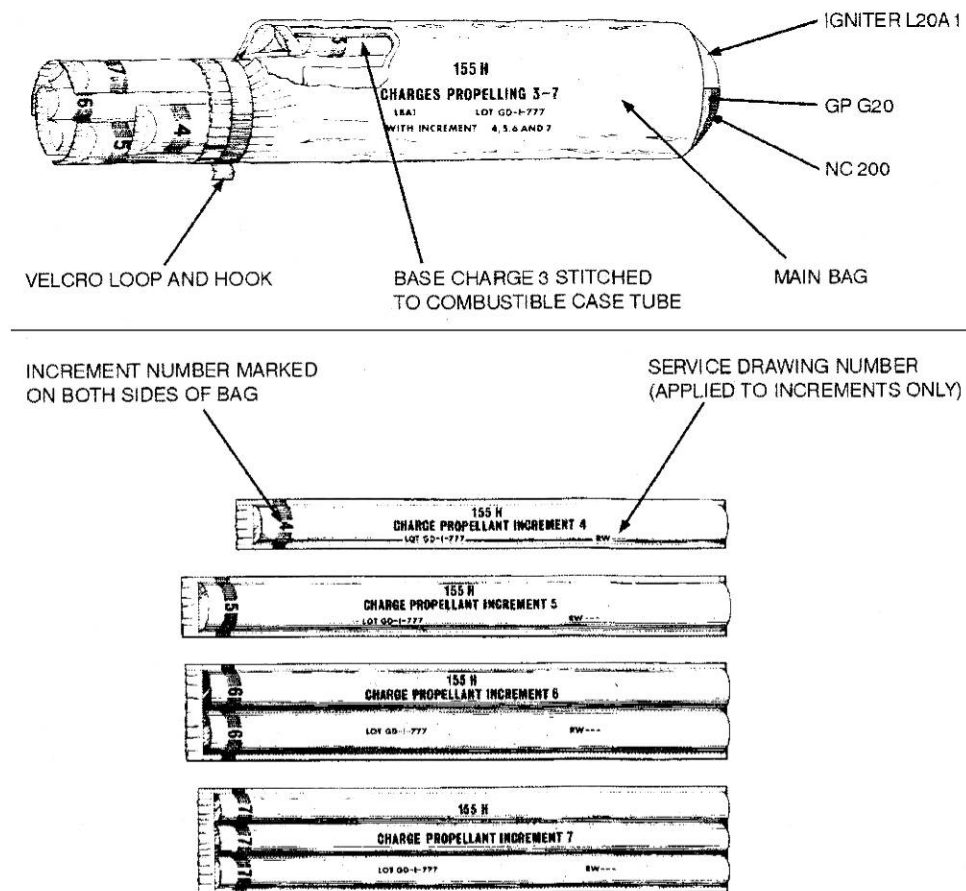


Figure 3-7. Schematic of the L8A1 propellant charge.

The 155-mm propelling charge L10A1 is a fixed charge that provides charge 8 and is used only for the L15 ammunition system (Fig. 3-6). The charge comprises a charge assembly, a combustible case, an end cap, and an L23A1 igniter (Fig. 3-8). The charge assembly consists of 12.25 kg of NBQ 2P/S propellant in a bundle format. The assembly is made in two stages: the propellant bundle, less the outer layer of propellant sticks, is tied in three places with polyester and cotton thread ties. The bundle is then wrapped in lead foil (a de-coppering agent) over the majority of its length, with the foil being secured by a further two ties. The second stage is the placement of the outer layer of propellant sticks and the tying of the bundle in five places, again using polyester and cotton thread ties. The combustible case is manufactured mainly from nitrocellulose and other combustible materials. The end cap is made of a combustible material (Nitrocellulose, etc.) and houses the L23A1 igniter. Table 3-1 shows the type, masses, and composition of each of the propellants in the increment bags making up the L8A1 and L10 A1 propellant charges.

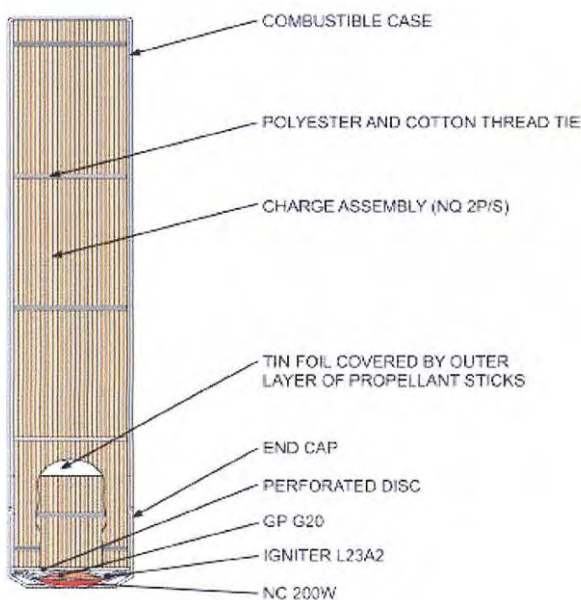


Figure 3-8. Schematic of the L10A1 propellant charge.

Table 3-1. Technical data for 155 mm charge propelling L8A1 and L10A1*

Charge and name	Propellants type and weight (g)	Mass (g) and Color **			
		NC	NG	NQ	Color
L4A1 RW498GF Charge 3	N M06 (1390)	262.8	259.7	760.6	BG
RW63AF Charge 4	N M06 (592)	111.9	110.2	323.9	O
RW73AF Charge 5	N/S M34-10 (1560)	295.0	290.3	853.6	G
RW69AF Charge 6	N/S M34-10 (2420)	457.6	450.4	1324.3	V
RW70AF Charge 7	N/S M34-10 (1490)	282.8	277.3	815.3	B
L10A1 RW532GF Charge 8	NBQ 2P/S (12250)	2316.5	2279.7	6703.2	Br

* Ammunition studied in this report, L8A1 (charge 3 to 7), L10A1 (charge 8).

** Increment Bag color: BG (Blue Grey), O (Orange), G (Green), V (Violet), B (Beige) Br (Brown).

The literature indicated that most of the triple-base propellant formulations, including those of Table 3-1, contain approximately the same amount of NC, NG and NQ (Stiefel and Summerfield 1988). The typical formulation is 18.91% NC, 18.61% NG, and 54.72% NQ, the rest being the stabilizer ethyl centralite and other inorganic salts. The different number and letters used for the propellant types differentiate the composition or geometry of the propellant or the charge. As an example, P means that potassium sulfate was used as a flash inhibitor in the charge whereas S means the propellant fibers are. According to discussions with Munitions

Safety Information Analysis center (MSIAC) and UK MOD personnel, the formulations used in our trial were all triple base containing 55% NQ. Percentages from the literature were used for our calculations in these tests. Table 3-2 shows the total masses of propellant that were used during our trial. From these masses were derived masses of NG and NQ that may disperse residues in the environment following the firings.

Table 3-2. Total masses of NG and NQ fired during the trial.

Series	No. of rounds	Total mass (kg)	Mass of NG (kg)	Mass of NQ (kg)
Series 1: Charge 5	30	106.26	19.77	58.15
Series 2: Charge 3	30	41.70	7.76	22.82
Series 3: Charge 8	19	232.75	43.31	127.36

3.4 Experimental

3.4.1 Test setup

In June 2009, DRDC Valcartier, in collaboration with CRREL, visited the British Army Training Unit Suffield at CFB Suffield to evaluate the dispersion and mass of residues deposited by the live firing of munitions utilizing triple base propellants. The British Ministry of Defense (MOD) supplied our team with an L131 self-propelled howitzer, a gun crew, and 80 triple base munitions for our trial. When we arrived on-site, the howitzer was already installed in a well-used firing pit gun position behind a small berm. A total of 80 rounds including 60 rounds having a High Explosives (HE) projectile equipped with a propellant charge L8, and 20 rounds having an inert projectile equipped with a propellant charge L10 were provided for a series of three test firings. The gun elevation was set at 35° angle from the ground. The speed of the wind was constant for the entire trial and was roughly 0–3 km/hr.

The first firing series consisted of 30 L8 rounds fired at charge 5 followed by a second series of 30 L8 rounds at charge 3. The last series consisted of firing 19 of the 20 L10 rounds at full charge. One L10 round was not fired because of a breech explosion of the gun during the firing of the 19th round. Prior to the commencement of firing, a baseline soil sample was taken. Particle deposition samples were taken following each firing.

3.4.2 Sampling strategy and nomenclature

3.4.2.1 Particle trap method

Prior to firing, DRDC installed residues collectors adjacent to and in front of the gun position. The setup consisted of arcs of particle traps placed 5, 10, 15, 20, 30, 40, 50 and 60 m in downrange of the gun muzzle (Fig. 3-9 and 3-10). Eleven particle traps were also placed on the surrounding sand berm where the gun was located (Fig. 3-11 and 3-12). These are called “gunside” locations. This allowed the collection of the residues directly deposited in front and beside the gun. Distilled water was poured inside the traps to improve the adhesion of the particles emitted during firings and also to contain them in the traps. The 56 traps located along the arcs were placed at the specified distances and locations using an observer standing at the muzzle of the gun who called out placement locations to the field crew. Traps were placed according to the setup map, with seven traps along each arc. The distance between the traps at the end of the 60-m arc was 34 m (Fig. 3-9). The inclusive segment of the sampling decision unit had an angle of 33°. This angle was used to calculate the area between the rows where the particles were collected. Metal holders were used to stabilize the traps against the muzzle blast in the first three rows and directly in front of the gun (Fig. 3-10, 3-12, and 3-13).

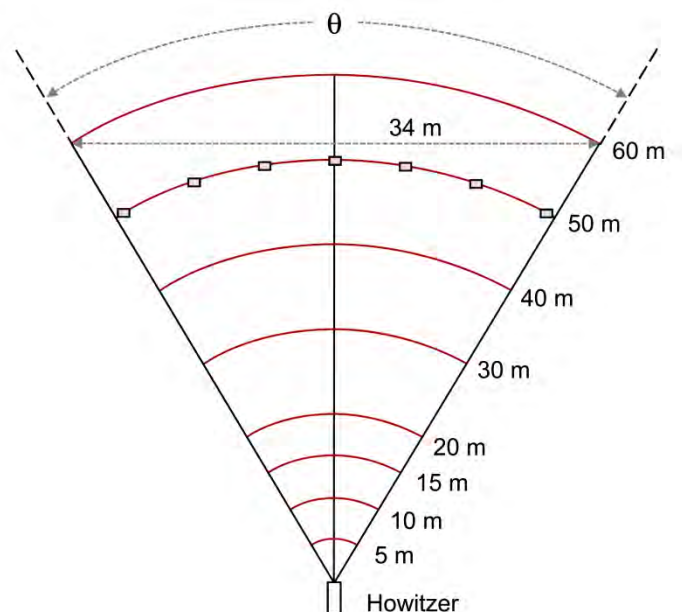


Figure 3-9. Half-circle setup of trays in front of the gun. Seven traps were installed along each arc, shown schematically on the 50-m arc.

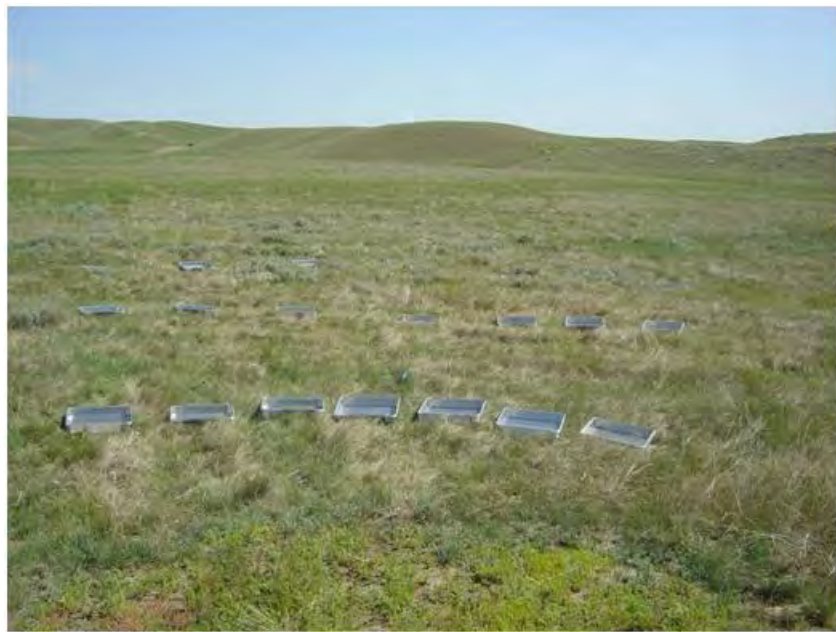


Figure 3-10. Particles traps setup in front of the gun.



Figure 3-11. Particles traps beside the gun.



Figure 3-12. Gunside particles traps.



Figure 3-13. Particles trap in holder.

At the end of each firing series, the particle traps of a specific row (arc) were combined to represent what was expelled at that specific distance. These samples were labeled according to the firing event, 1 to 3, one being the first series, etc. The second number gives the distance of the row. For example, all samples numbered 1-10m indicate samples collected following the first series of firing along the 10-m arc. This was repeated for each

row. Samples collected from the perimeter of the gun pit were also delineated according to the firing series and were named 1-gunside, 2-gunside, etc. One pail was used for the gunside traps following each firing. No bottles were used for these samples. Two types of samples were collected by DRDC, water samples in bottles and pails, described above, and soil samples. The water samples were named WB for water bottles and WP for water pails; the designation S was used for soils. This nomenclature was used in conjunction with the firing series and row or gunside labels to delineate the samples. In some cases, soil was kicked up into the traps by the muzzle blast. This soil was also collected for analysis and further delineated with an "ST" for soils in traps. From each of the pails used for the water trap collectors, 1 L of water was collected and poured into separate jars. This was done to test if nitroglycerin was adsorbed by the plastic of the pails. This resulted in samples collected from eight pails and eight water bottles for each series. At the end of the trial, 27 pails and 24 bottles were brought back to DRDC Valcartier for analyses.

3.4.2.2 . Soil collection method

In addition to the work performed by DRDC, researchers from CRREL and Envirostat collected soil samples in a parallel effort to determine triple-base propellant deposition rates for the firing of 155-mm projectiles utilizing different propellant loads. Random, systematic, replicate multi-increment sampling was used throughout the trials, concentrated on intensive sampling in a limited area in front of the gun. The self-propelled howitzer was dug into the firing position with the end of the cannon extending to the top of the berm formed in front of the site (Fig. 3-14). Rather than sample downrange transects, which DRDC Valcartier was doing, CRREL concentrated on intensive sampling in a limited area in front of the gun. Past experience with large-caliber weapon systems indicates that this is where the highest concentration of residue will occur. The decision unit (DU) extended from approximately 1 m up-range from the howitzer muzzle to 29-m down-range of the muzzle and 20 m on either side of the line of fire for a DU area of 1200 m² (Fig. 3-15). The area was grassy prairie with well-compacted, cohesive soils containing few small stones (Fig. 3-16). The DU was divided into 10 lanes traversing the line of fire with 11 cells in each lane.



Figure 3-14. Gun setup at firing position.

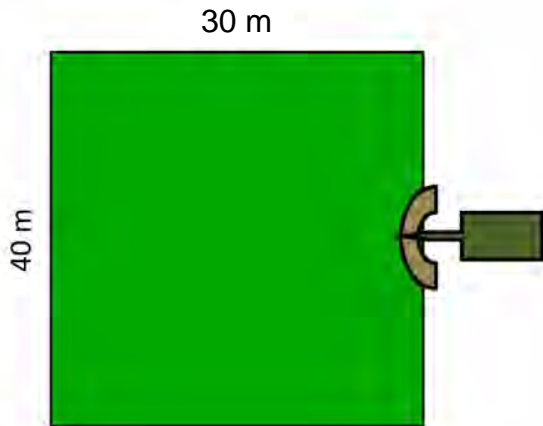


Figure 3-15. Firing point sampling decision unit configuration.

Five multi-increment (MI) samples of the well-used site were taken within the DU prior to firing to establish a baseline for the upcoming activity. Following each series of firing, five MI samples were taken from the same DU (Fig. 3-17). Samples were taken from each cell with the CRREL multi-increment sampling coring tool, using the 3-cm diameter bit and set to 1.5-cm sampling depth. The corer was set at a shallow depth to capture the newly deposited residue from the 155-mm howitzer. The sampling position in the first cell was randomly chosen and these positions repeated for all additional cells, creating a systematic, random, multi-increment sampling approach.



Figure 3-16. View of decision unit from downrange towards gun emplacement (up-range).



Figure 3-17. Sampling of firing point following the firing of the final projectiles.

In all cases, samples were built with over 100 increments. Samples were collected in clean polyethylene bags; the test number, number of increments, and sampler's initials were written on the bag. The bag was then closed with a tie-wrap that also held a tag containing the sample information. When completed, the sample bag was placed within a second, larger,

clean polyethylene bag to prevent cross-contamination while being transported to the lab.

In addition to these soil samples, 16 systematic, random, multi-increment soil samples were collected to represent the 0–30 m and the 30–60 m area between the DRDC traps in front of the gun position (see Appendix C, Table C-1 for a listing and results). This was done before the firings started and after each series of firings to verify if it was possible to measure residues on such large areas and also to confirm CRREL results for soils in front of the gun. Duplicate and triplicate samples were collected in each series. The number of increments for each sample varied from 50 to 75 per sample.

3.4.2.3 Burning of the excess propellant bags

After the firing point sampling was completed, excess propellant was moved to a separate location to conduct the burn point tests. Sand collected from an area away from the training range was used as a clean base layer beneath the burns. Four pads, sized 60 × 250 cm and 3 to 4 cm thick, were constructed 5 m apart from each other and oriented along the direction of the prevailing wind. Each pad was prepared using six bags of sand; samples of the sand were taken for baseline analysis prior to placement of the propellant.

The test burns consisted of burning either four charge 7 propellant bags or six charge 4 propellant bags. The bags, which contained long, thin strands of propellant, were laid overlapping along the long axis of the pads. Four tests were conducted: two with charge 7 bags and two with charge 4 bags (Fig. 3-18 to 3-20).

Following each burn, all surface residues and sand beneath the burn residue down to about 1 cm were collected in a single bag (Fig. 3-21). A subsurface sample was then taken that contained the remainder of the discolored sand. All samples were collected with a stainless steel scoop and placed in a clean PE bag. After sampling, no dark residues were present on the sand (Fig. 3-22).



Figure 3-18. Setup of four charge 7 propellant bags on sand.



Figure 3-19. Ignition of four charge 7 propellant bags on sand.



Figure 3-20. Setup of six charge 4 propellant bags on sand.



Figure 3-21. Sampling test pads following burning of propellants.



Figure 3-22. Test sites after completion of sampling.

3.4.3 Sample treatment and analytical methods

3.4.3.1 Collection and treatment of samples in particle traps

To avoid the degradation of the energetic material residues, particle traps were sampled immediately after the firing as outlined above. In this trial, use of the new holders resulted in no traps turning over, although several were displaced because of the muzzle blast from the gun. All the pails were sealed for transport and labeled according to the nomenclature explained earlier. Because the weather was mild and the trial was done quickly, no specific precautions were needed to protect the samples during transport to DRDC Valcartier. Upon arrival at the lab, the pails and soils collected in the pails were kept at -20°C until extraction.

3.4.3.1.1 Nitroglycerin analysis

Water samples in the bottles and in the pails were passed through a solid-phase extraction (SPE) filter cartridge for separation of the analyte. This technique retains the nitroglycerin and other energetic residues on a Porapak RDX cartridge¹, which was subsequently eluted with 5 mL of acetonitrile (AcN). Nitroguanidine is not retained by the cartridge; the filtrate was

¹ Sep-Pak, 6-cm³, 500-mg, Waters Corporation, Milford, MA.

placed under the hood in the dark to evaporate water almost to dryness. Nitroguanidine was recovered and analyzed by a different method described in the next section.

Prior to use, the cartridges must be conditioned to activate the Porapak RDX packing material. The SPE cartridge pre-treatment consisted of washing with 15 mL of AcN followed by 30 mL of reagent grade water. The aqueous sample was drawn under vacuum through the cartridge. The target flow rate was 10 mL/min. Following extraction of the total aqueous fraction, the SPE cartridges were dried by pulling full vacuum for a few minutes to remove residual water. After drying, 5 mL of AcN were loaded into the cartridge to elute the retained analytes. After an initial pulse of the vacuum pump started the AcN flowing, the remainder dripped through under gravity alone. The target flow rate was 1 mL/min. The concentrated extracts were diluted 1:1 (v/v) with reagent grade water, pipetted into autosampler vial, and analyzed via high-pressure liquid chromatography (HPLC) using EPA SW 846 Method 8330B (USEPA 2006). Depending on the volume of the water sample passed on the cartridge, the quantification limit was 0.3–5.0 ppb.

Prior to the HPLC analyses, extracts were maintained at 4°C according to Method 8330B. Analyses were performed with an Agilent HP 1100 HPLC equipped with a model G1322A degasser, a quaternary pump model G1311A, a model G1313A autosampler, and a model G1315A UV diode array detector monitoring at 205, 230, and 250 nm. The injection volume was 20 µL, and the column was a Supelcosil LC-8 (25 cm × 3 mm × 5 µm) eluted with 15:85 isopropanol/water (v/v) at a flow rate of 0.75 mL/min. The column temperature was maintained at 25°C during the analyses. Standards and solvents were diluted 1:1, acetonitrile to water (0.5 mL AcN/0.5 mL water).

For soil samples recovered from the traps, NG was analyzed at DRDC Valcartier using the same HPLC Method 8330B, a method that produces a 0.1 ppm detection limit (USEPA 2006). In our study, the HPLC method gave a detection limit of 0.1 ppm for all analytes in the calibration curve, and this detection limit was reduced to 0.02 ppm when the sample extracts were concentrated in a Zymark apparatus.

Soil samples were dried in a hood for 24 hours in the dark. The dried samples were homogenized by adding acetone to form a slurry, which was then

evaporated. Soils were sieved through 10-mesh sieves and extracted at DRDC Valcartier according to the following procedure: 10 g of soil were put into an amber glass vial and mixed with 20 mL of AcN. A vortex was applied for 1 minute, followed by a sonication period of 18 hours in a cooling ultrasonic bath in the dark. The samples were left to settle for 30 minutes. Acetonitrile (2 mL) was decanted from the vial and diluted with water (2 mL) containing calcium chloride (1%). The solution was filtered through a 0.45- μm filter to get 1 mL of solution ready to inject into the HPLC. Soil extracts were analyzed using exactly the same procedure and apparatus described earlier. A calibration curve using seven external standards at 0.1, 0.5, 1, 2, 10, 25, and 40 mg/L was used. When 10 g in 20 mL of AcN were used for the soil extraction, the detection limit for this method was 0.1 ppm.

To obtain a lower detection limit at 0.02 ppm, we filtered and concentrated to dryness 10 mL of AcN from the soil extract with a Zymark evaporator (model TurboVap LV) in a test-tube. Thereafter, we added 0.5 mL of water and 0.5 mL of AcN and used this mixture as the extract to inject for the analysis. All the soil extracts that did not show concentrations of energetic materials were re-injected after the treatment to the Zymark. All soil and water samples were analyzed as duplicates and were injected twice in the HPLC. The mean value is reported in Appendix C, Table C-1.

3.4.3.1.2 Nitroguanidine analysis

Water and soil samples were analyzed according to a method similar to the method developed by Walsh, M.E. (1989) for nitroguanidine. Prior to the HPLC analyses, extracts were maintained at 4°C. Once passed on the Sep Pak for the nitroglycerin analysis, the filtrate was evaporated to dryness and recuperated with a known volume of water. Analyses were performed directly on these samples with an Agilent HP 1200 HPLC equipped with a degasser G1322A, a quaternary pump model G1311A, an autosampler G1329A, and a UV diode array detector model G1315D monitoring at 263 nm. The injection volume was 20 μL and the column was a Grace C18/Cation mixed-mode (25 cm \times 4.6 mm \times 5 μm) eluted with 40:60 methanol/water (v/v) at a flow rate of 1.00 mL/min. The column temperature was maintained at 30°C during the analyses. Standards and solvents were diluted 1:1, methanol to water (0.5 mL MeOH/0.5 mL water).

For soils recovered from the traps, the procedure was similar to the soil treatment for NG except that, instead of adding acetonitrile to the soils,

water was added. The procedure was similar to the one used by CRREL and is described in the next section. Water extracts were injected and analyzed using the same apparatus and method.

3.4.3.2 *Soil samples processing and analysis*

At CRREL's analytical lab in Hanover, NH, the multi-increment soil samples were recorded in a logbook prior to processing. They were then spread out on a clean, lined aluminum tray and dried. The samples were ground for five 60-s grinds in a floating disk puck mill. For larger samples, grinding occurred in 500-g lifts. All lifts were then combined, stirred, and spread out on clean aluminum foil in a 1-cm thick layer. Four 10-g soil subsamples were taken, each of which was composed of 30 small increments randomly taken throughout the ground soil sample. Two subsamples were collected for NG analysis and the other two for NQ analysis. The remainder of the sample was then bagged and stored for re-sampling, if required.

The subsamples were processed from this point differently, reflecting the different chemical properties of the target compounds. The subsamples for NG analysis were immersed in 20 mL of acetonitrile (AcN), vortexed to mix, and placed on a shaker table overnight (Method 8330B) (USEPA 2006). A 1.00-mL volumetric pipette was then used to extract a 1.00 mL aliquot, which was added to 3.00 mL of reagent-grade water and swirled to mix. The solution was then filtered through a Millex-FH filter unit¹ into 2-mL vials for the chromatographic instrument injection. The sample was analyzed using high-performance liquid chromatography (HPLC). Select samples were also analyzed for NG using the GC-ECD (Method 8095A). These analyses were conducted for confirmation of the HPLC results, which were hampered by a background peak that interfered with the determination of low concentrations of NG.

For quality assurance, laboratory control samples were prepared. For nitroglycerin, these spiked samples consisted of 10 g of Lebanon, NH, Landfill Soil, a well-characterized local soil (50% silt-clay and 45% fine sand that contains approximately 0.5% organic matter), to which was added 1.00 mL of 10 mg/L NG plus 1.00 mL of a 10 mg/L mixed analyte solution of other energetic, including HMX, RDX, TNT, and 2,4-DNT (M8095A)².

¹ Millipore, PTFE, 0.45 µm.

² Restek Corporation, Belfonte, PA.

The samples were then air dried for 1 hour, after which 20 mL of AcN was added. The target concentration was 1 mg/kg for each analyte. A matrix spike and matrix spike duplicate (matrix spike/duplicate) was also prepared with a 10-g subsample of one of the baseline samples taken at CFB Suffield (09SUF03), with a target concentration of 1 mg/kg of NG. However, an interfering peak eluted within the retention window of NG, so a higher concentration matrix spike was required for the firing point samples. A second matrix spike/duplicate was prepared with 10 g of ground soil from another one of the five baseline samples (09SUF20). This spike contained 10 mL of 10 mg/L NG and 10 mL AcN to yield a target concentration of 10 mg/kg of NG. These spikes were used to determine the recovery rates for the site soils. Laboratory-grade clean sand was ground between samples and prepared for analysis to determine if carry-over or cross-contamination was occurring during the processing of the samples. Lebanon Landfill Soil blanks were also processed to determine if any laboratory contamination occurred during the sample processing.

The preparation procedure for the subsamples to be analyzed for NQ was similar with the following differences: 20 mL of reagent-grade water was added to each 10-g soil subsample to extract the analyte from the soil. The subsample was vortexed briefly and then shaken for two hours. The solids were allowed to settle. Then, 2.00 mL of each aqueous extract was mixed with 2.00 mL of aqueous calcium chloride (CaCl_2) solution to flocculate the suspended solids and facilitate filtration. Each sample was then capped, shaken, and the solids allowed to settle in a location away from light. The aqueous portion of the samples was then filtered through Millipore filter units¹ into 2-mL autosampler vials.

Nitroguanidine laboratory control samples consisted of 10 g of Lebanon Landfill Soil, 10 mL of 1000 $\mu\text{g}/\text{L}$ NQ solution, and 10 mL of water to yield a NQ target concentration of 1 mg/kg. Matrix spike/duplicates were also prepared from the baseline samples taken at CFB Suffield. A matrix spike/duplicate that was prepared with 20 mL of 1 mg/L NQ solution added to 10 g of ground soil from a baseline sample (09SUF03) for a target concentration of 2 mg/kg yielded a detectable peak above the background interfering peaks but was not large enough to evaluate NQ recovery. Therefore, a higher concentration matrix spike/duplicate was prepared with 2-g subsamples of the ground baseline sample and 4 mL of 10 mg/L

¹ Millipore, PVDF, 0.45 μm .

NQ solution to yield a target concentration of 20 mg/kg. This higher concentration resulted in a chromatographic peak that was quantifiable.

Nitroglycerin determinations were made on a modular system¹ composed of a Finnigan SpectraSYSTEM Model P1000 pump, a Finnigan SpectraSYSTEM UV2000 dual wavelength UV/VS absorbance detector (cell path 1 cm) set at 210 nm (to detect NG) and 254 nm (for other energetics), and a Finnigan SpectraSYSTEM AS3000 autosampler. Samples were introduced with a 100-µL sample loop. Separations were achieved on a 15-cm × 3.9-mm (4 µm) NovaPak C8 column² at 28°C and eluted with 1.4 mL/min of 15:85 isopropanol/water (v/v).

To conduct verification analyses with GC-ECD instrumentation, AcN extracts were filtered into autosampler vials, which were then placed into an HP 7683 Series autosampler tray that was continuously refrigerated by circulating a 0°C glycol/water mixture through the trays. A 1-µL aliquot of each extract was directly injected into the HP 6890 purged packed inlet port (200°C) containing a deactivated Restek Uniliner. Separation was conducted on a 6-m × 0.53-mm-ID RTX-TNT fused-silica column that has a 1.5-µm-thick film of a proprietary Crossbond phase. The GC oven was temperature-programmed as follows: 100°C for 2 minutes, 10°C/min ramp to 160°C, 20°C/min ramp to 250°C. The carrier gas was hydrogen at 1.1 psi inlet pressure. The µECD detector temperature was 280°C; the makeup gas was nitrogen at 45 mL/min.

A calibration standard for NG was prepared from an obtained analytical reference material³. The concentration of NG was 10 mg/mL in AcN in the solution used to calibrate the HPLC-UV and was 400 µg/L in the solution used to calibrate the GC-ECD.

Nitroguanidine determinations were made by HPLC using a modular system⁴ composed of a SpectraSYSTEM Model P1000 pump, a SpectraSYSTEM UV1000 single wavelength UV/VS absorbance detector (cell path 1 cm) set at 263 nm, and an Alltech 570 autosampler. Samples were introduced with a 100-µL sample loop. Separations were achieved on a 250- ×

¹ Thermo Electron Corporation of Waltham, MA.

² Waters Chromatography Division, Milford, MA.

³ Restek Corporation, Bellefonte, PA.

⁴ Thermo Electron Corporation of Waltham, MA.

4.6-mm mixed mode RP18 Cation 100-A 7- μm column¹ eluted with 1.5 mL/min water.

A calibration standard for NQ was prepared from an obtained analytical reference material²; calibration standards were prepared in water at 1 and 10 mg/L.

3.4.3.3 Burn points samples processing and analysis

Samples collected from the burn tests were processed for analysis using the same methods outlined for the firing points. Burn point samples were analyzed for NG and NQ by HPLC. Selected AcN extracts were also analyzed by GC-ECD to confirm the NG concentrations. The soil used for the propellant burn had no interfering peaks for either NG or NQ, so the matrix spike and matrix spike duplicates were prepared using baseline sample 09SUF01 that was spiked to yield target concentrations of 1 mg/kg for NG and 2 mg/kg for NQ.

3.4.3.4 Evaluation of the NG/NQ concentrations deposited in areas

To estimate the percentages of nitroglycerin and nitroguanidine deposited by the firing of the triple-base propellant, the sampled area had to be calculated. Considering that each trap measures 53 \times 48 cm, the surface of capture of a trap is 0.25 m². Each specified distance included 7 traps, totaling an area of 1.78 m². This area represents what was deposited at the specified distances. We assumed that the analyte concentrations were uniformly distributed between that distance and the firing point. If a hit was found at a preceding row, the calculation took into account the quantity found in that area and added the quantity for the area between these rows. By adding the concentrations calculated using the areas, we were able to estimate a total mass deposited by the firing and calculate the analyte residues percentages from the amount of propellant that was burned during each series of firings.

To calculate the area encompassed by the traps, the angle at the muzzle of the gun needed to be determined (Fig. 3-9). Knowing that the distance between the farthest points on the circle at 60 m was 34 m, the angle was calculated at 16.5°, meaning that the angle covering our entire surface in

¹ Alltech Associates, Inc., Deerfield, IL

² Restek Corporation, Bellefonte, PA

front of the gun was 33°. Based on that angle, the area up to the specified distance was calculated. For example, the areas from 0–5 m, 0–10 m, and 0–15 m were calculated and gave results of 7.2, 29 and 65 m², respectively. A simple calculation was used to determine the area between the distances from the gun.

All the different masses of NG and NQ obtained from the analyses of the water bottles, water pails, and soils in the traps were combined and represented the total mass deposited in the traps. Knowing the area corresponding to the traps for a specified distance (row) and knowing the surface area corresponding to that specific distance, a mass of NG and NQ was extrapolated to correspond to what was deposited on the entire area by the series of firing. These masses were compared to the total masses of propellant used (Table 3-2), and from that a percentage was derived.

To determine the area corresponding to the gunside, we had 11 traps around the butt (Fig. 3-11 and 3-12); we determined that 18 particle traps would have covered this entire area, thus resulting in a total area of 4.58 m². This area was used for the calculations of masses deposited at the gunside. All the quantities captured by the gunside traps were included in the calculation of the total masses deposited. Once all the masses collected in water, soils in traps and in the gunside were determined, percentages were derived from known mass of NG and NQ used during the firings (Table 3-2).

3.4.3.5 QA/QC

Quality assurance and quality controls were included in this study. Field blanks, trip blanks, and lab blank samples were done and revealed no anomalies. Analyses were done twice for energetic materials (lab replicates). A mean for the energetic results was calculated. It was not possible to get duplicate samples for the series of firing owing to time, materials, and costs to repeat the series. CRREL Quality Assurance (QA) samples consisted of field “blank” (pre-test) samples (2); lab blank samples consisting of clean sand grinding blanks (9) and Lebanon, NH, Landfill Soil (a local soil standard used at CRREL) blanks (4); and spiked samples using baseline soils (6) as well as Lebanon (NH) Landfill Soil (6). For the lab blanks and burn-pad pre-test samples, neither NG nor NQ was detected. The firing point samples had matrix interferences for both NG and NQ that raised the HPLC detection limits for both analytes. For the matrix spikes using the test site baseline soils, NQ recovery rates averaged 106%

for the pre-test propellant burn pad soil sample that was spiked at 2 mg/kg and was 76 % for the firing point baseline sample spiked at 20 mg/kg. NG recovery rates were 101% for both the pre-test propellant burn pad sample that was spiked at 1 mg/kg and for the pre-firing baseline sample spiked at 10 mg/kg. The landfill soil spikes averaged 99% recovery of NQ spiked at 1 mg/kg and 96% recovery of NG spiked at either 0.5 or 1 mg/kg. The NG concentrations determined by gas chromatography were in agreement with those determined by HPLC.

3.5 Results and discussion

3.5.1 Soil samples

Baseline samples taken in front of and adjacent to the firing position did not have detectable quantities of any of the analytes of concern. Both the CRREL and DRDC soil samples taken following each round of firing contained no detectable quantities of analytes as well (Appendix C)

3.5.2 Propellant residues in particle traps

During the trial in June 2009, 79 155-mm rounds using L8 and L10 triple base propellant charges were fired at CFB Suffield. Particle traps positioned in arcs in front of the gun were used to collect the propellant residues emitted during the live firing. Three series of firings were conducted and results from these series were compiled in Table 3-3.

According to our setup and strategy for sampling, residues were analyzed in the water bottles, in the water pails, and in the soils coming from the blast that were deposited in the traps. The reason for collecting water in bottles and pails was to evaluate if nitroglycerin was adsorbed by the plastic of the pail. Most of the results indicated that NG was not adsorbed on plastic but one result is not in accordance with this statement. We can still confirm that NG is not adsorbed on plastic. No residues were observed further than 10 m away from the muzzle of the gun except for one sample in the third series (Table 3-3). Most of the hits were in rows at 5 and 10 m away from the gun. These traps represent an area of capture for the particles and we were able to extrapolate percentages of NG and NQ that are ejected by the live firing of these munitions.

Table 3-3. Mass of NG and NQ detected in particle traps.

Description	Mass of compound (mg)					
	Water bottle		Water pail		Soil in traps	
	NG	NQ	NG	NQ	NG	NQ
<i>First Series of Firing at Charge 5</i>						
1-Gunside	na	na	0.27	5.2	0.32	0.41
1-5m	n.d	0.548	n.d	n.d	n.d	n.d
1-10m	0.018	0.14	0.30	0.78	n.d	n.d
1-15m	nd	nd	nd	nd	nd	nd
1-20m	nd	nd	nd	nd	nd	nd
1-30m	nd	nd	nd	nd	nd	nd
1-40m	nd	nd	nd	nd	nd	nd
1-50m	nd	nd	nd	nd	nd	nd
1-60m	nd	nd	nd	nd	nd	nd
<i>Second series of Firing at Charge 3</i>						
2-Gunside	na	na	nd	nd	nd	0.037
2-5m	0.087	0.39	0.026	nd	nd	nd
2-10m	nd	0.028	nd	nd	nd	nd
2-15m	nd	nd	nd	nd	nd	nd
2-20m	nd	nd	nd	nd	nd	nd
2-30m	nd	nd	nd	nd	nd	nd
2-40m	nd	nd	nd	nd	nd	nd
2-50m	nd	nd	nd	nd	nd	nd
2-60m	nd	nd	nd	nd	nd	nd
<i>Third Series of Firing at Charge 8</i>						
3-Gunside	na	na	nd	0.39	nd	1.2
3-5m	nd	0.54	nd	nd	nd	0.32
3-10m	nd	nd	nd	nd	nd	0.085
3-15m	nd	nd	nd	nd	nd	0.035
3-20m	nd	nd	nd	nd	nd	nd
3-30m	nd	nd	nd	nd	nd	nd
3-40m	nd	nd	nd	nd	nd	nd
3-50m	nd	nd	nd	nd	nd	nd
3-60m	nd	nd	nd	nd	nd	nd
na – Not applicable; nd – Not detected.						

Table 3-4 totals the masses of all the samples for each series. It is seen that firing at charge 5 leads to significantly higher deposition rates than firing at charge 3; this was not anticipated. According to discussions with one of

the authors (Archambault), an L8 round at charge 5 gives a pressure of 146 MPa while at charge 3, the maximum pressure is 68.5 MPa. Firing at charge 5 should have led to higher barrel pressures and temperatures, leading to better combustion. It was hypothesized that contamination was originally present on the ground at the firing location and that this contamination could have been suspended and transported into the traps by the muzzle blast from the first firings. However, neither the replicate baseline (pre-firing) soil analyses performed by CRREL nor the analyses of soil samples collected by DRDC Valcartier before and after each series of firing corroborated that hypothesis. On the other hand, use of L10 at full charge should have produced 345 MPa of maximum pressure, leading to the cleanest reaction of all. This was not observed in the NQ results; charge 8 NQ percentages are more similar to those at charge 3 than at charge 5. However, NG appeared to burn cleanly at the full charge, as NG is not detected in any of the series 3 samples. In addition, NG and NQ concentrations deposited are similar within the same series. This is surprising as NQ percentage in the propellant is almost three-fold the one of NG. NQ concentrations should have been higher than NG in each series but this was not observed. At this moment, we do not have any explanation that could illustrate what happened. These firings should be repeated to confirm this situation.

Table 3-4. Mass and percentages of NG and NQ deposited in front of the gun

Series ¹	Mass of compound (mg)				Percentage (x 10 ⁻⁵)
	Water bottle	Water pail	Soil in traps	Total ²	
1 (NG)	0.29	5.2	0.52	6.0	3.0
2 (NG)	0.35	0.10	0	0.45	0.59
3 (NG)	0	0	0	0	0
1 (NQ)	3.9	21.	0.68	26.	4.4
2 (NQ)	1.9	0	0.06	2.0	0.69
3 (NQ)	2.17	0.64	5.1	7.9	0.62

¹ Series 1 – 30 Charge 5; Series 2 – 30 Charge 3; Series 3 – 30 Charge 8.
² Total masses deposited in the area by the series of firing.

Nevertheless, the percentages of both analytes are very low when firing at all charges and this corresponds to what was anticipated. We found that firing 155-mm howitzer gun triple-base ammunition leads to the accumulation of solid propellant residues in the vicinity of the gun at $0.59\text{--}3.1\times10^{-5}\%$ by weight of unburned NG and $0.62\text{--}4.4\times10^{-5}\%$ of NQ.

Percentages of NG are lower than NQ in general and this could be explained by the fact that because of the generally low concentrations, the NG concentrations may have fallen under the limit of detection. Also, NG is present at lower percentages in the gun propellants.

It should be noted that the percentages of both NQ and NG are very low compared to other weapons; this makes the triple-base propellants the best formulation tested in our live firing experiments so far. In previous studies, artillery firings of 105-mm rounds deposited at a rate of 0.5% W/W of the original concentration of 2,4-DNT (Ampleman et al. 2008; Walsh, M.R., et al. 2007b). Even the open burning of these triple-base propellants produced low levels of contamination; this demonstrates a well balanced formulation, with a chemical reaction that leads to low residues emissions in the environment. This was the first time these triple-base propellant formulations were evaluated in a live-fire situation and, as anticipated, the energetic residues levels from use are very low.

3.5.3 Samples from the burn tests

The analytes of interest for the burn points were the same as for the firing points: NG and NQ. The pre-burn sand samples taken from the burn pads built for these tests were analyzed and neither NG nor NQ was detected (detection limits 0.02 mg/kg NG, 0.5 mg/kg NQ). Whole-area samples were taken from the surface and subsurface areas of each of the burn pads following completion of the propellant burns. Burns 1 and 2 used four charge 7 increments while burns 3 and 4 used six charge 4 increments. Mass for the combined samples from the four pads ranged from 6.5 to 14 kg (Table 3-2). Analyses found both NG and NQ in all samples. For the charge 7 burns, an average of 8.0 mg of NG and 63 mg of NQ were recovered (Table 3-5). For the charge 4 burns, an average of 16 mg of NG and 200 mg of NQ were recovered. A sample composed of debris that was collected downwind and off the burn pads was also analyzed and no analytes of interest were detected. This means that the analytes of interest had a tendency to stay at the burning locations.

As mentioned, both NG and NQ were found in all burn point samples. Although easily detected, the recovered propellant masses are a small percentage of the original propellant mass (Table 3-2). For NG, about 0.0007 and 0.002% of the original NQ mass was recovered from the charge 7 burns; for the charge 4 burns, NG was recovered at about 0.002% and NQ at about 0.01% (Table 3-5). This is very efficient burning propellant, as is

evident from the very low residue rates of even unconfined burning of the propellant.

Table 3-5. Percentages of NG/NQ deposited by the open burning tests.

Burn test	Sample	Compound mass (mg)		% of compound deposited ¹	
		NQ	NG	NQ	NG
Burn 1 (4 bags charge 7)	Surface 1	52	6.9		
	Subsurface 1	19	2.3		
	Total	71	9.2	0.0022	0.0008
Burn 2 (4 bags charge 7)	Surface 2	49	5.6		
	Subsurface 2	6.0	1.3		
	Total	55	6.8	0.0017	0.0006
Burn 3 (6 bags charge 4)	Surface 3	149	11		
	Subsurface 3	108	7.0		
	Total	256	18	0.013	0.0027
Burn 4 (6 bags charge 4)	Surface 4	99	7.5		
	Subsurface 4	47	6.1		
	Total	146	14	0.007	0.0021

¹Percentages are related to the total amount found in the combined surface and subsurface samples.

3.6 Conclusion

Following the characterization of Otterburn ranges in collaboration with the UK Ministry of Defense (MOD) and DRDC Valcartier, the UK MOD agreed to supply DRDC Valcartier with a 155-mm self-propelled howitzer, a supply of triple-base munitions, and a gun crew to perform this unique study. The trial was organized by the BATUS at CFB Suffield, Canada, and was conducted by DRDC Valcartier and U.S. Army ERDC/CRREL in June 2009. This work was conducted under the auspices of the Trilateral Technical Cooperation Programme. CRREL's participation was supported through a collaborative U.S./Canadian project funded by the U.S. Department of Defense's Strategic Environmental R&D Program, Project ER-1481. This trial was the first study to evaluate the dispersion of triple-base propellant residues deposited by the live firing of these munitions. The results obtained in previous trials conducted at different CFBs in Canada and at U.S. bases were for single- and double-base propellants. No results were available prior to this study on triple-base propellants.

A total of 79 155-mm rounds were fired during the exercise using a British L131 (AS90) Braveheart 39-calibre 155-mm Howitzer Self-Propelled Gun. During the trials, DRDC placed 56 particle traps in front of the gun using a semi-circular pattern, with rows of traps installed at specific distances away from the gun. In addition to this, 11 traps were positioned around the gun. For the trial, the traps were located in front of the gun at distances of 5, 10, 15, 20, 30, 40, 50, and 60 m. Holders were used for the first three rows to avoid the traps flipping from the muzzle blast during firings.

Our particle trap setup resisted the muzzle blasts well. Water was poured in traps to catch the particles. Soils were projected in the traps by the violent blast. This resulted in water samples and soils samples from the traps. To evaluate the possibility that nitroglycerin was adsorbed on the plastic of the pail used to recover the water samples, glass bottles were filled with water coming from the combined water for each row that was poured in the pails. Using this strategy, we collected 24 water samples in bottles, 27 water samples in pails, and 6 soil samples from the traps after firing three series of 30 L8 at charge 5, 30 L8 at charge 3, and 19 L10 at charge 8. Analyses of all DRDC samples were done at the laboratory in Valcartier. In a parallel effort, CRREL used the multi-increment sampling strategy to collect soils between the DRDC traps in front of the gun. They covered an area of 30 × 40 m and took five replicate samples before and after each firing series. Over 110 increments were taken for each sample. Soil samples collected by CRREL were analyzed at their laboratory. Furthermore, 16 systematic, random, multi-increment soil samples were collected to represent the 0- to 30- and the 30- to 60-m areas between the DRDC traps in front of the gun position.

At the end of the firing trials, burn tests with some of the excess propellant bags were conducted to evaluate the residues deposition of each component of these triple-base propellants. Four burn tests were conducted using four charge 7 bags in two events followed by the open burning of six charge 4 bags in two events. Four sand pads were constructed for the burning and soils were taken before and after every burn tests. The bags, which contained long, thin strands of propellant, were laid overlapping along the long axis of the pads. Following completion of each burn, all surface residues and discolored sand down to about 1 cm were collected in a single bag.

Results from the DRDC particle traps indicated that most of the residues fell within the 10-m area in front of the gun. Most of the residues were found in the rows 5 and 10 m from the gun; the one exception was a hit in soils found in a trap at the 15-m distance. Nothing was detected in any other traps of the setup. It was found that firing 155-mm howitzer gun triple-base ammunition leads to the accumulation of solid propellant residues in the vicinity of the gun at $0.59\text{--}3.1 \times 10^{-5}\%$ by weight of unburned NG and $0.62\text{--}4.4 \times 10^{-5}\%$ of NQ. In comparison, the latest investigation of residues deposited from 105-mm artillery guns found that 0.4–0.6% of 2,4-DNT is ejected during firing (Ampleman et al 2008; Walsh, M.R., et al. 2007b). Likewise, our February 2009 study found that 0.0026% of unburned 2,4-DNT is deposited from the firing of 90 tank gun ammunition rounds. The current study clearly demonstrated that triple-base propellants are the best formulations tested in our live firing experiments so far.

Results also showed anomalies when comparing the charge 5 with the charge 3 series of firings. Combustion of propellants in guns follows the laws of physics: the higher the pressure and temperature in the barrel for a given propellant compound, the better is the combustion and the fewer residues are expelled at the muzzle of the gun. Our findings indicate that firing at charge 5 led to higher deposition rates than firing at charge 3. Comparing the maximum pressure for an L8 round at charge 5 (146 MPa) with the maximum pressure at charge 3 (68.5 MPa), we would have expected more residues with the smaller charge. It was hypothesized that contamination was originally present on the ground at the firing location and this contamination could have been moved by the blast of the first firings, leading to this particular situation. However, soil analyses conducted by CRREL and DRDC Valcartier did not corroborate that hypothesis. On the other hand, use of L10 at full charge should have given 345 MPa of maximum pressure, leading to the cleanest reaction of all. This was not observed in the NQ results; the NQ percentages from the L10 firing are more similar to those for charge 3 than for charge 5. On the other hand, NG was not detected after the full charge firing, indicating that it burned completely at the higher temperature and pressure conditions. At this moment, we do not have any explanation that could illustrate what happened. These firings should be repeated to confirm this situation.

As stated, the pre-firing baseline soil samples collected by CRREL did not corroborate the hypothesis of having contamination in the ground before the firings; none of the soil samples contained detectable quantities of

energetic materials. Extensive analytical chemistry was employed to validate this finding, and, in the end, it was concluded that if contamination exists at that firing position, it is below the limit of detection. In a sense, this corroborates the fact that these triple-base propellants are well balanced formulations that leave very few residues upon firing. More practices and more weapon systems should use these formulations.

In addition to this, DRDC Valcartier soils collected between the traps before and after each series of firing also showed no NG or NQ presence. This is in good agreement with and corroborates the CRREL results. That we confirmed that no NG or NQ was present on-site before the firings clearly showed that the reason for higher deposition when firing the first series at charge 5 does not reside in the explanation of being on a contaminated site. At these low concentrations, the precision of our results may explain these anomalies. Nevertheless, we realized that particle traps are efficient at capturing particles emitted by artillery gun, especially during summer conditions, and the amount of residues deposited is in good agreement with what was anticipated.

The burn tests also confirmed that the triple-base propellants burn well. NG and NQ were observed in all samples but at lower levels than following the burning of single-base propellants. Although easily detected, the recovered propellant masses are a small percentage of the original propellant mass. Following the charge 7 burns, an estimated average of 0.0007% of the original NG mass and 0.002% of the original NQ mass was recovered. For the charge 4 burns, an estimated average of 0.002% of the NG and 0.01% of the NQ was recovered. This is a very efficient burning propellant, as is evident from the very low residue rates of even unconfined burning of the propellant.

In conclusion, it can be said that this trial was a success and that we accomplished the objective of this study, which was to analyze residues expelled by the live firing of triple base propellant. The next step would be to repeat the study to see if we can validate the percentages obtained during the trial. The most important finding from this work is that the triple base propellants burn efficiently and led to the lowest contamination compared to other propellant formulations tested. The use of these propellants should be increased. Another important finding is that even if the open burning of these propellants is cleaner, burning on the ground should be avoided.

4 Fixed and Mobile Burn Pans for the Burning of Excess Artillery Propellant Charge Bags

Sonia Thiboutot, Guy Ampleman, Michel Kervarec, Annie Gagnon, André Marois, Firmin Boucher, and Michael Walsh

4.1 Summary

Sampling conducted on military training ranges and residue deposition studies from the disposal of excess propellants done under SERDP ER-1481 have shown that burning of excess propellant results in the accumulation of 2,4-DNT, NG, and other contaminants in the surface soil. To prevent this, we developed and tested propellant burn pans for the controlled disposal of excess propellants. This chapter describes the design and testing of four Canadian fixed burn pan prototypes (DRDC) and one U.S. mobile burn pan prototype developed under SERDP ER-1481.

The Canadian fixed burn pans were constructed of high-temperature stainless steel or aluminum, measure $3 \times 5 \times 0.1$ m, and are equipped with a lightweight removable cover of reinforced aluminum. The depth of the pan was kept low to avoid the risk of transition from combustion to detonation. A rectangular channel guides the ignition of the propellant bed. The U.S. prototype is constructed of stainless steel, measures $1 \times 2 \times 0.3$ m, and has a 0.45-m-high expanded-metal stainless steel top. It has an access door at one end for burn initiation. Burning trials with the Canadian prototypes were conducted in February 2009 and November 2009. A joint trial was conducted using both the Canadian and U.S. prototypes in March 2010. Over 5000 kg of excess single-base artillery propellant bags were processed during these trials. The burn pans reacted well to the high burning temperatures, with a cooling time of less than 45 minutes, leading to a high disposal throughput. The collection of the post-burn residues was easy. A small proportion of propellant grains and lead was projected outside the U.S. pan while the screens developed for the Canadian table prevented this phenomenon. A Standardized Operating Procedure has been published in Canada for the use of the fixed burn pans, which will soon be

fielded in Canadian Ranges and Training Areas. Development of the U.S. burn pan continues, with efforts concentrating on incorporating the Canadian screen concept and lightening the total weight of the structure.

4.2 Introduction

Over the past decade, researchers from Canada and the U.S. have developed cutting-edge expertise in characterizing Ranges and Training Areas (RTAs) for the deposition of munitions constituents and in studying the environmental fate of energetic materials (EM) (Jenkins et al. 2008; Thiboutot et al. 2008c, d; Ampleman et al. 2007; Thiboutot et al. 2007b; Diaz et al. 2007; Pennington et al. 2006b; Brochu et al. 2008). Major environmental issues have been identified. Amongst them, the burning of excess propellant bags on surface soils has been shown to be a major potential source of soil and groundwater contamination. The field expedient open burning (OB) of propellant is a regular activity associated with the firing of artillery guns, such as the 105- and the 155-mm howitzers. Both guns use a propelling charge system composed of multiple charge bags to fire a projectile to the required distance. The number of charge bags used during the firing depends on the range of the target. Firing is typically conducted using the fewest charge bags to minimize the wear and tear on the barrel and gun as well as to avoid ricochet of the projectile. Furthermore, the safety templates of most RTA artillery ranges do not allow the firing at full charge. Following a gun firing operation, unused propelling charge increments were burned near the gun positions. This procedure entails piling the unused bags on the soil surface soil, or on the snow or ice surface during winter, and igniting them. In recent years, development of Modular Artillery Charge Systems (MACS) for the 155-mm gun has virtually eliminated the need for disposal of discarded propelling charges. However, the OB of propelling charge increments will remain for years to come with the M67 propelling charges for the 105-mm ammunition and until the current stock of M3- and M4-series propelling charges for the 155-mm howitzer ammunition is either exhausted or declared surplus to the requirement in favor of the MACS.

The Canadian OB specifications recommended laying out propellant on the ground surface parallel to the wind direction using a maximum density of 7.5 kg of propellant per 1 m (5 lb per linear ft). The recommended ignition train used combustible material consisting of a railroad fuse and 2 m of M700 time fuze cord (Department of National Defence Canada 1974, 2005) (Fig. 4-1 and 4-2). The burning, either on snow cover or on the

ground, does not lead to complete combustion and the presence of residues was obvious (Fig. 4-3 through 4-5).



Figure 4-1. Ignition train material.



Figure 4-2. Burning setup on snow.



Figure 4-3. Burning on snow.



Figure 4-4. Left over residues after burning on snow.



Figure 4-5. Left over residues after burning on concrete pads in Gagetown RTA (solidified lead beads).

Various artillery propellant burning sites sampled across North America consistently showed the presence of 2,4-dinitrotoluene (2,4-DNT) as a contaminant. Few papers on the measurement of the accumulation of these residues have been published up to now, but recent studies clearly

demonstrated that the incomplete burning of single-base propellants leads to the accumulation of 2,4-DNT in the environment (Diaz et al. in press; Walsh et al. 2010; Walsh et al. 2009). Both energetic-containing residues and “kicked-out” raw propellant grains have been found at burn and test sites, with the most occurring on wet and snow-covered ground. The quantities are significant; up to 18% of the original nitroglycerin (NG) load for mortar propellants remained on the surface soils. In the reports under publication by Diaz et al. (in press) and published by Walsh, M.R., et al. (2009a, 2010a), propellant bags from 105- and 155-mm howitzers (both M1 single-base composition) were burned in various configurations, and these independent studies determined that the field expedient burning led to 1% by mass of unburned 2,4-DNT.

In Canada, the expedient burning was also suspected to lead to the accumulation of dioxin and furans, as they were detected on a former burn site (Brochu et al. 2008). A study undertaken by Poulin et al. (2009) demonstrated that the Canadian protocol leads to the production of these toxic contaminants. Use of the railway fuse was suspected to be the source of dioxins and furans; other ignition trains are currently under study by Director, Ammunitions and Explosives Regulations (DAER).

An estimated 20,000 kg of excess propellant was burned during 2001 at RTAs across Canada (Diaz et al. in press). Based on an estimated accumulation rate of 2,4-DNT from field expedient OB of 1% w/w, these disposal operations will deposit 200 kg of 2,4-DNT in the surface soils of artillery firing positions. Results obtained in Canadian RTAs showed levels of 2,4-DNT over 500 mg/kg at various locations on propellant burn marks; lead concentrations were also higher than accepted thresholds at these locations.

A recent fate study conducted by *Institut National de la Recherche Scientifique—Eau, Terre et Environnement* (INRS-ETE) using large scale columns demonstrated that 1 m² of burning residues on the soil surface (or approximately 500 g of burned residues) may lead to the contamination of more than 7500 m³ of groundwater following the first infiltration of precipitation (Martel et al. 2011).

Field expedient burning of excess artillery propellant bags has therefore proven to be an important source of contamination and this stressed the need for the development of an environmentally sound alternative dispos-

al method. Based on the results cited earlier, the DAER's office at Canadian Headquarters banned the field expedient burning of excess artillery propellant in April 2008. The rationale behind the ban of the field expedient OB of M1 single-base propellant was that it results in a significant deposition of 2,4-DNT and lead on the soil surface that can:

1. Act as a source zone for soil contamination.
2. Cause surface water and groundwater contamination that could result in the contamination of drinking water aquifers.
3. Become a source of airborne contaminants to personnel through the inhalation of emissions from wind erosion and dust arising from ashes and nanoparticles resulting from past OB activities conducted near firing positions.
4. Require the application of costly remediation measures to clean the contaminated sites to maintain access for continued use and ensure sustainability of RTAs.
5. Cause the temporary or permanent closure of a site to conduct remediation to remove contamination sources.

Development was undertaken of an environmentally sound solution that would enable the sustainment of military training and force readiness by minimizing the impacts of this activity. An assessment of the potential options for the replacement of field expedient OB of propellant was written in 2007 by the Directorate of Armoured Vehicle Project Management in Canada (Boulay et al. 2007). Various options were analyzed in this document and the recommendation at that time was to ban the field expedient OB and to centrally demilitarize the discarded charge bags. However, this recommendation was not implemented because of a lack of sufficient funding. During a search for alternative solutions, a literature review showed that a very few papers were dedicated to the characterization of former burning sites, to guidelines for permitting OB, and to the development of liners for the OB of propellant (Jeenigs 2004; Tetrattech Inc. 2002; Kovero and Tervo 2002). Nothing published to date indicates an alternative sustainable solution to the practice of field expedient OB.

To replace field expedient OB with a cost effective, safe, and environmentally responsible OB process, Defence Research and Development Canada—Valcartier (DRDC Valcartier) developed various iterations of fixed burn structure prototypes, while the Engineer Research and Development Center's Cold Regions Research and Engineering Laboratory

(ERDC/CRREL) developed a mobile burn pan in parallel with the Canadian efforts. This chapter presents the results obtained with the prototypes and draft recommendations for the implementation of the selected burn table.

This work, co-sponsored by the Strategic Environmental Research and Development Program (SERDP) and by Director Land Environment (DLE), was conducted between February 2008 and June 2010.

4.3 Artillery propellants and environmental and health considerations

This investigation initially studied M67 and M4 propellant charges from 105- and 155-mm howitzers. Discarded M67 charges were brought back from the RTAs by the artillery units using safe explosive transport boxes and stored in a Munitions Experimental Test Center (METC) Valcartier magazine. The M4 charges were legacy units that needed to be demilitarized. Small amounts of single-base mortar propellant charges were consumed in some of the later tests.

4.3.1 105-mm Artillery propellant

The propelling charge of the 105-mm caliber howitzer, referred to as M67, includes seven bags filled with grains of single-base composition M1 propellant with a combined mass of approximately 1.28 kg (Department of National Defence Canada 2004). Chemical constituents of the M1 propellant are presented Table 4-1. The propellant for each charge increment is loaded into a cloth bag that is marked with the increment number and the lot number of the propellant (Fig. 4-6). Charges 1 and 2 use 0.38-mm, single-perforation propellant for quick burning; charges 3 to 7 use 0.71-mm multi-perforated (seven hole) propellant for slower burning. The mass of propellant in each bag is presented in Table 4-2. Charge 5 incorporates a piece of lead foil ($114 \times 198 \times 0.05$ mm) as a decoppering agent for the barrel. Figure 4-7 shows an example of bags from charges 6 and 7, opened to expose the propellant grains within. The burning trial processed mainly bags of charges 6 and 7, with a few bags of charge 5.

Table 4-1. Chemical composition of M1 propellant.

Constituents	Proportions (%)
Nitrocellulose	85 ± 2
2,4-Dinitrotoluene	10 ± 2
Dibutylphthalate	5 ± 1
Diphenylamine (added)	0.9 ± 1.2

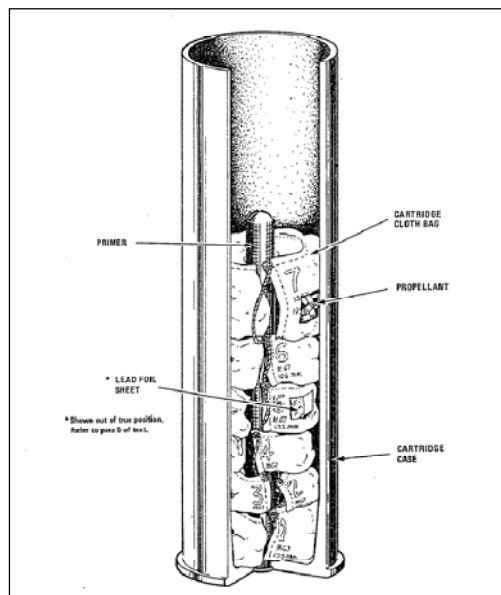


Figure 4-6. M67 Propelling charges.

Table 4-2. Mass of propellant in the M67 propelling charges.

Charge	Propellant mass (kg)
1	0.245
2	0.040
3	0.072
4	0.110
5	0.114
6	0.260
7	0.409



Figure 4-7. M1 propellant grains in bags 6 and 7.

4.3.2 155-mm Artillery propellant

Propellant bags consisting of green bag M3 propelling charges from 155-mm caliber howitzers were used in two burning trials (Department of National Defence Canada 2006). The full charge consists of approximately 5.9 kg of M1 multi-perforated (0.864-mm) granular propellant. The propellant is contained in cartridge cloth bags, divided into a base charge (3) and four increment charges (4–7). The mass of propellant charge in each bag is given in Table 4-3. The chemical composition of the M1 propellant is the same as that in the M67 105-mm charge (Table 4-1). An igniter charge consisting of 99 g of clean burning igniter powder in a red cloth bag is sewn to the rear of the base charge. The composition of the igniter is 98% minimum nitrocellulose (NC), 1.5% \pm 1.0 diphenylamine, 0.1% maximum potassium nitrate, and 0.2% graphite glaze. A flash reducer pad containing 57 g of potassium nitrate is assembled forward of the base charge. Similar 28.4-g pads are assembled forward of increments 4 and 5. Figure 4-8 shows charge 4 and 5 bags and a potassium nitrate flash reducer pad.

In 2003, Canada acquired new 155-mm guns using MACS. MACS use a build-a-charge concept, in which all increments are identical in the lot, eliminating the need to dispose of unused increments. Unused increments are retained for future use and MACS propellants can be safely transported and handled in the same manner as other conventional propellants. This means that expedient burning of excess bags will no longer be required when this system of propellant charges is fully implemented. However, Canada still possesses a large inventory of

conventional M3A1 propelling charges that will be consumed during training in the upcoming years.

Table 4-3. Mass of propelling charge M1 in the M3A1.

Charge	Propellant mass (kg)
3	1.814
4	0.524
5	0.779
6	1.261
7	1.530



Figure 4-8. Bags of 155-mm charge 4 and 5 and the flash reducer pad

4.3.3 Environmental and health impacts

Technical grade DNT is composed of approximately 78% 2,4-DNT, 19% 2,6-DNT, and small amounts of 3,4-DNT, 2,3-DNT and 2,5-DNT (U.S. Department of Health and Human Services 1998). DNTs are absorbed through the gastrointestinal tract, respiratory tract, and skin in most species. 2,4-DNT and 2,6-DNT have been classified as possible human carcinogens by the International Agency for Research on Cancer (IARC). The USEPA recommendations define a safe lifetime daily maximum oral dose of 0.002 mg/kg per day for 2,4-DNT, and 0.001 mg/kg per day for 2,6-DNT. In addition to the EPA recommendations, the U.S. Occupational

Safety and Health Administration (OSHA) regulations state that an average 8-hour exposure to total DNT in workplace air should not be more than 1.5 mg/m³ of air. The USEPA drinking water advisory values for DNT are as follows: 2,4-DNT, child = 0.3 mg/L and adult = 1.0 mg/L; for 2,6-DNT, child = 0.4 mg/L and adult = 1.0 mg/L. These recommendations are applicable primarily to workers involved in the manufacturing of DNT. Although these recommendations do not readily apply to military personnel exposed to DNT as a result of their handling, firing, and disposing of the propellant containing DNT, it must be kept in mind that DNT is a regulated toxic substance.

DNT dissolves easily in water and any quantity of DNT remaining on the ground will be dissolved by rainwater and eventually reach the water table, as was demonstrated by INRS-ETE in their soil column studies with propellants (Martel et al. 2011). Water containing dissolved DNT will percolate through sandy soil until it reaches the underground water table. Once the contaminants have reached the groundwater or have been entrained in surface water run-off, they can migrate off the range and affect neighboring lands. All the compounds in propellant formulations have human health exposure threshold limits and their values can vary as a function of the province (Canada) or state (U.S.) environmental laws.

Diaz et al. (in press) compiled thresholds for compounds of concern present at firing positions that were available from various sources. This information is presented in Table 4-4, which includes thresholds for two Canadian provinces (Quebec and Ontario) (Canadian Council of Ministers of the Environment [CCME]), and two locations in the U.S. (Maryland and EPA Region III, which includes Delaware, District of Columbia, Maryland, Pennsylvania, Virginia, and West Virginia). The right column in Table 4-4 also gives the criteria calculated by the National Research Council (NRC) Biotechnology Research Institute (BRI) in Montreal, Quebec (Robidoux et al. 2006). BRI calculated these values using the CCME model adapted for the military scenarios expected in training areas on military bases. Residential and industrial criteria are listed separately in the upper and lower sections of Table 4-4, respectively. Industrial values are typically used in the training area scenario. As stated earlier, the range of concentrations measured at artillery firing positions at locations exhibiting previous propellant disposal events varied between 500 and 800 mg/kg, which are greater than all the thresholds presented.

Table 4-4. Soil standards from U.S. EPA, Quebec, and Ontario.

Compound	Soil standard (mg/kg)					CCME military ¹
	Residential–Parkland					
	Quebec	Ontario	Canada (CCME)	Maryland	Region III (U.S.)	Canada
2,4-DNT	na ²	1.1	na	16	160	7.0
2,6-DNT	na	na	na	na	78	8.1
Dibutylphthalate	6	na	na	780	7.8x10 ³	na
Lead	500	200	140	400	na	na
Industrial						
2,4-DNT	na	na	na	1.8	200	
2,6-DNT	na	na	na	na	100	
Dibutylphthalate	7x10 ⁴	na	na	2x10 ⁴	1x10 ⁵	
Lead	1000	1000	600	400	na	

¹Criteria calculated by Biotechnology Research Institute, National Research Council Canada.
² na – not available.

4.4 Design, construction, and safety aspects

4.4.1 Design and construction of the fixed Canadian burn pan

4.4.1.1 First prototype

Many factors were taken into consideration in the design of the initial prototype burn table. During deflagration in gun barrels, M1 type propellants have a flame temperature of around 2200°C (Kovero and Tervo 2002). This high temperature was used as a parameter in the selection of the table materials. Safety was also a key element in the design, as well as ergonomics and the ease of operation. The table's operability under various harsh environmental conditions was also considered during the design. The following requirements were identified after consultation with the users and explosive ordnance disposal (EOD) experts:

1. Removable, reinforced lightweight cover to resist rain and the accumulation of snow.
2. Table frame must be made of either aluminium or high quality stainless steel (SS) to resist high temperatures and corrosion.

3. Elevation from the soil surface to allow air circulation and reduce cooling times.
4. Concrete pad mounting surface—the table will be brought to the destruction area. The concrete pads will add containment of any projected grains or ash outside the table and discourage the growth of vegetation.
5. Safe ignition system to initiate the powder.
6. Rounded corners to allow easy ash collection.
7. Containers for the accumulation of ashes.
8. Sides should not be too high to avoid users piling up bags, which could lead to a transition from deflagration to detonation.
9. Low height sides might favor the loss of propellant grains through the ejection of propellant grains from the intense gaseous emissions generated by the burning process. Protective screens might be later added to minimize this while allowing air intake for the efficient and complete burn process.
10. Design must allow the transportation of the table using a forklift.

All these requirements were carefully taken into consideration and led to the table design illustrated in Figures 4-9 and 4-10.

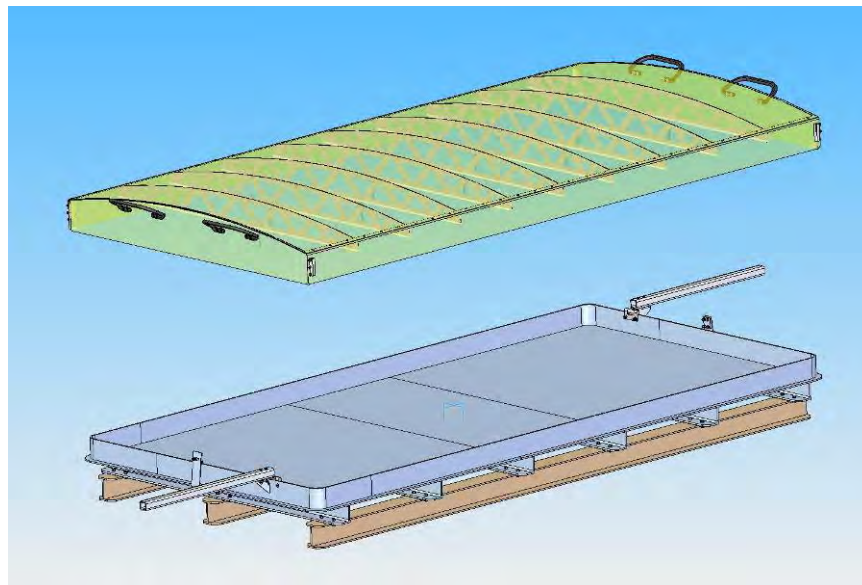


Figure 4-9. Initial table design with removable cover and integrated ignition tool.

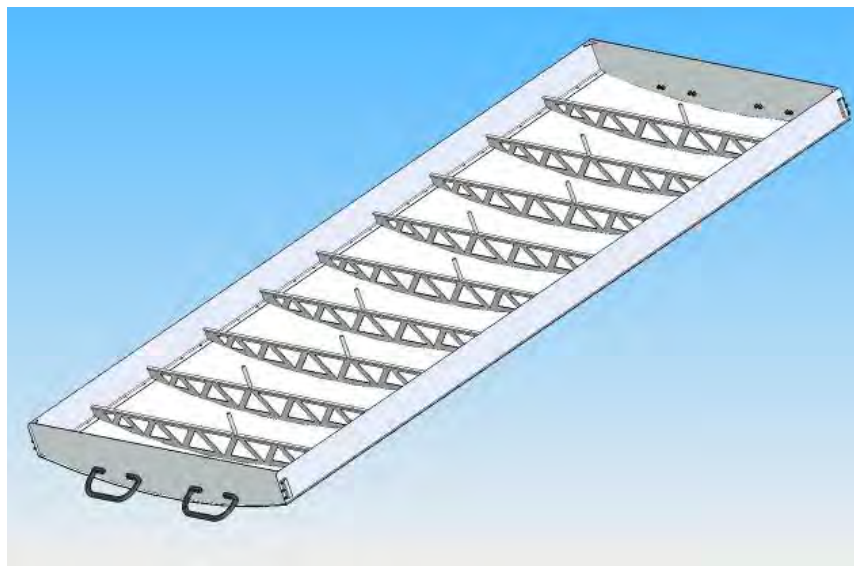


Figure 4-10. Inverted view of the aluminium table cover.

Initial drawings of the prototype were made using Solid Edge® software (Siemens PLM Software, Plano, Texas, U.S.). The drawings were further refined by Alain Cinq-Mars. A few meetings were held during the design process to refine the drawing details and obtain a final product, which was sent to our contracting office for construction of the prototype. The contract was awarded to Industry Samson¹. The following table dimensions and specifications were given to the private firm that built the prototype under contract for DRDC:

1. Table frame dimensions: $3 \times 1.5 \times 0.1$ m.
2. Height with cover: 40 cm.
3. Two rectangular ignition ports at both ends (time cord fuze holder): constructed with aluminium alloy 6061-T6. Dimensions of the port were: $3.8 \times 3.8 \times 0.32$ cm to provide light weight and strength.
4. Material selected for main frame: heat resistant stainless steel (RA310S alloy) of 0.64 cm thickness.
5. Material selected for cover: aluminium alloy 5252-H32 of 0.023 cm thickness.
6. Material selected for the reinforcement was aluminium alloy 6061-T6 of $\frac{1}{8}$ in. thickness.

The RA310S stainless selected for the table main frame possesses an excellent resistance to oxidation and corrosion under high temperature condi-

¹ 5796 St-Laurent Street, Levis, Qc, Canada, G6V 3V7.

tions because of its high chromium and medium nickel contents. The main industrial applications of this alloy include fluidized bed coal combustors, radiant tubes, refractory anchor bolts, burners, and combustion chambers (Robidoux et al. 2006).

The prototype received at DRDC Valcartier in November 2009 met our specifications and was stored until the February trial. The cover included the requested reinforcement system that proved to withstand the weight of two adult males standing on the table cover.

4.4.1.2 Other sets of prototypes

Following the February 2009 trial, new prototypes were designed and built for further testing. To reduce the cost, two materials were studied to replace the 0.635-cm-thick SS table used for the first prototype: 1) the same alloy SS at 0.32 cm thick, and 2) aluminium at 0.635 cm thick. Using aluminium would also reduce the table weight and make it easier to transport. The weight of the three table types was estimated to be: SS (0.32 cm): 714 lb, SS (0.635 cm): 974 lb, and aluminium (0.625 cm): 450 lb. In the new prototypes, the table height was raised to improve the ergonomics of the process; the first prototype proved to be too low for easily loading the propellant bags. The increased height would also improve air circulation and make it easier to move with the forklift.

The main table frame was modified to include vertical screens to minimize the projection of grains outside the table. After examining various options, we chose to use 1-m-high vertical screens mounted to holders along the outside periphery of the table. This would avoid the risk of having propellant grains trapped in the holders and then crushed when inserting the frames, leading to high shear and friction that could result in the premature ignition of the propellant in the table. The frame holders were hollow by design to avoid any accumulation of grains.

Four different screens were designed and tested based on their potential to stop the ejection of propellant grains. The perforated sheets selected for the screens were acquired from McMaster-Carr Supply Company (www.mcmaster.com). The openings were kept small to prevent the ejection of unburned propellant grains while also avoiding too much confinement in the burning process. The need for a good oxygen intake for an efficient burning process was also taken into consideration. Another set of angle baffles made of aluminium was designed. The baffles were to be at a 30°

angle with the table bottom and measured 0.5 m tall. The various shields were labeled types “a” to “e”; their specifications are presented in Table 4-5. For the second trial, the table prototypes were labeled table 1, 2, 3, respectively, for the SS 0.32 cm, SS 0.635 cm, and aluminum table main frame.

Table 4-5. Specification of the sheets selected for the screens.

Shield	Design	Sheet description	Mesh opening size (cm)	Percentage of open area
a	Sheet	Diamond shape	0.795 x 2.54	60%
b		Woven wire cloth square, interlaced	0.726	74%
c		Woven wire cloth square, welded	0.659	60–69%
d		Round hole perforated sheet	0.635 (diameter)	58%
e	Baffle	na	na ¹	na

¹ na – not applicable

4.4.1.2.1 Other set of screens

Based on the warping of the main screen frames in the November 2009 Nicolet trial, a stronger frame was designed to include reinforced screen frames. Both aluminum and SS frames were manufactured to test the long-term heat and corrosion resistance of the shields.

4.4.1.2.2 Construction

The contract for building the three tables and five sets of shields (four types of perforated aluminium sheets and the angled baffles) was awarded to APN Inc.¹. The detailed prototype drawings were provided to APN by the DRDC prototype group.

4.4.2 Design and construction of the mobile burn pan

The mobile burn pan was designed and built following the initial prototypes of the Canadians’ fixed burn pan. The design leveraged off the results of the testing of their pans as well as experiences with open burning of ar-

¹ 2659 Du Parc Technologique Blvd, Quebec, Quebec, Canada, G1P 4S5.

tillery propellants and burning propellants in various sized and shaped existing structures.

The initial mobile pan design was all stainless steel, with a removable stainless “bonnet” topped with expanded stainless grating to impede the ejection of propellant charge bags during deflagration (Fig. 4-11). A removable stainless steel false bottom is incorporated into the design to inhibit heat transfer to the bottom of the pan, thus helping prevent the combustion of any vegetation that may be in contact with the pan bottom. When flipped over, the bonnet fits into the main pan, allowing ease of shipment. Although heavy (≈ 240 kg), the complete unit can be moved by four personnel. The assembly was designed to easily fit in the bed of a standard U.S. Army 2-wheel $\frac{3}{4}$ -ton cargo trailer with a welded box cargo body (M101A2, M101A3, and M116A2). Polyethylene pads on the feet of the pan reduce damage to the trailer cargo box. An access door, shown closed in Figure 4-11b, allows access to the propellant in the pan when setting up a burn. The door is to be closed during deflagration. The bonnet is easily handled by two personnel, reducing risk exposure during the loading of propellant in the pan. A single technician can then configure the initiation train for the burn process.



a. Pan (foreground) with bonnet removed.

b. Assembled unit.

Figure 4-11. CRREL mobile propellant burn pan: first prototype.

The pan is of all-welded construction. However, the joints were not continuously welded. Loose hardware was kept to a minimum.

4.4.3 Safety considerations

Prior to fielding any prototype for the burning of excess propellant, the user's safety was carefully examined and evaluated. To minimize the hazard

elements, the ignition process, the maximum load of propellant per burn, the acceptable meteorological conditions for use, and the time for structure cool-down prior reuse were carefully studied.

4.4.3.1 Ignition of propellant bed

Ignition ports on the Canadian table were designed to allow safe ignition of the propellant bed. The ignition device would be placed in the table in the propellant bed and attached to the M700 blasting time fuze cord, which would be inserted in the rectangular channel. The channel would ensure that the cord could not roll on itself and ignite the propellant bed before the EOD technician could reach a safe distance away. On the U.S. design, a small port in the pan door allows feeding of the time fuze cord outside the pan for safe lighting. The cord used in the U.S. will not cross-ignite, negating the need for a guide channel as on the Canadian design.

4.4.3.2 Maximum load of propellant bed: critical height

Another consideration was the maximum mass of propellant that could be loaded on the table in one burning event. When propellant is ignited, it starts to burn energetically, a process known as deflagration. Under certain conditions, the deflagration can transition to detonation. This is possible when the confinement of the burn leads to a process where the reaction products cannot escape and the gas pressure builds up. This increases the rate of deflagration until the pressure waves generated in the burning region compact and compress the propellant in the path of the wave to a critical density. This autocatalytic reaction can build up and allow the formation of the shock conditions necessary for detonation to occur, as illustrated in Figure 4-12. This process must be absolutely avoided as it represents a major threat to the personnel that will operate the burning table and to the table itself.



a. Burning.



b. Detonation.

Figure 4-12. Transition from burning to detonation in GD-OTS experiments (courtesy of General Dynamics—Ordnance and Tactical Systems Canada—GD-OTS).

The Canadian prototype structure, measuring 3×1.5 m, could allow loading of a propellant bed that would exceed the imposed safety limit of 7.5 kg per m set by the Canadian Forces (CF) Procedural Manual C-09-008-002/FP-000 (Department of National Defence Canada 2005). In this manual, this limit was set to avoid a potential transition of the burning process to deflagration or detonation. However, no scientific basis supported this limit, and it was concluded that its main rational was that by

applying this limit, it was not possible to reach a “critical height” (CH) of propellant—the height over which transition to a higher order reaction is possible. Consultation with GD-OTS, the main Canadian propellant producer in Canada, revealed that, in fact, the thickness of propellant in the bed is indeed the key parameter in potential transitions to detonation. GD-OTS employees manipulate large batch quantities of propellant daily; they also regularly burn excess production lots, based on pre-established CHs. Pierre-Yves Paradis, Research and Development Coordinator at GD-OTS, carried out specific experiments in 2004 and 2005 to determine the CH of the propellant they manufacture (ExproTech D&T Department 2005). The initial assumption at the basis of their experiments was that a real risk for transition to deflagration–detonation is present whenever propellant columns are exceeding the critical height in steel, aluminium, and cardboard containers, especially when ignition starts from the bottom of the propellant bed. This is representative of propellant in a manufacturing environment, as well as in storage conditions, and applies directly to the conditions prevailing when burning excess propellants on a table.

Their approach was partly based on previously published data (Hooker 1990; Bosch and Perena 1988; Vandebeek 1988; Goliger and Lucotte 1981; Napadensky et al. 1980; Napadensky et al. 1978; Johnson 1977) and it involved a mass combustion with confinement, using a fiber drum buried in gravel and sand up to a pre-determined level of propellant. They used heavy cardboard forming tubes of 40.6 cm diameter with variable heights of propellant beds. The ignition was made from the bottom and propellant heights were varied from 30.5 to 122 cm. The detection of transition to deflagration or detonation was made by measuring time of peak pressure at a known distance, which allowed the calculation of the pressure wave velocity. By running many experiments and modeling the CHs, they concluded that for M1 type propellants, the CH value was 180 cm. They established the CH of M1 propellant to be 107 cm to include a supplementary safety factor. The table described in their report allows a propellant bed of 10 cm thickness; furthermore, the ignition always takes place at the surface of the propellant bed. Our setup is, therefore, 10 times below the CH limit value determined by GD-OTS. Even so, all the tests that were conducted within this project were carried out taking into account a potential transition from deflagration to detonation.

After a number of repetitions without any transition events, and based on GD-OTS study and a thorough literature review, we are able to ascertain

that the probability of transition to detonation is extremely low under the conditions specified for the prototype table operation.

4.4.3.3 Table cooling-down time and meteorological conditions

It was critical from a safety standpoint to estimate the time for the table to cool down after a burning to avoid placing propellant bags on a table that was hot enough to trigger auto-ignition of the material. During the second and third Canadian trials, as well as for the U.S. trial, experiments were run using thermocouples placed in various locations when burning was conducted to measure the time for cooling down under various meteorological conditions.

The meteorological conditions under which the table could be used were carefully examined. The metallic composition of the burn table may allow solar radiation heating of the structure to a point where it would not be safe to operate in summer conditions. The prevalence of rain and snow were also considered as they might interfere with the burning process. Wind conditions were also examined. Stormy conditions, strong winds, and especially electrical storms must be avoided.

4.5 Test trials

4.5.1 February 2009 trial

The initial trial was held on the Valcartier test site located within Garrison Valcartier on 9 and 10 February 2009. The first prototype table designed and built without screens was laid down on a concrete pad.

The objectives of the February trial were to:

1. Monitor the table response to the burning conditions.
2. Characterize the burning residues (quantity of residues and the ratio of 2-4 DNT in the residues).
3. Verify the extent to which propellant grains are projected outside the table.
4. Measure the time for cool down.
5. Verify the degree of difficulty of collecting ashes from the table.
6. Measure the overall efficiency of the table.
7. Verify the impact of the bag placement in the table on the efficiency of the burn.

8. Validate that the use of the table does not allow transition to detonation.

Four burn tests were conducted on 9 February. Three tests used 150 kg of M1 propellant (bags 5, 6 and 7 only, mostly 6 and 7) that created a full table load and one test used 75 kg of propellant. For the three first burns, the propellant was laid out on the table to cover its entire surface with a single or double layer of bags; for the fourth burn, bags were placed in the center of the table to minimize the projection of grains. They formed a low-lying pyramid with two to three layers of bags in the center and a single layer of bags around the edge (Fig. 4-13 through 4-15). On 10 February, three more burn tests were conducted. The first, Test 5, used 75 kg of M1 propellant. Tests 6 used a mix of M67 and M3 bags as well as bulk M1 propellant grains. Test 7 used 104 kg of old M3 propellant charges that were stored by METC Valcartier and needed to be demilitarized (Fig. 4-16).



Figure 4-13. Transfer of propellant bags for burning test.



Figure 4-14. Prior to burning with 150 kg of M67 propellant load.



Figure 4-15. Prior to burning with 75 kg M67 propellant load.



Figure 4-16. Prior to burning with 104 kg of M4 propellant load.

The three burn tests on 10 February were conducted after the table height had been elevated to 1 m so that it was easier to load. Another reason for elevating the table was to increase the time the ejected propellant grains were airborne before reaching the frozen soil surface and becoming extinguished. The table was raised using concrete blocks as illustrated in Figure 4-17.

The meteorological conditions during the February trial were as follows: on the 9th, it was sunny with a light wind to the west, temperatures were between -24 and -18°C; on the 10th, it was sunny with no wind, temperatures ranging from -19 to -14°C.

Table 4-6 presents the date and time, propellant type, and mass burned for each burn test conducted over the 2 days.



Figure 4-17. Table on concrete blocks and prior to burning 75 kg of M67 propellant.

Table 4-6. February 2009 burn trial.

Trial	Date (m/dd/yy)	Time	Propellant	Quantity (kg)
1	2/09/09	10:00	M67	150
2		10:45	M67	150
3		13:40	M67	150
4		14:05	M67	75
5	2/10/09	09:50	M67	75
6		10:15	Mix of M67, M3, and bulk M1	Approx. 150
7		10:50	M3	104 of M1

4.5.2 November 2009 trial

A large scale trial was held at METC-Nicolet on November 2009 using the three new prototypes. This site possessed a large quantity (20,000 kg) of excess artillery propellant that was beyond its service life and judged unsafe to keep. Excess charge bags that had been accumulated by Valcartier artillery units had also been brought to Nicolet for disposal and were available. The trial was held at the Batterie 1 location and involved the METC team and the DRDC Valcartier team.

The objectives of the November trial were to:

1. Compare the various tables made of SS and aluminium and evaluate their resistance to the burn conditions.
2. Compare the effectiveness of the various shields to minimize projection of residues outside the table as well as to evaluate their resistance to the burning conditions.
3. Measure the burning temperatures behind the table, in the flame, in the table, and from radiant heat at locations adjacent to the table.
4. Validate if ignition in the table center would improve the burning process.

The three prototype tables that were tested were referred as:

- 1: RA310S Alloy SS (0.32 cm).
- 2: RA310S Alloy SS (0.635 cm).
- 3: Aluminium (0.635 cm).

The five screens or shields that were tested were referred as:

- a) Perforated sheet, diamond shape.
- b) Interlaced square.
- c) Welded square.
- d) Round hole perforated.
- e) Angle baffles.

4.5.2.1 Trial setup

The tables were located behind a wall to protect the personnel from possible detonation. Ignition and burning were recorded using a remotely controlled camera (Fig. 4-18 and 4-19). The presence of a fire fighting unit from GD-OTS was requested for the duration of the trial. Temperatures were recorded using thermocouples that were placed on the table, under the table directly on the steel or aluminium bottom, and below the table at 0.5 m from the bottom (Fig. 4-20). On the second day, radiation temperatures were monitored at distances of 5, 15 and 40 m from the table.



Figure 4-18. Shelter at Batterie 1 and protective wall.



Figure 4-19. Remotely controlled camera and acquisition system.

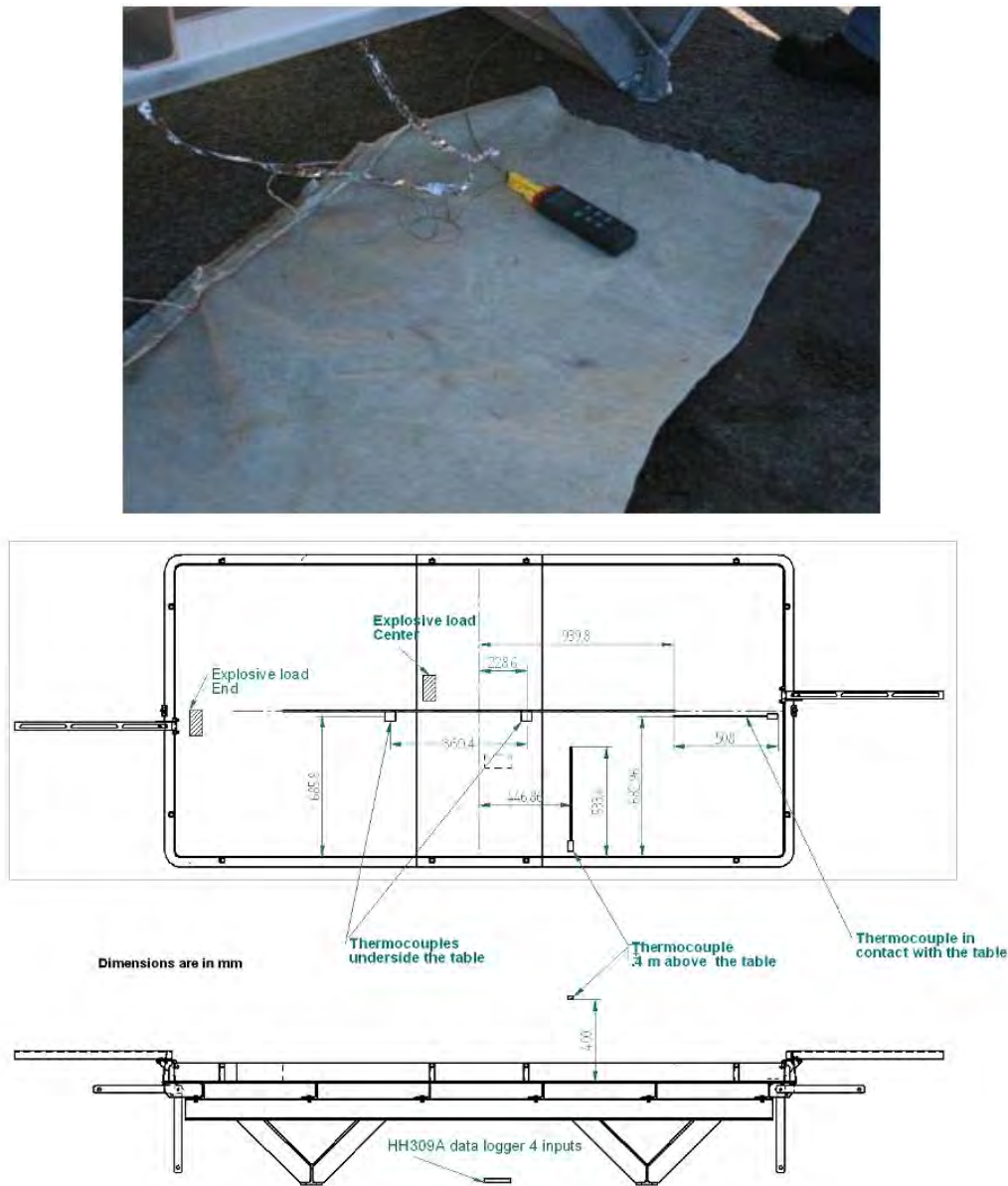


Figure 4-20. Thermocouples and data logger protected using an asbestos liner.

Table 4-7. November 2009 Nicolet burn trial.

Trial	Date (mm/dd/yy)	Time	Propellant ¹	Quantity (kg)	Table	Screen
1	11/17/09	10:15	V	200	1	a
2		13:00	V	300	2	b and c
3		14:15	V	250	2	e
4	11/18/09	09:30	N	195	2	d
5		10:30	N/V	295 (195/100)	3	d
6		14:00	N/V	295 (195/100)	3	d
7	11/19/09	09:05	N/V	368 (293/75)	3	d
8		10:30	N-Vrac	290	3	d
9		13:00	N-Vrac	240	2	d
10		14:15	N-Vrac	200	2	D

¹ V– Valcartier excess propellant; N– Nicolet excess propellant; N-Vrac– Nicolet Vrac propellant.

Ten burns were conducted over 3 days. Table 4-7 presents the date, time, propellant type, and quantity burned, as well as the type of table and screens used. The weather conditions for the Nicolet trial were sunny, winds between 0 and 5 km/hr in southeast direction, and temperatures ranging from -4°C in the mornings to 8°C in the afternoons. Trial 7 involved burning a total mass of 368 kg of propellant—almost twice the 200-kg limit that we had earlier imposed for the table use. This was done to validate that, even at this quantity, there would be no transition to detonation. Ignition was accomplished using an electric squib instead of a flare. In one trial, burn initiation was done in the middle of the table to test if a better burn would result from a central ignition.

4.5.3 March 2010 trial

A 2-day joint test exercise with CRREL was held at the DRDC test site on 30 and 31 March. Burn tests were conducted with both the static and mobile burn pan systems. This trial involved eight burns, four with the Canadian pan and four with the U.S. prototype.

The main objectives of the Canadian trial were the testing of aluminium and SS reinforced shields and the trial implementation of the proposed Standard Operating Procedure (SOP) for the table's future use by Canadian military units. A burning without charge 5 bags was also conducted to

avoid loading the table with lead. This came from a concern raised that small (nano) particles of lead might be lofted into the atmosphere during the burning process.

The main objective of the U.S. trial was the initial testing of the mobile propellant burn pan prototype. The U.S. team was also interested in observing the performance of the Canadian fixed table with the objective of improving any shortcomings of the U.S. design, allowing the U.S. team to benefit from the Canadian's experience and expertise.

A total of 1218 kg of M1 artillery (105 and 155 howitzer) and mortar propellant charges were burned in the two prototypes over the course of the trial. Table 4-8 details the eight burns that were conducted.

The meteorological conditions prevailing were sunny skies, relatively windy (5-10 km/h), with temperatures between -10 and -2°C.

The detailed objectives of this trial were to:

1. Test the new reinforced shields with aluminium and SS frames.
2. Test the draft SOP (under the responsibility of DAER).
3. Perform a burn without charge 5 bags.
4. Test alternative ignition methods (under the responsibility of DAER and DAEEME).
5. Measure to what extent material is ejected from the table and analyze if this material contains 2,4-DNT.
6. Test the proposed personal grounding devices.
7. Provide a test site and excess propellants for the U.S. testing of their mobile prototype.
8. Test of U.S mobile burn pan with large propellant loads.
9. Determine what residues remained in the mobile pan, with a special interest in heavy metals (lead).
10. Derive an estimate of ejected propellant from the mobile pan.
11. Measure structural temperatures of the mobile burn pan.

Table 4-8. March 2010 burn trial.

Trial	Date (mm/dd/yy)	Time	Propellant burned		Table
			Mass (kg)	Type: Source	
1	3/30/10	10:02	106.4	M1: 105 mm	U.S.
2		10:35	120	M1: 105 (no lead)	CA-Al framed shields
3		11:15	120	M1: 105 mm	U.S.
4		13:05	50	M1: mortar ?: rocket motor	U.S.
5		14:00	200	M1: 105 mm	CA-Al framed shields
6	3/31/10	09:10	112	M1: 155 mm	U.S.
7		10:05	250	M1: 105 mm	CA-Al and SS framed shields
8		10:55	260	M1: 105 and 155 mm	CA-Al and SS framed shields

Figure 4-21 shows the Canadian fixed table and the reinforced shields that were tested. Figure 4-22 shows the table loaded with bags 4, 6, and 7 to meet objective 3. Figures 4-23 and 4-24 present the grip and bracelet included in the Canadian grounding devices to be tested. And, finally, Figures 4-25 and 4-26 present the U.S. table.



Figure 4-21. Table with new reinforced shields.



Figure 4-22. Table loaded with charge bags 4, 6 and 7.



Figure 4-23. Grip to hold the conductive strap to the table.



Figure 4-24. Conductive bracelets tested in the trial.



Figure 4-25. U.S. table prototype.



Figure 4-26. U.S. table prototype prior to ignition.

4.6 Sample analysis

4.6.1 Energetic materials

All samples were analyzed at DRDC-Valcartier. High Performance Liquid Chromatography (HPLC) analyses for 2,4-DNT were performed with a Agilent HP 1100 equipped with a G1322A degasser, a G1311A quaternary pump model, a G1313A autosampler, and a G1315A ultraviolet (UV) diode array detector monitoring at 205, 230, and 250 nm. The injection volume was 20 μ L and the column used was a Supelcosil LC-8 column 25 cm \times 3 mm \times 5 μ m eluted with 15:85 isopropanol/water (v/v) at a flow rate of 0.75 mL/min. The column temperature was maintained at 25°C during the

analysis. Standards and solvents were diluted 1:1, acetonitrile to water (0.5 mL acetonitrile/0.5 mL water). The 14 compounds analyzed using this method are HMX, RDX, 1,3,5-trinitrobenzene (TNB), 1,3-dinitrobenzene (DNB), nitrobenzene (NB), trinitrotoluene (TNT), tetryl, NG, 2,4-DNT, 2,6-DNT, 2-amino-DNT, 2-nitrotoluene (NT), 3-NT, and 4-NT. Nitrocellulose was not analyzed as is a polymeric material and cannot be extracted or quantified.

4.6.2 Hazardous materials analysis

A representative sample of burning residues from the fixed burn pan was analyzed.¹ The sample was extracted by the external laboratory following the hazardous material protocol. Leachable materials including metals were analyzed by induced coupled plasma coupled to mass spectrometry (ICP/MS).

4.7 Results

4.7.1 February 2009 trial

4.7.1.1 General observations

Burning temperatures could not be measured because the thermocouples were not functioning at the time. However, the flame temperature was recorded using a remote OMEGA Laser TruRMS supermeter™. The maximum temperature recorded, 580°C, occurred during the third burn test. The ambient meteorological conditions were cold enough to allow the table to quickly return to less than 10°C and allow residue collection to occur in less than 15 minutes. The seven burns each occurred quickly, lasting less than 30 s per burn, with an impressive height of the flame at maximum burn (Fig. 4-27 through 4-29).

¹ Pamela Cushing from Director General Land Equipment and Program Management (DGLEPM) after the Nicolet trial and sent to SM Environment, 75 Queen Street, office 5200, Montreal, Quebec, Canada, H3C 2N6.



Figure 4-27. Ignition of the propellant bed.



Figure 4-28. Three seconds after ignition.



Figure 4-29. Maximum intensity of burning 10 s after ignition.

The intense burns projected residues and unburned propellant grains outside the table. We collected and weighed the residues surrounding the table following the trials. Of the 831 kg of propellant burned, we estimated that less than 1 kg ($\approx 0.1\%$) of the propellant was kicked out during the trial. In general, residues were projected to a distance of 60 cm outside the table upwind and 1.5 m downwind (Fig. 4-30 and 4-31).



Figure 4-30. Residues projected outside the table, trial 1.



Figure 4-31. Residues projected outside the table, trial 3.

After each burn, residues were collected from the floor of the pan in 5-L plastic pails using a shovel and a dust collector (Fig. 4-32 and 4-33). The remains of the ignition flare caught the pails on fire for trial 6, so plastic pails will not be used in the future.



Figure 4-32. Burning residues collection.



Figure 4-33. Burning residues from trial 3.

Residues were brought back to DRDC, weighed, and processed to separate the lead from the organic ashes. Acetonitrile was added to the ashes in the pails and the solution decanted. This process was repeated three to five times until only lead particles remained in the pails. The residues in the pails were dried and weighed. The decanted acetonitrile portion contained both a soluble fraction and an insoluble fraction that floated on its surface. The process was completed using an ultrasonic bath for 30 minutes to ensure that all soluble compounds were extracted. The insoluble ashes were filtered, dried, and weighed. The soluble fraction was isolated and processed through HPLC for the measurement of 2,4-DNT.

Figures 4-34 to 4-36 illustrate the lead and organic matter segregated from the burning residues collected from trial 1. The right-hand side of Figure 4-34 shows the remains of the ignition flare. Table 4-9 presents the mass of propellant processed, the total amount of residues collected, the quantities of segregated ash and lead, and the percent and quantity of 2,4-DNT collected.

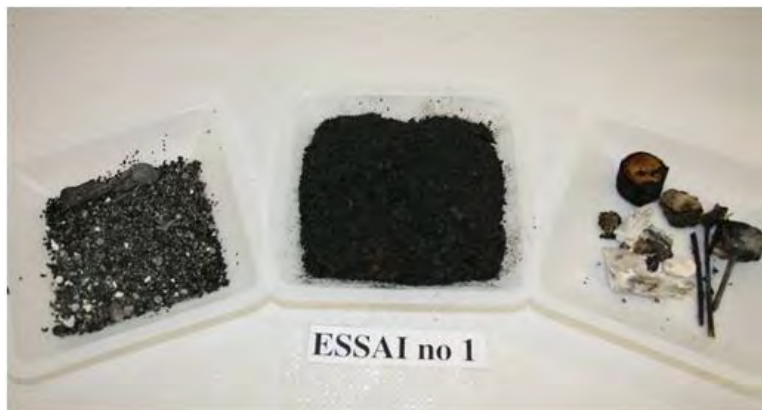


Figure 4-34. Inorganic (left), organic (center) and flares (right) residues segregated, trial 1.



Figure 4-35. Close-up of the lead deposited in the burn table.



Figure 4-36. Close-up view of the organic matter deposited in the burn table.

Table 4-9. February 2009 burn trial results.

Trial	Mass of propellant burned (kg)	Residue Mass (g)			% of residues deposited	Mass of 2,4-DNT deposited (g)	% of 2,4-DNT residual
		Total	Ash	Lead			
1	150	417	187	230	0.3	5.2	0.003
2	150	750	178	572	0.5	3.5	0.002
3	150	934	155	779	0.6	1.8	0.001
4	75	432	192	240	0.6	2.9	0.004
5	75	300	124	176	0.4	2.6	0.003
7	104	408	379	29	0.4	1.7	0.002

In the following, we address the objectives of this trial.

4.7.1.2 Monitor the table response to the burning conditions

The table responded perfectly to the burning conditions as no warping was observed and the removal of burning residues proved to be easy.

4.7.1.3 Characterize the burning residues (quantity of residues and percentage of 2,4-DNT)

The proportion of ashes versus lead varied from one burning to another depending on the number of charge 5 bags that were included per burn. The exact numbers of charge 5 bags was not monitored, so no mass balance can be calculated for lead. However, it can be stated that a large proportion of lead remains in the table in metallic form.

The mean percentage of waste produced per burn is 0.5% w/w for a mass reduction of 95.5%. The mean deposition rate of 2,4-DNT on the table is 0.003 %, which is three orders of magnitude smaller than what is deposited when burning on the soil surface (1%). This means that the residual waste contains mainly lead, ashes, and traces of 2,4-DNT and can be processed as hazardous waste.

4.7.1.4 Verify the extent to which propellant grains are projected outside the table

Approximately 0.1% of residues were projected outside the table. This was a concern and the shields were developed to minimize this phenomenon as much as possible. The projection distances varied between 0.5 and 2 m.

4.7.1.5 Measure the burning temperature and the time for cool down

No thermocouples were available at the time of trial. The flame temperature recorded using a remote sensing device was approximately 600°C. The time for cooling down in the winter conditions was around 10 minutes. After the safety clearing was done by the EOD technician, the table temperature was back to around 20°C.

4.7.1.6 Verify the degree of difficulty of collecting ashes from the table

It was very easy to scrape the ashes from the table using a shovel. Other scraping tools will be investigated in future trials. The use of a dust mask, sun glasses or safety glasses, and gloves will be recommended as minimal personal protection equipment. There are two problem areas related to the collection of the residues: the remains of the railway fuses used to ignite the propellant and the remains of the flash ignition reducer pellets included in the 155-mm propelling charge stuck to the bottom of the pan. The railway fuses will be eliminated from the ignition train owing to their production of dioxins and furans, resolving this issue. The flash reducing pellets will remain in future processing of 155-mm propelling charges, but this is still manageable.

4.7.1.7 Measure the overall efficiency of the table

The table performance was very good. No warping was observed, allowing very high burning throughput. The residues in the pan were easily and quickly collected. There was large mass reduction and low levels of remaining 2,4-DNT. The ignition tool on the table proved to be helpful and

well designed. However, we observed that the ignition cord could stick to the channel and future channels will be designed with a few openings in them to minimize this problem. The table allowed the burning of a large quantity of bags at once and allowed a burn repetition in a shorter time than when burning directly on the soil (24 hours waiting time is mandatory when burning on the soil surface).

The table height allowed a fast cool-down and the steel also resisted the high temperatures well, as the table responded very well to the burning with no structural damage. The ergonomics of the table needs improvement as loading the charge bags on the low table proved to be difficult on the backs of the users. The table height will be raised.

The table was easy to move using a forklift. The table cover was lightweight, easily transported by two persons, and offered a strong resistance through its reinforced structure; it easily supported two adults standing on it.

4.7.1.8 Verify the impact of the bag placement in the table on the efficiency of the burning

The burning at full load of 150 kg (vs. 75 kg) led to better combustion and less projection of residues outside the table. The full loading of the table will thus be recommended.

4.7.1.9 Validate that the use of the table does not allow transition to detonation.

The burnings were stable and no transition to detonation was observed.

Tests were conducted in parallel with research to verify the source of dioxins and furans: the flare was highly suspected to be the source. It will then be replaced by other ignition means in future trials.

Improvements to the structure and further tests needed based on this first trial are as follows:

- Minimize the ejection of residues outside the table using screens or baffles.
- Open the ignition tube partly to minimize adhesion of the ignition cord.
- Monitor the burning behavior during other meteorological conditions.

- Monitor the burning temperatures using thermocouples.
- Look for other material for the table main frame for cost reduction.

4.7.2 November 2009 trial

The Nicolet trial involved the destruction of both excess charge bags from Valcartier and obsolete propellants stored in Nicolet. It was conducted over 10 burns. Table 4-10 presents the results obtained for the trial.

The burning residues were collected using both a shovel and an ice breaker. The ice breaker proved to be a very efficient tool to scrape the residues from the table. The residues were deposited in a 45-gallon drum, a method that will be recommended for future users of the table. A representative sample was sent to an external lab for dangerous goods assessment and was found to contain high concentrations of leachable lead (2450 mg/kg).

Table 4-10. November 2009 Nicolet burn trial results.

Test	Table	Screen	Observations	Maximum temperature reached (°C)	Burning duration (s)	Time for cooling down (min)
1	1	a	Severe warping of table frame; screen reduced grain projection but not completely	410	33	N.A. ¹
2	2	b-c	Table 2 reacted well; screens b and c: projections 0.5 m away	190	30	32
3	2	e	Less effective burn: lack of oxygen, projections up to 1.5m	260	29	30
4	2	d	Good burn, few projections	190	20	30
5	3	d	Good resistance of the Al table, no projections	250	25	22
6	3	d	Good burn	270	18	26
7	3	d	High load/ 15–20 cm height. More projections but no transition to detonation	450	19	29
8	3	d	Very fast burn; radiation monitored at 10 and 33 m	Max temp = 255 Rad at 10 m = 15 Rad at 33 m = 8	14	22
9	2	d	Radiation monitored at 5 m	Max temp = 650 Rad at 5 m = 70	20	N.A.
10	2	d	Good burn	275	20	N.A.

¹ N.A. – Not Available

In the following, we address the objectives of this trial.

4.7.2.1 Compare the various tables made of SS and aluminium and evaluate their resistances to the burning conditions

The 0.32-cm SS table did not resist the burning conditions and warped after the first burn. The thinner SS material cannot be used for the table frame owing to insufficient strength. The aluminium table reacted very well to the burning conditions and no warping or corrosion was observed. At the completion of the burn trial, the table was washed with water and wiped to determine if the aluminium material was attacked, which did not occur. The conclusions are that both the 0.635-cm SS and aluminium table frames can be used. The aluminium version has the advantages of being lighter and lower in cost, while being potentially less corrosion and resisting damage in the long term. If the table is to be frequently lifted to the disposal location, the SS version is recommended.

4.7.2.2 Compare the efficiencies of the various shields to minimize the projections of residues outside the table and determine the shields' resistance to the burning conditions

Shields a, b, and c led almost to the same result. They minimized grain projection when compared to the table without shields, but projections up to 0.5 m away from the table were still observed. Shield e, the angle baffle design, led to two unwanted situations. First, the burning process was poor and a lack of oxygen caused by the baffles was obvious. A much larger quantity of unburned residues was observed. Secondly, grain projection was worse than without any shield, and grains were projected as far as 1.5 m away from the table (Fig. 4-37). This was attributable to the turbulences caused by the baffles. This design has thus been abandoned.

Shield d proved to be highly efficient at keeping the grains inside the table and allowed enough oxygen intake to ensure complete combustion (Fig. 4-38). Shield d was therefore selected as the preferred shield for further testing.

A problem observed was the warping of the shield frames. The frames were not built strong enough to resist the intense heat generated and the temperature differences between both sides of the shield. This needed improvement and stronger shields frames were designed for the next trial.



Figure 4-37. Trial 3 using shield e, after burn.



Figure 4-38. Full burning using the model d shields.

4.7.2.3 Measure the burning temperatures directly behind the table, in the flame, in the table, and from radiation at distances from the table

As presented in Table 4-10, the maximum temperatures measured directly in the flame varied from 190 to 650°C. Flame temperatures were mostly in the 250°C region. The high degree of variation observed can be explained by the difficulty of measuring precisely the flame temperature at the same location from trial to trial and the rapidity and intensity of the burning process. Figure 4-39 shows two of the thermocouples used to measure the flame temperature. One, seen in the foreground, was approximately 0.5 m from the table; the other, at 5 m behind the table (marked by the orange cone), measured the radiation temperature at that distance. In the gun barrel, the burning process is confined, leads to a sharp pressure increase, and temperatures as high as 1200°C are theoretically reached. That is not the case in an unconfined environment and the flame temperatures are much lower, as observed here. This is a good thing from a lead volatilization perspective, as lead could be melted but not volatilized. On the other hand, the lower burning temperature might cause the production of incomplete oxidation compounds, less environmentally friendly than the completed oxidized end-products such as carbon dioxide. The two thermocouples installed on the surface of the table reacted similarly in all trials, and in general they came back to 30°C within 30 minutes. At that temperature, the table can be reused safely for another burn. Figure 4-40 presents an example of temperature acquisition curves that were obtained throughout the trials.

Radiation temperatures at distances of 5, 10, and 40 m away from the table were also monitored. The maximum temperatures measured were 8°C (40 m), 15°C (10 m), and 70°C (5 m). At the time, the ambient temperature was about 2°C. A small rise in temperature was still observed 40 m away, without representing a risk to human health. The minimum distance in the SOP took that into account and a safety factor was added for a windy situation as the temperature rise will be more intense in the wind direction.



Figure 4-39. Thermocouples in the flame and 5 m away (orange cone) for radiation measurement.

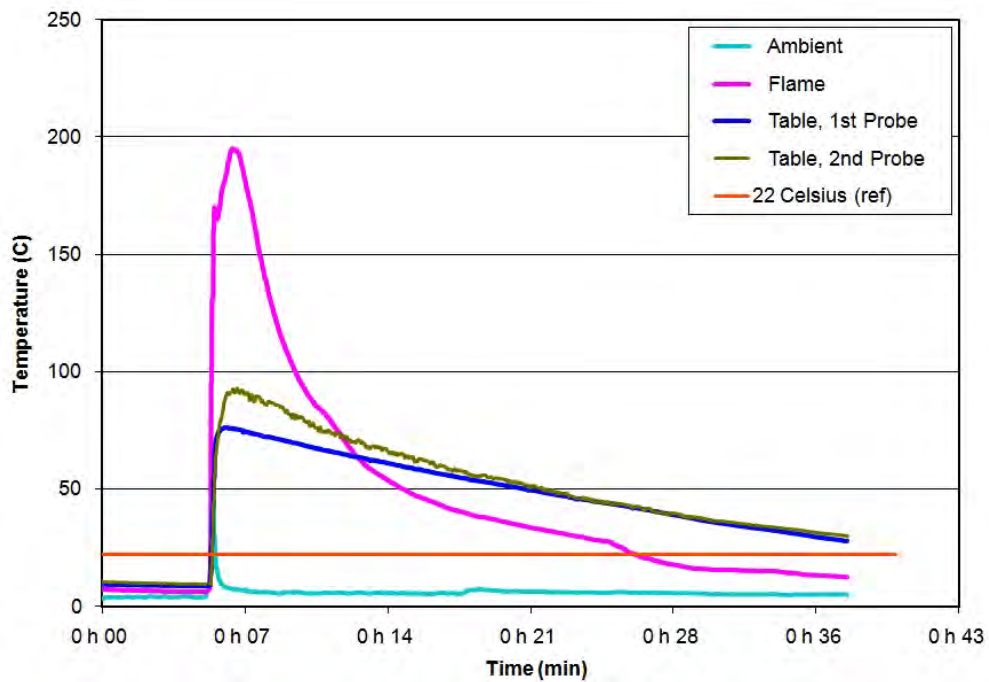


Figure 4-40. Temperatures monitored during trial 2.

4.7.2.4 Verify if ignition of the burn in the center of the table would improve the burning efficiency

Two trials involved the ignition of the propellant bed in the center of the table. In both cases, the burning did not proceed faster or better. Placing the ignition train in the center of the table increases the risks because the

ignition port cannot be used and the installation is made over the propellant bed. Thus, this configuration for ignition was abandoned.

4.7.3 March 2010 trial: Canadian trial results

The March trial involving both Canadian and U.S. burn tables was conducted in spring conditions, complementary to the former trials. Results of the Canadian table tests will be reported first.

4.7.3.1 Test the new reinforced shields with aluminium and SS frames

Both frames reacted very well to the burning conditions. However, a little warping was still observed in both cases. We hypothesized that the cohesion between the frames and the round-hole perforated sheets was too stiff and caused the warping. We decided to include a flammable washer in the shield design that would burn in the first use and allow a movement between the frames and the sheets, thus minimizing the warping. A new set of shields was designed and ordered for further testing. The aluminium-framed shields were much lighter in weight, which greatly improves their ease of manipulation. The aluminium frame was selected based on its similar robustness, lower cost, and lighter weight.

4.7.3.2 Test the draft SOP (under the responsibility of DAER)

Execution of the draft SOP was successfully accomplished and the SOP was further improved using feedback from all team members. Many modifications were made and pictures were taken to better illustrate the SOP.

4.7.3.3 Perform a burn without charge 5 bags

No charge 5 bags were consumed during trial 3. The loading time was greatly increased since all the charge 5 bags had to be removed individually from the propellant bed. Instead of a table loading time of approximately 15 minutes, the loading time was around 60 minutes. Furthermore, it involved a lot of manipulations of the charges bags, which could potentially generate static electricity and represents a danger of inadvertent propellant ignition. Lead particles are not thought to be lofted into the atmosphere, and the lead residues can be easily managed as hazardous waste when collected afterward from the table. Based on these factors, removing charge 5 bags prior ignition is not recommended.

4.7.3.4 Test alternative ignition methods (under the responsibility of DAER and DAEME)

An alternative propellant ignition method was successfully implemented and DAER will soon publish the alternative ignition train recommended for use with the table.

4.7.3.5 Measure to what extent material is ejected from the table and analyze if this material contains 2,4-DNT

The DRDC test site location was favorable for collecting the larger ash particles that were ejected from the table. The tables were placed on a large concrete pad and there was also a snow cover that made it easy to locate and collect these large particles. After the four burns on the Canadian table, the particles were deposited in an area estimated to be approximately 10 m². They were collected and brought back to DRDC to be weighed and extracted to measure the remaining 2,4-DNT. Most of what was collected was the remains of the cotton cloth used for the bags. Figure 4-41 presents an image of a representative particle collected. The total mass of gathered residues was 2.4 g. Hypothetically, if only 10% of what was ejected was collected (which is believed to be the worst case scenario, because care was taken to ensure that most of the particles were collected), it can be estimated that, at the worst, around 25 g of unconsumed cotton cloth particles were dispersed after burning 830 kg of propellant, which represents 0.003% w/w. The remains were extracted and contained 0.5 mg of 2,4-DNT. By multiplying this by a safety factor of 10, then at the most, 5 mg (<0.001%) of DNT was dispersed after processing 830 kg of propellant. This amount is negligible and does not represent an environmental threat.

4.7.3.6 Test the personal grounding device

Both the bracelet and grip worked properly and was a great improved over the former versions of grip and bracelet. The use of this new device will then be implemented in the SOP.



Figure 4-41. Representative large particle collected near the burning location.

4.7.4 March 2010 trial: U.S. results

Four burns were conducted in the CRREL mobile burn pan. The first two were with M1 single-base 105-mm howitzer propellant. The third was with a mixture of single-base M1 mortar propellant and rocket propellant of unknown composition. The final burn was with M1 155-mm howitzer propellant (Table 4-8). All propellant was contained in its original charge bags. All burns were initiated by the Canadian UXO technician.

A total of 388.4 kg of M1 propellant was burned. The largest burn of M1 propellant was 120 kg, the one mixed mortar–rocket burn contained about 50 kg of propellant. Ten 0.28-m² collection trays were placed outside the burn pan to capture ejected grains. The area covered by these trays represents 20 m² outside the burn pan area and included most of the area containing ejected propellant grains. These trays were collected following the end of the U.S. trials and analyzed by DRDC in Valcartier.

Results of the tray content analyses included both lead as well as organics. The lead content in the trays was 46 g. The organic material totaled 5.85 g. Duplicate analyses of the organic material resulted in 2,4-DNT masses of 0.32 and 0.33 g. Extrapolated over the 20-m² area surrounding the burn pan we get an estimate of 2.3 g of 2,4-DNT ejected from the propellant burns. No NG was detected, leading us to conclude that all the detectable energetics were derived from the M1 propellant burns. The nominal mass

of DNT in M1 propellant is 10%. This gives us approximately 39 kg of DNT for the burns. The ejected propellant thus represents $5.9 \times 10^{-3}\%$ of the initial DNT load.

Temperatures of the pan were fairly mild, with a maximum temperature not exceeding 130°C. The ambient temperature at the time of the tests was $\pm 5^\circ\text{C}$ with winds of under 3 m/s. Cool-down was rapid, with the maximum pan temperature reaching 30°C within 7 minutes. The pan was reloaded within 15 minutes following the cessation of the previous burn.

The ejection of lead was significant, and small particles were recovered from the pan bottom, the bonnet screen, and the trays. Only the lead on the trays was measured. We are unsure of the percentage of lead ejected as the lead content of all the 105-mm howitzer charge bags was not known.

In addition to lead, potassium nitrate, used as a flame suppressant in the artillery charges, was found both inside and outside the burn pan. Small pieces of charge bags were observed outside the pan as well as enmeshed in the bonnet grating, a result of the violent deflagration of the propellants. Observation of the burn indicates that flames from the burn blew through the unwelded seams and door of the pan as well as the interface of the bonnet with the pan.

4.8 Conclusion and future implementation

A Canadian burn table for the safe destruction of artillery excess propellant was successfully developed. The end product has been obtained through many trials and iterations to optimize the burning process ensure the safety of the personnel that will conduct the destruction, and minimize the environmental footprint of the global operation. Using the burn table allows a mass reduction of 99.5%, generates mostly ashes, and resulted in residues containing only 0.003 % of the original mass of 2,4-DNT in the burned propellant. Lead that was contained in charge 5 bags of the M67 105-mm caliber propellant remained in the pan. The mixed organic and inorganic residues in the table are easily collected and can be processed as hazardous waste. A minimal amount of material is ejected outside the table and is composed mostly of partially burned cotton cloth.

The Canadian burn table project was presented to various audiences during its development. This allowed great teamwork and continuous feedback on the project orientation and direction. The close collaboration,

support, and involvement of DRDC, DLE, DAER, DAEME and G4 Ammo allowed the rapid development and fielding of this new asset and the success of the whole process. A procedure for the safe return of the excess charge bags by the artillery units to the ammunition stores has been published. The proposed plans recommend that excess charge bags be brought back to ammo supply by the artillery units, stored by the ammo supply units, and burned once or twice a year under favorable meteorological conditions. The ignition protocol will be modified to eliminate the use of the perchlorate-based railroad flare. An SOP for the use of the table will be published by DAER. The implementation of the burn table is under way and 11 units across Canada shall be deployed in early 2011. Excess artillery and mortar propellants will then be destroyed across Canada with minimal environmental impact. The close collaboration of the artillery units, ammo supply units, and environmental officers will be critical for the success of the implementation of the protocol. Residues will need to be processed as hazardous wastes by the base environmental officers. In term, the Army's RTAs will become more sustainable with the implementation of this new disposal process.

The U.S. mobile pan worked well, handling large (120-kg) loads of propellants without warping of the structure. Although the amount of ejected DNT was small over the course of the tests (<0.007%) we would like to see even less contamination resulting from the burn. The pan is also heavier than we would like. We have thus redesigned the system, using aluminum rather than stainless in the base structure and incorporating the Canadian perforated steel into the sides of the bonnet. Seams will be continuously welded to prevent blow-out. We anticipate a total weight of less than 160 kg for the unit when completed. We are currently trying to line up sites to test the new structure.

5 Fate and Behavior of Energetic Material Residues in the Unsaturated Zone: Sand Columns and Dissolution Tests

Richard Martel, Sébastien Lange, Sébastien Côté, Sonia Thiboutot, and Guy Ampleman

5.1 Summary

Use of energetic materials is central to the training of military personnel for combat operations. During live-fire training, these materials are not fully consumed, leading to deposition and accumulation of energetic compounds on training lands. The goal of this project was to study the transport in unsaturated soil of energetic materials (EM) derived from actual training activities. These activities included propellant residues (2,4-DNT) from an artillery firing position, explosives residues (HMX, TNT, and RDX) from an anti-tank impact area, and burn residues from a gun propellant disposal site (2,4-DNT). The source materials were spread on top of six large columns filled with uncontaminated sand. The columns (60-cm diameter × 60-cm tall) were watered at 8°C to simulate autumn rain or spring snowmelt for an equivalent period of 2 years following the Valcartier, QC, precipitation pattern. Effluents containing dissolved energetic compounds were sampled regularly and analyzed for EM. Ammonium perchlorate was added as an inert tracer to evaluate the transport pore volume and the retardation factor of each EM.

After a 1-1/2-year experiment, no EM was detected in the effluent from the artillery firing position tests, indicating that the propellant had reached a condition in which the target analyte (DNT) was no longer able to diffuse out of the propellant grains. HMX and TNT leached rapidly from the EM in the anti-tank impact area and may affect between 500 and 5000 L of groundwater per 1 m² of contaminated soil. The 2,4-DNT also leached readily from the gun propellant burn residues and may affect between 2200 and 3400 L of groundwater per 1 m² of contaminated soil, indicating that burning residues and Octol residues represent a direct hazard for groundwater.

Complementary water drop dissolution tests were conducted to define the input function of EM at the top of the large columns and correlate results from both setups. These tests used the same contamination sources and conditions as the column tests, as well as with Composition B particles, with and without suction. Effluent was collected regularly and analyzed for EM and showed good mass balance at the completion of the tests. Water drop tests results suggest that the residence time of applied water in contact with the particles, the duration of the test, the compositional heterogeneity of the formulations, and the specific surface of EM are the principal parameters that control EM dissolution. Seasonal precipitation rates and water volume did not influence EM dissolution. It has proven difficult to correlate the water drop test results with what was observed on the large sand columns owing to compositional heterogeneity affecting the smaller samples used in the water drop tests, the water drop size, and frequency that affect the effective water volume for dissolution. Another setup was proposed to ensure the consistency of the dissolution and the large sand column tests.

5.2 Sand columns

5.2.1 Introduction

For more than a decade, research efforts have been dedicated to the study of the environmental impact of military live firing activities on surface soils and groundwater. However, few studies have been conducted on the fate of EM in the unsaturated (vadoze) zone. The main goal of this ER-1481 task was to study the fate and transport of EM residues recovered from three different locations on three active Canadian Forces bases: an anti-tank impact area at Canadian Force Base (CFB)—Gagetown, a firing position for artillery at CFB Petawawa, and an expedient propellant burn test site at CFB Valcartier. At the anti-tank impact area, the residues resulted from the use of M-72 or Carl Gustav antitank rockets that disperse 2,4,6-trinitrotoluene (TNT) and octahydro-1,3,5,7-tetranitro-1,3,5,7-tetrazocine (HMX) particles of various sizes upon detonation or impact. At the CFB Petawawa artillery firing position, the main EM is 2,4-dinitrotoluene (2,4-DNT). The third type of ammunition residues studied were from the test burning of excess propellant bags left over from artillery training exercises, contains 2,4-DNT and 4-A-2,6-DNT (4-amino-2,6-dinitrotoluene). Contaminated soils from these three sources were spread on six large soil columns (two columns per source of contamination) containing uncontaminated sand from the Arnhem training range of CFB Val-

cartier. Water was applied to the columns for a period equivalent to 2 years of precipitation, following the precipitation pattern at Valcartier. Spring and autumn are the snowmelt and rainy seasons, respectively; summer and winter are considered the dry seasons. The laboratory temperature was set at 8°C, except during the summer period, when it was set at 20°C. To evaluate contaminant transport through the unsaturated zone (soil column), water effluents were sampled frequently in wet seasons and analyzed to determine EM concentration.

5.2.2 Methodology

5.2.2.1 Sand sampling for column filling

Uncontaminated sand that was used to construct the soil column was collected from a gravel pit close to Arnhem range at CFB Valcartier. Shovels were used to transfer the sand into 200-L plastic drums with large polyethylene bags inside. Before their use, the shovels were alternatively decontaminated with hypochloric acid, acetone, and acetonitrile and rinsed with distilled water. Then, sand was transported to the laboratory and dried by spreading it on a polyethylene tarp in a layer 5–10 cm thick. The sand layer was tumbled after 2 days to allow a more uniform drying. Finally, when the sand was at its residual humidity, it was sieved at a diameter smaller than 9 mm to remove large particles and put back in polyethylene bags for storage. The Arnhem sand physico-chemicals properties are presented in Table 5-1.

Table 5-1. Arnhem sand physico-chemicals properties (from Bellavance-Godin 2009).

CEC	2.29 m _{eq} /100g _{soil}	Fine sand %	24
Total organic carbon %	0.1	Very fine sand %	7
Gravel %	3	Silt %	< 1
Very coarse sand %	8	Clay %	< 1
Coarse sand %	18	Classification (USDA)	Sand
Medium sand %	40	D ₅₀ (mm)	0.375

5.2.2.2 Preparation of the fiberglass wicks

To drain the sand column, fiberglass wicks were installed at the bottom of the column. The bottom surface was made to include seven conical-shaped depressions, each with a hole at the center. In each depression, nine fiber-

glass wicks, measuring $25\text{ cm} \pm 0.5\text{ cm}$ long, were positioned in a star pattern with 10 cm of fiberglass inside the depression (radius of conic depressions) (Fig. 5-1). Fiberglass was used because its sorption of EM is negligible. The 15 cm of the fiberglass wicks exterior to the column creates suction on the water inside the sand column and allows it to drain evenly into the 2-L glass cylinders that were put under each of the seven column outlets. This stopped any loss of water from the effluent.



Figure 5-1. Fiberglass wicks positioned on the bottom of each column.

5.2.2.3 Sand column filling

Sand columns were filled and compacted to a bulk density (ρ) of 1.70 (± 0.01) kg/m³. Sand layers 5 cm in height (H) equivalent to a mass (M) of $23.7\text{ kg} \pm 1.4\text{ kg}$ were sequentially added and compacted to reach the bulk density according to eq 1:

$$M = \pi \times r^2 \times H \times \rho \quad (1)$$

where: r = the column radius of 29.8 cm. Therefore:

$$M = 3.14 \times 29.8^2 \times 5 \times 1.7$$

or $M = 23,713\text{ g}$ ($\approx 24\text{ kg}$) of sand for a 5-cm soil layer.

Between each sand layer, the sand was scarified to 0.5 cm deep with a scraper to link the adjacent layers and ensure good hydraulic contact. During the compaction, the mass of sand for each layer was noted to calculate

the average bulk density and the average total porosity of the entire soil column (Table 5-2). Thus, to stay constant during the compaction, each column was marked inside at every 5 cm, and each soil layer was compacted uniformly to the marked layer height to avoid any bulk density variation into the column (Fig. 5-2). The average total porosity obtained for all sand columns was $0.36 \pm 0.01 \text{ cm}^3/\text{cm}^3$, and the average bulk density was $1.70 \pm 0.01 \text{ kg/m}^3$.

In each soil column, three TDR probes were installed during filling: one at 55, one at 35, and one at 15 cm from the soil surface. These sensors were used to measure the water content of the soil column during the experiment.

Table 5-2. Mass of Arnhem sand for each 5-cm layer, with the average bulk density and the total porosity of each column.

Lower depth (cm)	Upper depth (cm)	Mass of uncontaminated sand (kg)					
		Column A	Column B ¹	Column C ¹	Column D	Column E ¹	Column F ¹
65	60	23.6	23.6	23.6	23.6	23.6	23.6
60	55	23.6	23.6	23.6	23.6	23.6	23.6
55	50	23.6	23.6	23.6	23.6	23.6	23.6
50	45	23.6	23.6	23.6	23.6	23.6	23.6
45	40	23.6	24.0	23.6	23.6	23.6	23.6
40	35	23.6	23.6	23.6	23.6	23.6	23.6
35	30	23.6	23.6	24.0	23.6	23.6	23.6
30	25	23.6	23.6	23.6	23.6	23.6	23.6
25	20	23.1	23.6	23.6	23.6	23.6	23.6
20	15	23.6	23.6	23.6	23.6	23.6	23.6
15	10	23.6	23.6	23.6	24.9	25.4	23.6
10	5	23.6	23.6	23.6	23.6	23.6	23.6
5	0 ¹	23.6	23.6	23.6	23.6	24.9	23.6
Total mass (kg)		306.3	307.2	307.2	308.1	309.9	306.8
Bulk density (kg/m ³)		1689.08	1694.05	1694.05	1699.01	1708.94	1691.84
Total porosity ² (m ³ /m ³)		0.36	0.36	0.36	0.36	0.35	0.36

¹ The upper layer included clean sand and contaminant material (see Section 5.2.2.5 *Pre-test preparation*).

² Average total porosity was calculated with the equation $1-\varphi b/\varphi s$, where φb is the average bulk density and φs is the sand particles density (2650 kg/m^3).



Figure 5-2. Soil compaction in the sand column.

5.2.2.4 Residues and soil sampling

Contaminated soils resulting from three different activities were collected to seed the column surfaces for these tests. Soil containing propellant residues was sampled following the artillery powder burning test on snow at CFB Valcartier. The propellant burned was single-base M1 propellant for 105-mm artillery guns composed primarily of nitrocellulose (NC) and 2,4-DNT. These residues had different size fraction and can reach few millimeters. These residues contained up to 159,000 mg/kg of 2,4-DNT (Table 5-3), and nitrocellulose. They were spread on columns A and D.

Soil from the Wellington antitank impact area at CFB Gagetown was sampled in October 2008. The soil was contaminated with octol, which contains HMX and TNT. There is also potential NG and perchlorate contamination from unspent rocket fuel.

Soil contaminated with propellant residues was collected from the artillery firing position Hotel Tower at CFB Petawawa in the autumn of 2008. The soil sample is a multi-increment sampling taken over the first 30 m in front of the firing position. Both NG and 2,4-DNT were the target contaminants in these soils. This soil was put on columns C and F.

Table 5-3. Initial EM content of the residues put on the large sand columns.

Residues	Repetition	Concentration (ppm)				
		HMX	TNT	NG	2,4-DNT	4-A-2,6-DNT
Soil sample from the Wellington anti-tank impact area at CFB Gagetown	a	800	16	44	nd ¹	nd
	b	730	25	53	nd	nd
Soil sample from the Hotel Tower artillery firing position, CFB Petawawa	a	63	nd	nd	10	2
	b	120	nd	nd	190	3
Residues from artillery propellant bag burning test on snow at CFB Val-cartier (Analyses conducted by INRS)	a	nd	nd	nd	160,000	na ²

¹ nd – not detected
² na – not analyzed

Soils with residues were directly frozen after their collection to avoid EM degradation. They were dried outdoors in an opaque basket at DRDC-Valcartier, and then passed through a 9-mm sieve. The sieve was cleaned between every sieving series with acetone and distilled water to avoid any cross contamination. Finally, the contaminated soils were put back in the freezer until their placement on top of the sand columns.

A preliminary analysis was done on each of the range soil samples to determine the initial content of each EM (Table 5-3). Some discrepancies were observed and all of these sources zone samples were analyzed after homogenization using a grinding technique.

5.2.2.5 Pre-test preparation

Before the residues or contaminated soil were placed on top of each soil column, water equivalent to one pore volume was applied (~65 L, Table 5-4). The columns were then drained for approximately 10 days until no water outflow was observed. A water mass balance was done between inflow and outflow to determine the average volumetric water content in each column before the experiment began (Table 5-4).

Mass of the source zone material put on top of the columns was defined by the field conditions. Residues from the Hotel Tower artillery firing position at CFB Petawawa were spread as a 2-cm-thick, contaminated dry soil layer (9.5 kg) on the top of the clean soil. This source zone contained 1.0 g of 2,4-DNT. The residues from the CFB Gagetown Wellington anti-tank range impact area were spread as a 1.5-cm (7-kg) layer of contaminated dry soil, so the contamination of this source zone has 5.4 g of HMX and

140 mg of TNT (Table 5-3). The 150 g of residues from the gun powder burning test were spread on the top of the large sand column to make a source zone containing 24 g of 2,4-DNT. Thus, to obtain the same conditions for the six columns, 5.0 cm of clean sand was added in columns A and D, 3.5 cm in columns B and E, and 3.0 cm in columns C and F to obtain a soil column 65 cm high (Table 5-2).

Table 5-4. Pore volume, average initial volumetric water content, weight of contamination sources and weight of perchlorates for the large sand column test.

Column	Total porosity (m^3/m^3)	Pore volume (L) ¹	Average initial volumetric water content (m^3/m^3)	Weight of contamination sources (g)	Weight of ammonium perchlorate (g)	Weight of perchlorates (g) ²
A	0.36	65.28	0.19	151	1.40	1.19
B	0.36	65.28	0.19	7000	1.41	1.19
C	0.36	65.28	0.20	9500	1.40	1.19
D	0.36	65.28	0.16	152	1.40	1.19
E	0.35	63.47	0.17	7000	1.40	1.19
F	0.36	65.28	0.24	9500	1.40	1.19

¹ With a column volume of 181.34 L.
² ClO₄: is equivalent to 84.64% of NH₄ClO₄ (due to molecular weight).

Ammonium perchlorate (1.4 g/column) was added as an inert tracer for each soil column to evaluate the transport pore volume and the retardation factor of each EM tested (Table 5-4). The perchlorate was dissolved in 200 mL of distilled water and sprayed on the top of each large sand column with an atomizer before the first spring simulation. The large sand column tests were started with a spring simulation on 15 October 2009.

5.2.2.6 Effluent sampling and analyses

We used 42 glass 2-L cylinders under the six soil columns (seven per column) to recover the column effluent. Before their use, they were washed with water and acetone and rinsed with ultra-pure water. A lid was put on top of the cylinders to avoid any contamination before use. At each sampling event, the seven cylinders per column were emptied into a carboy and weighed. We poured 1 L of the effluent into an amber glass bottles (to prevent photo-degradation) and they were immediately frozen until the time of analyses to prevent EM degradation. For the analysis, they were thawed and two subsamples were retrieved, one for EM analysis with

HPLC-UV using USEPA 8330B method (USEPA 2006) and one for perchlorates analyses using ion chromatography.

5.2.2.7 Test schedule

- 15 October to 15 November 2009: spring simulation with 8 hours/day of watering and a watering of 0.074 L every 15 minutes during 31 days at 8°C for a total water volume of 73 L.
- 16 November 2009 to 14 January 2010 (59 days): summer simulation without watering at 20°C.
- 15 January to 16 March 2010: autumn simulation with 24 hours/day of watering at the rate of 0.088 L every 4 hours during 60 days at 8°C for a total water volume of 32 L.
- 17 March to 15 April 2010 (30 days): winter simulation without watering at 8°C.
- 15 April to 15 May 2010: spring simulation with 8 hours/day of watering and a watering of 0.074 L every 15 minutes during 31 days at 8°C for a total water volume of 73 L.
- 16 May 2009 to 22 June 2010 (59 days): summer simulation without watering at 20°C.
- 23 June to 24 August 2010: autumn simulation with 24 hours/day of watering at the rate of 0.088 L every 4 hours during 60 days at 8°C for a total water volume of 32 L.

5.2.3 Results

5.2.3.1 Temperature, inflow and outflow results

Owing to the test schedule, results of the second fall will be not presented in this chapter. Water content in each soil column and temperature are presented from the beginning of the test to 29 June 2010.

Temperatures recorded with a Campbell CR10X data logger¹ ranged from 10 to 12.5°C for the spring, autumn, and winter simulations and 21 to 24°C for the summer of the first and second simulation years, respectively (Fig. 5-3). The variation in laboratory temperature is attributable to the efficiency of the cooling system.

¹ Campbell Scientific Corp., Edmonton, AB, Canada.

Figures 5-4 and 5-5 present the inflow and outflow for each column. Inflow and outflow were similar for each column, with a difference of ± 19 to 26 L at the end of the second spring. In column D a slight difference was observed from the start because a nozzle was stuck in the open position during the first 24 hours. Outflow in spring started immediately, whereas outflow in fall was retarded by approximately 12–15 days because of the soil rewetting after the prior “season’s” small inflow.

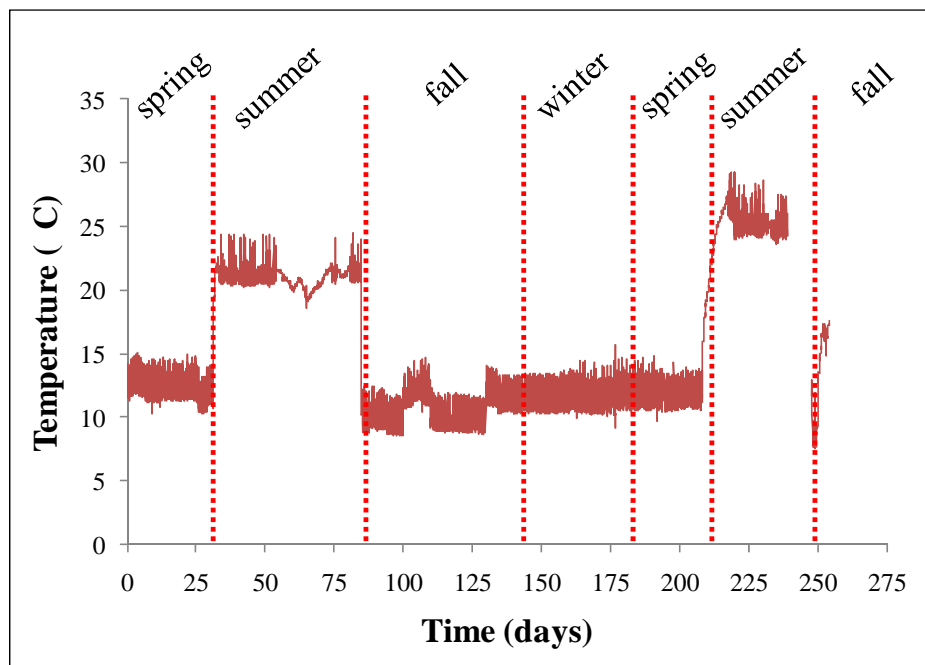


Figure 5-3. Laboratory temperature recorded by the CR10X.

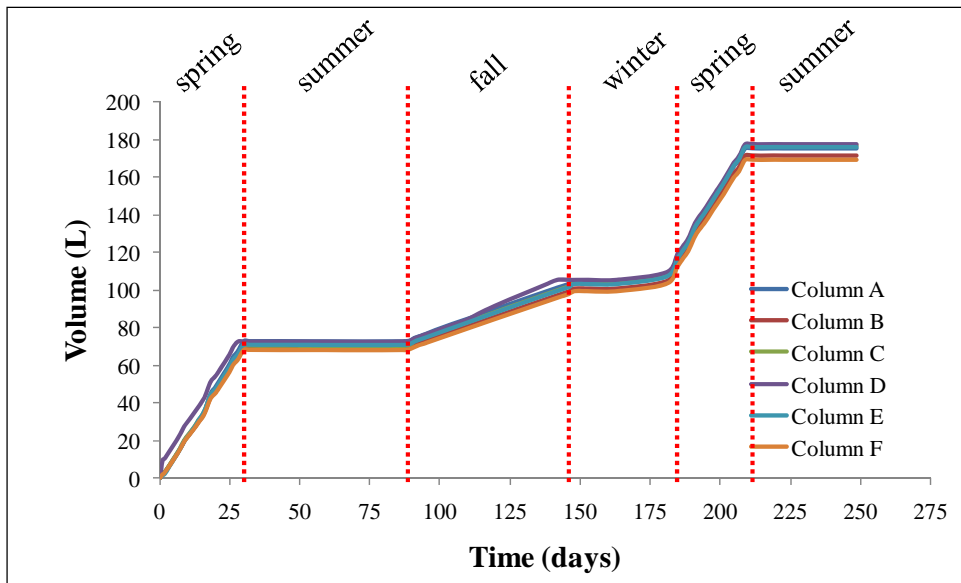


Figure 5-4. Cumulative measured inflow for each column.

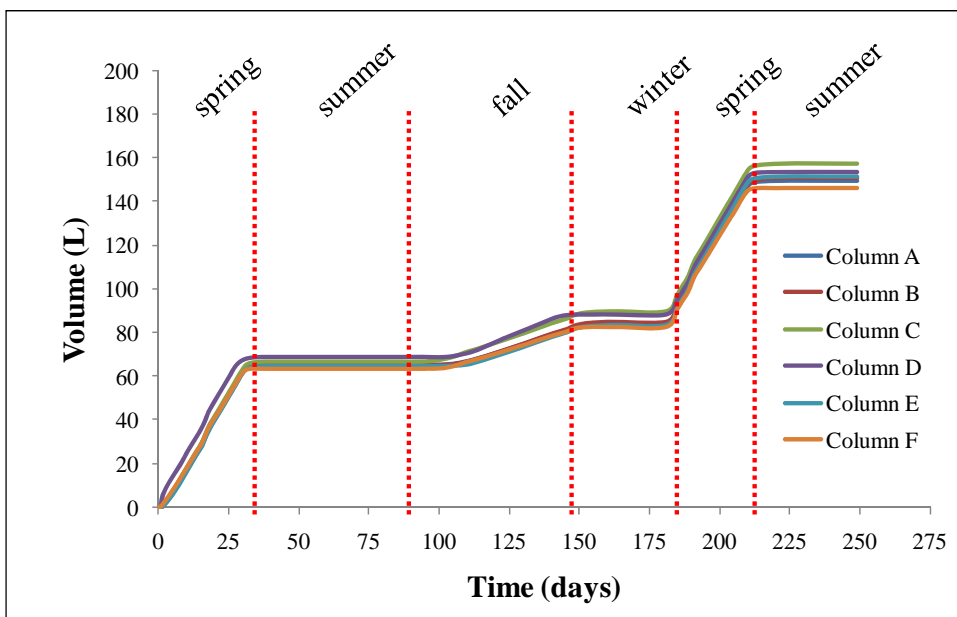


Figure 5-5. Cumulative measured outflow for each column.

5.2.3.2 Time domain reflectometry results

The moisture content in each column was monitored using time domain reflectometry probes (TDR 100) connected to a CR10X data logger. Three measurements were done per column every hour at the monitored depths 0.15, 0.35, and 0.55 m from the soil column surface. Figure 5-6 depicts the moisture content of each soil columns at the three depths over the course of the tests.

Figure 5-6 shows that volumetric water content (θ_v) increases with depth in the soil columns. The variance in θ_v is also less at depth, as the soil column attenuates the difference between rainfall events. During the first spring simulation, θ_v at 0.15 and 0.35 m depths increased slightly at the beginning of the cycle and then remained constant until the end of spring. Spring results also show that θ_v differs somewhat between the columns. While θ_v at 0.55 m depth is similar in all six columns ($0.35 \text{ m}^3/\text{m}^3 \pm 0.04 \text{ m}^3/\text{m}^3$), the two shallower depths vary considerably. Columns A, B, C, and E have similar θ_v at 0.15 and 0.35 m depths (0.15 and $0.25 \text{ m}^3/\text{m}^3$, respectively); columns D and F have a higher θ_v at these two shallow depths. The θ_v at the 0.35-m depth is similar to that at the 0.55-m depth in column F and slightly less in column D. The θ_v at 0.15 m depth in column F is almost twice the value in the other columns. Columns D and F were more saturated at the beginning of the test, indicating that these columns had not been drained enough prior to initiating the runs. They retained more water

during the drainage period, which may be acrivable to a finer texture of the soil particles. This assumption regarding columns D and F will be validated by particle size analyses at the completion of the test.

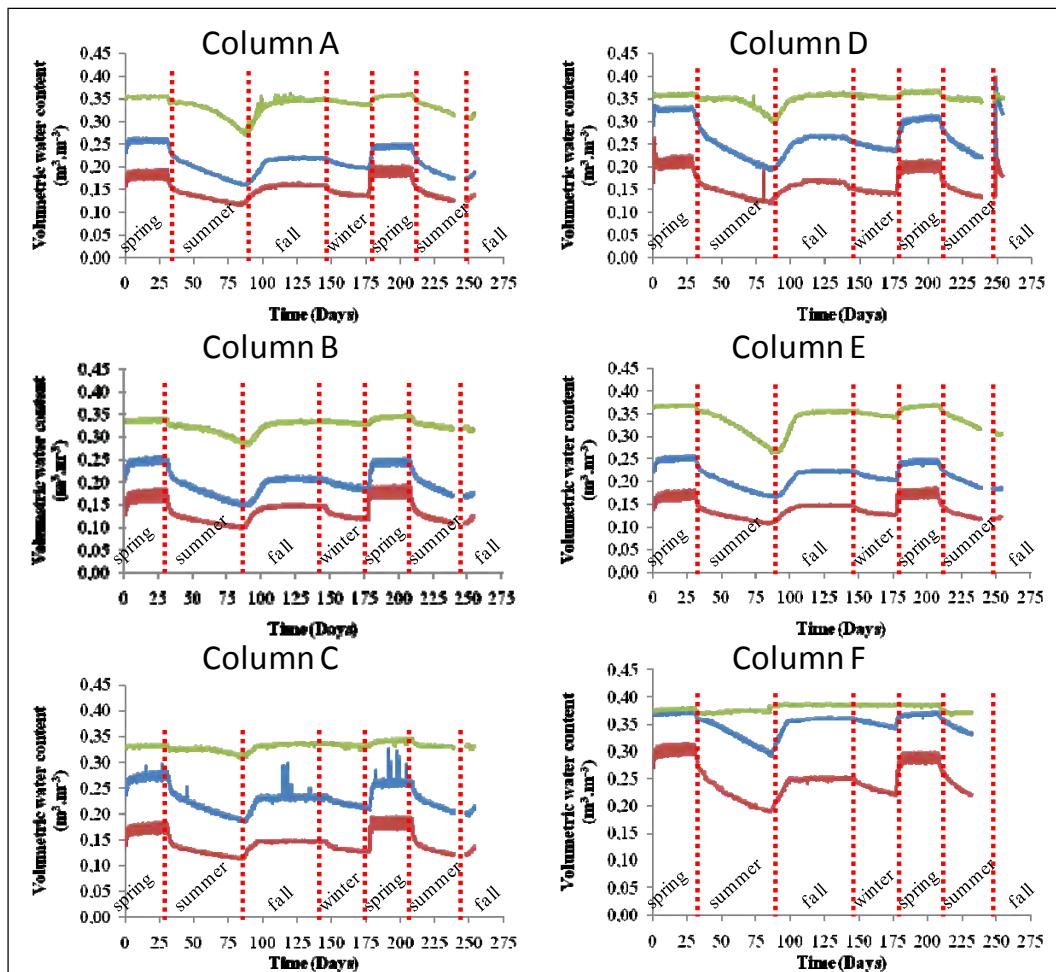


Figure 5-6. Volumetric water content as a function of time for columns A and D (burn residues), columns B and E (octol contaminated soils), and columns C and F (artillery FP). The red, blue, and green curves are the volumetric water content at the 0.15-, 0.35-, and 0.55-m depths respectively.

At the beginning of the summer simulation, θ_v decreases rapidly at all measurement depths during the first 1–4 days, and then the rate of decrease slows and becomes constant. The drying pattern seems to be attenuated with depth, although a higher difference is observed for θ_v at 0.35 m depth. The decrease in θ_v at the 0.55-m depth during summer is quite large in columns A and E, whereas it is negligible in columns C and F.

At the start of the fall simulation, θ_v increases again and reaches a steady state condition after few days at all depths. The θ_v at all three depths is

slightly less than during the spring simulation; this is likely attributable to the smaller autumnal inflow compared with the spring inflow.

At the beginning of the dry winter period, θ_v at all depths decreases in a way similar to the summer simulation; the decrease is attenuated with depth. At the beginning of the second spring, the θ_v increase again and reaches steady state condition in 2–4 days, returning to the θ_v of the first spring simulation. The pattern for the second summer period is similar to the first summer simulation, although the decrease seems to be more gradual for θ_v at 0.55 m depth for all columns.

At the end of the second summer period, 10 days of data are missing because of a problem with the apparatus program. Also, note that θ_v increases rapidly in Column D at the beginning of the second fall. A broken nozzle resulted in a period of constant watering. All the water volume for the fall was applied in 2–3 days; consequently, the experiment with this column was immediately stopped.

The θ_v is more variable at the top of the column (at 0.15 m) than deeper, particularly during spring; fluctuations occur daily because of the flow pattern cycle (8 hours of watering followed by 16 hours without watering). These daily fluctuations were attenuated during other seasons' simulations because there was either no watering (summer and winter) or watering was done on a 24-hour schedule (autumn).

5.2.3.3 Perchlorate concentrations in the effluent

Perchlorates were analyzed following the method described in Table 5-5. Analyses were performed on a Dionex ICS-2000 ion chromatography system equipped with an AS40 automated sampler.

All data in subsequent sections are presented in relation to the pore transport volume of each column. In a saturated regime, one pore volume is the water volume required to completely fill the pore spaces of a given soil volume that includes both pores and particles. Thus, the breakthrough curve of a fluid traveling at the average linear velocity is achieved when one pore volume has passed through a column of soil. In an unsaturated regime such as in this experiment, the pore volume is filled with water and air, so one pore volume will not represent the point at which all the water in a column has been theoretically replaced. In this experiment, the transport pore volume through the unsaturated zone is defined using perchlo-

rate as a tracer. Perchlorate is used because it is known to flow through soil without adsorption, transformation, or biodegradation under aerobic conditions.

Table 5-5. Ion chromatography conditions for the analysis of perchlorate.

Column	IonPac AS11 analytical, 4 x 250 mm with IonPac AG11 guard, 4 x 50 mm	
Mobile phase	100 mM sodium hydroxide at 1.0 mL/min.	
Detection	Suppressed conductivity, ASRS (4 mm), AutoSupression external water mode	
Working pressure	900 psi	
	Retention time (minutes)	Calibration range ($\mu\text{g/mL}$)
ClO_4^-	6.7	ND

Transport pore volume as a function of perchlorate concentration for the six columns can be derived from the following graphs. The maximum perchlorate concentration should be reached at 0.5 total pore volumes or at one transport pore volume. According to this assumption, transport pore volume for columns A, B, C, D, E, and F is 34, 54, 56, 56, 55, and 68% of the total pore volume, respectively (Fig. 5-7 and 5-8, Table 5-6). Transport pore volume corresponds to 25.5, 35.4, 36.6, 36.6, 34.9, and 44.4 L for columns A, B, C, D, E, and F respectively (Table 5-6).

Table 5-6. Transport pore volume for each column and recovery percentage of perchlorates.

Column	Total pore volume (L)	Percentage of total pore volume corresponding to transport pore volume (%)	Transport pore volume (L)	Recovery of perchlorates at the end of the second spring (%)
A	65	49	26	85
B	65	54	35	86
C	65	56	37	90
D	65	56	37	110
E	63	55	35	89
F	65	68	44	79

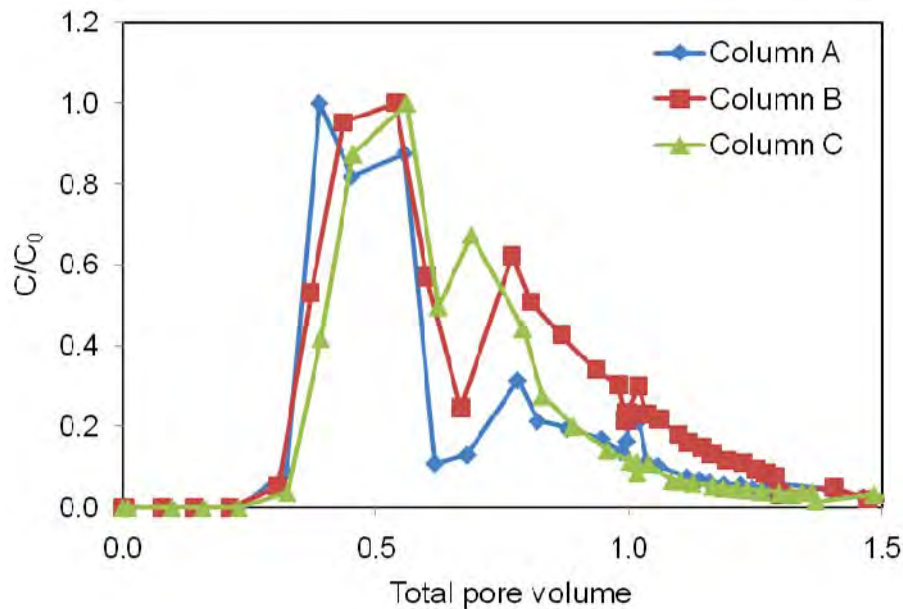


Figure 5-7. Perchlorate concentration vs. total pore volume for columns A, B, and C.

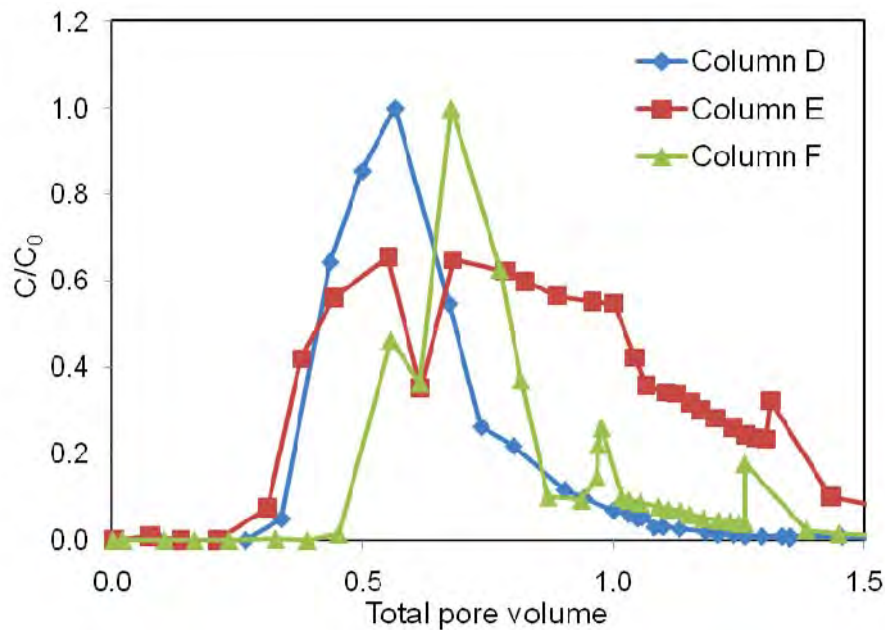


Figure 5-8. Perchlorate concentration vs. total pore volume for columns D, E, and F.

5.2.3.4 Columns with propellant residues from CFB Valcartier

Figures 5-9 and 5-10 depict EM concentrations obtained for the column A and D tests. Only 2,4-DNT and 4-A-2,6-DNT were detected in the column effluent, with similar concentrations in the two columns. 2,4-DNT is the

first organic compound to appear in column effluent at approximately 0.8 to 1 transport pore volume. An increase in 2,4-DNT concentration was measured for column A between 1 to 1.6 transport pore volumes and between 0.8 to 1.5 transport pore volumes in column D. In both columns, 2,4-DNT concentrations stay stable at 9000 µg/L until the end of the spring. At the beginning of autumn, 2,4-DNT concentrations decrease and stay stable at 6000 µg/L until the end of the second spring.

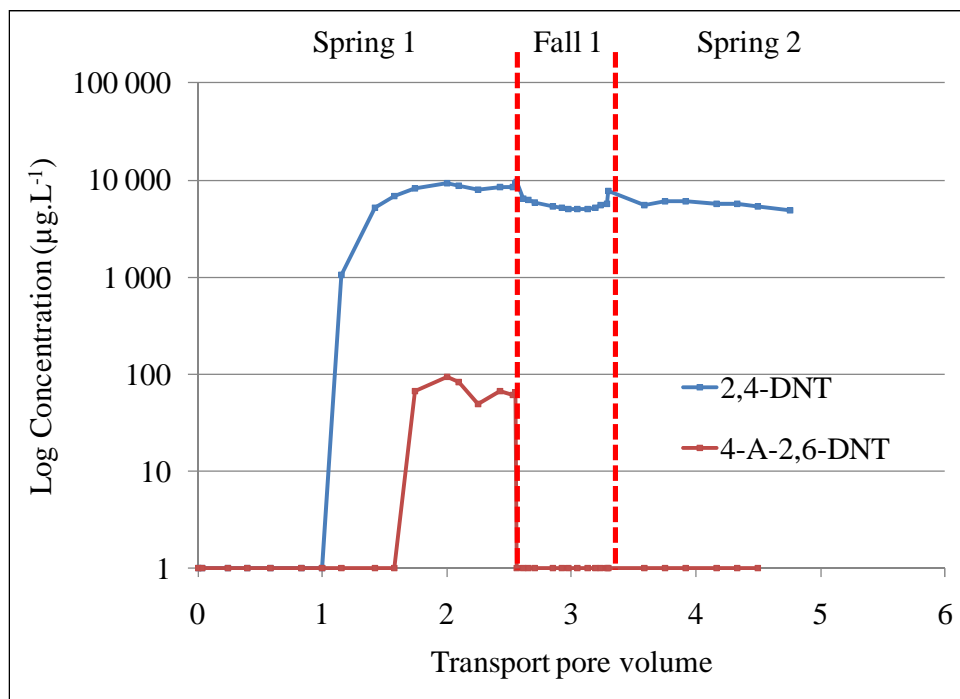


Figure 5-9. Concentrations of 2,4-DNT and 4-A-2,6-DNT in column A effluent.

Movement of 4-A-2,6-DNT is retarded compared to 2,4-DNT. However, the pulse of 4-A-2,6-DNT is finished at the end of the first spring, while the 2,4-DNT pulse continues with concentrations slightly lower (6000 µg/L) in the autumn and the second spring. In these two columns, little pulses of 2,4-DNT are observed at each seasonal transition (Fig. 5-9 and 5-10). This is probably attributable to the lack of watering during the winter and summer simulations. Also, 4-A-2,6-DNT needs to be quantified in the source term that was put on top of the column; these analyses are in progress.

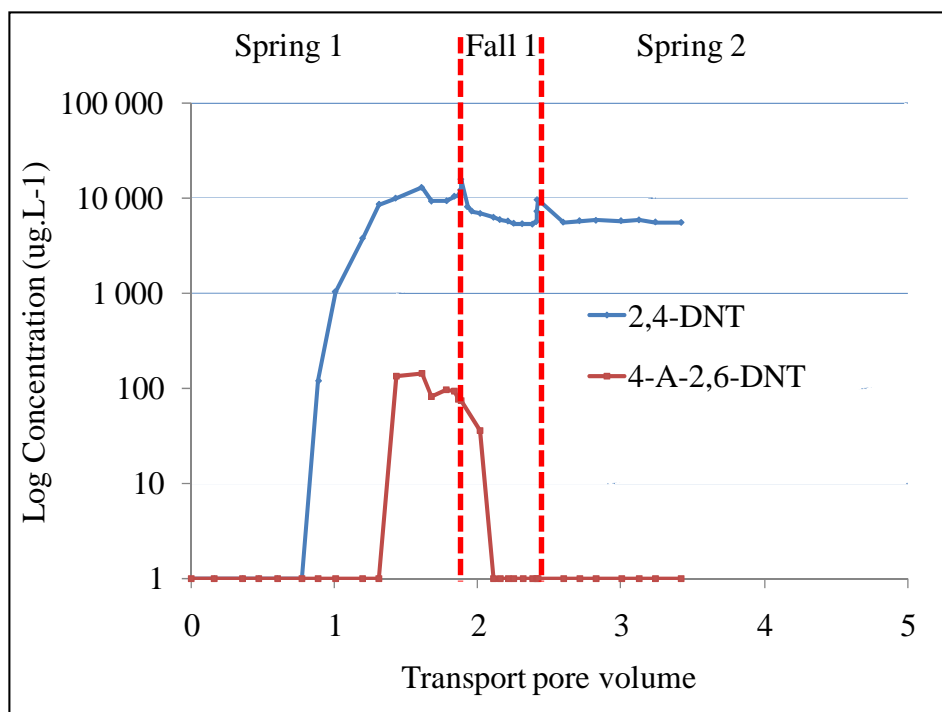


Figure 5-10. Concentrations of 2,4-DNT and 4-A-2,6-DNT in column D effluent.

Table 5-7 shows the dissolved mass of EM that was flushed between the beginning of the test and the end of the second spring. It also includes the water volume that could potentially be contaminated above the water quality guidelines (Ministere du Developpement Durable, de l'Environnement, et des Parcs [MDDEP], Quebec 2002; Ontario Ministry of the Environment 2004) for the columns and for 1 m² of soil contaminated by burning residues.

The masses of 2,4-DNT flushed from columns A and D, respectively, were 580 and 630 mg. Thus, less than 3% of the initial 2,4-DNT mass (Table 5-3) was flushed between the beginning of the test and the end of the second spring.

The water guideline for 2,4-DNT from the MDDEP, Quebec (2002) is 910 µg/L; thus, the average contamination of 2,4-DNT during this period is more than five times higher than the groundwater guideline (4.7 and 5.0 mg/L_{water outflow} for columns A and D, respectively). It is more than 8700 times higher than the groundwater guideline of the Ontario Ministry of the Environment (2004), where the limit is 0.5 µg/L. Thus, 2,4-DNT leachate from single-base propellant residues presents a significant hazard to groundwater quality.

Table 5-7. Dissolved EM mass between the beginning of the test and the end of the second spring, and equivalent groundwater volume contaminated at the drinking water guideline for columns A and D and for 1 m² of single-base propellant residues on the ground.

Column	EM	EM dissolved mass (mg)	Column surface area (m ²)	Measured outflow volume (L)	Water guideline ¹ (µg/L)	Equivalent contaminated water volume/column area (L) ²	Equivalent contaminated water volume (L/m ²) ²
A	2,4-DNT	580	0.28	120	910 ^a	630	2,300
					0.5 ^b	1,200,000	4,100,000
	4-A-2,6-DNT	1.8			na ³	na	na
D	2,4-DNT	630	0.28	130	910 ^a	960	3,400
					0.5 ^b	1,300,000	4,500,000
	4-A-2,6-DNT	2.5			na	na	na

¹ a: groundwater guideline of Ministere du Developpement Durable, de L'environnement et des Parcs, Quebec (2002).
^b: groundwater guideline of Ontario Ministry of the Environment (2004).

² outflow volume contaminated at the corresponding water guideline.

³ na: drinking water guideline is not available for 4-A-2,6-DNT.

Depending on the dissolved mass of 2,4-DNT, the water volume that may be contaminated, based on the water guideline concentration from MDDEP, Quebec (2002), is higher than 0.63 m³ for each column with propellant residues; it is also higher than 1100 m³ based on the water guideline concentration from Ontario Ministry of the Environment (2004). Also, using the column 0.28-m²surface area, we can estimate that more than 2.2 m³ and more than 4100 m³ of groundwater may be contaminated for each square meter of surface soil contaminated with propellant resides based on the Quebec (2002) and Ontario (2004) water guidelines, respectively. No data were available in the literature for 4-A-2,6-DNT.

5.2.3.5 Columns with contaminated soils from the Wellington anti-tank impact area at CFB Gagetown

Figures 5-11 and 5-12 graph the EM concentrations found in the effluent from Columns B and E, which were seeded with impact area source materials. The only compounds detected were HMX and TNT. The HMX and TNT concentrations in water are very similar in the two columns, as was found with the analytes from the propellant column tests. HMX is the first EM to appear in the columns' effluent, at approximately 0.8 transport pore volumes. The HMX concentration increases rapidly between 0.8 and 1.8

transport pore volumes and more slowly until the end of the second spring, reaching a maximum concentration of about 1000 µg/L. This slowly increasing rate is probably ascribable to the low solubility (4 to 5 mg/L; Lynch et al. 2001, 2002) and the dissolution kinetics of HMX in water.

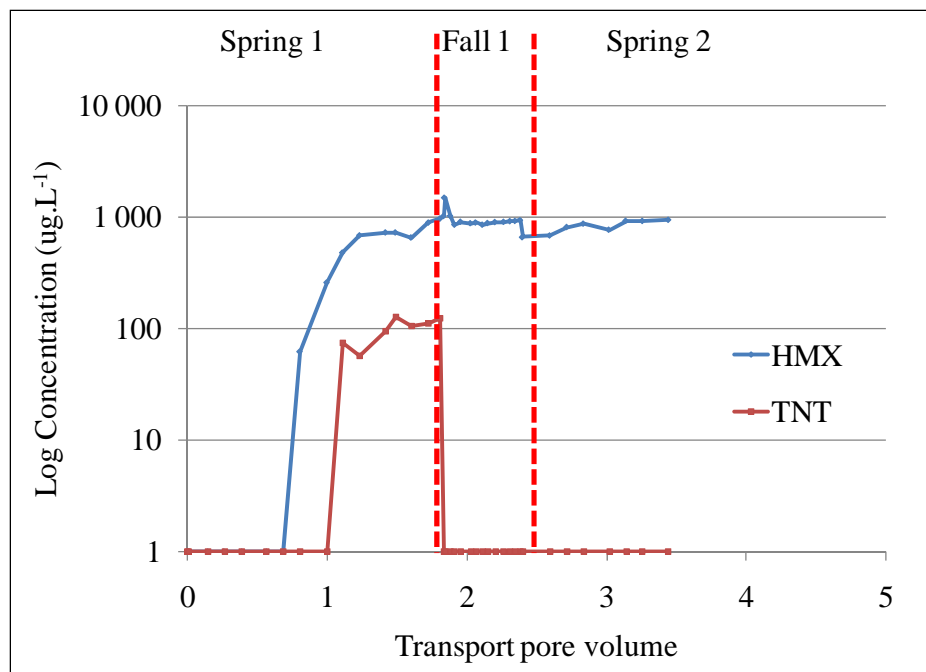


Figure 5-11. HMX and TNT effluent concentrations in Column B.

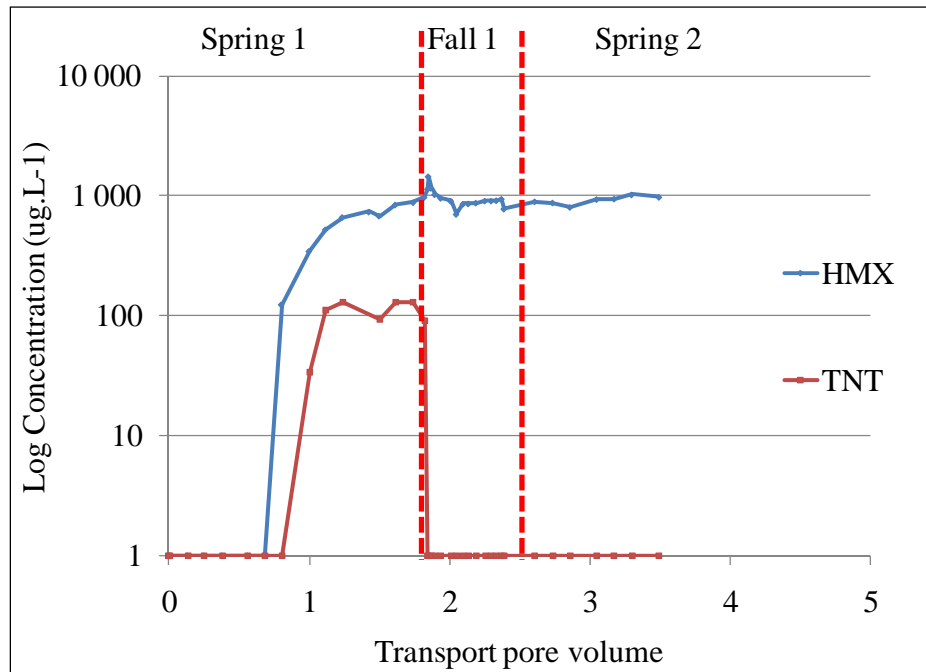


Figure 5-12. HMX and TNT effluent concentrations in Column E.

TNT appears in the column effluent later than HMX, at approximately 1 and 1.1 transport pore volumes for columns B and E, respectively. In these two columns, the TNT concentrations increase very fast, stabilizing at approximately 130 µg/L midway through the first spring until the end of that spring when the concentrations fall very fast, reaching non-detectable levels thereafter.

A pulse of HMX was observed starting the second half of the first spring. The end is unknown at this point but may be determined with the second fall's results. Meanwhile, a complete dissolution pulse was observed for TNT during the second half of the first spring. The TNT pulse is totally flushed from the column within less than 0.8 transport pore volumes. TNT is retarded when compared to HMX.

Table 5-8 presents the dissolved masses of HMX and TNT that were flushed between the beginning of the test and the end of the second spring, along with the water volume contaminated for the columns and for 1 m² of contaminated soil according to USEPA (2009) drinking water guideline. A total of 40 and 41 mg of HMX and 2.7 and 2.8 mg of TNT were flushed from columns B and E, respectively; thus, less than 1% of the initial HMX mass and 2% of the initial TNT mass (Table 5-3) were flushed between the beginning of the test and the end of the autumn.

Table 5-8. Dissolved EM mass between the beginning of the test and the end of the second spring and equivalent groundwater volume contaminated at the U.S. drinking water guideline (USEPA 2009) for columns B and E and for 1 m² of contaminated soil from the Wellington anti-tank impact area at CFB Gagetown.

Column	EM	EM dissolved mass (mg)	Column surface area (m ²)	Measured outflow volume (L)	USEPA (2009) Drinking water guideline (mg/L)	Equivalent contaminated water volume / column area (L) ¹	Equivalent contaminated water volume (L/m ²) ¹
B	HMX	73	0.28	122	0.4	180	650
	TNT	2.7			0.002	1,400	4,900
E	HMX	78	0.28	122	0.4	200	700
	TNT	2.8			0.002	1,400	5,000

¹ Outflow volume contaminated at the drinking water guideline (USEPA 2009)

The drinking water guideline (USEPA 2009) for HMX is 0.4 mg/L; thus, the average contamination of HMX during this period is slightly higher than the groundwater guideline (0.60 and 0.64 mg/L_{water outflow} for columns

B and E, respectively). The TNT drinking water guideline is 0.002 mg/L (USEPA 2009); consequently, the average contamination of TNT (0.034 and 0.033 mg/L_{water outflow} for columns B and E, respectively) during this period is more than 15 times higher than the groundwater contamination guideline. Thus, HMX and TNT present a hazard for groundwater quality. Depending on the HMX and TNT dissolved mass, the water volume that may be contaminated at the drinking water guideline concentration is higher than 180 and 1300 L for HMX and TNT, respectively, for each column with contaminated soil from the Wellington anti-tank impact area at CFB Gagetown. Thus, we can estimate that more than 650 and 4800 L of groundwater may be contaminated by HMX and TNT, respectively, for a surface of 1 m² of contaminated soil from the Wellington anti-tank impact area at CFB Gagetown.

5.2.3.6 Columns with contaminated soils from the Hotel Tower artillery firing position at CFB Petawawa

Column effluent samples analyzed from the beginning of the test to the end of the second spring showed no detectable EM. This is probably related to the age of the residues and the retention of 2,4-DNT in the nitro-cellulose (NC) matrix. Because of this, column F was emptied during the second summer simulation and soil samples were taken within the soil profile to analyze its EM content. The results will indicate whether it is worthwhile to continue the experiment with column C, which contains the same contamination source, for one more year. EM analyses are in progress. Also, soil samples were taken to define the bulk density and the volumetric water content of the soil profile at the end of the experiment.

After the experiment was complete, bulk density (ρ_b) and volumetric water content (θ_v) of column F was studied at 0.05- or 0.10-m depth intervals (Fig. 5-13). After careful removal of 0.05 m of soil, one sample of 190 cm³ was taken with the core method to measure the ρ_b (Grossman and Reinsch 2002). Approximately 100 g of soil was sampled at every depth for measuring the gravimetric soil water content (θ_g) using the method of Topp and Ferré (2002). θ_v was calculated with $\theta_v = \theta_g \rho_b / \rho_{water}$ (Grossman and Reinsch 2002).

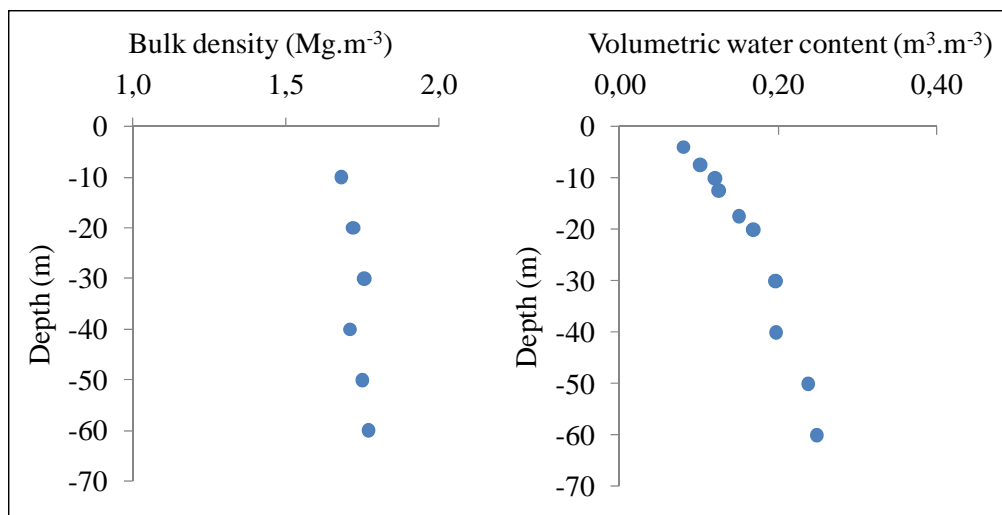


Figure 5-13. Profile of the bulk density (left) and the volumetric water content of column F.

5.3 Dissolution tests

5.3.1 Introduction

Water drop dissolution tests were also done on various residues that were or will be used in the large sand column tests to define the input function of EM at the top of the large sand columns. These tests were done to complement the experiments of Lewis (2006) and Bellavance-Godin (2009). They were also done with residues used for the on-going large sand column tests previously described in this chapter.

5.3.2 Methodology

All tests were done at INRS laboratory under a controlled environment at 8 or 20°C (Fig. 5-14). A series of tests is in progress but only the results of the completed tests (Table 5-9) will be discussed in the next section.

The dissolution test protocol consisted of measuring by HPLC-UV the EM content in the various tested residues and placing on a fritted glass funnel a mass of residues that was proportional to the mass of residues on top of the large sand column (see Appendix D, Table D-1). Residues were homogeneously spread on the fritted glass funnel's surface (except for the octol flake in Test 2).

The flow rate of the water dropping on the residues was controlled by a syringe pump (Fig. 5-14). The flow corresponds to infiltration rates measured during spring and autumn at CFB Valcartier or CFB Petawawa, de-

pending on contamination sources origin (see Appendix D, Table D-2). Two years of precipitation were simulated with two springs and two autumns. As winter and summer do not contribute to recharge, they were not considered in this experiment (real time is presented Appendix D, Table D-2).

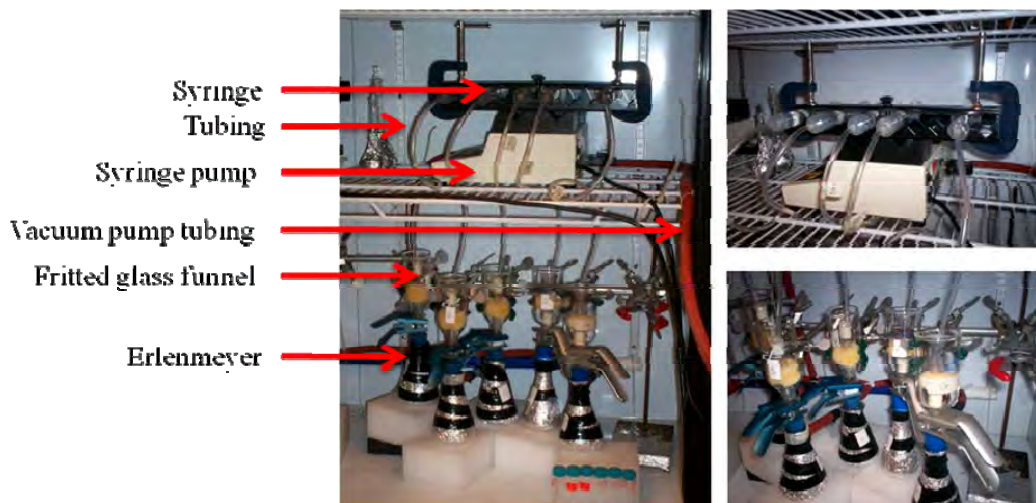


Figure 5-14. Dissolution experiment: the entire setup (left), the syringes pump (top right), and the fritted glass funnels with their connection to the vacuum pump (bottom right).

Different parameters were studied during these tests, such as pH of the water, temperature, and soil tension, which was simulated with a vacuum pump that reduced or increased the residence time of the water in contact with the residues. Effluent was collected every 48 hours and analyzed by HPLC-UV using method USEPA 8330 B. Cartridges were inserted in the tubing between the vacuum pump and the fritted glass funnel to recover the volatile part of the EM. Two types of cartridges were used: the HLB 6 cm³ for residues of NG and its metabolites and Porapak RDX 6 cm³ (with divinylbenzene/vinylpyrrolidone copolymer) for the residues that contain HMX, RDX, and TNT. These cartridges were analyzed at the end of every simulated season.

After 2 years of simulated precipitation, the remaining residues on the fritted glass were collected and extracted with acetonitrile (for RDX, TNT, HMX) or methanol (NG and metabolites). They were analyzed to determine the quantity of EM not dissolved during the dissolution test.

5.3.3 List of dissolution tests with water drops

Table 5-9 is a summary of all tests, including those that are done, those in progress, and those that will be conducted.

Table 5-9. Description of all dissolution tests that were done and in progress.

Test	Rep.	Test description					
		Type of residues	Flow rate of vacuum pump ¹	pH	Temperature (°C)	Status	
1	1	Propellant in soil from anti tank range firing position (Range Wellington at CFB Gagetown)	Valcartier	N	Not adjusted, demineralised water	8 ± 2	Done
	2			N			
	3			Y			
	1	Composition B particles sampled on snow after 81-mm mortars sympathetic detonation	Valcartier	N	4.7	8 ± 2	Done
	2			Y			
	3			Y			
	1	Propellant in soil from anti tank range firing position (Range A at CFB Petawawa)	Petawawa	N	Not adjusted, demineralised water	8 ± 2	Done
	2			Y			
	3			Y			
2	1	Octol in flakes	Valcartier	N	Not adjusted, demineralised water	8 ± 2	Done
	2			Y			
	3			Y			
	1	Octol powder	Valcartier	N	Not adjusted, demineralised water	8 ± 2	Done
	2			Y			
	3			Y			
3	1	Propellant in soil from anti-tank range firing position (Range Wellington at CFB Gagetown)	Valcartier	N	Not adjusted, demineralised water	8 ± 2	In progress
	2			Y			
	3			Y			
	1	Octol in soil from the impact area of the anti-tank range Wellington at CFB Gagetown	Valcartier	Y	Not adjusted, demineralised water	8 ± 2	In progress
	2			Y			
	3			N			
	1	Gun powder in soil from burning test at CFB Valcartier	Valcartier	Y	Not adjusted, demineralised water	8 ± 2	In progress
	2			Y			
	3			N			
4	1	Octol in soil from the impact area of the anti-tank range Wellington at CFB Gagetown	Valcartier	Y	Not adjusted, demineralised water	20 ± 2	Not started
	2			Y			
	3			N			
	1	Gun powder in soil from burning test at CFB Valcartier	Valcartier	Y	Not adjusted, demineralised water	20 ± 2	Not started
	2			Y			
	3			N			
5	1	Propellant in soil from artillery firing position Hotel Tower, at CFB Petawawa	Valcartier	Y	Not adjusted, demineralised water	20 ± 2	Not started
	2			Y			
	3			N			
	1	Propellant in soil from artillery firing position Hotel Tower, at CFB Petawawa	Valcartier	Y	Not adjusted, demineralised water	20 ± 2	Not started
	2			Y			
	3			N			

¹ Y— with vacuum pump; N— without vacuum pump.

5.3.4 Results

The two first dissolution tests (Table 5-9) are completed and the third one is in progress. No results are currently available for the in-progress test.

5.3.4.1 Results of the 2 years dissolution tests with propellant residues in soil from anti-tank range firing positions, Wellington Range, CFB Gagetown, sampled on September 20th, 2006

The dissolution tests were done at 8°C on three samples of contaminated soil with propellant residues from firing positions at the Wellington anti-tank ranges at CFB Gagetown. Table 5-10 presents the soil physico-chemical parameters of this contaminated soil and Table 5-11 shows the initial mass of NG that was put on the fritted glass of the dissolution test setups. One setup was connected to a vacuum pump, creating a tension of 0.1685 bars, and the two others were not connected to the vacuum pump (Table 5-9). For the sample under suction, HLB 6 cm³ cartridges were placed on the vacuum line to recover the volatile part of EM (NG and its metabolites).

Appendix D, Tables D-1 and D-2 present the setup parameters of the test and Table D-3 presents an example of data processing. Figure 5-15 presents the cumulative NG mass lost of the residues expressed as a percentage of the initial mass of NG (Table 5-11) as a function of cumulative eluted water volume.

The three samples behaved similarly during the simulation. Results show that 16 to 19% of the initial NG content is flushed during the dissolution test; however, NG dissolution occurs only during the first spring. After that, the NG dissolution rate is negligible. Thus, results suggest that NG is present in two fractions: a mobile NG fraction (16 to 19%) that it is immediately flushed and an immobile fraction that stayed in the residues, likely owing to the NC matrix of the propellant that immobilizes the NG (Martel et al. 2008). Results show also that the vacuum did not affect the NG dissolution rate.

Table 5-10. Physico-chemical parameters of contaminated soils from firing positions of anti-tank ranges at Wellington Range, CFB Gagetown (from Bellavance-Godin 2009).

Classification (USDA)	medium sand
Clay content (%)	0.1
Silt Content (%)	2.6
Very fine sand content (%)	14.6
Fine sand content (%)	21.2
Medium sand content (%)	39.1
Coarse sand content (%)	22.2
Very coarse sand content (%)	0.2
pH	5.35
Electrical conductivity (ms/cm)	0.327
Oxydo-reduction potential (mV)	274
Total Organic Carbon (%)	1.19
Fe (mg/Kg)	1630
NO ₂ -NO ₃ (mg-N/Kg)	286
Ca (m _{eq})	0.031
K (m _{eq})	0.0038
Mg (m _{eq})	0.015
Na (m _{eq})	0.0003
CEC (m _{eq} /100g)	1.55

Table 5-11. Initial NG content in residues from anti-tank range firing position (back of the firing position) at CFB Gagetown.

Sample	Initial soil mass (g)	Initial NG content (mg)	Spring time (days); flow rate (mL/h)	Autumn time (days); flow rate (mL/h)
A	2.047	6.28	10; 0.19	11; 0.074
B	2.041	6.26		
C	2.045	6.27		

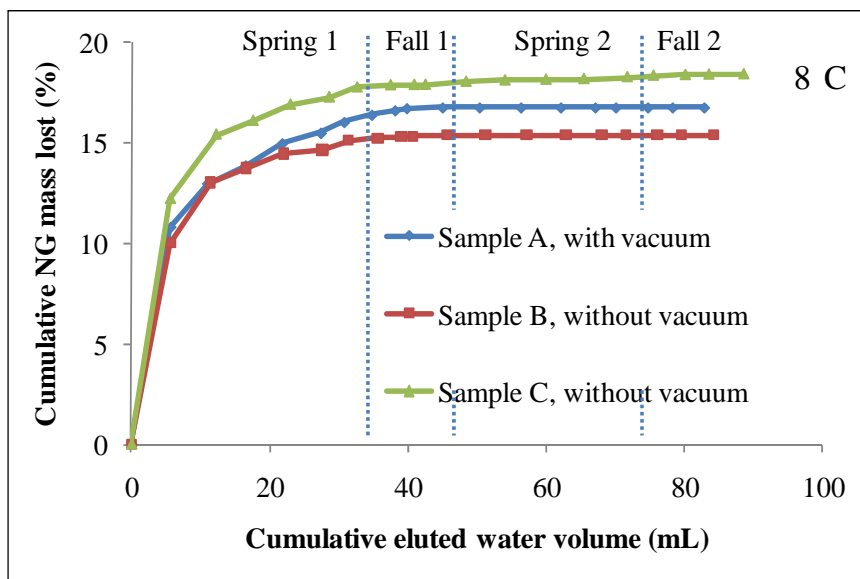


Figure 5-15. Cumulative NG mass lost on residues from Wellington firing position at CFB Gagetown expressed as a percentage of the initial mass of NG as a function of cumulative eluted water volume.

Figures 5-16 and 5-17 show the production of NG metabolites during the test. Only two metabolites resulting from the NG degradation were measured in the eluted water: 1,2-dinitroglycerine (1,2 DNG) (Fig. 5-16) and 1,3-dinitroglycerine (1,3 DNG) (Fig. 5-17). Metabolites 1-mononitroglycerine and 2-mononitroglycerine were not detected in the eluted water. Production of these metabolites was very weak and irregular. Production rates were slightly greater for 1,2-dinitroglycerine, because it is the first NG biodegradation metabolite to appear and, consequently, the more abundant. Nevertheless, metabolite production began at the end of the first spring and occurred over the subsequent seasons, suggesting that they originated from the degradation of the immobile NG fraction. The mobile NG fraction is probably flushed too rapidly to be degraded into metabolites. Also, as for NG, the NG metabolites production was unaffected by applying suction to the setup.

Results of this test show that only a fraction of NG (15 to 20%) is soluble and mobile (Table 5-12). Also, 80 to 85% of the residues NG is not readily soluble but released NG can be degraded in the source zone, resulting in NG metabolites production in the mobile aqueous phase.

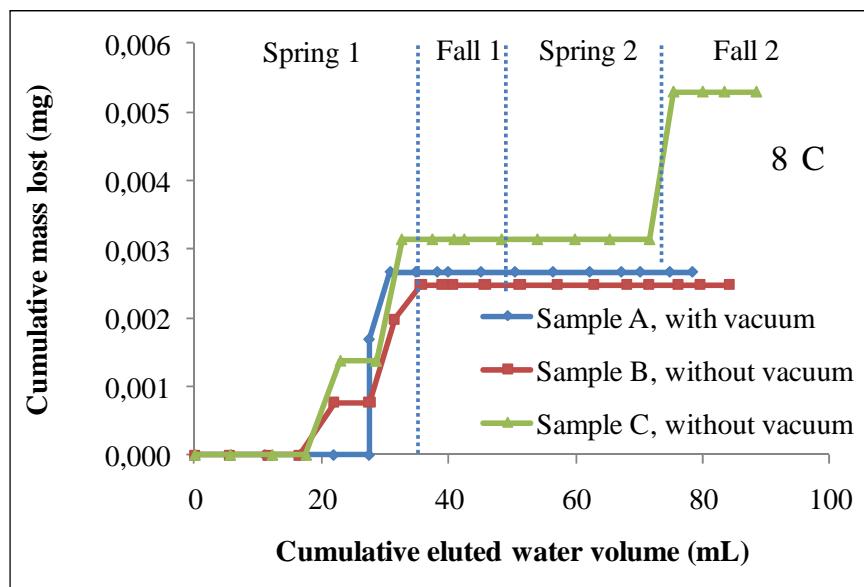


Figure 5-16. Cumulative mass lost of 1,2-dinitroglycerine relative to the cumulative eluted water volume on residues from Wellington firing position at CFB Gagetown.

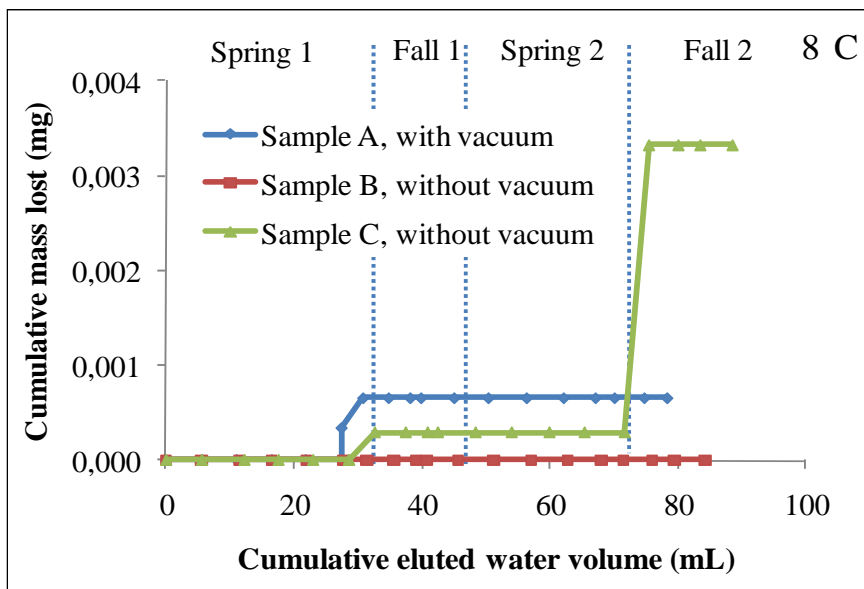


Figure 5-17. Cumulative mass lost of 1,3-dinitroglycerine related to the cumulative eluted water volume on residues from Wellington firing position at CFB Gagetown.

The NG metabolites produced were eluted a little slower compared to the NG elutions. This delay was not observed by Bellavance-Godin (2009). It may be attributable to the spring watering, which is not the same in these two experiments (24 hours/24 hours for water drop dissolution test and 8 hours/24 hours for large sand column test). Another test is underway to confirm this assumption (see Section 5.3.4.4).

Table 5-12. Initial and final residues from anti tank range firing position (back of the firing position) at CFB Gagetown.

Sample	A: Initial mass of NG on fritted glass (g)	B: Final mass of NG, 1,2 DNG and 1,3 DNG on the fritted glass (mg)	C: Total dissolved mass of NG, 1,2 DNG and 1,3 DNG in eluted water (mg)	D: Mass in the fritted glass of NG, 1,2 DNG and 1,3 DNG (mg)	E: NG mass in the cartridges on the vacuum line (mg)	F: EM mass balance (%): $[(B+C+D+E)/A]*100$
A	6.28	na ¹	1.17	0.0000	na	nd
B	6.26	na	1.01	0.0039	nap	nd
C	6.27	na	1.20	0.0000	nap	nd

¹na: not analyzed; nap: not applicable; nd: not determined.

Figure 5-18 shows that only one dissolution peak is observed. Dissolution started rapidly at the beginning of the test and faded away at approximately 50 mL of eluted water for sample A and B, while it continued to decrease slowly until the end of the simulation for sample C. These observations are in accordance with what was observed by Bellavance-Godin (2009) on the large sand column test with this same soil (Fig. 5-19).

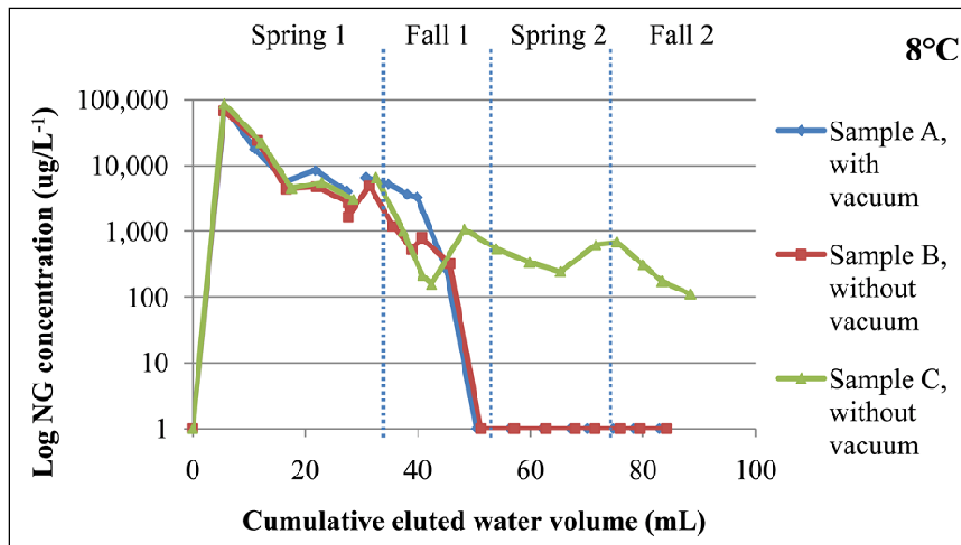


Figure 5-18. NG concentration in eluted water from drop test relative to the cumulative eluted water volume on residues from Wellington firing position at CFB Gagetown used for sand column test.

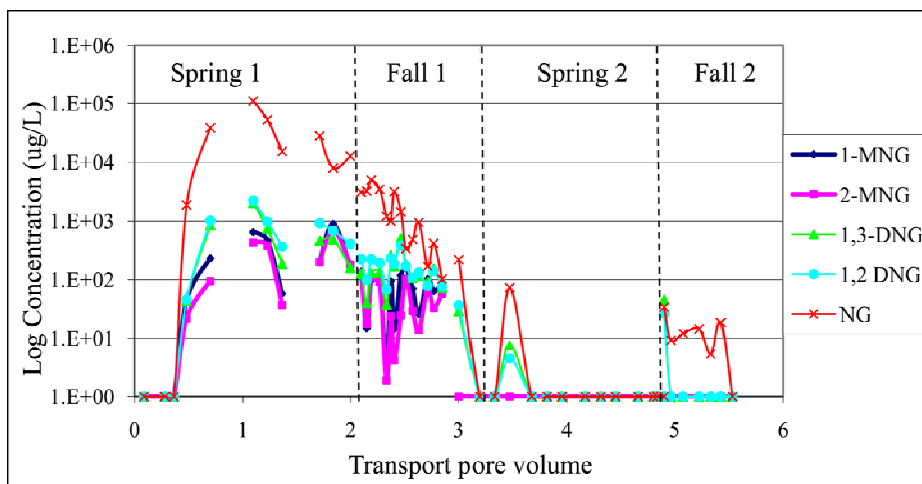


Figure 5-19. NG, DNG, MNG leachate concentration vs. transport pore volumes from column C-Valcartier (from Bellavance-Godin 2009).

5.3.4.2 Results of the 2 years dissolution tests with Composition B particles sampled on snow after 81-mm mortar sympathetic detonation (Lewis 2006; Lewis et al. 2009)

Dissolution tests using water drops were done at 8°C on three samples (Table 5-13). Two setups were connected to a vacuum pump pulling 0.17 bars of suction and one setup was not connected to the vacuum pump. For the two samples under suction, Porapak 6 cm³ RDX cartridges (with divinylbenzene/vinylpyrrolidone copolymer) were placed on the vacuum line to recover the volatile part of the EM.

Table 5-13. Initial contents of the EM in the Composition B residues on top of the fritted glass funnel and the applied flow rates.

Residues	Replicate	Initial mass of residues (mg)	Content of EM (mg) ¹			Total mass of EM in residues (mg) ²	Spring time (days) flow rate (mL/hr)	Autumn time (days) flow rate (mL/hr)
			RDX (43%)	HMX (2.6%)	TNT (29.1%)			
Composition B particles sampled on snow after 81-mm mortars sympathetic detonation (Lewis 2006)	I	28.3	12.17	0.736	8.24	21.1	10 0.19	11 0.074
	G	24.8	10.66	0.645	7.22	18.5		
	H	29.0	12.47	0.754	8.44	21.6		

¹ Defined in a fourth sample with 3 replicates.
² Total EM mass is different from the initial mass of residues due to impurity as black soot.

Appendix D, Tables D-1 and D-2 list the test setup parameters and Table D-4 presents an example of data processing. Figures 5-20 to 5-25 depict the cumulative EM mass lost expressed as a percentage of initial EM mass relative to the cumulative volume of eluted water that flowed through the samples on the funnels for 1 year and 2 years of simulation.

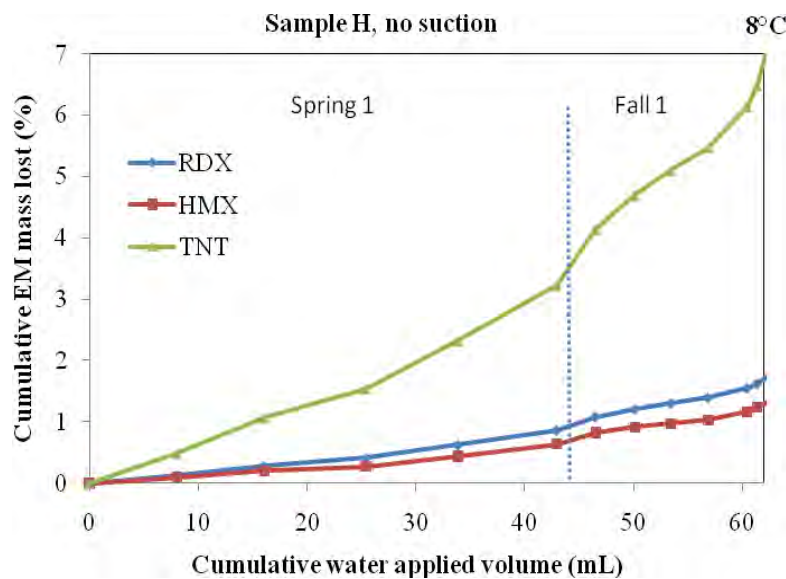


Figure 5-20. Cumulative EM mass lost expressed as a percentage of the initial mass of each EM in sample H as a function of cumulative eluted water volume (no suction applied) during the first year of simulation.

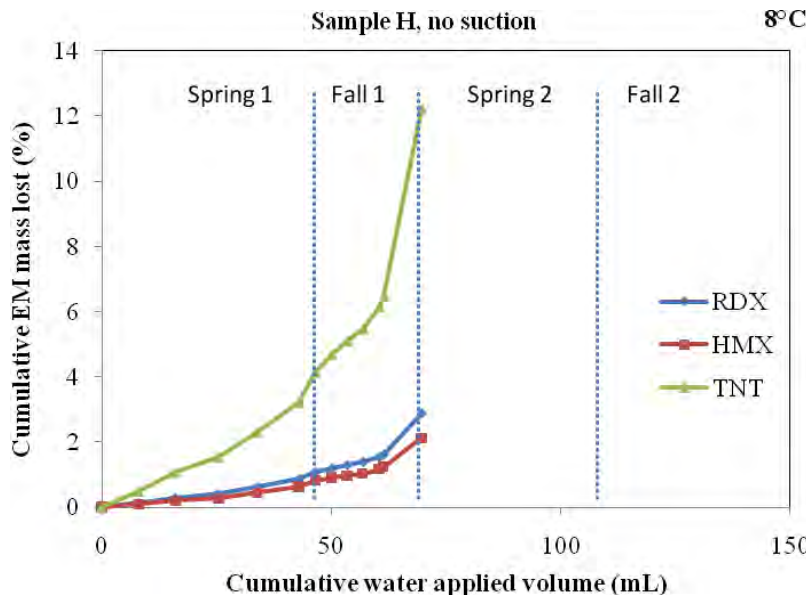


Figure 5-21. Cumulative EM mass lost expressed as a percentage of the initial mass of each EM in sample H as a function of cumulative eluted water volume (no suction applied) during 2 years of simulation.

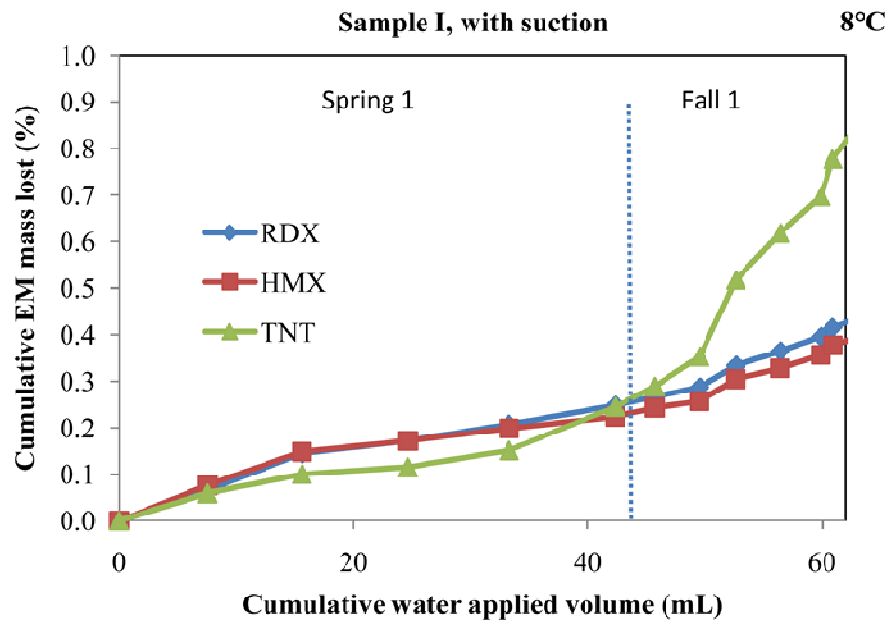


Figure 5-22. Cumulative EM mass lost expressed as a percentage of the initial mass of each EM in sample I as a function of cumulative eluted water volume (0.17 bar suction applied) during the first year of simulation.

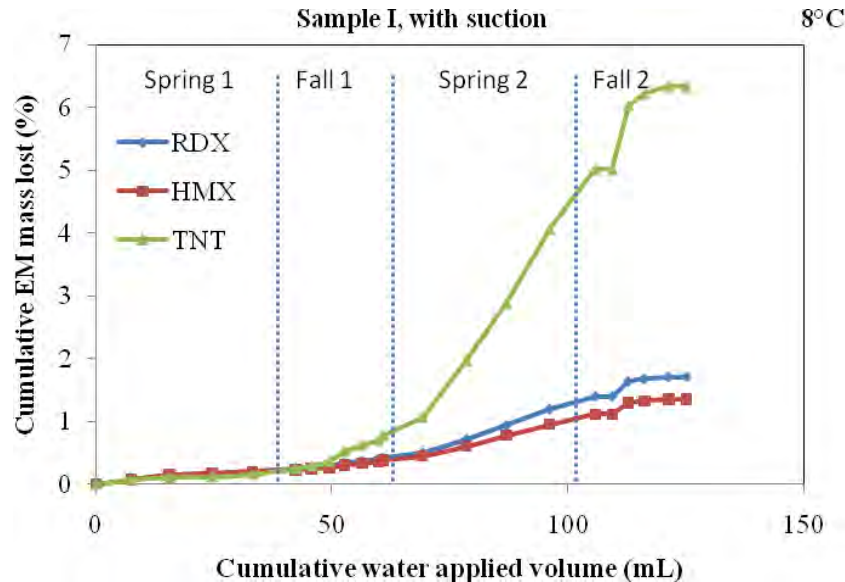


Figure 5-23. Cumulative EM mass lost expressed as a percentage of the initial mass of each EM in sample I as a function of cumulative eluted water volume (0.17 bar suction applied) during 2 years of simulation.

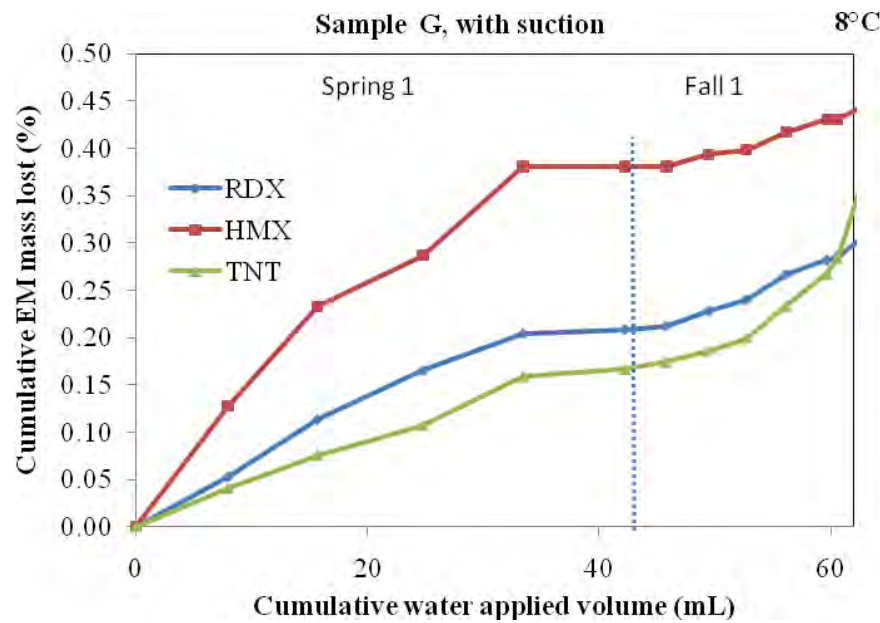


Figure 5-24. Cumulative EM mass lost expressed as a percentage of the initial mass of each EM in sample G as a function of cumulative eluted water volume (0.17 bar suction applied) during the first year of simulation.

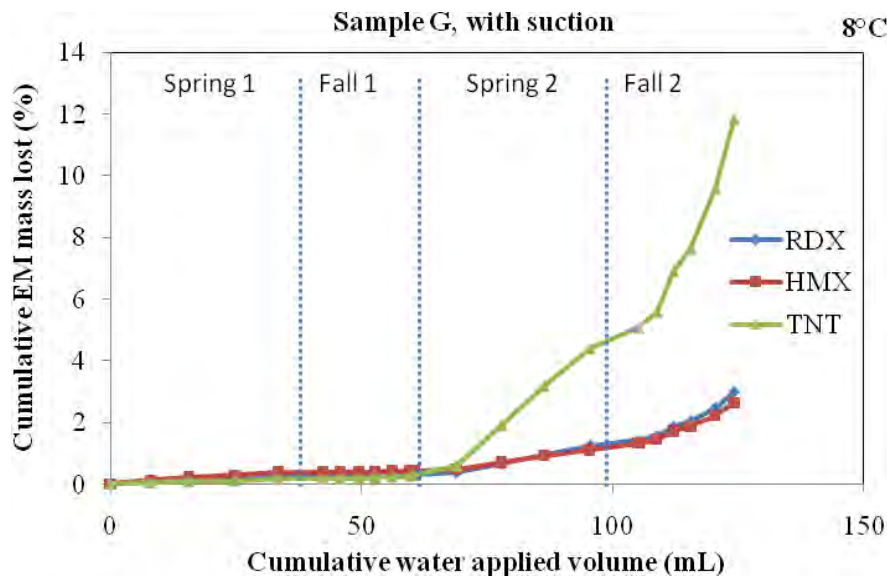


Figure 5-25. Cumulative EM mass lost expressed as a percentage of the initial mass of each EM in sample G as a function of cumulative eluted water volume (0.17 bar suction applied) during 2 years of simulation.

5.3.4.2.1 Results after 1 year of simulation

Results show that the dissolution rate of the Comp B particles without applied suction (sample H, Fig. 5-20) is larger than the dissolution rates ob-

served with suction applied (sample I, Fig. 5-22 and Sample G, Fig. 5-24). This phenomenon can be observed at the beginning of the experiment and was observed for RDX, HMX, and TNT, with TNT showing the strongest effect. Up to 7% of the initial TNT mass was lost within 1 year when no suction was applied. This rate is seven times higher than what was observed for the two other samples under suction. For HMX and RDX the difference in mass loss rate is two to four times higher in the sample without suction compared to the samples with suction.

For samples with suction (G and I), the dissolution rates of the various compounds varied. For sample I during the first spring, the TNT dissolution rate was lower than that observed for RDX and HMX, but the rate then increased at the beginning of fall (from 45 mL of cumulated eluted water volume). A mass of TNT that was unavailable at the beginning of the dissolution test may have become exposed to water drops after dissolution of RDX and HMX crystals that were protecting the TNT intra-crystalline matrix. For RDX and HMX, the cumulative mass lost seemed linear and thus seemed to present a similar, constant dissolution rate as for sample H without suction. This observation is logical because RDX and HMX are associated, HMX being an impurity in RDX (Lewis 2006, 2009).

In sample G, which had suction, HMX is the compound that presented the highest dissolution rate in relation to the initial mass. From the beginning of the experiment, a larger mass of HMX was dissolved compared with sample I. Thus, the HMX particles presented a higher surface area in this sample, which can explain its higher dissolution rate. The compound with the next highest dissolution rate was RDX, half that of HMX. TNT presented the smallest dissolution rate. The TNT matrix localized between the numerous RDX/HMX particles was probably protected by these particles and, consequently, water drops could not dissolve it (Fig. 5-26).

These observations during the first year of simulation showed that the TNT matrix is exposed for dissolution only when RDX/HMX crystals are dissolved, as in sample I. Consequently, the ratio of the surface area to the mass of TNT in contact with the eluting water is small at the beginning of the experiment. Therefore, the dissolution rate of the RDX/HMX particles controls the TNT dissolution rate, as was observed by Lever et al. (2005) and Taylor et al. (2009). Fracturing of the residue particles resulting from the dissolution of the RDX and HMX crystals, as observed by Taylor, could also be a factor in the variance of the TNT dissolution rate.

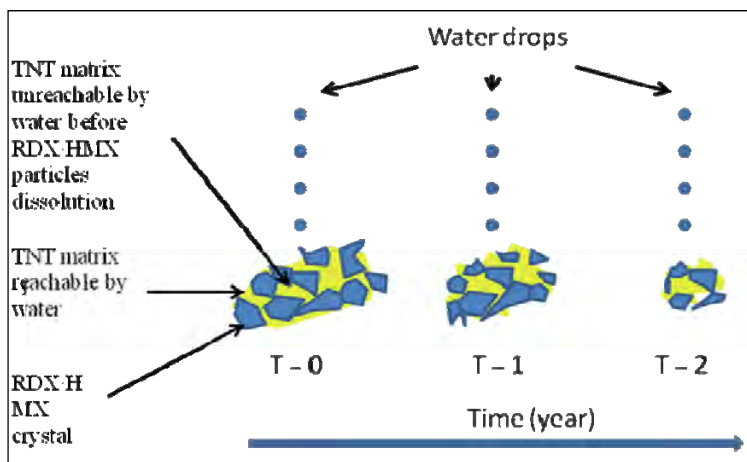


Figure 5-26. Conceptual model of dissolution of Composition B as a function of time.

The different flow rates applied during the first spring and fall (Table 5-13) resulted in little or no change in the dissolution rates (as observed on Fig. 5-20, 5-22 and 5-24). Thus, it is not the applied flow rate that modifies the dissolution rate of various EM, but the residence time of water in contact with particles (as shown in Fig. 5-27). The residence time of water in this experiment was controlled by the suction created by the vacuum pump.

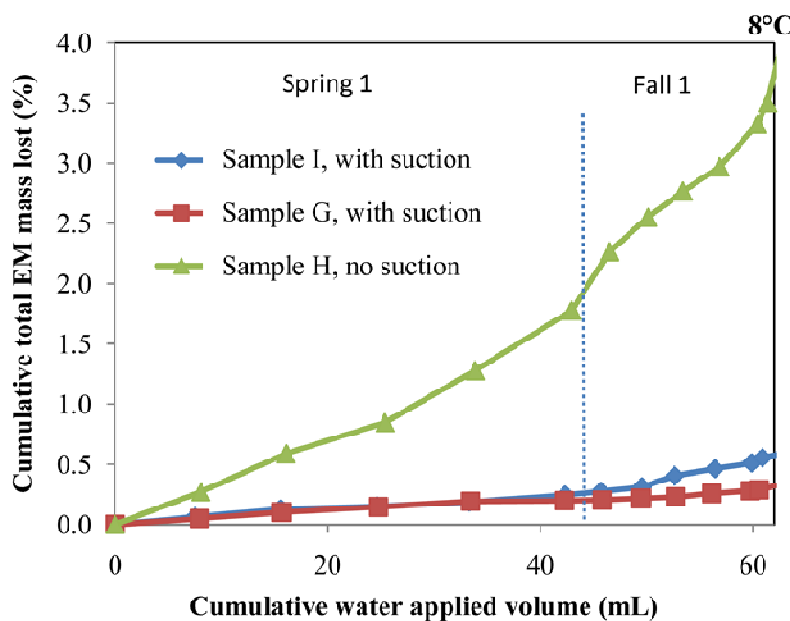


Figure 5-27. Percentage of total EM mass lost (RDX + HMX + TNT) relative to the initial EM mass of three samples according to the cumulative water applied volume having circulated in each of these samples during the first year of simulation.

5.3.4.2.2 Results after 2 years of simulation

For sample H (Fig. 5-21: no suction), the water drop test was stopped at the beginning of the second year because flow through the fritted glass funnel was blocked. The experiment was stopped after 69.6 mL of water was applied and 2.9, 2.1, and 12% of the initial mass of RDX, HMX, and TNT, respectively, had dissolved from the residues. For the two setups in this test connected to the vacuum pump, the general shapes of the dissolution curves were very similar. The dissolution rate of sample I (Fig. 5-23) was half that of sample G (Fig. 5-25) for all the EM. Sample I had dissolution of 1.7, 1.3 and 6.3% of the initial mass of RDX, HMX, and TNT, respectively, compared to the equivalent sample G results of 3.0, 2.6, and 12%. This is different from what was observed after the first year of simulation, at which time the dissolution rate of sample I was slightly higher than that of sample G. Furthermore, the delay of the increase in TNT dissolution rate was longer for sample G (~70 mL) than for sample I (~50 mL). These observations confirm that sample G had more RDX/HMX crystals protecting the inner TNT matrix from dissolution with water drops than were present in sample I.

At the end of the experiment, the dissolution rate of all three EM in sample I became nil after 110 mL of applied water. In contrast, the dissolution rates in sample G continued to increase until the last sample collected over the 2 years of simulation. Nevertheless, in these two samples, the final content of EM on the fritted glass funnel was not nil (Table 5-14). In addition, at the end of 2 years, the fritted funnels seemed to be partially blocked, as was observed earlier for sample H. Recrystallization and precipitation of EM on top of the fritted glass funnel was hypothesized to be the cause of the blockage, although some soot was found as well.

Figure 5-28 shows that the dissolution rate of the total EM mass is higher for sample H, which was not under suction, than for the two other samples (I and G), which were under suction. Compared to samples G and I, the dissolution rate of EM in sample H is two times faster. Thus, to dissolve the same EM mass in a sample not under suction, the volume of water that is required is half that for a sample under suction. Furthermore, a distinction was observed for the dissolution rates between the first and the second years for samples I and G, with a significant increase of the dissolution rate at the beginning of the second year for all of the three EM. In contrast, the dissolution rate of these components for sample H was more significant following the first year.

Table 5-14. EM contents in Composition B residues at the end of the dissolution experiment and mass balance of the experiment.

Rep.	A: Purity (%) ¹	B: Final EM mass on fritted glass (mg)			C: Total EM dissolved mass (mg)			D: EM mass on fritted glass (mg)			E: Final total mass (B+C+D) (mg)			F: EM mass balance [(E/A)*100] (%)		
		RDX	HMX	TNT	RDX	HMX	TNT	RDX	HMX	TNT	RDX	HMX	TNT	RDX	HMX	TNT
I	75	15.0	0.81	8.22	0.208	0.010	0.522	0.944	0.056	0.396	16.2	0.878	9.14	133 ²	119 ²	111 ²
G	61	10.0	0.55	4.89	0.317	0.017	0.853	0.816	0.050	0.397	11.2	0.614	6.14	105	95	85
H	86	12.6	0.80	7.39	0.360	0.016	1.03	0.251	0.017	0.128	13.2	0.828	8.55	106	110	101

¹ Impurity is black soot
² Possible interaction with plastic containers

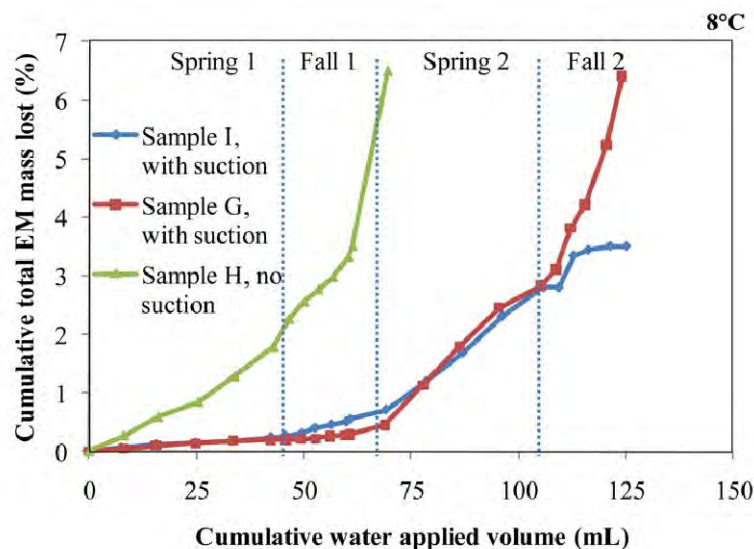


Figure 5-28. Percentage of total EM mass lost (RDX + HMX + TNT) according to the initial EM mass of three samples as a function of the cumulative water volume applied on these samples during 2 years of simulation.

Samples G and I followed a similar trend until 110 mL of water was applied. At the end of 2 years of simulation, the total dissolved mass of EM was twice for sample G (6.5%) than for sample I (3.5%). In sample I, the EM seemed to become inaccessible to the water (Fig. 5-26).

Differences between sample H (no suction) and the two other samples with suction (G and I) were explained by the contact time between the applied water and EM particles. In samples G and I, this contact time was reduced by the applied suction compared to sample H. Thus, the dissolution rate for samples I and G decreased when compared to sample H because water was in contact with EM particles for a shorter time.

The dissolution rate tests showed strong sample heterogeneity, not in their initial mass, but in their assemblage and in their surface area exposed to water during the experiments. Also, the residence time of water in contact with EM particles seems to be the main parameter that controls EM dissolution. Thus, it is possible to deduce that EM dissolution in the training ranges is more significant when the soil volumetric water content is near saturation. The same observation can be made when impact holes created by artillery fire are filled with water and thus increase the EM dissolution rate of EM particles.

5.3.4.2.3 Mass balance and source of error

After 2 years of simulation, we determined the dissolved part, the non-dissolved part, and the part of EM that was reprecipitated in and on the fritted glass funnel. The percentage of recovery was very good—between 85 and 110% of the initial mass of each EM (Table 5-14). The volatile part of the EM measured with cartridges was insignificant and not considered in Table 5-14. The recovery of EM in sample I was overestimated because of laboratory bias caused by interaction with plastic during the extraction procedure with acetonitrile before the HPLC-UV analysis of the samples.

Table 5-14 shows that EM dissolved fraction is probably underestimated in the water drop test owing to EM content on the fritted glass. The suction applied by the vacuum pump for samples I and G had dried the particles and increased the recrystallization of the EM in the fritted glass. The EM was first dissolved by water and then recrystallized in the porous media of the fritted glass. Consequently, the dissolved EM fraction of each sample presented in Table 5-14 is underestimated. This observation is a bias to the field situation because:

1. The pore size of the fritted glass funnels is smaller than the soil pore size of most soil.
2. The recrystallization is probably higher in the water drop test than in the field situation because of the high flow rate of air circulation in the lab setup.
3. Most of the time, the real soil suction in the field is different from the vacuum pump suction and, thus, the soil is not drying in the same way as for the water drop test experiment.

As a result, EM recrystallization in soil layers is probably lower than what was observed in the fritted glass of the water drop test. Consequently, the

EM concentrations in the underlying water in the field are probably higher compared to the concentration of the eluted water during the drop test.

The compositional heterogeneity of EM particles is a source of error and has an influence on the initial content of EM in the three subsamples. It was not possible to quantify the EM in these subsamples before the experiments, and the estimation was based on another subsample. The specific surface area of each EM subsample exposed to water drops may be different. The water content of the final mass of particles on the fritted glass funnels may vary and has an impact on the final EM mass. The volume estimation of the eluted water sample at each sampling date, the EM mass that was recrystallized in the fritted glass pores, and the volatile EM portion were also sources of error but were evaluated in detail (Table 5-14).

5.3.4.2.4 Comparison with dissolution experiment on large sand column test (Lewis 2006; Lewis et al. 2009)

The water drop test results are in agreement with those published by Lewis et al. (2009) for the experiment with the same contamination sources on a large sand column where 10% of the initial mass of EM was dissolved and eluted in 1 year. The difference between these two experiments may be explained by the characteristics of the water drop size and the effective water volume. An effective water volume corresponds to the water volume in contact with EM particles. The droplets size for the large sand column test was smaller (micro-droplet of 1 to 3 mm) and applied on a larger surface (2826 cm^2). Thus, the effective water volume in contact with Comp B particles is larger in the sand column test than in the dissolution test on the fritted glass funnel with big droplets (7–8 mm) applied to a smaller surface area (1.7 cm^2). The lesser effective water volume in contact with Comp B particles on the fritted glass funnel tests may explain the smaller dissolution rate of the fritted glass funnels dissolution test than in the large sand column test.

Figures 5-29 to 5-31 show the concentration of each EM as a function of the cumulative water volume applied in water drop test and show some differences with the large sand column experiment conducted by Lewis (2006). During the first year and for the large sand column test, two concentration peaks were observed: the first one at the end of the spring and the second one at the beginning of the autumn when the water flow was restarting (Lewis 2006). For the water drop test, the summer and winter were not simulated; spring and autumn ran one after the other and this

separation between the two peaks was not distinct. The water drop tests showed that concentrations were low during the first year for all EM while they were 10 times higher in the second year (Fig. 5-30 and 5-31). This behavior is different from the dissolution tests on the large soil column that showed the highest dissolution concentration during the first spring. This observation is astonishing for the column tests because water must flow through the 0.60-m soil column; in the water drop test, water flow has no delay. Dissolution seems faster in the large sand column tests than in the water drop test.

Differences between these two tests may be explained by the effective water volume in contact with EM particles (water droplet size/EM surface ratio) in combination with the residence time of the water in contact with particles. The spring is simulated in 10 days in the water drop test and in 31 days in the sand column tests. The small residence time between the water and EM particles in the water drop tests prevents EM dissolution. Also, the small effective water volume in the water drop tests slows down the dissolution rate.

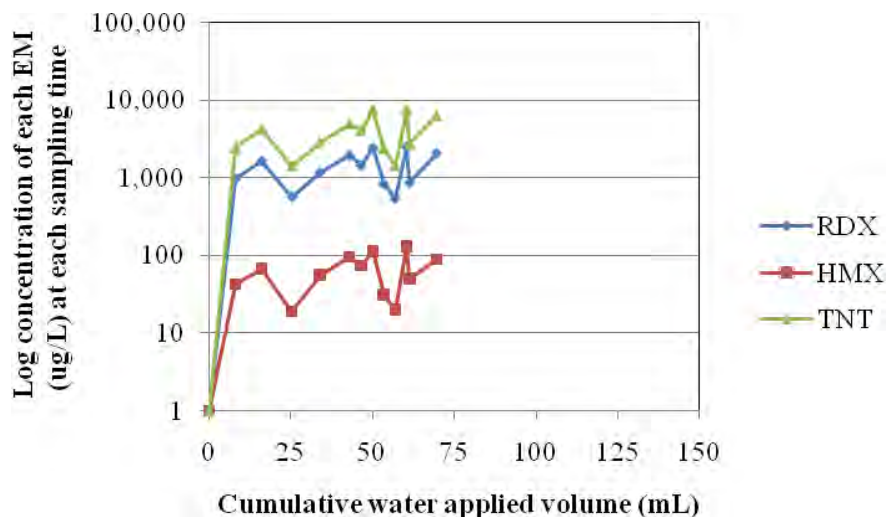


Figure 5-29. Concentration of each EM (RDX + HMX + TNT) in the effluent of water drop test H at each sampling time as a function of the cumulative water volume applied during 1 year of simulation.

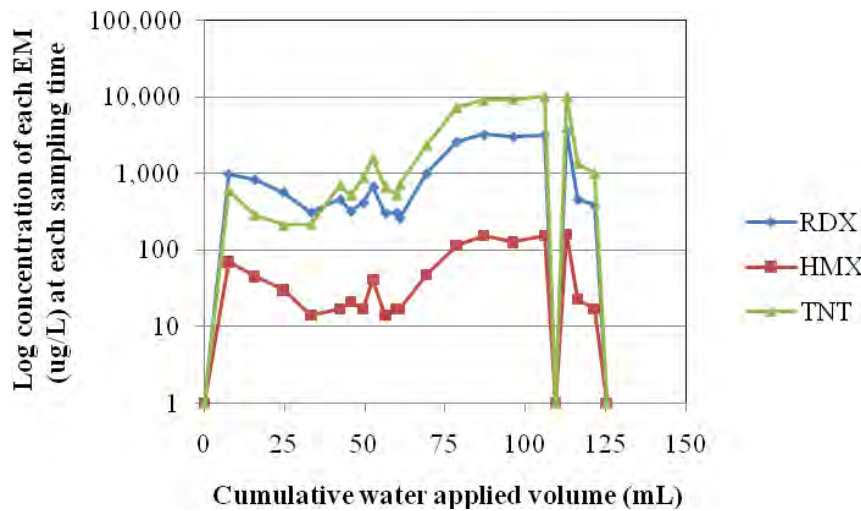


Figure 5-30. Concentration of each EM (RDX + HMX + TNT) in the effluent of water drop test I at each sampling time as a function of the cumulative water volume applied during 2 years of simulation.

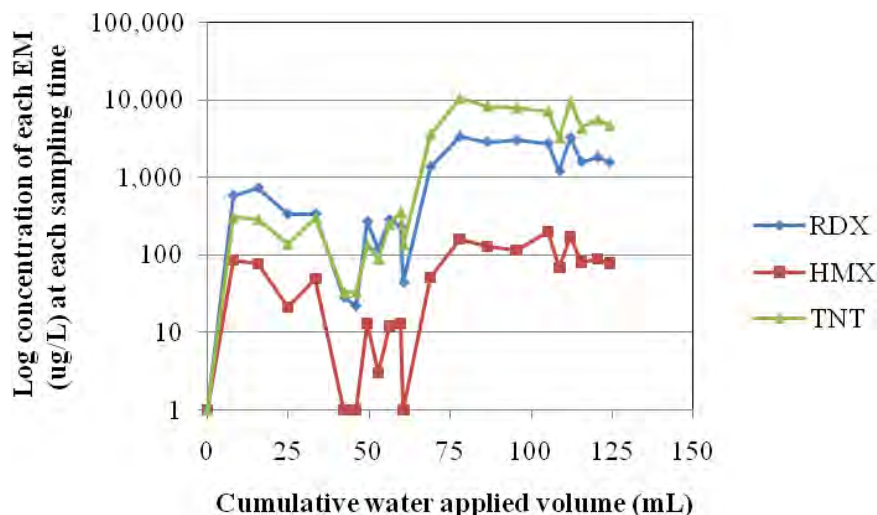


Figure 5-31. Concentration of each EM (RDX + HMX + TNT) in the effluent of water drop test G at each sampling time as a function of the cumulative water volume applied during 2 years of simulation.

Maximum EM concentrations in the effluent samples of the water drop tests are in the same range as for the large sand column tests, but the timing when the EM concentrations reach their maximum was earlier in the large sand column test.

If a stronger correlation between the water drop tests and the sand column tests is desired, the design of the water drop tests must be changed. The

season simulation must be the same length of time in both experiments. The same flow rate pattern must be used to increase the time of simulation for the water drop tests, which will increase the effective water volume. The residence time of water must be adjusted for the spring to simulate a cycle of watering (8 hours) followed by no watering (16 hours) because the wet/dry cycling is important. Simulation of autumn stays the same for both experiments, with watering 24 hours/day, but the autumn simulation time for the drip tests must be extended to 60 days to match that of the large sand column test. Simulation of summer and winter should introduce a dry period between spring and autumn.

5.3.4.3 Results of the 2-year dissolution tests with pure Octol flakes and powder

Dissolution tests on three samples of Octol powder and three samples of Octol flakes were conducted with water drops at 8°C (Table 5-15). For each form of Octol, two setups were connected to a vacuum pump that created a suction of 0.17 bar and one was conducted at atmospheric pressure.

Table 5-15. Initial EM content in Octol powder and in Octol flakes on top of the fritted glass funnel used as well as the applied flow rates.

Residues	Replicate	Initial residues mass (mg)	EM content (mg) ¹		Spring (days); flow rate (mL/hr)	Autumn (days); flow rate (mL/hr)
			HMX	TNT		
Octol powder (70% RDX; 30% TNT)	D	41.3	28.9	12.4	10; 120	7.3; 0.74
	E	55.7	39.0	16.7		
	F	62.9	44.0	18.9		
Octol flakes (69.5% RDX; 31.5% TNT)	G	210 (1 big flake)	146	66.1		
	H	55.3 (1 small flake)	38.4	17.4		
	I	110 (2 flakes)	76.1	34.5		

¹ Defined on a fourth sample with 3 replicates

For the two samples under suction, Porapak 6 cm³ RDX were placed on the vacuum line to recover the volatile part of the EM.

Appendix D, Tables D-1 and D-2, contain the setup parameters of the test and Table D-4 presents an example of data processing.

Figures 5-32 to 5-37 present cumulative EM mass lost expressed as a percentage of initial EM mass as a function of cumulative eluted water volume

that had passed through the samples on the fritted glass funnels for 2 years of simulation. Because the dissolution rates for these forms of Octol are linear (Fig. 5-32 to 5-37), no distinction was evident between the first and the second years of the simulation. Because of the low concentration of HMX detected in the effluent, all concentrations were multiplied by 10 for better visualization of the results in the next graphs.

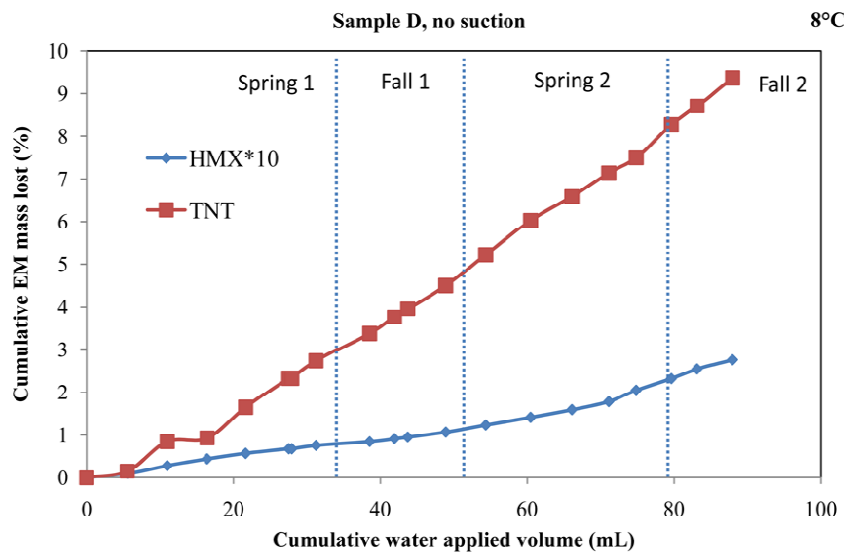


Figure 5-32. Cumulative EM mass lost expressed as a percentage of the initial mass of each EM in water drop test D (Octol powder) as a function of cumulative eluted water volume (no suction applied) during 2 years of simulation.

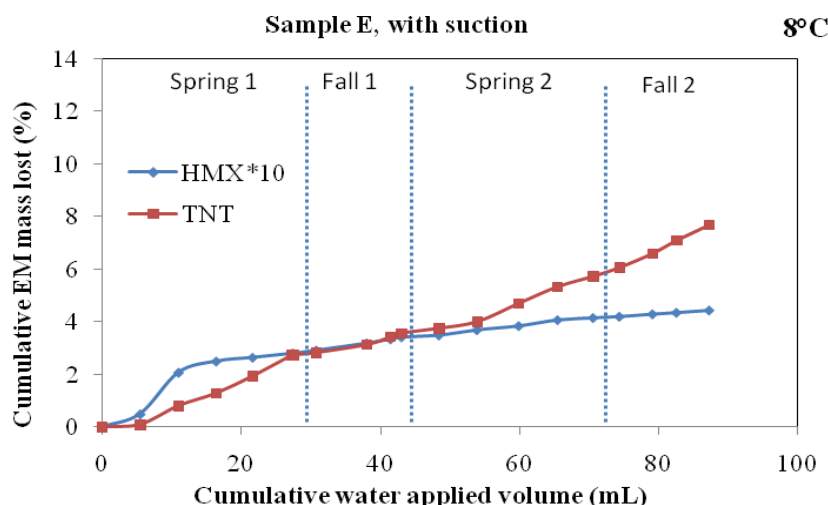


Figure 5-33. Cumulative EM mass lost expressed as a percentage of the initial mass of each EM in water drop test E (Octol powder) as a function of cumulative eluted water volume (0.17 bar applied suction) during 2 years of simulation.

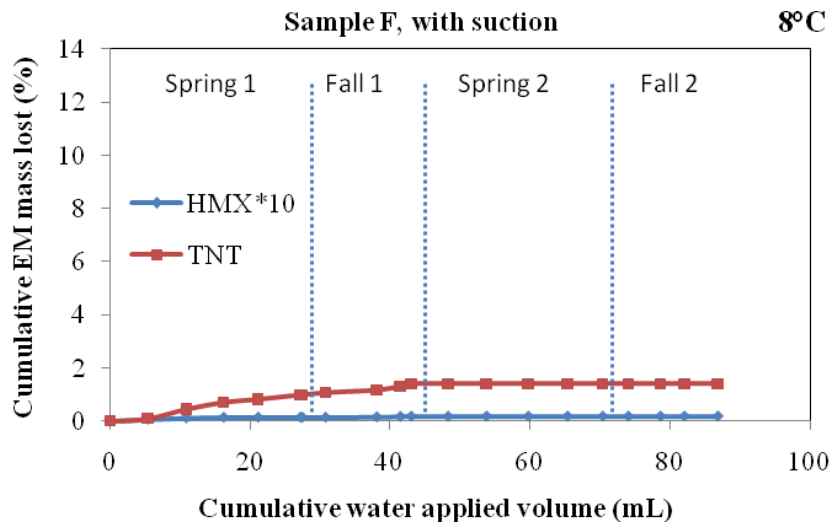


Figure 5-34. Cumulative EM mass lost expressed as a percentage of the initial mass of each EM in water drop test F (Octol powder) as a function of cumulative eluted water volume (0.17 bar applied suction) during 2 years of simulation.

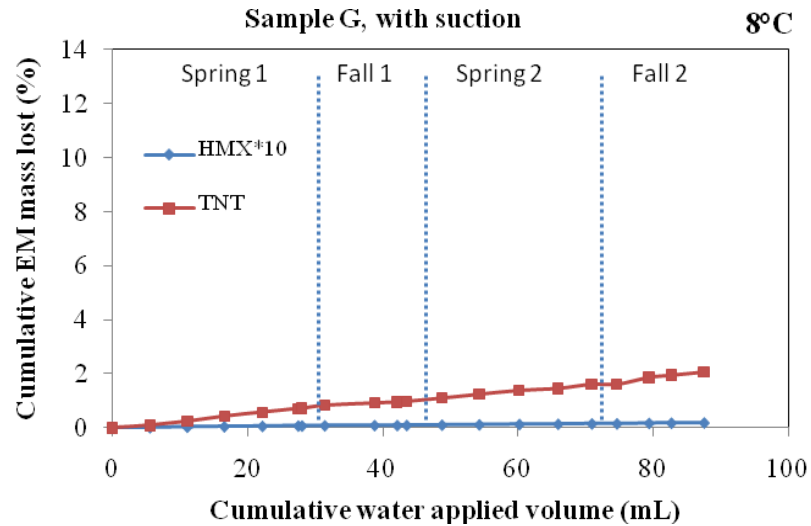


Figure 5-35. Cumulative EM mass lost expressed as a percentage of the initial mass of each EM in water drop test G (1 Octol flake) as a function of cumulative eluted water volume (0.17 bar applied suction) during 2 years of simulation.

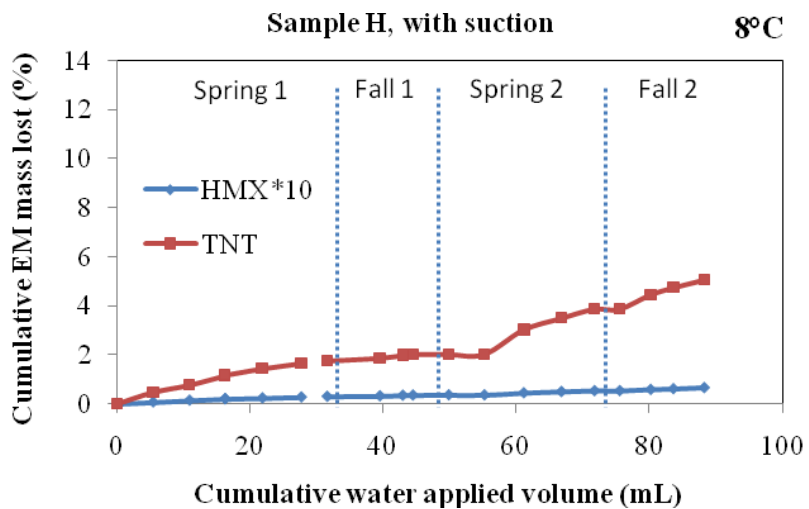


Figure 5-36. Cumulative EM mass lost expressed as a percentage of the initial mass of each EM in water drop test H (2 Octol flakes) as a function of cumulative eluted water volume (0.17 bar applied suction) during 2 years of simulation.

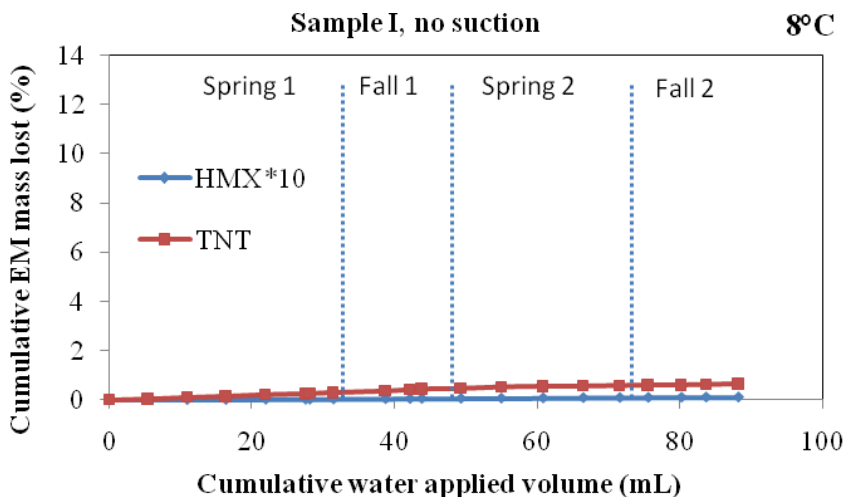


Figure 5-37. Cumulative EM mass lost expressed as a percentage of the initial mass of each EM in water drop test I (1 Octol flake) as a function of cumulative eluted water volume (no suction applied) during 2 years of simulation.

The dissolution rate of Octol powder or flake was independent of the seasonal flow rate. The dissolution rate was linear during the 2-year experiment without any variation, with the exception of sample E (Fig. 5-33), where the HMX dissolution rate showed an increase at 5 mL of applied water volume. Nevertheless, for these six tests, the dissolution rates of TNT were 20 to 120 times higher (samples E and G, respectively) than the dissolution rate of HMX, even though Octol is a mixture of 70% HMX and

only 30% TNT. This difference may be explained by difference in the solubilities of these two compounds (~100 mg/L at 20°C for TNT and ~3.8 mg/L at 20°C for HMX [Lynch et al. 2001, 2002]).

Octol powder samples (D, E, and F) under suction showed a TNT dissolution rate smaller than the sample not under suction. As with the other energetic formulations previously described in this chapter, the cause of the lower dissolution rate is likely related to the residence time between Octol particles and water. The same pattern did not apply for HMX; the HMX dissolution rate of sample E (under suction) was two times higher than for sample D (no suction). For sample F, the dissolution rates for TNT and HMX became nil after 50 mL of applied water, although more than 85% of the initial EM mass remained on the fritted glass funnel (Table 5-16).

For the Octol flake samples (G, H, and I), a difference was observed between samples under suction (G and H) and the sample not under suction (I). Sample I without suction had the smallest dissolution rate. This result is contrary to what is observed for Comp B and Octol powder. Dissolution rates of TNT and HMX for samples in flake form appear to be smaller than those when Octol is in powder form. This is probably attributable to the low specific surface area reachable by water to dissolve EM when Octol is in flakes (smaller surface area to mass ratio).

Figure 5-38 shows that the dissolution rate of Octol was linear for these six samples and independent of the flow rate. It also shows that the dissolution was not complete after 2 years of simulation in all samples, with the exception of sample F, which had a no dissolution mass from the beginning of the second year.

Table 5-16. EM contents in Octol at the end of the dissolution experiment with the water drop test.

Sample	Form of Octol	A: Initial EM mass on the fritted glass		B: Final EM mass on the fritted glass		C: Total dissolved mass of EM		D: Mass of EM inside the fritted glass		E: Final total mass (B+C+D)		F: EM mass balance (E/A*100)	
		HMX	TNT	HMX ¹²	TNT ¹²	HMX ²	TNT ²	HMX ²	TNT ²	HMX	TNT	HMX	TNT
		mg	mg	mg	mg	mg	mg	mg	mg	mg	mg	%	%
D	Octol in powder	28.91	12.39	26.3465	9.5607	0.0796	1.1594	0.1384	0.0321	26.5645	10.7522	91.89	86.78
E	(70% RDX; 30% TNT) ³	38.99	16.71	36.0396	13.6184	0.1883	1.0256	0.5484	0.0526	36.7763	14.6966	94.32	87.95
F		44.03	18.87	42.4034	15.8496	0.0080	0.2114	0.1514	0.1864	42.5628	16.2474	96.67	86.10
G	Octol in flakes	143.7815	66.1185	142.8984	66.6722	0.0284	1.0421	0.0214	0.056	142.9482	67.7703	99.42	102.50
H	(69.5% RDX; 31.5% TNT) ³	37.8805	17.4195	39.2194	15.3513	0.0269	0.6718	0.0419	0.062	39.2882	16.0851	103.72	92.34
I		75.0075	34.4925	78.7182	33.7284	0.0090	0.1701	0.0064	0.0133	78.7336	33.9118	104.97	98.32

¹ Determined by analysis of the final particles because the HMX/TNT ratio is probably different.

² Determined by HPLC-UV analysis with USEPA 8330B method.

³ Purity is 100%.

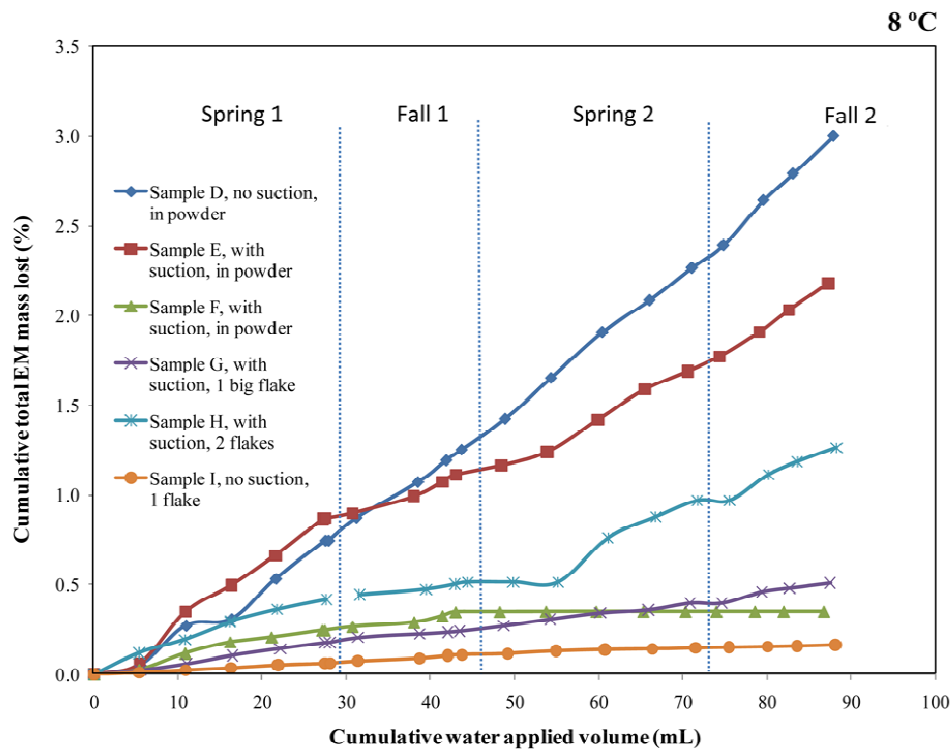


Figure 5-38. Percentage of total EM mass lost (HMX + TNT) based on the initial EM mass of six Octol water drop tests (D, E and F—powder form; G, H and I—flake form) as a function of the cumulative water volume applied on these samples during 2 years of simulation

These two forms of Octol (flake and powder) show different dissolution rates for HMX and TNT, but they have a similar range for each EM. Nevertheless, it was difficult to compare the flake and powder results because we don't know if all the water droplets interacted with the flakes on the fritted glass funnel. This is not the case for powder, because it was spread on the entire surface area of fritted glass funnel and the water drops had to pass through the powder. Thus, for the sample with Octol in flake form, the effective water volume that produced dissolution is probably less than that applied. In addition, the water flow rate (seasonal and yearly) did not appear to have an effect on the dissolution rates of TNT and HMX in Octol form, contrary to what was observed with Comp B. Also, results show that the suction effect and, consequently, the residence time of water in contact with EM particles seem to have less of an effect with Octol than with Comp B. One explanation for this phenomenon is the different composition of Octol compared to Comp B. Although the TNT content is similar (29.1% in Comp B and 30% in Octol), the main component content is different (43% RDX in Comp B and 70% HMX in Octol). This may explain the lower dissolution rate observed for Octol, as the solubility of RDX is 10 times higher

than that of HMX (Lynch et al. 2001, 2002). The crystalline skeleton of HMX particles is more stable in Octol than the RDX particles in Comp B and consequently protects the intra-crystalline TNT matrix (Fig. 5-39). The low dissolution rate of HMX tends to preserve particles of Octol and TNT inside and consequently the specific surface area for dissolution decreases more slowly relative to Comp B with RDX.

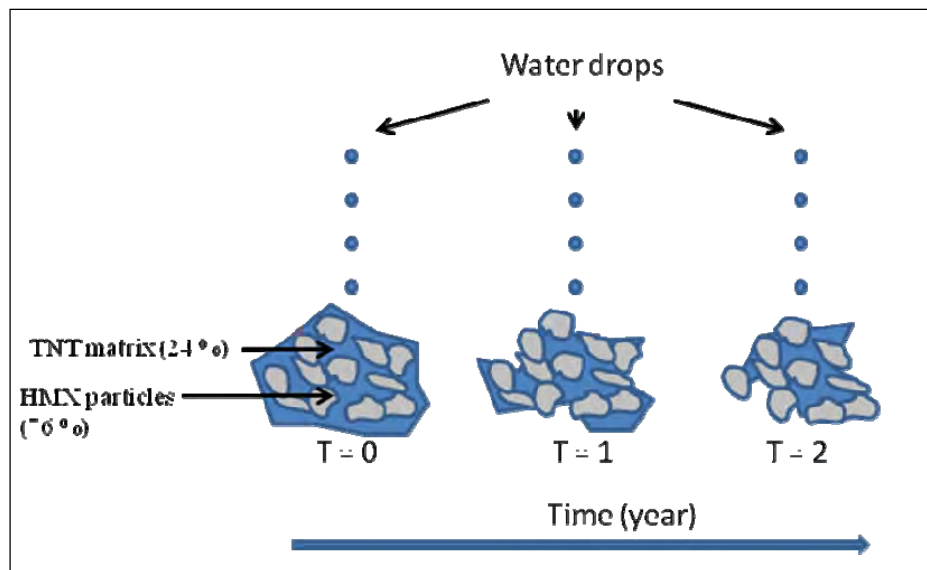


Figure 5-39. Conceptual model of dissolution of Octol on fritted glass funnel during water drop test as a function of time.

Combining the dissolved, undissolved, and precipitated fractions of EM after 2 years of simulation, we found the percentages of recovery compared to the initial mass of HMX and TNT to be, respectively, between 91–105% and 86–103% (Table 5-16). The volatile part of EM measured with cartridges was insignificant and not considered in Table 5-16. A higher fraction of TNT was not recovered at the end of the test compared to the HMX recovered mass and the missing EM mass is higher for Octol in powder than in flakes. The deficiency of TNT may be ascribable to the TNT having unknown degradation products that are volatile or soluble in water and cannot be analyzed with the usual analytical method (USEPA 8330B). EM content in the fritted glass is a high fraction, particularly for samples in powder form. Nevertheless, the total dissolved mass lost is larger for Octol in powder form than in flake form, attributable to the larger specific surface area of Octol in powder than in flakes. The total HMX dissolved mass is higher for Octol in powder than for Octol in flake, while the total TNT dissolved mass seems similar between these two Octol forms.

As was the case for Comp B, the compositional heterogeneity of Octol particles can be a source of error that would influence the initial content of EM in the three subsamples. It was not possible to quantify the EM before the experiment, and the HMX/TNT ratio may not be the same for each sample. The specific surface area of each Octol subsample exposed to water drops was different, particularly between powder and flake. Also, the water drops may not have all interacted with the Octol flakes, which was not likely the case for the Octol powder. Thus, the effective water volume is different and was probably overestimated for the Octol flakes. The water content of the final mass of particles on the fritted glass may vary and has an impact on the final EM mass. The volume estimation of the eluted water sample at each sampling date, the EM mass that was recrystallized in the fritted glass pores, and the EM volatilized fraction were also sources of error but were evaluated in detail (Table 5-16).

5.3.4.4 Setup of the third dissolution test

As described earlier in this chapter, a third set of water drop dissolution tests at 8°C with the three sources of contaminant on the large sand column tests are in progress (see Section 5.2). Soil from the Wellington anti-tank impact area at CFB Gagetown, the artillery firing position Hotel Tower at CFB Petawawa, and residues from an artillery gunpowder bag burning test on snow at CFB Valcartier are under study (Table 5-17). For each source, two setups were used—one connected to a vacuum pump recreating a tension of 0.17 bar and one not connected to the vacuum pump. For the two samples under suction, Porapak 6-cm³ RDX cartridges were placed on the vacuum line to recover the volatile part of the liberated EM. The soil with propellant residues from the firing position sampled on 20 September 2006 at Wellington range at CFB Gagetown (Table 5-9) was also studied with a different watering setup to reproduce the same watering pattern as on the large soil columns. Thus, for the spring simulation, the flow rate was established with a watering (8 hours) and no-watering (16 hours) 24-hour cycle. The watering for the autumn simulation will be the same as the previous water drop tests: a constant watering during 24 hours/day for 7.3 days compared to 60 days for large sand column test. A summer dry period of 7 to 10 days at 20°C between spring and autumn will be necessary to dry the particles. The dissolution water drop test, with this new watering pattern, on the soil with propellant residues sampled at Wellington range at CFB Gagetown will allow us to compare the effect of the daily watering–no-watering cycle during the spring simulation. This third

test began on 12 March 2009; no results were available at the time of this report.

Appendix D, Tables D-1 and D-2 present the setup parameters of the test.

Table 5-17. Parameters of the third dissolution tests—initial EM contents in the soils samples placed on the fritted funnel and the applied flow regimes.

Residues	Replicate	Initial residues mass on fritted glass (g)	Vacuum	Spring (hours per day; number of days); flow rate (mL/hr)	Autumn (hours per day; number of days); flow rate (mL/hr)
Soil with propellant residues sampled at Wellington range at CFB Gagetown	A	2.043	N	8; 31; 120	24; 7.33; 0.74
	B	2.044	Y		
	C	2.042	Y		
Soil sample from the artillery firing position Hotel Tower at CFB Petawawa	D	3.856	Y	8; 31; 120	24; 7.33; 0.74
	E	3.895	Y		
	F	3.873	N		
Residues from artillery gun powder bag burning test on snow at CFB Valcartier	G	0.091	N	8; 31; 120	24; 7.33; 0.74
	H	0.072	Y		
	I	0.101	Y		
Soils samples from the Wellington anti-tank impact area at CFB Gagetown	J	2.845	Y	8; 31; 120	24; 7.33; 0.74
	K	2.820	Y		
	L	2.884	N		

5.4 Conclusion

Both experiments (the large sand column tests and the dissolution tests with water drops) presented in this chapter are almost completed, but are still ongoing. Results obtained with these tests should allow us to complete collecting the needed information on dissolved EM on top of the large sand columns to complement the original ER-1481 project. The columns and dissolution tests carried out in the extension of project ER-1481 led to detailed information on the dissolution rates of three types of energetic residues that occur in training areas: Octol (HMX and TNT) on anti-tank ranges, and 2,4-DNT at artillery firing positions and propellant disposal areas. The combination of columns and drip tests led to a better understanding of the fate of EM under various conditions.

Large sand column tests on a soil sample from the Wellington anti-tank impact area at CFB Gagetown, a soil sample from the artillery firing posi-

tion Hotel Tower at CFB Petawawa, and residues from artillery propellant burning test on snow at CFB Valcartier are still in progress. Two columns are under study for each contamination source. The results to date are reproducible from the two columns. Results through to the end of the second spring of the 2-year simulation are available.

An HMX pulse was observed in the Octol-contaminated soil column during the second half of the spring (maximum at ~1000 µg/L), but the end of the pulse is unknown. It will be probably be determined with the second falls' results. A complete dissolution pulse was observed for TNT (maximum at ~130 µg/L) during the second half of the spring. The TNT pulse was retarded compared to the HMX pulse. We estimated that more than 650 and 4800 L of groundwater may be contaminated by HMX and TNT, respectively, for a surface of 1 m² of contaminated soil from the Wellington anti-tank impact area at CFB Gagetown.

For residues from the artillery propellant burn test on snow at CFB Valcartier, we observed a major pulse of 2,4-DNT (maximum at ~9 000 µg/L) and, after a little delay, a pulse of 4-A-2,6-DNT (maximum at ~90 µg/L). The pulse of 2,4-DNT was not finished at the end of the second spring, during which concentrations decreased slowly. The pulse of 4-A-2,6-DNT was completed during the second half of the spring. Owing to the high concentrations of 2,4-DNT and 4-A-2,6-DNT that move very rapidly in the unsaturated zone and may contaminate more than 4100 m³ of groundwater per square meter of propellant residues, we recommend that field expedient burning of gun powder bag be stopped to prevent further groundwater and soil contamination.

For the soil sample from the artillery firing position Hotel Tower at CFB Petawawa, EM were not detected in the column effluent samples until the end of the second spring. One of the two test columns was excavated and sampled to analyze for EM content in the soil profile; analyses are in progress. The hypothesis here would be that any available 2,4-DNT had been leached out prior to our sampling of the source, and the remaining 2,4-DNT is irreversibly bounded into the NC matrix.

Dissolution tests on soils contaminated with NG from propellant residues on Wellington range at CFB Gagetown showed that a portion of NG is eluted mainly during the first spring. The following year NG is not available for dissolution because the remainder is embedded in the NC matrix.

This is similar to the phenomenon that we observed for the artillery firing position soils.

A dissolution test on Comp B particles showed that the applied water flow rate has no influence on the dissolution rate. The residence time of water in contact with EM particles is the main parameter affecting EM dissolution. Variability in dissolution rates of the three compounds (RDX, HMX, and TNT) shows also that Comp B particles may present a high compositional heterogeneity (proportion of RDX/HMX particles to the TNT matrix). This heterogeneousness may explain the differences observed in dissolution rates and is probably attributable to the surface area of each EM exposed to water drops. Comparing the water drop test results to Lewis' (2006) results shows that care must be taken with the test methods to correlate the experiments. The drip test protocol should include a longer spring with a watering–no-watering cycle and a summer period to dry the particles to more closely match the parameters of the column tests.

Dissolution tests were made with Octol in flake and powder form. The residence time of water in contact with these EM particles has less influence on the dissolution process than for the particles of Comp B. The low dissolution rate of HMX in water may be the reason for the difference. Octol in powder form has a dissolution rate three to six times higher than Octol in flakes; this is related to the specific surface area, which is larger in powder than in flakes.

The third series of water drop tests with the three sources of contamination that are the same as those studied on the large sand columns are in progress.

We had difficulty correlating the water drop test results with what was observed on the large sand columns. We hypothesize that this was caused by compositional heterogeneity affecting the smaller samples used in the water drop tests, along with the water drop size and frequency that affect the effective water volume for dissolution. Another setup was proposed to ensure compatibility between the dissolution tests and the large sand column tests: three new large columns without clean sand will be used in the same laboratory as the large sand column to ensure the same environmental conditions exist between these two tests. Also, the duration of the test, watering, contamination sources mass and size, and sampling frequency will be done with the same setup and devices, but contamination sources will

be spread directly on a 1-cm inert material layer. Thus, there will be no retardation time between their dissolution and their analyses in effluent column samples. The results obtained for the various sources of contaminations in columns and in drop tests allow us to gain a better understanding of the complex dissolution processes of the heterogeneous EM formulations that are deposited in the surface soils of ranges and training areas. Conceptual models for the dissolution of Octol and Composition B, two formulations that are widely used in North American weapons, were proposed.

6 A Simple Device for Initiating High-Order Detonations

Michael R. Walsh, Marianne E. Walsh, and James W. Hug

6.1 Introduction and background

The collection of energetics residues from live-fired munitions is often a difficult proposition. Locating the detonation point and accessing it safely on an active impact area are usually very difficult when allowed. Cross-contamination is always a consideration, and unless work is done on a seasonally ice-covered impact area, will be impossible to avoid. Conducting tests on low-ordered ordnance is difficult because of the low incidence of this type of detonation. And precisely positioning a fired round adjacent to an item of unexploded ordnance (UXO) to determine the effect of a close-proximity detonation is not likely.

For SERDP Project ER-1481, one of the tests we proposed was to determine the effect of a close-proximity high-order detonation from a fully functioning round on nearby unexploded ordnance. This test was a follow-up to a test conducted by Lewis et al. (2009) in Canada in which they generated pitted or breached rounds by detonating unfuzed mortar projectiles with a block of C4 explosive over a second unfuzed mortar projectile. For their tests, the objective was to create damaged rounds to determine explosives leaching rates into soils. For the ER-1481 tests, we were more interested in the damage to and reaction of the adjacent UXO to a high-order detonation from a fully functioning round. Thus, the use of an external donor charge was not desired for the initiation of the detonation.

6.2 Objective

The objective of this study was to develop, test, and implement a simple system that will replace a fuze in a high-explosive (HE) projectile and enable researchers to cause the projectile to detonate high-order, thus simulating a live-fire high-order detonation of a point detonating projectile.

6.3 Materials and methods

The tests that were planned for the close-proximity detonations required the use of 81-mm HE mortar rounds. Thus, the initiation system had to function with that specific round. We also wanted a simple system that was safe, easily implemented, and utilized common materials available to explosive ordnance disposal (EOD) units on military installations, where the tests would need to be conducted. The initiation system should mimic the explosive train designed to detonate HE filler of the projectile.

The simplest fuze used for most projectiles is called a point-detonating fuze. These fuzes arm shortly after leaving the barrel of the weapon system and function upon impact with the ground. A small charge is activated upon impact, causing a shock wave to propagate into a larger booster charge at the base of the fuze. The detonating booster charge, located next to the HE filler in the main body of the round, transfers a much larger shock wave into the main charge, causing the filler to detonate. The body of the projectile then shatters, sending steel fragments (frag) and a shock wave radially out from the detonation point. The detonation consumes over 99.99% of the HE filler. Our objective was to mimic this chain of events to enable us to conduct realistic tests without the need to fire a round from a mortar.

Fuzes are generally made of aluminum alloy. Thus, we chose a standard aluminum alloy (6061-T6) as the basis of our design. We obtained data on the standard fuze used with the rounds we were to test, incorporating this into the design. Thread size and length and the geometry of the booster cup were critical parameters when matching fit and performance of the device. The booster charge mass was used to finalize the booster cup design. As C4 is a common explosive available to EOD units, we designed the cup around this compound. To initiate the booster charge, we settled on a standard military blasting cap routinely used for initiating demolition blocks, which incorporate C4 explosive. The port for insertion of the blasting cap is 2 mm shorter than the cap, so that when the top of the cap is flush with the top of the initiator system, it will be partially embedded in the booster charge, giving us coupling between the two charges.

6.4 Testing

Prior to using the initiator device in the close-proximity tests, we conducted two tests to determine if the device would perform as needed. The

first test was of the device alone, fully configured, as it would be for use in a round. The second test was a detonation test to determine if the system would actually initiate a high-order detonation in the rounds to be used for the close-proximity detonation study.

The rounds used for the test were M374 81-mm HE mortar rounds. We chose these rounds because the rounds used by Lewis et al. (2009) were 81-mm HE rounds. The rounds come without fuzes and have a cast zinc nose plug that can be easily removed for the installation of the initiation device. The mortar round contains 950 g of Composition B (Comp B) explosive (60% RDX:39% TNT). Propellant charges were removed prior to detonation of the round, although the propellant initiation charge was left in the tail of the round. We anticipated that this energetic material would have no effect on the tests, as it is not as shock sensitive as the explosive filler. Table 6-1 contains data on the munitions used for these tests.

Testing was conducted at the Demo III demolitions training range on Fort Richardson, AK. We were assisted by the U.S. Army Alaska Range Control Office, the 716th EOD detachment, and James Hug, UXO Tech-3 out of the U.S. Army Engineer Division, South Pacific, Albuquerque District office. Snow depth varied, averaging about 60 cm. Frozen soil underlaid the snow cover. Temperatures during the tests were near freezing with calm winds and mostly sunny skies.

Table 6-1. Munitions used for the detonation system tests.

Description	DODIC	Energetic formulation	Component	Energetic mass (g)
Mortar Cartridge M374	C236	Comp B	—	950
			RDX	570
			TNT	370
Ignition Cartridge M66A1	Part of C236	M9 Propellant	—	7.5
		NG		3.0
Booster Charge M112 ¹	M023	C4	—	23
			RDX	21
Blasting Cap M6	M130		Lead Azide	0.27
			RDX	0.94

¹ M112 Demolition Charge: 520 g each. Portion used for each booster charge is 23 g.

6.4.1 Testing of the device

A device was loaded with 23 g of C4 explosive, enough to fill the booster cup (Fig. 6-1). An M6 blasting cap was then inserted through the access port at the top of the device partially into the booster charge. The cap was then set off electrically. The remains of the device were recovered and inspected to determine if the system would function in a loaded HE round.



Figure 6-1. Device with C4 booster installed.

6.4.2 Test of the total system

After the successful test of the initiator device, we carried out three tests of the total system. Prior to testing, we obtained a baseline sample within the test area. A small (10- × 10- × 2-cm deep) Teflon®-lined hand scoop was used to sample the area using the standard protocol for sampling for energetics on snow-covered ranges (Walsh, M.R., et al. 2007b).

Following the baseline sampling, one initiation device was loaded with the booster charge and installed in a fully loaded mortar round. The round was placed vertically with the nose down in an untrafficked area of the range (Fig. 6-2). The round was then detonated electrically. Following inspection of the detonation area, the plume area surrounding the detonation was sampled using multi-increment (MI) sampling.



a. Preparing to screw the device into the 81-mm HE body.



b. Round in place ready for detonation.

Figure 6-2. Test setup for the initiation system.

Using the 10- × 10-cm scoop, we took triplicate MI samples within the visually demarcated plume area, which included the detonation crater (Fig.

6-3). Triplicate MI samples were taken within a 3-m annulus surrounding the first plume periphery to determine if the plume demarcation was sufficiently large.



Figure 6-3. Detonation plume following first system test.

Samples were collected in lab-grade polyethylene (PE) bags. The bags were labeled on the outside with the sampling information (except the number of increments) prior to sampling. After the sample was taken, the number of increments was written on the bag and the information transferred to a permanent tag and into a field book. The tag was then wire-tied onto the

cinched sample bag top and the bag placed into an outer PE bag at the transfer station to reduce the chances of cross contamination.

Two more tests were done in the same manner in different locations of the Demo III range. The same procedure for sample collections was used. When all the initiator system tests were completed, the samples were transferred to a lab on post for processing.

On post, the samples were processed for shipment to the analytical lab at CRREL in Hanover, NH. The sample bags were placed in clean plastic bins and allowed to melt overnight in the logistics room adjacent to the lab. They were then filtered, the filters containing the solid residues stored in 4-oz, amber, wide-mouth jars in a refrigerator, and two aliquots of 500-mL each taken from the filtrate, stored in amber Teflon-capped bottles, and placed in the refrigerator. When all the samples were filtered, one of the bottles from each of the samples was filtered through a PorPak RDX¹ cartridge to remove the energetic compounds from the water. The cartridges were then eluted with 5.0 mL of acetonitrile into a 7-mL vial and placed in the refrigerator.

At the end of the tests, the filters and vials were shipped to CRREL for final processing and analysis. Energetic compounds were extracted from the soot fraction on the filters using acetonitrile. Samples were mixed on a platform shaker set at 150 rpm for 18 hours. The acetonitrile extracts from the solid phase extraction of the melted snow and of the solid residue on the filters were analyzed by high-performance liquid chromatography (HPLC). Analyte concentrations were determined following the general procedures of SW 846 Method 8330 to determine nitroaromatics and nitrarnines by HPLC (USEPA 2006). The HPLC method has an analytical error that is very small, about 2% relative standard deviation (RSD) for replicate injections.

Before HPLC analysis, 1 mL of each acetonitrile extract was mixed with 3 mL of reagent-grade water. Determinations were made on a modular system² composed of a SpectraSYSTEM Model P4000 pump, a SpectraSYSTEM UV2000 dual wavelength ultraviolet/visible absorbance detector set at 210 and 254 nm (cell path 1 cm), and a SpectraSYSTEM AS300 auto-

¹ Sep-Pak, 6-cm³, 500-mg; Waters Chromatography Division, Milford, MA.

² Thermo Electron Corporation of San Jose, CA.

sampler. Samples were introduced with a 100- μ L sample loop. Separations were achieved on a 15-cm \times 3.9-mm (4- μ m) NovaPak C8 column¹ at 28°C and eluted with 1.4 mL/minute of 15:85 isopropanol/water (v/v).

Calibration standards were prepared from analytical reference materials obtained from Restek Corporation (Bellefonte, PA). The analytical reference materials were 8095 Calibration Mix A (1 mg/mL) and a single-component solution of NG (1 mg/mL). A spike solution at 1000 μ g/L was prepared from 8095A Calibration Mix and the single-component solution of NG (10,000 μ g/L). Spiked water samples at 2 μ g/L were prepared by mixing 0.10 mL of the spike solution to 500 mL of water in a volumetric flask. Following SPE, the extract target concentration was 200 μ g/L for each analyte.

We used a detection limit of 0.02 mg/L for HMX, RDX, and TNT, and 0.05 mg/L for NG. Values below these limits are labeled as ND in the data.

6.5 Results

6.5.1 Test of the device

The initiator device worked as planned when tested alone. Only one test was necessary based on the visual inspection of the device after initiation. The booster load was completely gone and the booster cup end of the device was severely damaged, indicating a high-order detonation (Fig. 6-4). Fracturing of the aluminum alloy device is a good indication of a high shock event as the aluminum is quite ductile.

6.5.2 Test of the system

The areas of the plumes were 260, 220, and 200 m², respectively. The plume produced from the live fire high-order detonation of an 81-mm mortar projectile was measured previously as 224 m² (Hewitt et al. 2003).

¹ Waters Chromatography Division, Milford, MA.

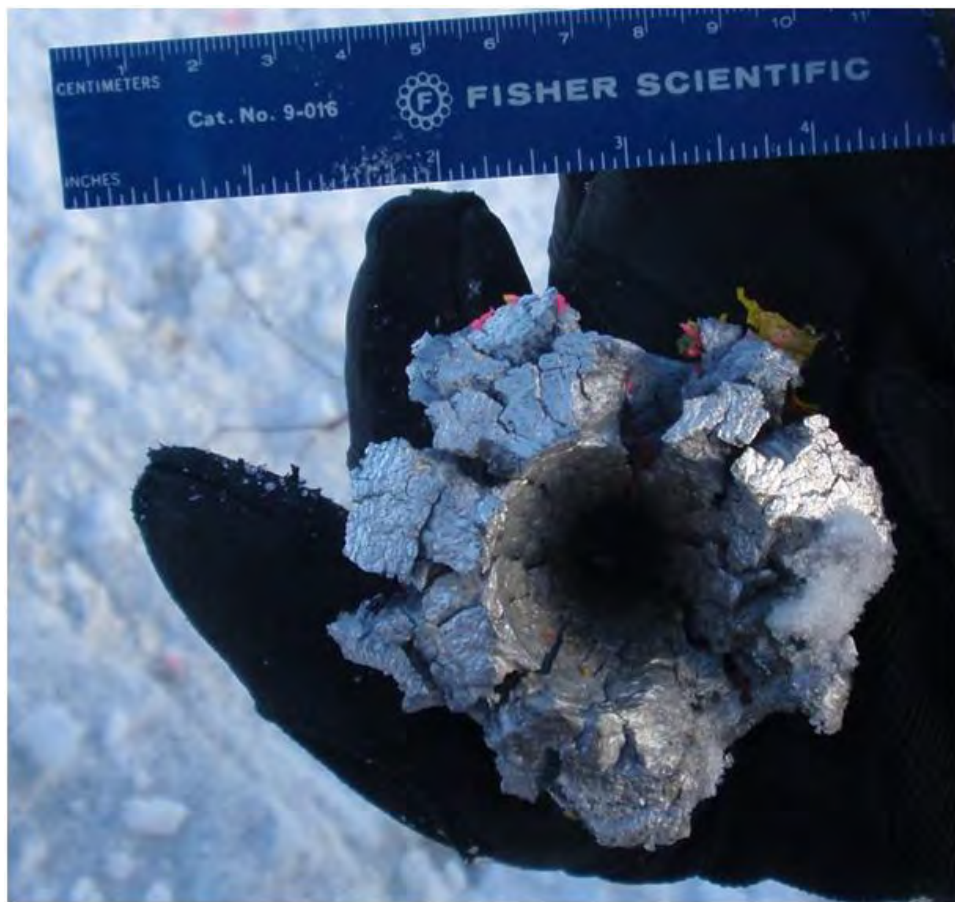


Figure 6-4. Initiator device after blast.

A map of the visually demarcated plumes is shown in Figure 6-5. The plumes did not overlap. Two of the three aluminum tail assemblies were recovered with no steel from the projectile body attached, an indication of a high-order detonation. No metal fragments were found in the plumes, also indicating that the detonations were efficient. Some underlying soil was kicked up by the detonations, which may have introduced some cross-contamination from previous activity on the range.

The initial mass of energetic compounds was the sum of the Comp B filler (953 g), the RDX in the C4 of the booster charge (21 g), and the RDX in the blasting cap (0.94 g). The estimated masses of Comp B residues (HMX, RDX, and TNT) in the detonation plumes are in Table 6-2, and the complete data set is in Appendix F, Table F-1. To calculate the mass of un-reacted energetics deposited on the snow, we multiplied the concentration of each plume (mass/unit area basis) by the measured area of the plume (Walsh, M.R., et al. 2007b). The residual mass (%) was calculated by dividing the mass of energetics recovered by the initial mass of energetics. For

all the samples that had non-detect values for some of the energetics, the minimum detectable mass, based on the analytical detection limit, was substituted for zero in the calculation for percent residual mass.

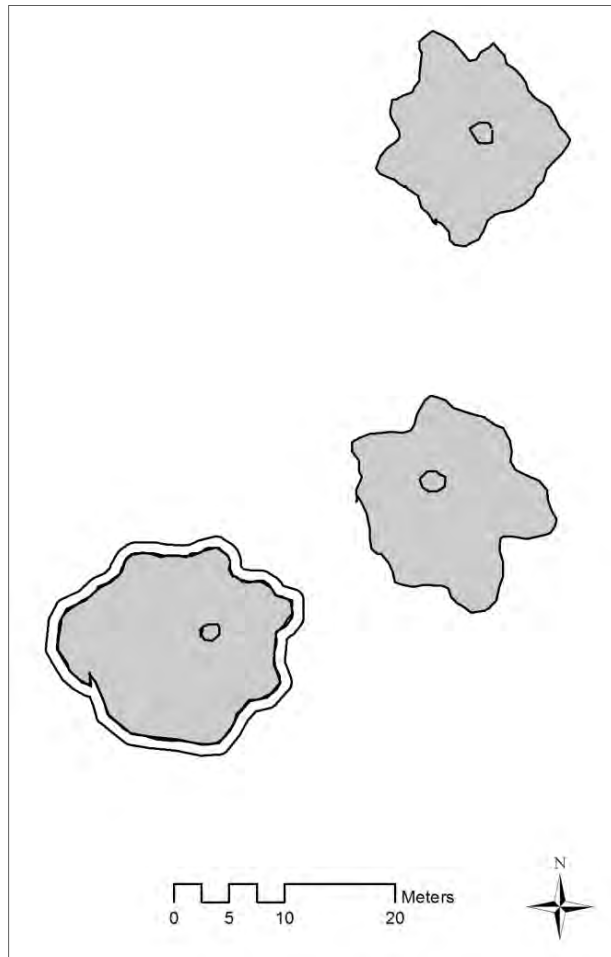


Figure 6-5. Initiator test detonation plumes.

NG was also detected in the snow samples. The source of the NG is the ignition cartridge in the tail assembly of the projectile. The cartridge contains 7.45 g of M9 propellant, of which 3 g is NG. Mean recoveries of NG were 0.81, 0.48, and 0.61 g or 27, 16, and 20% for plumes 1, 2 and 3, respectively.

Table 6-2. Mass of energetic compounds recovered in detonation plumes.

Sample description		Mass (mg) in plume			Residual ¹ (%)
		HMX	RDX	TNT	
Plume 1	Rep 1	<0.7	1.7	<0.6	<0.0003
	Rep 2	4.7	72	<53	<0.013
	Rep 3	<1.2	1.9	<0.5	<0.0004
Plume 1 mean		2.2	25	<18	<0.005
Plume 2	Rep 1	<0.4	1.7	<0.69	<0.0003
	Rep 2	<0.4	2.9	<1.6	<0.0005
	Rep 3	<0.4	<0.4	<0.4	<0.0001
Plume 2 mean		<0.4	<1.7	<0.90	<0.0003
Plume 3	Rep 1	<0.3	1.5	<0.3	<0.0002%
	Rep 2	<0.3	<0.3	<0.3	<0.0001
	Rep 3	<0.3	<0.3	<0.3	<0.0001
Plume 3 mean		<0.3	0.7	<0.3	<0.0001
Meta-mean (n=3)		<0.97	<9.1	<6.4	<0.0018

¹ Residual (%) = Sum of the masses (mg) of HMX, RDX, and TNT recovered/sum of masses (mg) of Comp B Filler and RDX in initiator device

6.6 Discussion

The initiation system successfully mimicked the fuze of a fired point-detonating projectile. The devices were easy to configure and install and were reliable. All three rounds used in the system tests went high-order (>99.99% average energetics consumption). Because we tested on snow overlying soil and did not have the segregating layer of ice separating our tests from previous range activity, there was a chance of cross-contamination. This may have happened during our first system test, which took place near the more active area of the range. The higher value for energetics from one of the triplicate plume 1 samples (plume 1, rep 2) is likely an artifact from previous activities. Past research with the 81-mm HE mortar projectile shows that the residual mass of RDX plus HMX from 14 live-fire detonations averaged 8.5 mg/round or 0.0014% of the original mass (Hewitt et al. 2007). This compares to less than 10 mg/round from the three detonations in this test. Blow-in-place residues from the same rounds using a block of C4 averaged 153 mg/round, or 0.014%—an order of magnitude higher (Walsh, M.R, et al. 2005a). The test detona-

tions most closely resembled the live-fire high-order detonations rather than the BIP detonations.

Based on the visual performance of the system (prior to sample analysis), we proceeded to use the initiators for the close-proximity detonation tests, which commenced the following day. Over the course of 3 days and 23 tests, all 11 mortar projectiles assembled with the CRREL initiation system detonated high-order.

6.7 Conclusions

The design of the high-order detonation initiator system proved to be a success. All rounds configured with the system, both during the tests described in this chapter and those in the following two chapters, detonated high-order. The use of the initiator systems opens new avenues to research of energetics residues by enabling the controlled detonation of rounds in a manner that closely simulates a live-fire high-order detonation, while under closely controlled test configurations. Without the initiators, our tests on close-proximity detonation damage to adjacent rounds would not have been possible.

7 Close-Proximity Detonations: a Study of the Damage to 81-mm Mortar Projectiles

Isabelle Poulin, Susan Taylor, Michael R. Walsh, Susan Bigl, Marianne E. Walsh, Anna Wagner, and James Hug

7.1 Summary

Unexploded ordnance (UXO) is the greatest single-point source of explosives on operational ranges. However, these rounds are fully enclosed on impact and the explosive filler is isolated from the environment until the body of the projectile is penetrated. Penetration of the rounds will expose high-explosive (HE) energetic material (EM) to the environment. Once HE is released from the metal casing, it can dissolve and be transported to groundwater. Although the likelihood that fragments from a high-order detonation will damage UXO on training ranges is thought to be small, the probability increases with higher densities of surface and near surface UXO. Our objective was to measure the damage produced on UXO from a close-proximity high-order detonation of a second projectile.

To produce damaged UXO, we detonated 81-mm mortar projectiles near unfuzed 81-mm rounds that simulated UXO. To initiate the detonating round, we used a system designed to fit in the fuze well that triggers the explosive train in a way similar to a functioning fuze. Of the 23 unfuzed rounds, placed between 0.30 and 1.20 m from the detonating round, the casings of five were not penetrated, four casings were pierced (penetration and exposure of the explosive), five were broken open (large area of exposure of energetic material with scattering of particles on the ground), six were partially detonated, one detonated high-order, and two were not recovered. The patterns of damage observed on all the UXOs are described herein. How the rounds were damaged can help identify similarly damaged UXO in the field. The test were performed in March 2010 at Fort Richardson—U.S. Army Alaska.

7.2 Introduction

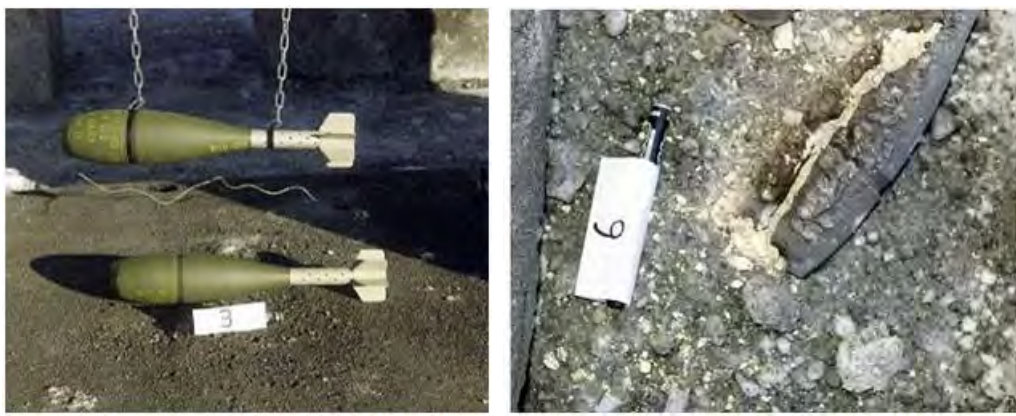
Live-fire training is a necessary component of readiness for U.S. and Canadian armed forces. Long-term use of military training ranges requires that each installation comply with environmental regulations that protect human health and the environment. For example, residues from live-fire training should not migrate beyond installation boundaries at concentrations above those that would impact ground and surface water resources for the surrounding communities.

High-order detonations deposit very little explosives residues on range soils (Hewitt et al. 2003; Hewitt et al. 2005; Walsh, M.R., et al. 2005b, c; Jenkins et al. 2006a; Pennington et al. 2006a). Low-order detonations release their explosive fill quickly and are a significant short-term source; however, corroded UXO release their explosives over longer time scales (Pennington et al. 2006a). Taylor et al. (2004b) analyzed the rate of the occurrence of these different fates and concluded that partial detonations are the largest contributor to explosive loads on ranges today. However, they noted that little information existed on the rate at which high-order detonations partially detonate or breach nearby rounds. Both of these fates would leave most of their explosive fill undetonated or unburned and would be large point sources of contamination. The number of UXO/m² of surface area has not been measured for many sites, and varies greatly at sites where it has been measured. For example, in the case of Massachusetts Military Reservation, discounting the impact area that has not been searched extensively, the values for the number of UXOs per acre ranges from 4 to 89 (Taylor et al. 2004b).

We selected the 81-mm HE mortar round (M374A2) for study because it is a commonly used round, it was previously used in tests intended to rupture rounds by Lewis et al. (Lewis 2007; Lewis et al. 2009), and its dud rate (2.3% [Jenkins et al. 2006b]) and the dispersion of its fragments are known (Lahaye and Abi-Zeid 1994).

Because breached rounds found on training ranges could not be transported back to the laboratory to be used in fate and transport studies (safety concerns owing to the presence of fuzes on the rounds), Lewis et al. (Lewis 2007; Lewis et al. 2009) did tests to create unfuzed, breached rounds. One of Lewis's experimental setups is shown in Figure 7-1a. The round on top was detonated using either a shaped charge or different amounts of C4 (see Appendix G for details on the tests). The casing of the

underlying munition was either cracked or pierced when the distance between the two rounds was between 0.15 and 1.57 m. At shorter distances, both rounds detonated high-order and separations over 1.57 m were not tested. For these tests most of the damage was found to be in the center of the round between 85° and 105°, where 0° was at the nose of the projectile and 180° was the tail. Because the two rounds were parallel, the fragments split the casings of the unfuzed rounds along their entire length (Fig. 7-1b). The authors concluded that fragments and not the pressure wave detonated or damaged the UXOs.



a. Setup to produce breached mortar. b. Breached mortar on top of soil column.

Figure 7-1. Lewis' work.

Individual breached rounds were placed on top of large-scale sand columns. These columns were in a climate-controlled laboratory where a sprinkler system produced the desired rainfall rates. Lewis et al. (2009) found immediate and high concentrations of explosives in solutions leaving the base of the column.

Arena tests are used to determine the fragmentation pattern of a munition detonated high-order. The munition is placed in the center of a horseshoe shaped test area where the structures stop the munition fragments (Fig. 7-2). The velocity of the fragments can be measured when specific surfaces on the structures are penetrated, while wood bins collect the fragments. The metal fragments are separated by a magnetic apparatus, and are then sieved into various sizes. The 81-mm round C70A1 (Canadian mortar) produced more, but smaller and faster, fragments than the large HE rounds (Fortier 2007). Because the fragments are small, air drag reduces their velocities more quickly than it does larger fragments, and the fragments do not penetrate targets as effectively as fragments from larger HE rounds. The average velocity of the fragments varies between 500 and

1750 m/s (Fortier 2009). All the fragments from a high-order detonation of the C70A1 weighed less than 13 g (Lahaye and Abi-Zeid 1994). For a C70A1, the total number of fragments recovered was approximately 3600 (fragments larger than 60 mg—this mass is the limit in terms of lethality [Lahaye and Abi-Zeid 1994]). The fragmentation of a round is a process with high intrinsic variability (Lahaye and Abi-Zeid 1994). To the authors' knowledge, arena tests are not used to study partial detonations.



Figure 7-2. Typical setup for arena tests. The munition is placed in the center stand. (Photo courtesy of Claude Fortier, DRDC Valcartier.)

The work reported here was designed to determine the fraction of the surface of UXO broken open by fragments from a nearby high-order detonation. This is currently unknown and is needed to determine the likelihood that HE particles are dispersed onto range soils. Our tests differ from those conducted by Lewis et al. (2009), whose aim was to produce breached UXO. We placed most of the detonating rounds vertically, nose down, to simulate the orientation of a fired munition that detonates on impact. To simulate a high-order field detonation, we used a specially designed initiator, not C4 or shaped charges. Lastly, we recorded the damage on each of the UXOs and the mass distribution of the scattered Composition B particles. We documented simple surface dings, penetration of the round by fragments (ranging from small holes to cracks that split the round open), partial detonation, and sympathetic high-order detonations.

7.3 Experimental design

7.3.1 Munitions used

The munitions used for this study were 81-mm mortar rounds, model CRTG M374A2, lot LS-67-68A6-73. These mortars came with propellant rings, but these were removed for the trials as they would have been expended in flight both for the UXO and the donor round. The explosive fill in the 81-mm mortar is 950 g of Composition B (60% cyclo-1,3,5-trimethylene-2,4,6-trinitramine [RDX], 39% trinitrotoluene [TNT]). A new initiator was designed and used for these tests that simulate the functioning fuze of a live-fired projectile (see Chapter 6).

7.3.2 Test locations

The trials were conducted from 13 to 18 March 2010 at demolition range 3 at Fort Richardson, AK. All trials were done on a snow-covered surface. The demolition area has a road bisecting it. One side of the range was used for initial testing of the initiation system and disposal of munitions at the end of the trial, and the other side for the close-proximity detonation tests. The snow was approximately 50 cm deep and, to facilitate testing, access lanes were packed by a snowmobile and a sled for testing the initiation caps. A large area for the detonation tests was packed as well. The compressed snow sintered into a fairly hard surface, which was used 2 days later for the tests. Each detonation was carried out in a different location within the packed area to minimize cross-contamination.

7.3.3 Tests sequence and setup

These tests used one 81-mm mortar that was detonated with the fuze adaptor described earlier near one to five UXOs of the same caliber without fuzes. Table 1 summarizes the details of the setups. To determine the damage produced to the target rounds relative to the detonating round, the unfused mortar projectiles were marked before the trial with an “X” on the side facing the detonating round and with the word “up” on the top side. The nomenclature for the tests was Test N (originally named “Proxi” N), with N being a number from 1 to 11. When multiple UXOs were used in a same test, the rounds were named “round Na” and “round Nb,” where round “a” is the one on the left hand side of the fuzed mortar (when placed in front of the setup, the access road is in the back and forest area is in the front), and “b” is for the right hand side of the fuzed mortar. Setup 4 (be-

low), with a spiral of five rounds, used lowercase letter designations “a” through “e.”

Table 7-1. Summary of the setups used in the close-proximity trials.

Trial number	Orientation of fuzed round	Position of UXO	No. of UXOs	Distance from the fuzed round (m)	Fig. no.
Test 1	Vertical, nose down, slightly tilted	Horizontal in front of the fuzed round	1	0.50	7-3
Test 2	Vertical, nose down, slightly tilted	Horizontal behind the fuzed round	1	0.50	7-3
Test 3 Test 5 Test 7 Test 8	Vertical, nose down, slightly tilted	Horizontal symmetrical on each side of the fuzed round	2	0.50	7-4
Test 6 (one UXO damaged)	Vertical, nose down, slightly tilted	Horizontal symmetrical on each side of the fuzed round	2	0.50	7-4
Test 4	Vertical, nose down, slightly tilted	Horizontal symmetrical on each side of the fuzed round	2	0.30	7-4
Test 9 Test 10	Horizontal	Horizontal on each side of the fuzed round, parallel	2	0.50	7-5
Test 11	Vertical, nose down	Spiral pattern	5	0.40, 0.60, 0.80, 1.00 and 1.20	7-6

7.3.3.1 Setup 1: Vertical incoming round, single UXO

The fuzed 81-mm mortar was placed almost vertical to the snow surface, with the nose in the snow to simulate an incoming mortar fired from a remote location and detonating on contact with the surface. For the first test (Test 1 in Table 7-1), the UXO was placed in front of the detonating round, i.e., on the side where the angle between the fuzed mortar and the ground was the largest (Fig. 7-3). For the second test (Test 2 in Table 7-1), the UXO was placed behind the fuzed round, i.e., on the side where the angle between the fuzed mortar and the ground was the smallest (Fig. 7-3).

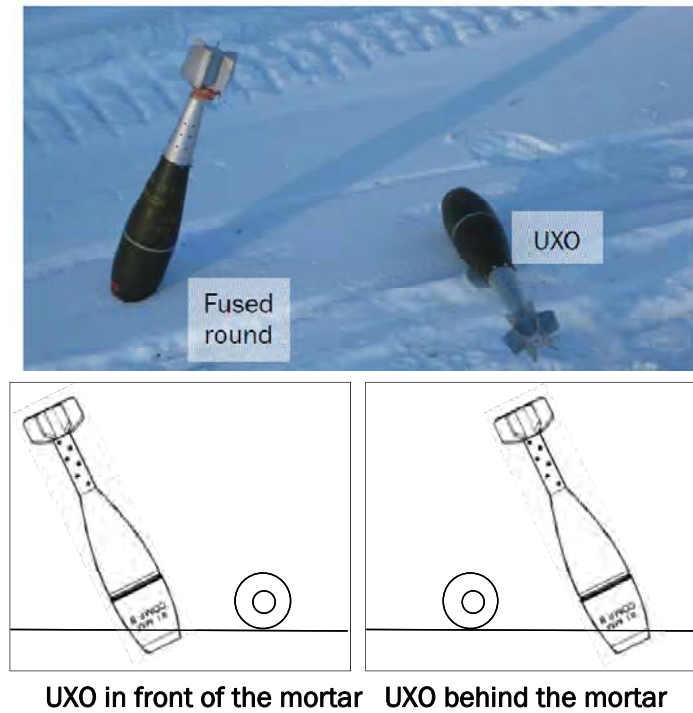


Figure 7-3. Setup 1, vertical incoming round, one UXO on the side.

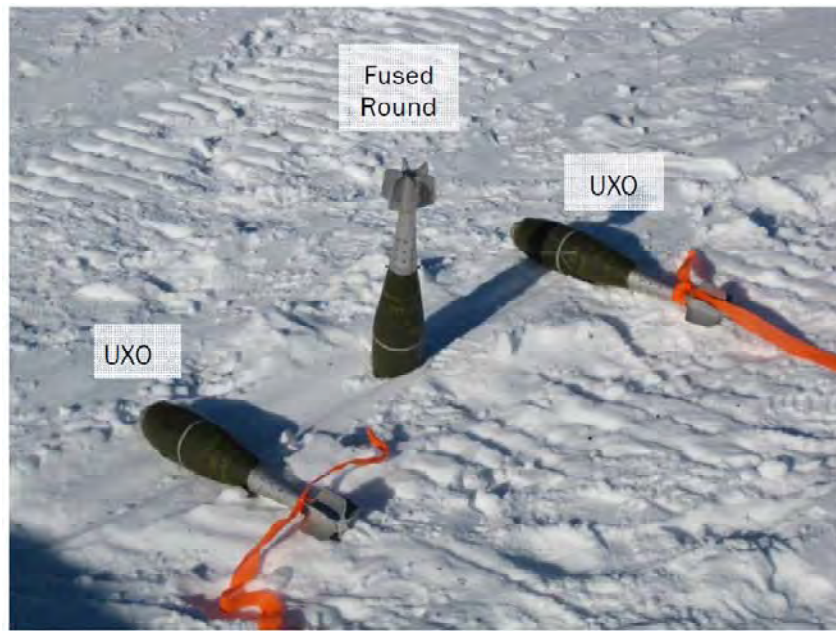


Figure 7-4. Setup 2, vertical incoming round, two UXOs on the side.

7.3.3.2 Setup 2: Vertical incoming round, two UXO

This seup is very similar to setup 1. To accelerate the trial progress, instead of having only one simulated UXO, two UXOs were placed beside the

fuzed round, which was placed almost vertically (Fig. 7-4). Distances of 0.30 and 0.50 m between the detonating round and the UXOs were tested. The UXOs were parallel, and the setup was symmetrical on each side of the fuzed round, allowing us to study multiple UXOs with one detonation.

7.3.3.3 Setup 3: Horizontal detonating round, parallel to UXOs

The detonating round and the UXOs are laid parallel on the ground, approximately 0.50 m apart (Fig. 7-5). Although it seems unlikely that a detonation would occur in this orientation, as the incoming round detonates when it hits the ground and it does so in a vertical position, nose down, this configuration was tested to compare the results with those obtained by Lewis (Fig. 7-1a).

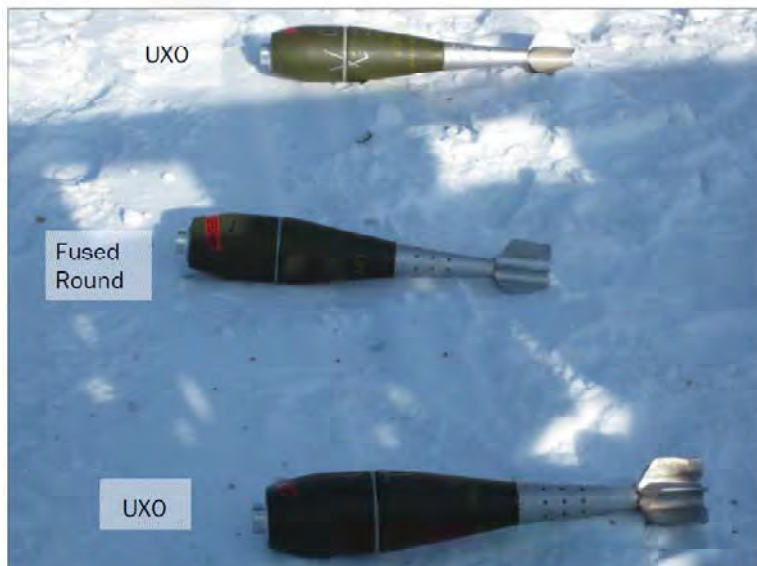


Figure 7-5. Setup 3, horizontal incoming round, two UXOs on the side (similar to Lewis's setup).

7.3.3.4 Setup 4: Vertical incoming round, UXOs different distances away

In this setup, the detonating round was placed vertically as for setup 1 and 2, but this time with five UXOs placed horizontally on the ground in a spiral pattern. The first was 0.40 m from the fuzed round, the others at increasing distances from the detonation: 0.60, 0.80, 1.00 and 1.20 m (Fig. 7-6). This setup was not repeated.

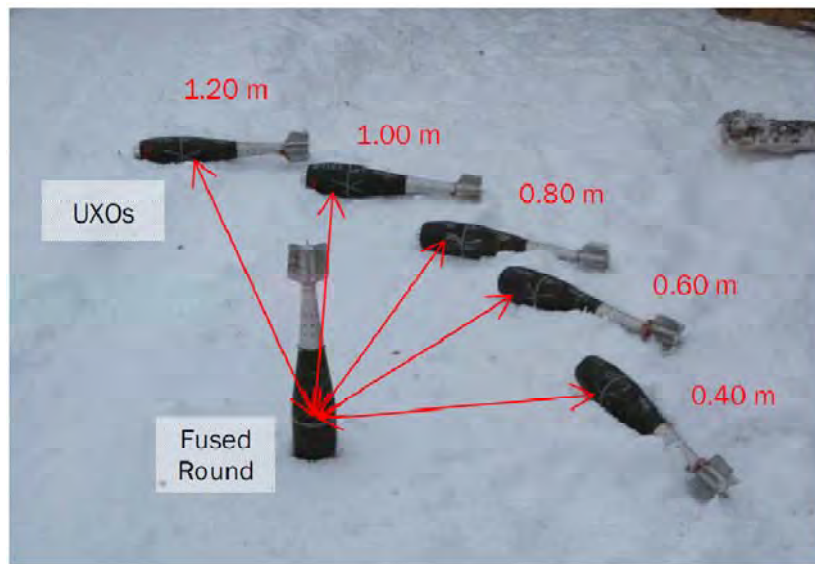


Figure 7-6. Setup 4, vertical incoming round, five UXOs on the side.

7.3.4 Detonating the rounds

Once a setup was complete, researchers moved to a safe location. Explosive ordnance disposal (EOD) personnel then inserted a detonator into the C4 filled adaptor and placed the fuzed round in position. The detonator was connected to a hard-wire system and the detonation was initiated remotely.

7.3.5 Data collected on UXO rounds

After the detonation and the site was deemed safe by EOD, researchers returned to the site. First, the dimensions of the crater made by the fuzed mortar were recorded to ensure it detonated high-order. Next, the distance from the center of the crater to the damaged UXO was measured. If the UXO was broken into multiple pieces, the distance from the crater was recorded for each piece of metal. All UXOs were photographed in place then moved to a table where the damage was recorded in detail.

All the UXO were damaged to greater or lesser degrees. The number and dimensions of dings (marks on the casing, but not pierced), holes (casing pierced) or breaches and cracks (casing open in a longitudinal direction) in each of four regions—nose, upper body, lower body and tail—along the length of the round were tabulated (Fig. 7-7). Calipers were used to measure the outside diameter and depth of the dings, and to measure the outer and inner dimensions of the holes. A maximum of three marks (the largest) were measured. For rounds that suffered from partial detonations, the

area of deposition was estimated and all visible HE fill on the snow surface was collected.



Figure 7-7. Regions used when identifying damage to an 81-mm mortar.

7.4 Results

7.4.1 Damage to the UXO

Five different types of damage were seen: dings, holes, breaches/cracks, partial detonation, and high-order detonations. They can be defined as follows. The STANAG definitions (NATO Standardization Agency 2009) of the various detonation types for sympathetic detonation test of insensitive munitions are presented in Appendix H for comparison.

7.4.1.1 Dings

These are damages to the casing, most of them looking like small craters (spherical or oval shape, with a depression in the center). The depth of this crater varied from very shallow (paint removal) to depths close to the thickness of the metal. The metal casing was not perforated, and there was no exposure of the explosive filler. Typical dings are presented in Figure 7-8.

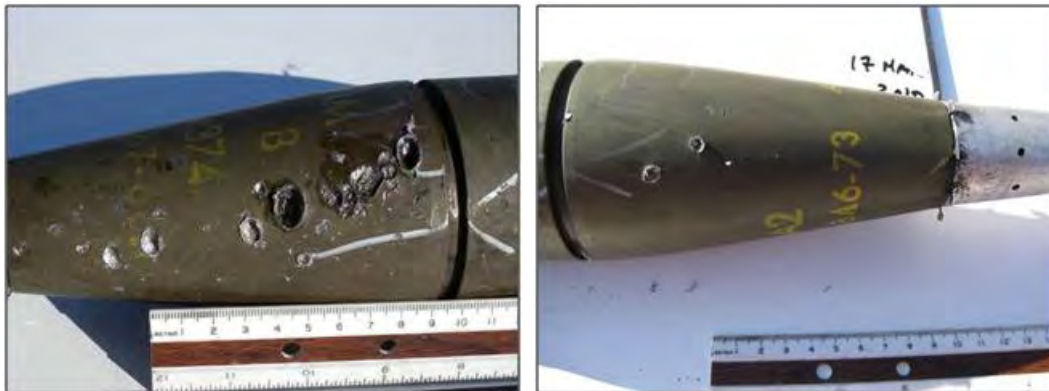


Figure 7-8. Typical dings to an 81-mm mortar (simulated UXO).

7.4.1.2 Holes

These are damages to the casing with a spherical or oval shape that went through its entire thickness, perforating it. The explosive filling was exposed, but there was no clear sign of explosives residues scattered outside the casing. Size varied between 1.4 and 48 mm. When holes were observed on the tail/fin, they do not expose energetic material. Figure 7-9 shows examples of typical holes.

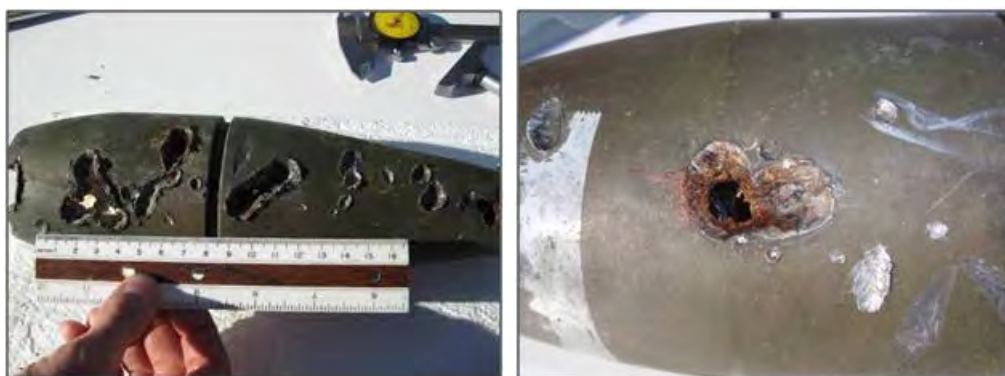


Figure 7-9. Typical holes to an 81-mm mortar (simulated UXO).

7.4.1.3 Breaches and cracks

These are damages to the casing with an irregular, rectangular shape, leading to the exposure of the explosive filling. These cracks led to the scattering of explosive particles outside of the munition. For the cases where the fuze adaptor was blown away, which led to the scattering of energetic particles and the exposure of an important area of explosive filler, these damages were labeled cracks. Typical cracks are presented in Figure 7-10.



Figure 7-10. Typical breaches/cracks to an 81-mm mortar (simulated UXO).

7.4.1.4 Partial detonation

This is damage to the casing that produced large pieces. In most cases, the pieces were distorted from the internal pressure. Some metal pieces could not be retrieved. Most of the explosive fill was scattered on the ground; a portion was still present on the metal parts and some fraction was probably burned. Owing to the scattering of many particles, the exposed surface area of energetics was the highest. Typical residues after a partial detonation are presented in Figure 7-11.



Figure 7-11. Typical 81-mm mortar metal pieces obtained after a partial detonation of a simulated UXO.

7.4.1.5 High-order detonation

The precise identification of a high-order detonation requires placing sensors around the detonation point to measure the blast wave. In practice, a detonation was classified as high-order on the basis of the sound of the detonation and the absence of a shell carcass (Taylor et al. 2004b). The high-order detonation formed a crater in the ground. No traces of pieces from the explosive filling were found. Previous tests (Hewitt et al. 2005; Pennington et al. 2006a; Walsh, M.R., et al. 2008) have shown that a high-order detonation leads to very little contamination from unburned energetic material. Figure 7-12a presents a typical crater from a high-order detonation of an 81-mm mortar (simulated UXO). In comparison, Figure 7-12b shows a large oval large crater caused by of two detonations: one high-order detonation of the fuzed round and one sympathetic high-order detonation of the simulated UXO. The craters observed for the detonating 81-mm mortars were approximately 1.7×1.8 m.



Figure 7-12. Typical craters from high-order detonations of 81-mm mortars.

7.4.1.6 Summary of damages

Of the 23 unfuzed rounds, placed between 0.30 and 1.20 m from the detonating round, the casings of five presented dings only (not penetrated) as the most important damage, four casings presented holes (penetrated and exposed explosive) as the most important damage, five presented cracks (large area of exposure of energetic material with scattering of particles on the ground as the main damage), six presented an partial detonation, one detonated high-order and two were not recovered. Figure 7-13 shows the summarized results; Table 7-2 presents the overall results. The gray region in Figure 7-13 represents the damages that led to direct environmental contamination, i.e., where the casing is either penetrated or ruptured and where the energetic material is exposed or particles scattered outside the munitions. Previous work (Hewitt et al. 2005; Pennington et al. 2006a; Walsh, M.R., et al. 2008) shows that, as a rule of thumb, one low-order detonation leads to 10,000 to 100,000 times more contamination than does a high-order detonation.

Table 7-2 and Figure 7-13 show that, for a given distance, many types of damage are observed. For example, a UXO placed 1 m from a vertical incoming round had both dings and holes. For UXO placed 0.5 m from a vertical incoming round (setups 1, 2 and 4 as presented above), two UXOs partially detonated, and the others had a combination of dings, holes, and cracks. The details of the damage types for each setup and each UXO are presented in the next section.

Table 7-2. Damage types observed for the different setups and replicates.

Setup	Distance between the detonating mortar and the UXO (m)	Replicates	Damages
Vertical incoming round, UXO lying on the snow	0.30	1/2 (Test 4, round 4a)	Projectile not found
		2/2 (Test 4, round 4b)	Partial detonation
	0.40	1/1 (Test 11, round 11a)	Partial detonation
	0.50	1/12 (Test 1)	Dings + hole
		2/12 (Test 2)	Dings
		3/12 (Test 3, round 3a)	Dings + holes + cracks
		4/12 (Test 3, round 3b)	Dings
		5/12 (Test 5, round 5a)	Dings + hole
		6/12 (Test 5, round 5a)	Dings
		7/12 (Test 7, round 7a)	Dings + holes + cracks
		8/12 (Test 7, round 7b)	Partial detonation
		9/12 (Test 8, round 8a)	Partial detonation
		10/12 (Test 8, round 8b)	Dings + cracks
		11/12 (Test 6, round 6a)	Dings
		12/12 (Test 6, round 4b)	Dings + holes + cracks
	0.60	1/1 (Test 11, round 11b)	Partial detonation
	0.80	1/1 (Test 11, round 11c)	Dings
	1.00	1/1 (Test 11, round 11d)	Dings + hole
	1.20	1/1 (Test 11, round 11e)	Dings + hole
Horizontal incoming round, UXO lying on the snow	0.50	1/4 (Test 9, round 9a)	Dings + cracks
		2/4 (Test 9, round 9b)	High-order detonation
		3/4 (Test 10, round 10a)	Partial detonation
		4/4 (Test 10, round 10b)	Projectile not found

Even though there were not as many replicates for the horizontal incoming round setup as compared to the vertical setup, one can note from Figure 7-13 that the damages observed seem to depend only on the distance, not the orientation. The damage that released the most HE (i.e., cracks and partial detonations) is observed mostly for distances less than 0.60 m. All the tests in which rounds partially detonated were for distances less than 0.60

m. For distances larger than 0.60 m, most of the damages were surfaces dings and small holes.

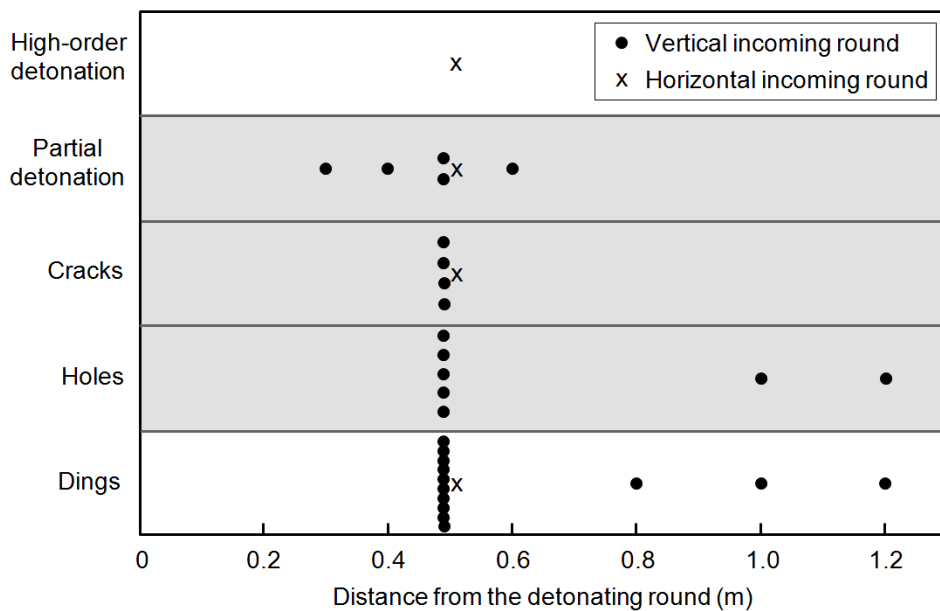


Figure 7-13. Overall results of damage types observed on the simulated UXOs.

In the case of the vertical incoming round at the 0.50-m setup, 12 “UXO” were tested. Various damages were observed; the distribution is shown in Figure 7-14. Again, the gray region represents the damages where environmental contamination occurs. Of the total of 21 damaged rounds, more than half (55%) scattered HE onto the ground.

The various types of damages observed for a fixed distance can be explained by the very nature of the mortar detonation and fragmentation itself. Indeed, the HE 81-mm mortar is designed to fragment upon detonation, leading to a wide range of fragment sizes and fragment velocities. The fragment production varies from one detonation to another because the mortar casing is made of one piece of metal, without pre-determined break points. As presented earlier, the fragmentation is a process with high intrinsic variability (Lahaye and Abi-Zeid 1994).

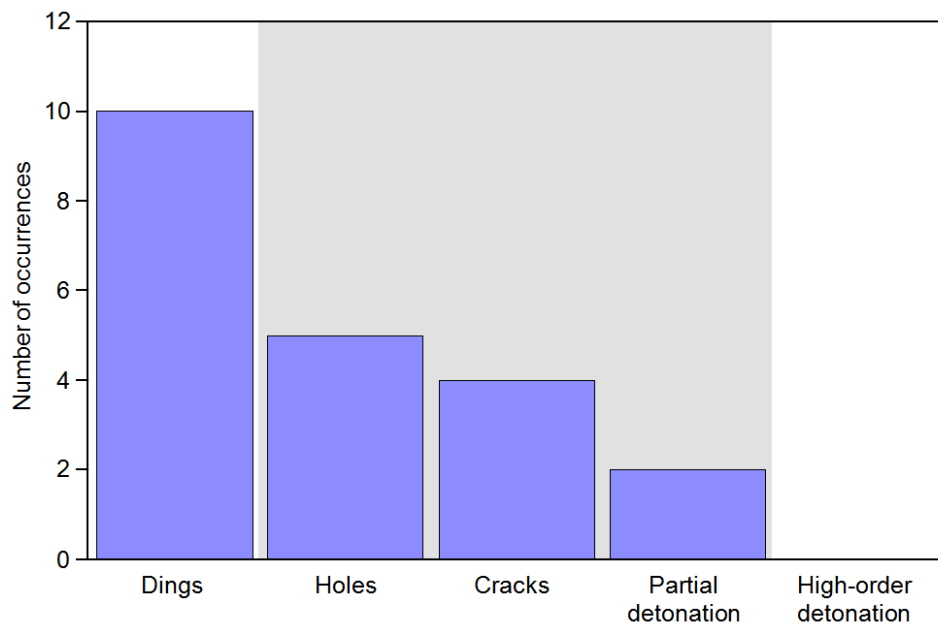


Figure 7-14. Distribution of damages observed on the UXO when the detonating mortar is at 0.50 m from the simulated UXO (vertical setup).

7.4.2 Detailed patterns of damage from vertical detonating rounds

7.4.2.1 Distance at 0.30 m: Replicate 1: Test 4, Round 4b

For this test, a vertically positioned mortar, detonated to simulate an incoming round, was positioned 0.30 m from two mortars lying on the ground. One of the UXOs was not found and the second, round 4b, was partially detonated. The significant damages are presented in Figure 7-15. An intact mortar is shown beside the damaged UXO for comparison. Both craters from these detonations measured 1.5×1.5 m.

For round 4b, the remainder of the projectile was recovered 123.6 m from the crater. The side of the casing was split open. Most of HE fill was scattered but some remained in the casing. The particle mass distribution for the HE is presented in Chapter 8 of this report.



Figure 7-15. Damage recorded and HE chunks collected in test 4, round 4b (vertical incoming round, 0.30-m distance).

7.4.2.2 Distance at 0.40 m: Replicate 1: Test 11, Round 11a

For this single replicate test, a fuzed mortar was place in the center of a spiral pattern with five UXO at different distances. The vertical detonating mortar induced a partial detonation of the UXO at 0.40 m, leading to the dispersion of EM particles on the test site. The metal pieces left after the partial detonation are presented in Figure 7-16. The detonation crater was oval (1.7×1.4 m), and the pieces were found at up to 2.9 m from the center of the crater.



Figure 7-16. Damages recorded for test 11, round 11a (vertical incoming round, 0.40-m distance).

7.4.2.3 Distance at 0.50 m

A total of 12 unfuzed mortars were exposed to the high-order detonation of another 81-mm mortar that was 0.50 m away. This section will present the 12 results.

7.4.2.3.1 Replicate 1: Test 1

For this first test at a 0.50-m distance, the vertical detonating mortar has induced many dings on the UXO, and made one hole. The most important damages are presented in Figure 7-17. Small dings (millimeter-size) were distributed mostly on the upper (15 marks) and lower body (13 marks). One large ding ($17.1 \times 12.8 \times 5.0$ mm deep) was observed near the nose and the fuze adaptor was broken. It is not possible to determine with certainty if this damage would have lead to the initiation of a real fuze. Other large dings were observed on the lower body ($8.3 \times 10.5 \times 0.5$ mm deep) and on the tail ($13.8 \times 16.6 \times 4.1$ mm deep). The only damage that led to the exposure of energetic material was a hole on the lower body of the round (2.4×1.4 mm of exposed surface). The mortar was found 2.85 m from the center of the detonation crater. The round would probably have been moved further, but the presence of a wood barrier kept it nearer the detonation point. Damages are recorded in Table 7-3. The crater size was not measured in this trial.



Figure 7-17. Damages recorded for the test 1 round (vertical incoming round, 0.50-m distance).

Table 7-3. Damages description for test 1 round.

Position	Total number	Damages (size of the largest in mm)		
		Dings	Holes	Cracks
Nose	1	17.1 x 12.8 x 5.0	n/a ¹	n/a
Upper body	15	(Ø > 2 mm)	n/a	n/a
Lower body	13	8.3 x 10.5 x 0.5	2.4 x 1.4	n/a
Tail	5	13.8 x 16.6 x 4.1	n/a	n/a

¹ n/a: not applicable.

7.4.2.3.2 Replicate 2: Test 2

In this second test at a 0.50-m distance, the vertical detonating mortar induced only surface dings on the UXO. None of the damage led to exposure of energetic material. Figure 7-18 shows the most important damages.

Small dings (millimeter-size) were distributed on the upper (11 marks) and mostly on the lower body (24 marks). On the lower body, three main large dings were observed ($10.1 \times 9.7 \times 0.3$ mm, $8.4 \times 6.3 \times 0.3$ mm, and $5.0 \times 3.8 \times 0.3$ mm). Other dings were observed on the tail and fins, even a

small hole, but it did not lead to exposure of EM. All the damages were observed on the same side of the mortar, which was found 15.5 m from the center of the detonation crater (crater size: 1.8×1.9 m). According to the visual observations by the EOD team, this projectile was kicked away by the blast and skipped across the snow surface. Damages are recorded in Table 7-4.

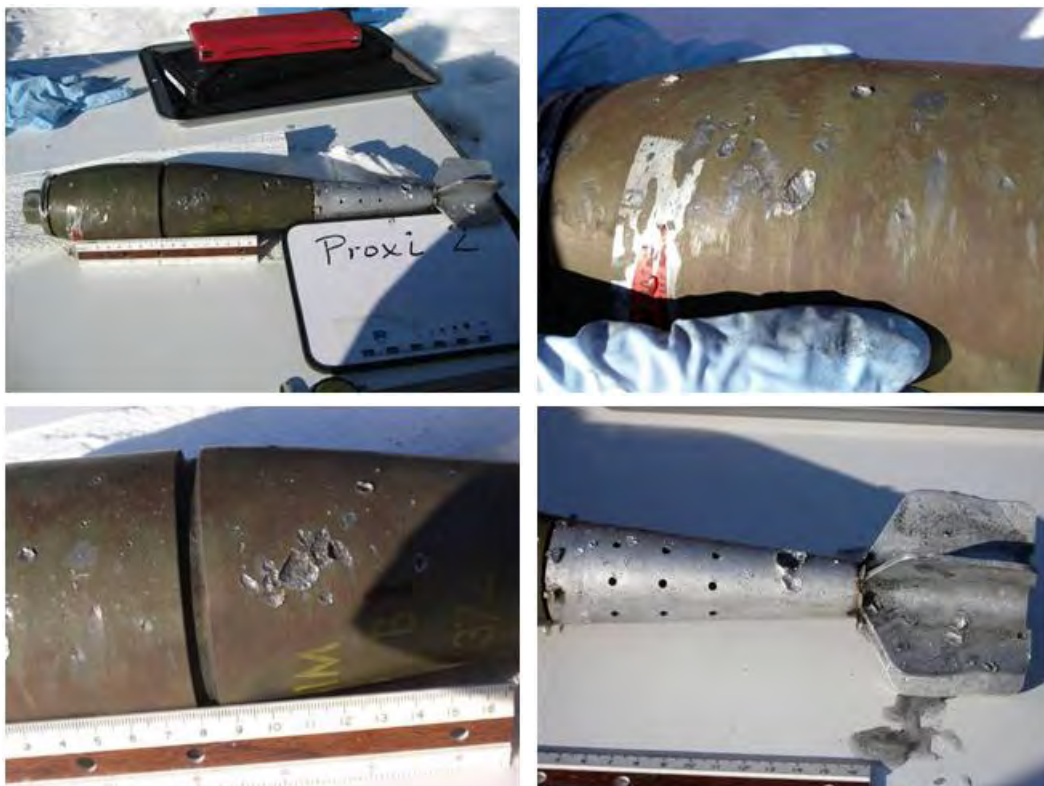


Figure 7-18. Damages recorded to the test 2 round (vertical incoming round, 0.50-m distance).

Table 7-4. Damages description for test 2 round.

Position	Total number	Damages (size of the largest in mm)		
		Dings	Holes	Cracks
Nose	0	n/a ¹	n/a	n/a
Upper body	17	9.8 x 6.7 x 1.4 4.3 x 4.3 x 0.7	n/a	n/a
Lower body	24 with $\varnothing > 2$ mm	10.1 x 9.7 x 0.3 8.4 x 6.3 x 0.3 5.0 x 3.8 x 0.3	n/a	n/a
Tail	9 Fins only : 14	13.5 x 13.5 x 4.5	Hole in one fin	n/a

¹ n/a: not applicable.

7.4.2.3.3 Replicate 3: Test 3, Round 3a

In this test, the vertical detonating mortar (distance 0.50 m) induced many holes in the UXO. The damages led to exposure of EM. Significant damages are presented in Figure 7-19. The largest holes were found on the upper body (38.2×28.0 mm and 25.8×12.9 mm). The most important damage is the loss of the nose, leading to a large opening (39.5 mm Ø) and the scattering of EM. It is not possible to determine with certainty if this damage would have led to the initiation of a real fuze. Except the nose loss, all the other damages were observed on the same side of the mortar. The mortar was found 10.8 m from the center of the detonation crater (crater size: 1.8×1.7 m). According to the visual observations by the EOD people, this projectile was stopped by hitting the wood barrier at about 1 m height. The damages are recorded in Table 7-5.



Figure 7-19. Damages recorded for test 3, round 3a (vertical incoming round, 0.50-m distance).

Table 7-5. Damage description for test 3, round 3a.

Position	Total number	Damages (size of the largest in mm)		
		Dings	Holes	Cracks
Nose	Missing nose	n/a ¹	n/a	Area exposed : 39.5 mm Ø
Upper body	11	Too small- not measured	38.2 x 28.0 25.8 x 12.9	n/a
Lower body	14	Too small- not measured	38.7 x 14.0 13.3 x 13.3	n/a
Tail	12, one fin is missing	Too small- not measured	n/a	n/a

¹ n/a: not applicable.

7.4.2.3.4 Replicate 4: Test 3, Round 3b

In this test, the vertical detonating mortar induced only dings on the UXO. The most important damages are presented in Figure 7-20. None of the damages led to the exposure of EM. The largest dings were found on the upper body ($23.9 \times 14.2 \times 5.1$ mm, $15.8 \times 15.8 \times 5.1$ mm, and $24.2 \times 10.2 \times 2.3$ mm). The dings are deep, but the casing was not ruptured. All the damages were observed on the same side of the mortar. The mortar was found at 4.15 m from the center of the detonation crater (crater size: 1.8×1.7 m). The damages are recorded in Table 7-6.

Table 7-6. Damage description for Test 3, round 3b.

Position	Total number	Damages (size of the largest in mm)		
		Dings	Holes	Cracks
Nose	3	Too small- not measured	n/a ¹	n/a
Upper body	14	23.9 x 14.2 x 5.1 15.8 x 15.8 x 5.1 24.2 x 10.2 x 2.3 12.0 x 12.0 x 6.9	n/a	n/a
Lower body	13	17.9 x 10.6 x 6.0	n/a	n/a
Tail	Missing tail	n/a	n/a	n/a

¹ n/a: not applicable.



Figure 7-20. Damages recorded for test 3, round 3b (vertical incoming round, 0.50-m distance).

7.4.2.3.5 Replicate 5: Test 5, Round 5a

In this test (fifth UXO at 0.5 m), the vertical detonating mortar induced only surface dings on the UXO and one hole. Damages are presented in Figure 7-21 and Table 7-7. Most of the dings were observed on the upper body (seven marks), with the largest being 12.8×5.4 mm and $7.0 \times 11.3 \times 1.4$ mm. The hole, with an opening of 5.7×5.4 mm, led to the exposure of EM. Damages were all on the same side of the mortar. The mortar was found at 5.2 m from the center of the crater (crater size: 1.7×1.8 m).

Table 7-7. Damage description for test 5, round 5a.

Position	Total number	Damages (size of the largest in mm)		
		Dings	Holes	Cracks
Nose	0	n/a ¹		n/a
Upper body	7	12.8×5.4 $7.0 \times 11.3 \times 1.4$	13.5×16.7 (outer mark) 5.7×5.4 (inner hole)	n/a
Lower body	1	$7.5 \times 5.8 \times 1.8$	n/a	n/a
Tail	3 + 5 on fins	Too small—not measured	n/a	n/a

¹ n/a: not applicable.



Figure 7-21. Damages recorded for test 5, round 5a (vertical incoming round, 0.50-m distance).

7.4.2.3.6 Replicate 6: Test 5, Round 5b

In this test, the vertical detonating mortar induced only dings on the UXO (Fig. 7-22), which did not lead to any exposure of energetic material. Most of the dings (five marks) were found on the upper body. As on round 5a, the largest was found on the upper body ($23.9 \times 14.2 \times 5.1$ mm, $15.8 \times 15.8 \times 5.1$ mm, and $24.2 \times 10.2 \times 2.3$ mm). The dings are deep, but the casing did not rupture. All the damages were observed on the same side of the mortar. The mortar was found at 3.65 m from the center of the detonation crater (crater size: 1.7×1.8 m). The damages are recorded in Table 7-8.

Table 7-8. Damage description for test 5, round 5b.

Position	Total number	Damages (size of the largest in mm)		
		Dings	Holes	Cracks
Nose	1	Too small- not measured	n/a ¹	n/a
Upper body	5	$14.4 \times 11.7 \times 3.8$ $20.7 \times 10.5 \times 1$	n/a	n/a
Lower body	3	$5.7 \times 6.5 \times 2.0$ $5.5 \times 5.1 \times 1.1$	n/a	n/a
Tail	0	n/a	n/a	n/a

¹ n/a: not applicable.



Figure 7-22. Damages recorded for test 5, round 5b (vertical incoming round, 0.50-m distance).

7.4.2.3.7 Replicate 7: Test 6, Round 6a

In this test, the vertical detonating mortar (distance 50 cm) was placed beside a previously damaged projectile (from test 2) to verify that repeated detonation near a UXO could lead to an easier rupture. Only surface damages, without exposure of EM, were observed (Fig. 7-23). Most of the dings were found on the lower body and the tail. The largest ding was found on the tail ($18.7 \times 18.7 \times 4.2$ mm). The mortar was found 1.65 m from the center of the detonation crater (crater size: 1.9×1.6 m). The damages are recorded in Table 7-9.

Table 7-9. Damage description for test 6, round 6a.

Position	Total number	Damages (size of the largest in mm)		
		Dings	Holes	Cracks
Nose	0	n/a ¹	n/a	n/a
Upper body	17	9.5 x 11.7 11.0 x 7.3	n/a	n/a
Lower body	33	13.9 x 9.8 x 4.3 8.0 x 12.5 x 3.9	n/a	n/a
Tail	17 + 21 on fins, one fin missing	18.7 x 18.7 x 4.2	n/a	n/a

1 n/a: not applicable.



Figure 7-23. Damages recorded for test 6, round 6b (vertical incoming round, 0.50-m distance).

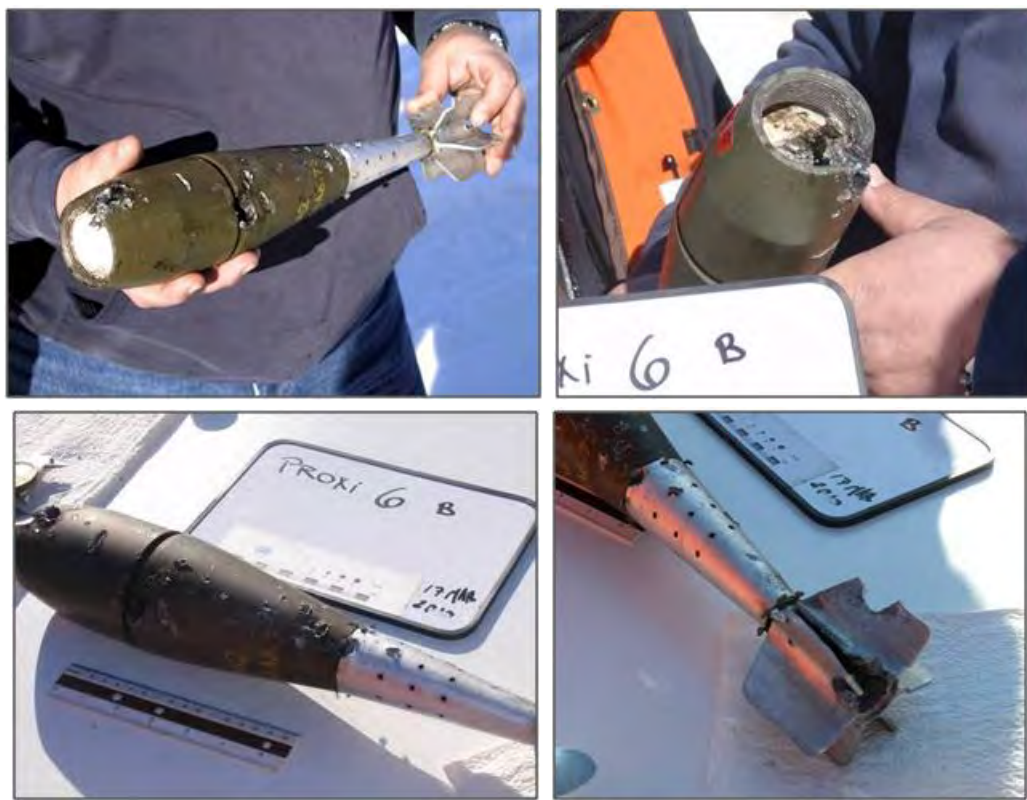


Figure 7-24. Damages recorded for test 6, round 6b (vertical incoming round, 0.50-m distance).

7.4.2.3.8 Replicate 8: Test 6, Round 6b

In this test, the vertical detonating mortar induced dings, holes, and cracks that led to the exposure of EM. The significant damages are shown in Figure 7-24. Numerous dings were observed on all parts of the round—upper, lower body, and tail, as well as two large holes (24.9×15.7 mm on the upper body and 23.9×20.3 mm on the lower body). The most significant damage was the loss of the inert fuze adaptor, leading to the exposure of an area in the shape of a half circle (39.5 mm Ø). As for the round 3b replicate, where the nose was lost, it is not possible to determine with certainty if this damage would have led to the initiation of a real fuze. Except the nose loss, all damages were on the side that was initially facing the fuzed projectile. The mortar was found 29 m from the center of the detonation crater (crater size: 1.9×1.6 m). The damages are recorded in Table 7-10.

Table 7-10. Damage description for Test 6, round 6b.

Position	Total number	Damages (size of the largest in mm)		
		Dings	Holes	Cracks
Nose	Nose is lost	n/a ¹	n/a	Exposed area: half-circle of 39.5 mm Ø
Upper body	15	18.5 x 6.1 x 2.8 14.6 x 7.7 x 2.0	24.9 x 15.7	n/a
Lower body	23	11.5 x 11.2 x 4.0	23.9 x 20.3	n/a
Tail	9 + 5 on fins (one fin is missing)	Too small- not measured	n/a	Cracked, lost one fin

¹ n/a: not applicable.

7.4.2.3.9 Replicate 9: Test 7, Round 7a

In this ninth replicate, the vertical detonating mortar (distance 0.50 m) has induced dings, holes, including a very large and long breach or crack that led to the exposure of EM (Fig. 7-25). Most of the dings were observed on the upper body (largest: 23.9 x 15.1 x 5.6 mm and 12.2 x 12.1 x 2.5 mm). The largest hole was also in the upper body, with an opening of approximately 48.2 x 28.0 mm. The projectile was breached (dimensions of approximately 120 x 11 mm) on the lower body. Many HE pieces were scattered on the ground. The mortar was found 3.2 m from the center of the detonation crater (crater size: 1.4 x 1.5 m). The damages are recorded in Table 7-11.

Table 7-11. Damage description for test 7, round 7a.

Position	Total number	Damages (size of the largest in mm)		
		Dings	Holes	Cracks
Nose	3	Too small- not measured	n/a ¹	n/a
Upper body	12	23.9 x 15.1 x 5.6 12.2 x 12.1 x 2.5	48.2 x 28.0	n/a
Lower body	9	13.7 x 11.4 x 4.5 15.3 x 8.6 x 2.2 14.2 x 7.3 x 1.3	n/a	Approx. 120 x 10 mm (Exact dimensions in Fig. 7-25).
Tail	12 + 9 on fins	Too small—not measured	n/a	n/a

¹ n/a: not applicable.

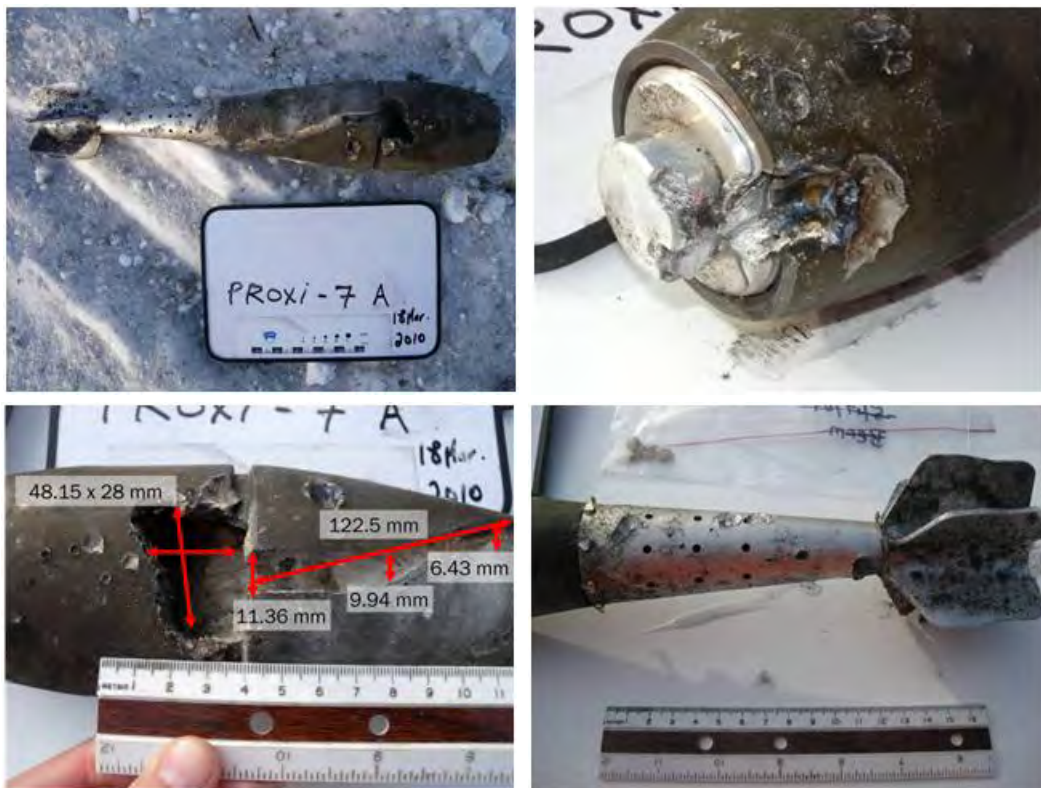


Figure 7-25. Damages recorded for test 7, round 7a (vertical incoming round, 0.50 m distance).

7.4.2.3.10 Replicate 10: Test 7, Round 7b

In this test, the vertical detonating mortar (distance 50 cm) induced a partial detonation reaction on the simulated UXO. Figure 7-26 shows the remaining metal pieces: piece “i” was $81.6 \times 33.1 \times 5.8$ mm and piece “ii” was $94.3 \times 69.7 \times 5.2$ mm. The nose and tail pieces were found at 7.8 and 29.3 m from the detonation crater, respectively. Piece “i” was projected to 4.3 m away and piece “ii” to 2.3 m away from the detonation crater (size: 1.4×1.5 m).

7.4.2.3.11 Replicate 11: Test 8, Round 8a

In this test, the vertical detonating mortar also induced a partial detonation of the simulated UXO. The remaining metal pieces are presented in Figure 7-27. On the remaining body piece, many dings (five marks) were observed, as well as indications of holes in the sides. A large ding ($20.5 \times 12.7 \times 5.9$ mm) caused by ductile deformation of the casing was observed: a dimple is present on the “inside” side of the fragment. The fuze piece was found 3.3 m from the detonation crater (size: 1.7×1.4 m); the metal piece was found at 3.7 m (dimensions: 131.3×60.7 mm).



Figure 7-26. Damages recorded for test 7, round 7b (vertical incoming round, 0.50-m distance).



Figure 7-27. Damages recorded for test 8, round 8a (vertical incoming round, 0.50-m distance).

7.4.2.3.12 Replicate 12: Test 8, Round 8b

In this test (the twelfth and final replicate at separation distance 0.50 m), the vertical detonating mortar induced dings and a large crack on the UXO that led to exposure of EM. The most significant damages are shown in Figure 7-28, along with a photograph showing HE spilled on the snow. Most of the dings were observed on the lower body (largest : $23.1 \times 14.1 \times 8.1$ mm—fragment of metal from the detonating round was still observable in the newly induced damage—and 11.1×15.8 mm). The crack was observed on the upper body, near the nose, with an opening of 77.3×69.5

mm (largest dimensions). The mortar was found 20.1 m from the center of the detonation crater (crater size: 1.7×1.4 m). Much damage was observed on the side that was initially facing the fuzed projectile, and the side facing up was cracked. The damages are recorded in Table 7-12.



Figure 7-28. Damages recorded for test 8, round 8b (vertical incoming round, 0.50-m distance).

Table 7-12. Damage description for test 8, round 8b.

Position	Total number	Damages (size of the largest in mm)		
		Dings	Holes	Cracks
Nose	3	Too small- not measured	n/a ¹	n/a
Upper body	9	Too small- not measured	n/a	n/a
Lower body	14	23.1 x 14.1 x 8.1 (fragments of metal lodged within the damage) 11.1 x 15.8	n/a	77.3 x 69.5 (opening)
Tail	Tail is missing	n/a	n/a	n/a

¹ n/a: not applicable.

7.4.2.4 Distance at 0.60 m: Replicate 1: Test 11, Round 11b

For this only replicate at a 0.60 m distance, the setup used was the previously presented spiral pattern with five UXO at different distances. The vertical detonating mortar has induced a partial detonation on the UXO at 0.60 m. The metal pieces left after the partial detonation are presented in Figure 7-29. The detonation crater was 1.73×1.40 m, and the piece was found at 1.8 m from the center of the crater.



Figure 7-29. Damages recorded for test 11, round 11b (vertical incoming round, 0.60-m distance).

7.4.2.5 Distance at 0.80 m: Replicate 1: Test 11, Round 11c

For this test, the fuzed mortar was again placed in the center of a spiral pattern with five UXO at different distances. The vertical detonating mortar induced only surface damages (dings) to the UXO at 0.80 m (Fig. 7-30). Most of the dings were observed on the upper body (four marks), but the largest were observed on the lower body ($10.4 \times 12.8 \times 1.6$ mm and 10.9×4.3 mm [depth not measured]). The tail was unscrewed. All the damages were on the side facing the detonating round (Table 7-13). The UXO was found 3.2 m from the center of the detonation crater (size: 1.73×1.40 m).



Figure 7-30. Damages recorded for test 11, round 11c (vertical incoming round, 0.80-m distance).

Table 7-13. Damage description for test 11, round 11c.

Position	Total number	Damages (size of the largest in mm)		
		Dings	Holes	Cracks
Nose	1	Too small—not measured	n/a ¹	n/a
Upper body	4	7.8 x 9.4 x 2.0 6.3 x 6.3 x 0.9	n/a	n/a
Lower body	2	10.4 x 12.8 x 1.6 10.9 x 4.3	n/a	n/a
Tail	Tail unscrewed	n/a	n/a	n/a

¹ n/a: not applicable.

7.4.2.6 Distance at 1.00 m: Replicate 1: Test 11, Round 11d

For this test, the setup with the spiral pattern with five UXO at different distances was used. The vertical detonating mortar was positioned 1.00 m away, inducing surface damages (dings) and perforated the casing of the UXO (Fig. 7-31). Most of the dings were observed on the lower body (11 marks, the largest: $13.4 \times 7.5 \times 3.4$ mm and $10.4 \times 6.2 \times 4.6$ mm). One hole was observed on the lower body, with an oval opening of 17.5×13.2 mm. The damages are presented in Table 7-14. The UXO was found 2.4 m from the center of the detonation crater (1.73×1.40 m).



Figure 7-31. Damages recorded for test 11, round 11d (vertical incoming round, 1.00-m distance).

Table 7-14. Damage description for test 11, round 11d.

Position	Total number	Damages (size of the largest in mm)		
		Dings	Holes	Cracks
Nose	0	n/a	n/a ¹	n/a
Upper body	2	6.0 x 4.1 6.6 x 4.0	n/a	n/a
Lower body	11	13.4 x 7.5 x 3.4 10.4 x 6.2 x 4.6	17.5 x 13.2	n/a
Tail	0	n/a	n/a	n/a
¹ n/a: not applicable				

7.4.2.7 Distance at 1.20 m: Replicate 1: Test 11, Round 11e

For the last test, the spiral pattern setup was used at a 1.20-m spacing. The vertical detonating mortar induced surface damages (dings) and perforated the UXO. The damages on the UXO are presented in Figure 7-32. Most of the dings were observed on the upper body (four marks, the largest: $22.5 \times 15.4 \times 5.7$ mm). A hole was also observed on the upper body: the opening was oval with internal dimensions of 36.2×15.5 mm. All the damages were on the side facing the detonating round (Table 7-15). The UXO was located 2.8 m from the center of the detonation crater (1.73×1.40 m).



Figure 7-32. Damages recorded for test 11, round 11e (vertical incoming round, 1.20-m distance).

Table 7-15. Damage description for test 11, round 11e.

Position	Total number	Damages (size of the largest in mm)		
		Dings	Holes	Cracks
Nose	0	n/a	n/a ¹	n/a
Upper body	4	22.5 x 15.4 x 5.7 6.0 x 5.1	n/a	n/a
Lower body	1	16.5 x 8.8 x 2.8	n/a	n/a
Tail	2 (pierced fins)	Too small—not measured	n/a	n/a
¹ n/a: not applicable				

7.4.3 Detailed patterns of damage from horizontal detonating round: distance at 0.50 m

7.4.3.1 Replicate 1: Test 9, Round 9a

For this first test of the “horizontal” setup series, the fuzed mortar was placed horizontally on the ground, parallel and slightly shifted from the UXO. As presented earlier, this setup was tested for comparison with previous Canadian work (NATO Standardization Agency 2009). At a distance of 0.50 m, the detonating mortar induced dings and a very large crack on the UXO. The damages to the UXO are presented in Figure 7-33. Most of the dings were observed on the lower body (41 marks) (largest: 31.0 × 10.7 × 7.1 mm and 19.0 × 11.4 × 2.7 mm). The crack runs through both the upper and lower body and has dimension (largest opening size) of 172.1 × 84.1 mm. The HE filling is highly exposed and chunks were found on the snow. The damages are presented in Table 7-16. The UXO was found 6.6 m from the center of the crater.



Figure 7-33. Damages recorded for test 9, round 9a (horizontal incoming round, 0.50-m distance).

Table 7-16. Damage description for test 9, round 9a.

Position	Total number	Damages (size of the largest in mm)		
		Dings	Holes	Cracks
Nose	3	Too small- not measured	n/a ¹	n/a
Upper body	31	6.8 x 6.8 x 3.6 10.4 x 7.1 x 2.8	n/a	172.1 x 84.1 mm in upper and lower body
Lower body	41	31.0 x 10.7 x 7.1 19.0 x 11.4 x 2.7	n/a	n/a
Tail	12 + 15 on fins	Too small—not measured	n/a	n/a

¹ n/a: not applicable

7.4.3.2 Replicate 2: Test 9, Round 9b

For this second replicate of the “horizontal” setup series at a distance of 0.50 m, the detonating horizontal mortar has induced a sympathetic high-order detonation on the UXO. Only the tail was recovered (Fig. 7-34) at 7.5 m from the center of the detonation crater. It should be noted that the cra-

ter was very large compared to those produced by the other detonated fuzed rounds. It was made by both the fuzed round and the sympathetically detonated round (2.3×1.73 m).



Figure 7-34. Tail recovered after sympathetic detonation of a UXO in test 9, round 9b (horizontal incoming round, 0.50-m distance).

7.4.3.3 Replicate 3: Test 10, Round 10a

For this third replicate of the “horizontal” setup series at a distance of 0.50 m, the detonating horizontal mortar induced a partial detonation of the UXO. Many metal pieces were recovered; they are shown in Figure 7-35. Chunks of HE were also recovered.

7.4.3.4 Replicate 4: Test 10, Round 4b

For this last replicate of the “horizontal” setup series at a distance of 0.50 m, the UXO near the detonating horizontal mortar was not found. We do not think it detonated as there was no crater produced. More likely the blast from the detonating round moved the UXO. No traces of a high-order detonation (crater) were observed; thus, it is most probable that the projectile or its pieces were pushed to a long distance either in the soft snow or in the wooded area. The damages are thus unknown.



Figure 7-35. Damages recorded for test 10, round 10a (horizontal incoming round, 0.50-m distance).

7.5 Discussion

7.5.1 Damage to UXO seen in the field

Damaged UXO are frequently observed in the field. The types of damage seen include dings, holes, cracked rounds, and casing pieces from low-order detonations. These types of damage are analogous to damage seen in our tests, although the field UXO are different types of rounds (Fig. 7-36 and 7-37).



a. 105-mm howitzer UXO,

Figure 7-36. Damaged howitzer projectile UXOs observed in the field



b. 155-mm howitzer UXOs.

Figure 7-37 (cont'd). Damaged howitzer projectile UXOs observed in the field.



a. 81-mm UXO.

b. 120-mm UXO.



c. 60-mm UXO.

Figure 7-38. Damaged mortar UXOs observed in the field.

7.5.2 Surface versus buried UXO

Duds can either be found on the ground or buried below the surface. According to Jenkins et al. (2006a), in the case of the 81-mm mortar, the HE-filled rounds make up most of the surface UXO, as compared to inert rounds. Nevertheless, buried HE rounds can be found up to 1.20 m deep. As presented earlier, the small fragments produced by the detonation of an 81-mm mortar are not very effective in penetrating protected targets. The metal casing of a UXO that protects the HE was indeed observed to be hard to penetrate. The distance between the detonating mortar and the UXO needs to be below 0.60 m in order to observe penetration or breaching damages, and even at this close distance, not all the damages are important enough to lead to HE exposure. In the case of buried UXO, the soil would quickly slow the fragments and detonation or breaching of the UXO would not occur unless the high-order detonation was directly above a shallowly buried UXO.

7.6 Conclusion

We observed a variety of damages on the unfuzed UXO rounds, from shallow surface dings, pierced casings, partial detonations, and high-order detonations. Arena tests carried out using mortar projectiles similar to the 81-mm rounds used in these tests show that the rounds produce thousands of fragments, some up to 13 g in mass, and demonstrate that fragmentation of the round is a process with high intrinsic variability. The tests we conducted show that the pattern of damage is unique for each of the rounds, even if the exact same setup were used. For the setup where the detonating round is almost vertical, simulating a fired incoming round, exposure of the energetic material inside the UXO casing occurred for distances up to 0.60 m. For the horizontal setup, where the detonating round was laid on the snow parallel to the UXO, the damage seems more severe. Of the four replicates, one was breached, one detonated high-order, the third partially detonated, and the fourth was not recovered. The damages observed are also more significant than what was observed by Lewis (Lewis 2007; Lewis et al. 2009). His conclusions were that partial detonation occurred at distances below 0.15 m. This difference may be attributable in part to the different detonation initiation, but can most likely be explained by the different mortar model. (Lewis's C70A1 vs. M374A2 in this work). These might lead to slightly different fragmentation and the high variability of the fragmentation pattern.

8 Particle Mass Distribution of High Explosives from Sympathetic Partial Detonations

Susan Taylor, Susan Bigl, Kathleen Jones, Isabelle Poulin, Michael Walsh, Marianne Walsh, Anna Wagner, and James Hug

8.1 Summary

Unexploded ordnance on training ranges is clearly damaged by nearby high-order detonations, as evidenced by holes and indentations in the casings made by hot metal fragments. Pierced, cracked, or partially detonated rounds can release large amounts of high explosives to the environment. The total mass deposited and the particle mass distributions of ejected high explosives are key pieces of information needed to estimate the amount of dissolved HE entering range soils. Here, we measured particle mass distributions of four partial detonations and one holed round, all damaged by a nearby high-order detonation, and compared these with previously measured mass distributions from partial detonations. We find that partial detonations of Composition B-filled projectiles produce smaller particles with narrower mass distributions than do similar detonations of rounds filled with TNT.

8.2 Introduction

A critical problem facing range managers is how to determine if explosives from training activities are likely to migrate off base, an outcome that might trigger federal regulatory actions able to close the base or restrict the type of training permitted (Racine et al. 1992a, Clausen et al. 2004). Transport of high explosives (HE) off military ranges can occur when substantial quantities of explosives are deposited on the soils, precipitation is high, and the transit time for water to reach groundwater is short (shallow groundwater or very permeable soils). HE are deposited on the soil when munitions containing HE are fired during training exercises.

A fired munition will experience one of many possible fates. Generally, it will detonate high-order and deposit very little explosives residue. Howev-

er, it is also possible that it will partially detonate (not consume the entire explosive fill) or dud (not detonate at all). A dud might penetrate the ground or come to rest on the surface. Whether on the surface or underground, an unexploded ordnance (UXO) will suffer one of the following fates: it can be intentionally blown-in-place, a round exploding nearby could detonate or partially detonate it, the casing might be split by the initial impact or by a nearby detonation, or the casing can remain intact and corrode over time (Taylor et al. 2004b).

Using available data on the rates of these different outcomes, Taylor et al. (2004b) concluded that partial detonations are the largest contributor of explosives onto ranges today. However, they noted that little information existed on the rate at which high-order detonations produce partial detonations or broken rounds, outcomes that breach the metal casing and expose the HE fill to dissolution and transport. Once the round is breached, however, the area of HE exposed or the size of the explosive pieces will determine how quickly the explosives dissolve. Given the initial mass distribution of HE pieces on the soil, the drop impingement dissolution model developed by Lever et al. (2005) can predict aqueous dissolution of HE. Unfortunately, both the initial HE mass and its distribution are poorly known, introducing order-of-magnitude uncertainties into forecasts of the dissolved mass influx to range soils.

Two studies have measured the particle distribution resulting from partial detonations. Taylor et al. (2006, 2004a) measured particle mass distributions for a partial detonation of a Composition B-filled 81-mm round and of two TNT-filled 155-mm projectiles. In a separate study, Taylor et al. (2010) measured the daughter particles resulting from crushing TNT (trinitrotoluene), Composition B (Comp B—a 60:39:1% mix of RDX:TNT:wax) and Tritonal (80% TNT 20% aluminum powder) chunks. Some of these crushed samples were placed outside to dissolve and their particle sizes measured again after 22 months of outdoor dissolution and weathering.

In this study, we collected and massed explosive particles released from four 81-mm “UXOs” that were partially detonated, and one that was broken open by fragments from a nearby high-order detonation, and compared the results with those found by the previous studies. We hoped to determine if explosives fracture in a quasi-predictable way that would help us estimate HE particle distributions on training ranges and how these

distributions change as particles weather outdoors, information needed if we are to predict the dissolved HE load entering range soils. This work is part of a larger study (Chapters 6 and 7 of this report) whose aim is to determine the likelihood of cracking or breaching UXOs by a close-proximity high-order detonation.

8.3 Experimental Methods

To simulate a close-proximity detonation, as might occur when a round detonates high-order close to a UXO, Walsh, M.R., et al. (Chapter 6 of this report) designed and tested an initiation system that behaves similarly to a fully functioning fuze. Using this system, we detonated 81-mm high-explosive (HE) mortar projectiles at 0.3- to 1.2-m distances from one or more unfuzed, 81-mm HE rounds. During these tests, 11 81-mm HE rounds were detonated high-order near 23 unfuzed 81-mm HE rounds that acted as proxies for UXO. Each 81-mm projectile contained 950 g of Comp B.

The tests were conducted on an approximately 50-cm-deep snow cover, which we mechanically compressed so that it sintered into a fairly hard surface. Each round was detonated in a different location within the packed area to minimize cross-contamination. The “UXOs” that were partially detonated or broken open scattered Comp B particles on the hardened snow surface, some over 100-m distances. We picked up centimeter-sized HE particles from the snow surface. These were spread out on aluminum trays in the laboratory and left to dry for 12 hours in the dark before massing. To collect the millimeter-sized HE particles, we used snow samples collected with a Teflon®-lined aluminum scoop. All these samples were put into plastic bags, labeled, and kept in a cooler away from sunlight until they could be melted at room temperature. The water was then filtered under vacuum (Whatman filters, GF/A glass microfiber filters, 90-mm diameter, 1.6-µm pores). The recovered particles were left to dry in the dark before massing.

We weighed the recovered Comp B particles on an O’Haus balance (Adventurer Pro, 310 g max). Particles larger than 1 cm in diameter were weighed individually and photographed. Smaller particles were massed in groups of 10. The explosive ordnance disposal (EOD) personnel detonated the HE pieces at the end of the tests.

We fit the ranked mass data, all particles except the dust, using a log-normal cumulative distribution, with a range between 0 and 1:

$$P_i = \frac{1}{2} \operatorname{erfc} \left[\frac{\ln(M_i/A_0)}{\sqrt{2A_1}} \right] \quad (1)$$

where P_i is the probability that the mass M_i , the mass of the particle, is not exceeded; A_0 and A_1 are parameters that are varied to fit the data, and erfc is the complementary error function. A_0 is a measure of the size of the pieces and is larger for distributions that contain gram chunks and smaller for those having milligram particles. A_1 is a measure of the slope of the distribution and is larger for distributions having a wider range of particle masses, than for those whose particles have a narrower range of masses. R^2 is a measure of the goodness of fit of the distribution to the data.

For data sets where we collected a lot of particles, test 4b, and the previously published partial detonation residues for two TNT-filled rounds and one Comp B round (Taylor et al. 2004a, 2006), we also fit a generalized Pareto distribution (GPD) to the tail of the measured mass distributions, which we defined as the largest 10 to 20% of the particles. The GPD is

$$\begin{aligned} F(x) = P(X \leq x | x \geq u) &= 1 - \left[1 - \frac{k(x-u)}{\alpha} \right]^{1/k} & k \neq 0 \\ &= 1 - \exp \left[\frac{-(x-u)}{\alpha} \right] & k = 0 \end{aligned} \quad (2)$$

In eq 2, u is the threshold mass, k is the shape parameter, and α is the scale parameter. The cases $k = 0$, $k < 0$, and $k > 0$ correspond to the extreme value distribution types I (shortest infinite tail), II (longer infinite tail), and III (finite tail length, $x < \alpha/k$). We used probability weighted moments to determine the parameters k and α . Thus, estimates of the GPD parameters are provided by:

$$\begin{aligned} k &= \frac{4b_1 - 3b_0 + u}{b_0 - 2b_1} \\ \alpha &= (b_0 - u)(1 + k) \end{aligned} \quad (3)$$

where

$$b_0 = \frac{1}{l} \sum_{i=1}^l x_{(i)}$$

$$b_1 = \frac{1}{l} \sum_{i=1}^l \frac{i-1}{l-1} x_{(i)}$$

(Wang 1991), where the $x_{(i)}$ are the ordered sample, $x_{(1)} \leq x_{(2)} \leq \dots \leq x_{(l)}$ of masses greater than the threshold u . We reasoned that the big pieces deposit most of the mass and that their distributions are the most important for quantifying HE loads on ranges.

8.4 Results and Discussion

8.4.1 Samples studied

Of 23 unfuzed rounds, the casings of four were hit, but not penetrated, by fragments from the high-order detonation (Fig. 8-1a); nine casings were penetrated to the fill (Fig. 8-1b); seven rounds partially detonated (Fig. 8-1c); one round detonated high-order; and two rounds were not recovered (Table 8-1). As a partial detonation can look similar to a cracked round, we used the diameter of the metal casing as our distinguishing criterion. Pressure from a partial detonation expands and distorts the round relative to rounds that are simply broken open. The carcass retrieved for round 4b (Fig. 8-2), for example, measured 11.1 cm at its widest point compared to 8.0 cm for an undetonated round. Depending on how much of the HE fill detonates, a partial detonation might scatter much of its explosive fill or just a small amount leaving the remainder in the shell (Fig. 8-1c). Cracked and holed rounds generally spill their HE adjacent to the carcass.

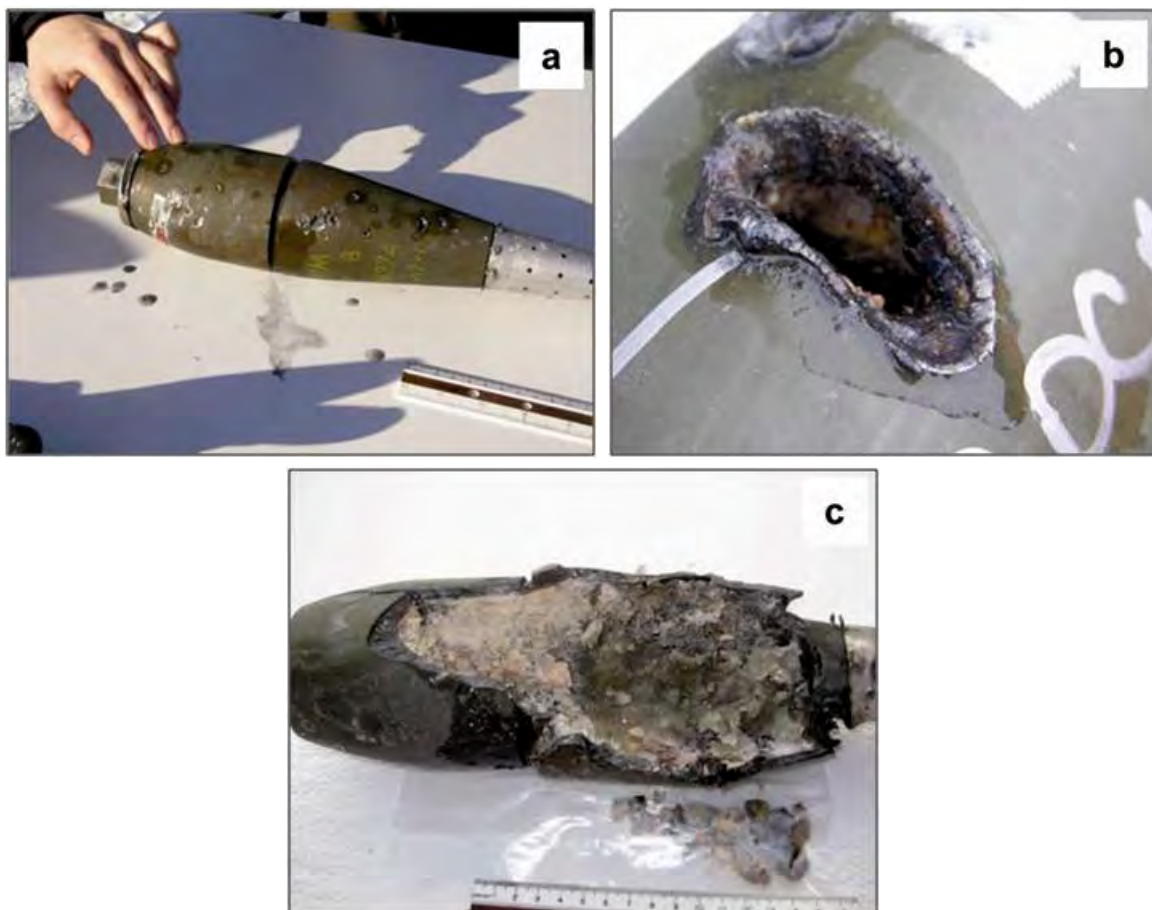


Figure 8-1. Types of damage caused by high velocity fragments from a nearby high-order detonation: a) dimples in round 2, b) a hole in round 11e, and c) a partial detonation where most of the HE fill remained in round 9b.

Table 8-1 Fate of the unfuzed rounds.

Condition	Test no. and round label	Studied here
Not pierced	2, 3b, 5b, and 11c	
Pierced to HE fill	1, 3a, 5a, 6a, 6b, 7a, 8b, 11d, and 11e	8b
Partially detonated	4b, 7b, 8a, 9a, 10a, 11a, and 11b	4b, 8a, 9a, and 10a
High-order	10b	
Not recovered	4a and 9b	



Figure 8-2. Cross-section of round 4b next to an undetonated 81-mm mortar projectile.

Nine of the 23 rounds scattered HE onto the snow. Although we collected the HE from all nine events, here we describe results only for tests 4b, 8a, 8b, 9a, and 10a because we can unambiguously link the HE recovered following the test to each of these rounds.

For test 4, we detonated a vertically positioned projectile (to simulate an incoming round) at a distance of 30 cm from two horizontally placed rounds (Fig. 8-3). One of the rounds, no. 4a, was projected over a plywood barrier and was not recovered; the second round, no. 4b, partially detonated. The craters from the high-order detonation and from 4b both measured 1.5 by 1.5 m and the largest piece of round 4b was recovered 123.6 m from the crater.

The side of round 4b was split open and some HE remained in the casing (Fig. 8-2). Most of the particles were scattered in a 10-m-wide swath at distances 0 to 41 m from the round's original position (Fig. 8-4). Within this swath, less than centimeter-size particles were distributed over the snow surface (Fig. 8-5). Individual centimeter-sized and larger pieces were found further away, up to 73 m from the detonation. From the 600-m² depositional "plume," we collected 839 HE pieces (Fig. 8-6) weighing 221 g or 23% of the Comp B originally in the round. The largest HE piece weighed 9.3 g.



Figure 8-3. Setup used for test 4, with vertical “incoming” round to be set off high-order and two “UXO” placed 30 cm from the round.

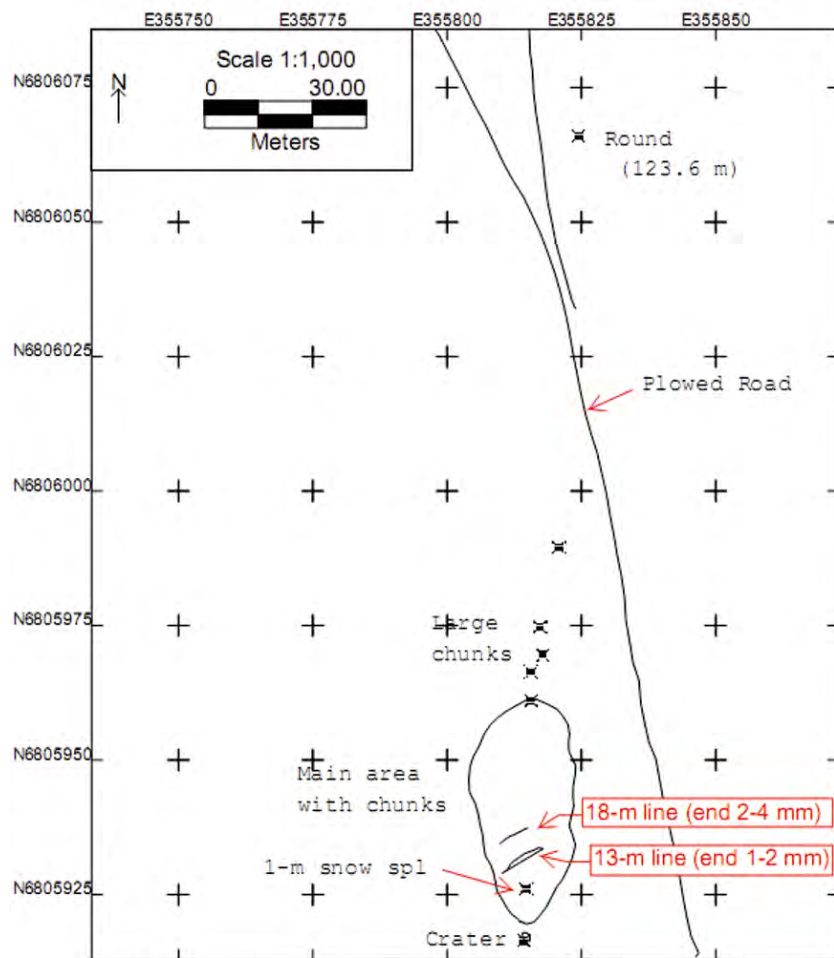


Figure 8-4. Location of the crater, centimeter-sized HE strewn field, and individual larger pieces including the remains of round 4b.

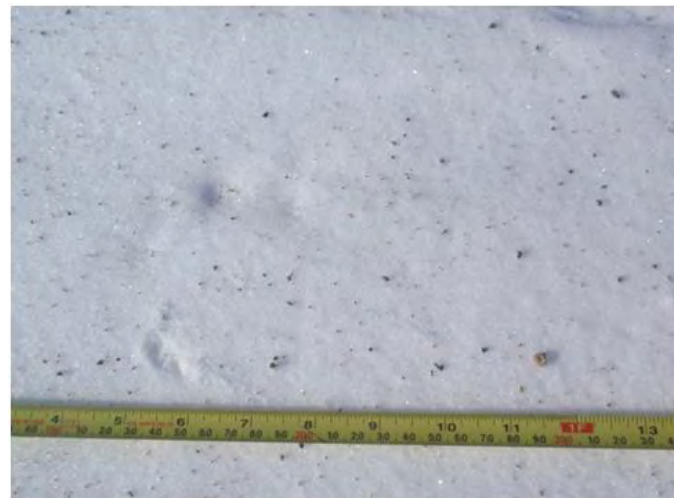


Figure 8-5. Sub-centimeter-sized HE pieces deposited close to detonation 4b.



a. Largest piece found.

b. Centimeter-size pieces recovered.



c. Shape of some of these cm-sized pieces.

Figure 8-6. Comp B left after the partial detonation of round 4b.

For test 8, we detonated a vertically positioned projectile at a distance of 50 cm from two horizontally placed rounds. UXO 8a partially detonated, whereas 8b was cracked and spilled HE onto about 1 m² snow (Fig. 8-7).

For both tests 9 and 10, we detonated a horizontally positioned round 50 cm from two horizontally placed UXOs, one on each side of the detonating round. Round 9a was opened along its entire length and partially detonated, as evidenced by its expanded central section (Fig. 8-8), and the particles deposition pattern was clearly linked to this round. Round 9b was not recovered and did not contribute any HE.



Figure 8-7. Residues recovered from round 8a (left) and round 8b.



Figure 8-8. Residues recovered from round 9a (left) and round 10a.

Round 10a also partially detonated and formed a 1.1-m² diameter crater. The round was broken into multiple pieces (Fig. 8-8) and HE was scattered over a 140-m² area (Fig. 8-9). Its twin, 10b, detonated high-order. Information about these rounds is summarized in Table 8-2.

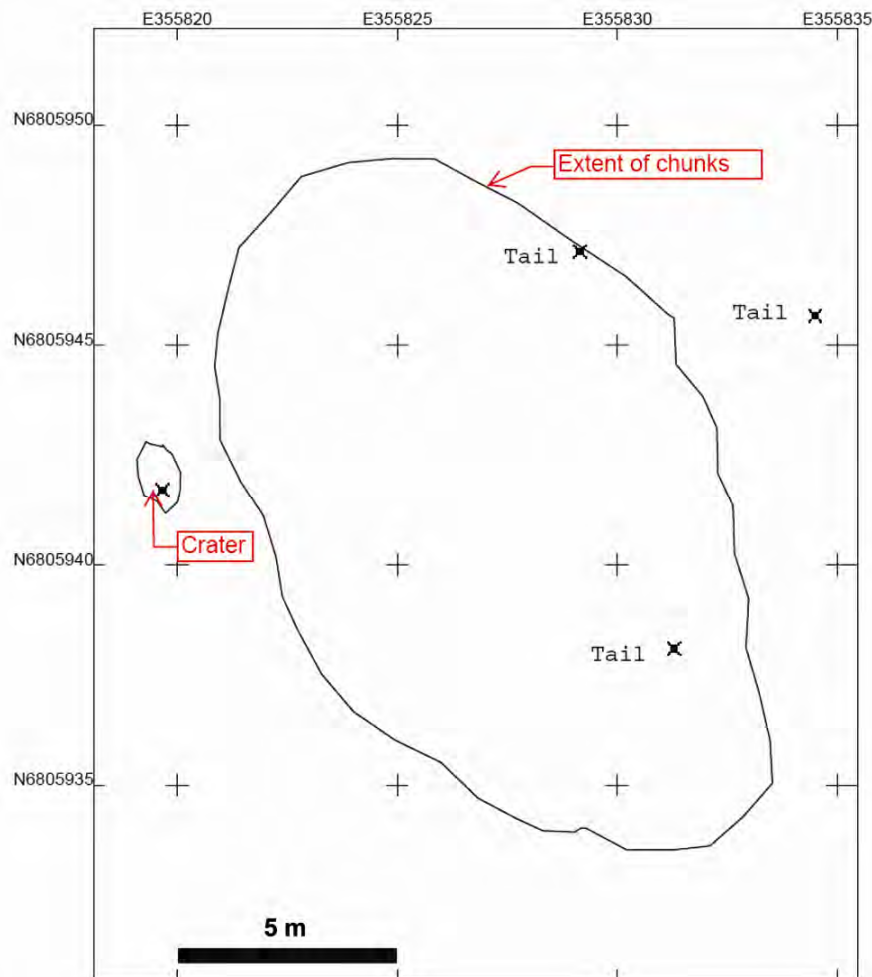


Figure 8-9. Crater and centimeter-sized HE scatter area for test 10a.

Table 8-2. Total mass and number of HE pieces recovered.

Round	Mass recovered (g)	No. of pieces	Mass of largest piece (g)	Scatter area (m ²)
4b	221	839	9.3	600
8a	25.6	12	3.1	
8b	21.7	20	3.6	2
9a	12.3	11	1.6	
10a	60.0	16	11.7	140

8.4.2 Mass distributions

Figure 8-10 shows the generalized Pareto distribution for the largest 10% of the pieces collected from round 4b, plotted alongside similar data from three other partial detonations—two from TNT-filled 155-mm howitzer rounds and from another Comp B-filled 81-mm round. Despite the order-of-magnitude differences in the masses recovered from the two TNT detonations, these two distributions are similar and quite different from those of the two Comp B detonations. The TNT rounds yielded tail shape parameters k of -0.73 and -0.77 , whereas the Comp B rounds have tail shape parameters of -0.35 and -0.49 . The more negative values of k indicate a fatter tail for the distribution; that is, there is a relatively larger fraction of large particles relative to small particles in the TNT partial detonations compared to the Comp B partial detonations.

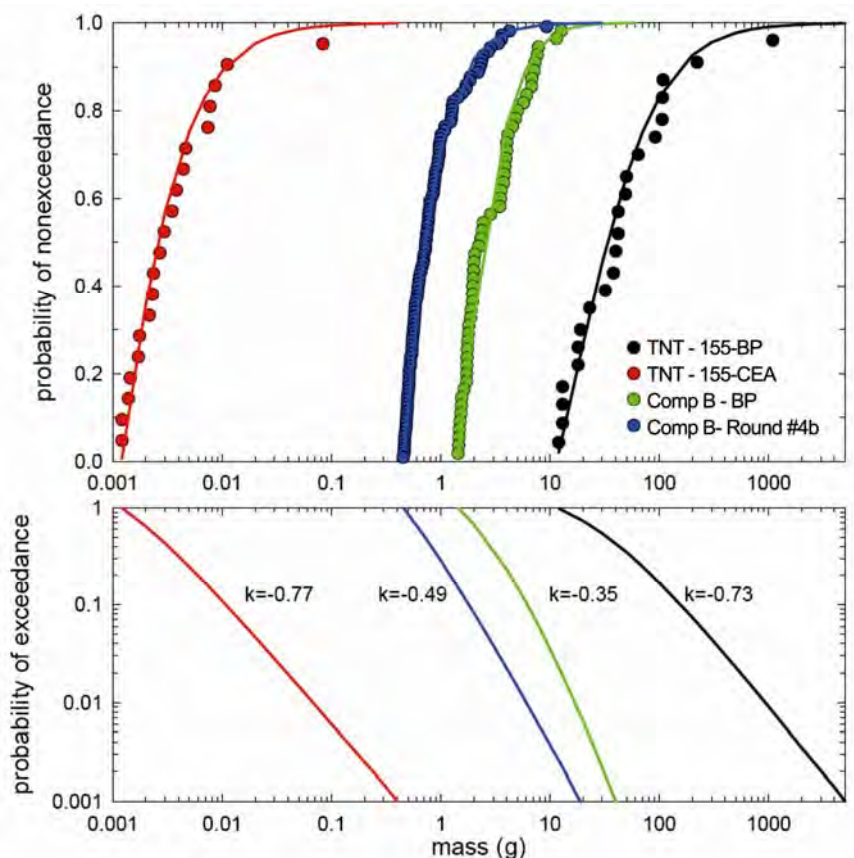


Figure 8-10. Piece size distribution for round 4b plotted along with distributions of low-order detonations previously published by Taylor et al (2004a, 2006). The largest 10% of the pieces were fitted using a generalized Pareto distribution. The k values for these distributions suggest that 155-mm TNT-filled rounds (black and red lines) produce mass distributions that are similar to one another but different from those resulting from Comp B filled 81-mm rounds (blue and green lines).

The same data were fitted using semi-log cumulative distributions (Fig. 8-11) so as to compare them with the fits for the rest of the tests (Table 8-3). The cumulative distributions shown in Figure 8-11 all have good curve fits ($R^2 > 0.9$) but the A_0 and A_1 parameters do not clearly differentiate the TNT from the Comp B distributions. One of the TNT and one of the Comp B distributions have high A_0 values and the other TNT and other Comp B distributions have low values, reflecting differences in the mass collected from these partial detonations, not differences between the explosives. The average of the two TNT A_1 values (1.7), however, is higher than the average A_1 values of the two Comp B-filled rounds (1.2).

Figure 8-12 shows semi-log cumulative distributions for the four remaining rounds, 8a, 8b, 9a and 10a, all Comp B-filled 81-mm mortar rounds. The A_0 values range between 0.57 and 1.54, the A_1 values between 0.40 and 1.4, and the R^2 values are just over 0.9. These distributions are composed of fairly large Comp B pieces, reflected in the A_0 values. The A_1 values (0.81 ± 0.41) are smaller than those measured for TNT, consistent with the finding that Comp B may produce narrower size distributions. Also of note is that the mass distributions between rounds 8a and 8b are not different, despite one coming from a partial detonation and the other from a cracked round.

For comparison, we reanalyzed the data on crushed explosives published in Taylor et al. (2010) by plotting them also as semi-log cumulative distributions (Fig. 8-13). Unlike the field-collected samples, where we probably did not collect all the scattered particles, we were able to weigh all of the daughter particles generated by these tests. The A_0 values for the crushed explosives range between 0.01 and 0.07, with an average of 0.020 ± 0.01 and do not show a systematic difference between the explosive compounds (Table 8-3). A_1 , on the other hand, appears to separate the explosives into two groups, Comp B with average values of 0.95 ± 0.36 , and TNT and Tritonal with average values of 1.93 ± 0.55 , showing that Comp B breaks into a narrower range of particle masses than does TNT or Tritonal. The R^2 values are generally over 0.9, with the exception of Trit1 (weathered), TNT14 (crushed), and Comp14 (crushed). Interestingly, these three samples have the highest A_0 values in their groups and produced fewer particles when crushed than their fellow pieces (Table 8-3), indicating that a few large pieces were produced.

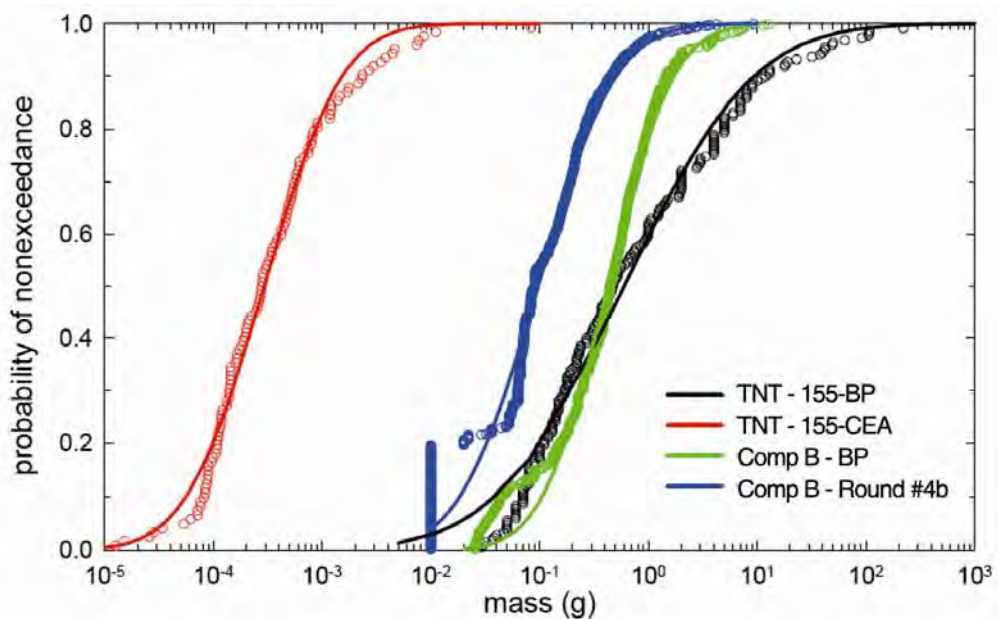


Figure 8-11. Same data shown in Figure 8-10 fitted using cumulative distributions.

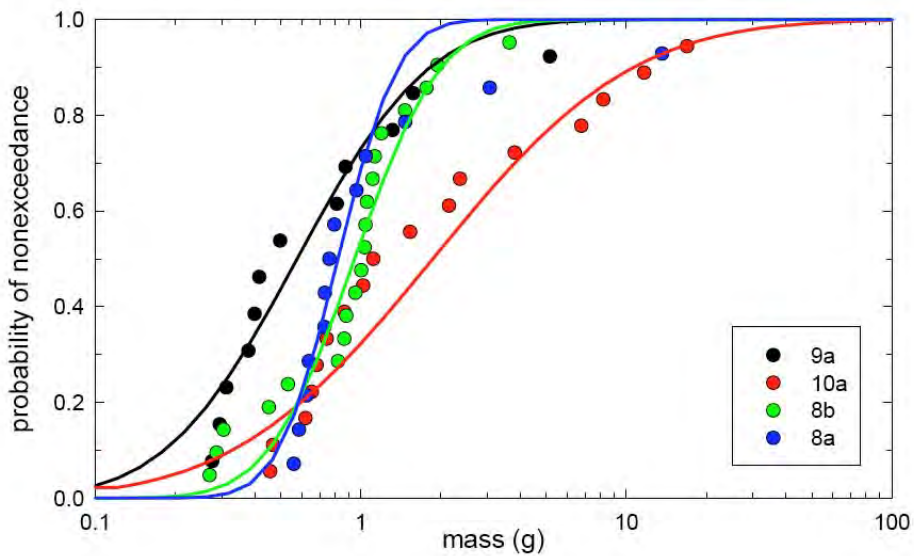


Figure 8-12. Plot of pieces collected from rounds 8a, 9a, and 10a, all partial detonations, and from round 8b, which was holed by a fragment.

Table 8-3. Parameters of a cumulative lognormal distribution found to best fit the measured mass distributions; ratio of mass of the largest HE piece found divided by the HE mass recovered M/M_0 ; and tail shape parameter k for the fit of a GPD to the tail of the distribution. For samples that were crushed in the laboratory, we also list the force needed to crush the HE piece and the number of daughter pieces. A_0 is a measure of the size of the pieces and A_1 is a measure of the slope of the distribution and is larger for distributions having a wider range of particle masses.

Sample Label	Test Type	A_0	A_1	R^2	M/M_0	k	
CEA 155 TNT	BIP Partial detonation	0.00	1.29	0.99	0.45	-0.77	
BP 155 TNT	BIP Partial detonation	0.60	2.15	0.98	0.44	-0.73	
BP 81 Comp B	BIP Partial detonation	0.43	1.09	0.99	0.03	-0.35	
4b Comp B	Pxi* Partial detonation	0.10	1.30	0.97	0.04	-0.49	
8a Comp B	Pxi* Partial detonation	0.82	0.40	0.90	0.12		
8b Comp B	Pxi* Cracked	0.95	0.58	0.92	0.17		
9a Comp B	Pxi* Partial detonation	0.58	0.90	0.92	0.13		
10a Comp B	Pxi* Partial detonation	1.54	1.35	0.94	0.19		
Sample Label	Test Type	A_0	A_1	R^2	M/M_0	Force (lb)	No. pieces
Trit 6	crushed	0.01	1.56	0.94	0.5	54	13
Trit 7	crushed	0.01	2.05	0.98	0.42	29	17
Trit 8	crushed	0.01	1.91	0.95	0.51	26	16
Trit 9	crushed	0.01	2.09	0.97	0.48	13	10
Trit 5 (14 mo)	Outdoor & crushed	0.01	1.73	0.99	0.68	110	22
Trit 5 (36 mo)	weathered	0.02	1.07	0.99	0.26		30
Trit 1 (36 mo)	Outdoor & crushed	0.04	3.03	0.80	0.66	76	3
TNT 12	crushed	0.01	1.88	0.99	0.77	7	7
TNT 13	crushed	0.03	2.23	0.90	0.57	7	7
TNT 14	crushed	0.07	1.15	0.61	0.31	7	7
TNT 15	crushed	0.01	0.95	0.95	0.42	3	10
TNT 5 (14 mo)	Outdoor & crushed	0.01	2.31	0.92	0.54	8	7
TNT 5 (36 mo)	weathered	Too few pieces			0.60		2
TNT 9 (36 mo)	Outdoor & crushed	0.01	2.29	0.95	0.47	12	7
Comp B 13	crushed	0.02	1.23	0.91	0.29	21	13
Comp B 14	crushed	0.03	0.44	0.78	0.28	4	5
Comp B 15	crushed	0.01	0.89	0.98	0.26	6	12
Comp B 16	crushed	0.02	0.87	0.93	0.28	23	11
Comp B 17	crushed	0.01	0.80	0.98	0.16	24	18
Comp B 11 (14 mo)	Outdoor & crushed	0.02	1.47	0.92	0.52	15	8
Comp B 11 (36 mo)	weathered	0.01	1.01	0.97	0.76		5
Comp B 1 (36 mo)	Outdoor & crushed	0.01	1.91	0.98	0.44	20	12

Pxi* = Proximity to High-order Detonation. Data from the crushed samples are from Taylor et al. (2010). Some of the explosive pieces were part of a 36-month weathering and dissolution experiment. Trit 5, TNT 5, and Comp B 11 were placed outside for 14 months, crushed, and then returned outside. Three other HE pieces (Trit 1, TNT 9, and Comp B1) were crushed at the end of the experiment. Mass of dust not included in the number of pieces.

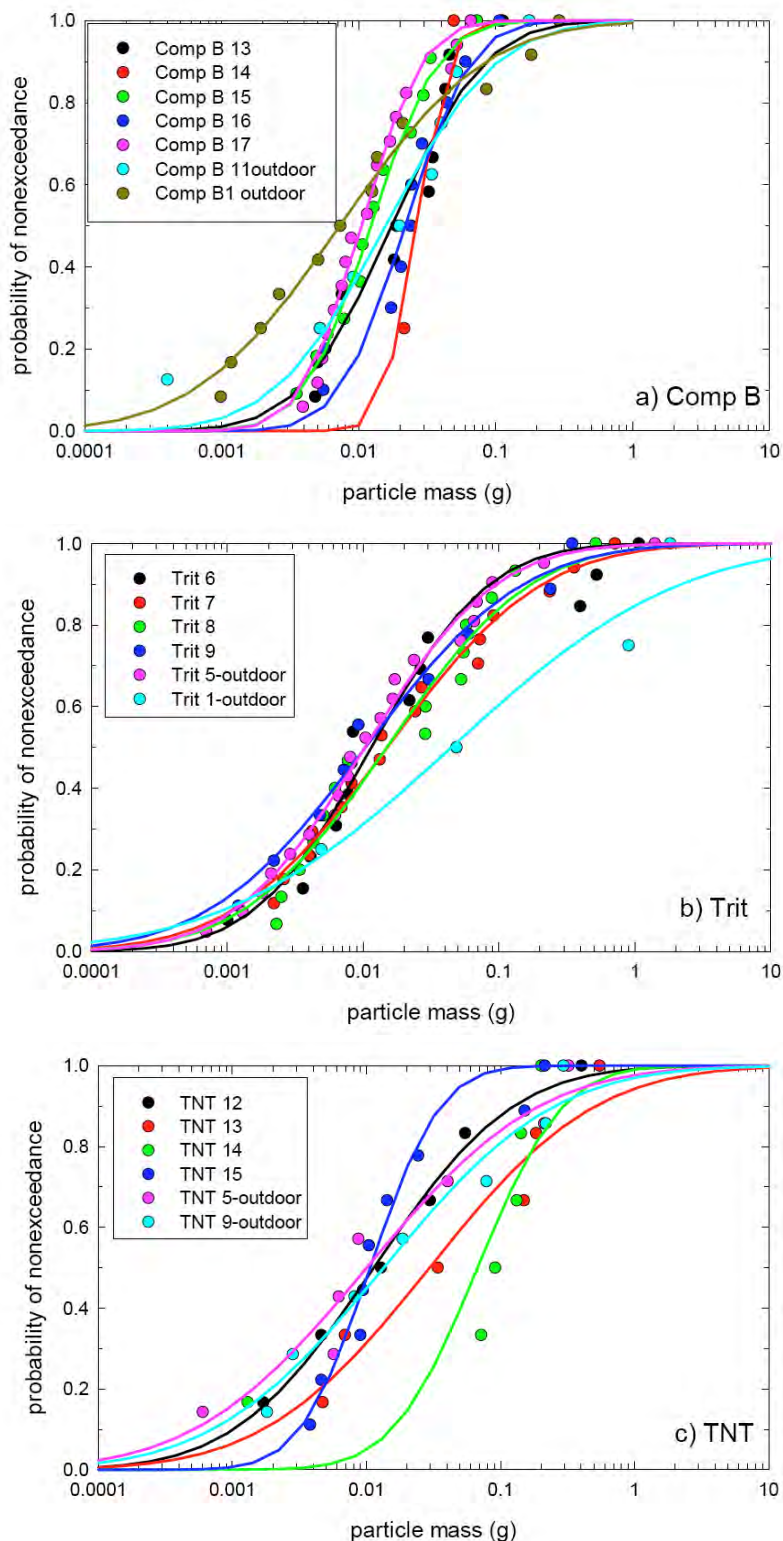


Figure 8-13. Particle masses plotted versus probability of not exceeding that mass for crushed and outdoor weathered chunks of a) Comp B, b) Tritonal, and c) TNT; data taken from Taylor et al (2010).

8.4.3 Mass of the largest HE piece

The mass distributions show that Comp B breaks into smaller pieces than does TNT and Tritonal. Another measure of this property is the ratio of the mass of the largest piece recovered (M) relative to the total mass recovered or the starting mass (M_0). We tabulated this ratio, M/M_0 , for all of the HE collected in the field and for the HE crushed in the laboratory (Table 8-3). For partial detonations, the ratio of the largest piece to the total mass collected ranged from 0.03 to 0.19 for Comp B and was 0.45 for TNT (only two tests). For the crushing tests, the largest Comp B pieces were on average 0.31 ± 0.11 of the mass of the original chunk; TNT and Tritonal pieces averaged 0.53 ± 0.13 of the original chunks (Table 8-3, Fig. 8-11). As Comp B is a mix of 60% 100- μm RDX crystals blended into 39% molten TNT (which becomes a fine-grained matrix), we speculate that the dissimilar grain sizes produce stresses and grain interactions not present in pure TNT or TNT mixed with micrometer-sized aluminum grains (Tritonal). Given this interpretation, we would expect similar behavior for any two or three component melt-cast explosive where one of the phases has crystals significantly larger than the matrix. Octol, an HMX-TNT mixture that also has dissimilar grain sizes, and some of the new insensitive munitions, come to mind.

8.4.4 Changes in mass distributions caused by weathering

HE particle masses are not static when exposed in the environment and their distributions are likewise not static. Particles can split because of mechanical forces and dissolve when in contact with precipitation. The slope of the distribution should flatten if large pieces split into many smaller ones and steepen if small particles are preferentially dissolved. The net change in the shape and magnitude of the mass distribution will depend on the relative rates of dissolution versus splitting.

We can test how mass distributions change using data collected by Taylor et al. (2010) in a study of weathering and dissolution of HE chunks and particles. Three outdoor test samples, Trit 5, TNT 5, and Comp B 11, were crushed after 14 months of outdoor exposure and their daughter pieces returned outdoors. The experiment ended after 36 months, at which time the daughter populations were weighed again. Dissolution should remove the smaller particles, leading to a narrower mass distribution and, consequently, smaller A_1 values. For the Trit 5 distribution, the A_1 value decreased from 1.7 to 1.1; for the Comp B 11 distribution, the decrease was

from 1.5 to 1.0 (Table 8-3). No distribution was fit to TNT 5, which had only two pieces remaining. Interestingly, Trit 5 split while it was outdoors (note the decrease in M/M_0 ratio and increase in number of pieces). Nevertheless, the value of A_1 decreased, indicating that dissolution controlled the shape of the distribution in this case. Although these data are limited, the distributions became narrower and moved to larger particle masses during outdoor exposure (Fig. 8-14).

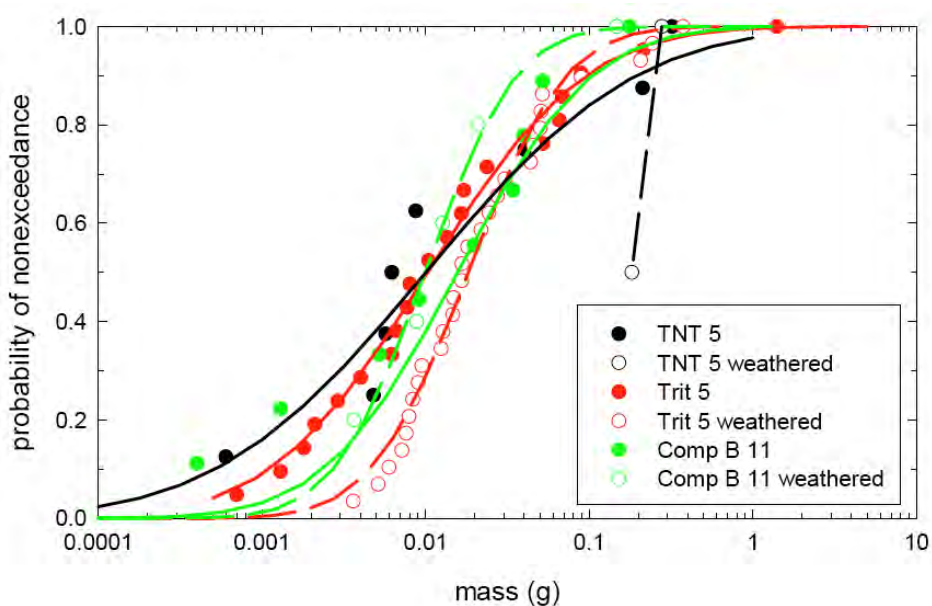


Figure 8-14. Change in particle distributions after 22 months of outdoor dissolution.

8.4.5 Implications for explosive particles in training range soils

HE particles scattered onto range soils dissolve and break apart because of weathering. The differences in the starting particle sizes and distributions deposited by Comp B- and TNT-filled rounds during partial detonations have implications for how these explosives weather in the field. The wider particle distributions seen for TNT and Tritonal suggest that the many small particles will dissolve, leaving the large pieces behind. The narrower distributions seen for Comp B, on the other hand, provide more surface area for dissolution, suggesting that TNT will dissolve from the Comp B, thus releasing RDX crystals into the soil. Consequently, Comp B pieces should be harder to find than TNT and Tritonal pieces, although the slowly dissolving RDX crystals should persist in the soils.

8.5 Conclusions

The high density of surface and near surface UXOs increases the likelihood that fragments from a high-order detonation will partially detonate or pierce the casing of a UXO. As partial detonations and cracked rounds leave much of their explosive fill undetonated or unburned, both of these fates could be large point sources of contamination, given climatic and geological conditions that allow precipitation wetting and dissolving of the exposed HE, which can reach groundwater. Both the total HE mass and its distribution determine the rate at which dissolution occurs.

We measured the HE particle masses that resulted when a “UXO” was damaged by a nearby high-order detonation. These data are compared to mass distributions from previously measured partial detonations and from crushing tests on HE pieces. Our results show a systematic difference between Comp B particle masses and distributions and those of TNT and Tritonal. Partial detonations of Comp B-filled rounds scatter smaller pieces of HE, with a narrower mass range, than do TNT-filled rounds.

9 Sampling for Comp B Residues using Shallow Wells at Two Low-order Detonation Sites

Marianne E. Walsh, Alan D. Hewitt, Michael R. Walsh, Charles M. Collins, Ronald N. Bailey, Susan R. Bigl, and Jeff Bryant

9.1 Introduction and background

High explosives are used worldwide during live-fire on military training lands. Incomplete detonations or breached unexploded ordnance deposit explosives on the soil surface that can subsequently dissolve and migrate to groundwater (Lewis et al. 2009). Few actual field investigations of the fate of detonation residues have been performed on training ranges because of the dangers associated with unexploded ordnance. Where monitoring wells have been installed, RDX, a nitramine, has been detected (Clausen et al. 2004; Morris and Fallin 2008; Bordeleau et al. 2008).

We monitored the persistence of Comp B residues from a live-fire training event with 120-mm HE M933 point detonating mortar projectiles on a salt marsh impact area over 4 years (Walsh, M.E., et al. 2010; Hewitt et al. 2009). The distribution, appearance, and persistence of Comp B residues from two low-order (incomplete) detonations were documented. To determine if dissolved Comp B residues were migrating down into the underlying sediments, the explosives concentrations in the sediment under two pieces of Comp B were measured to a depth of 40 cm. In addition, water from a flooding tide that had flowed over the Comp B residue was sampled during the ebb tide to determine if Comp B residues were washing off the mudflats and migrating to the river (Walsh, M.E., et al. 2008).

The Comp B residues were scattered 20 to 30 m asymmetrically from each crater in March 2006. The physical appearance of the Comp B residues varied from red stains on the sediment surface to clusters of millimeter-sized particles to individual Comp B chunks 3–4 cm long. Subsequent physical changes were the disaggregation of initially solid chunks into masses of smaller diameter pieces and formation of red phototransforma-

tion products that washed off with rain or tidal flooding (Walsh, M.E., et al. 2010). The solid residue was all dissolved by September 2010. Despite high surface concentrations of explosives under individual chunks of Comp B (>1000 mg/kg), subsurface concentrations were low. Over 90% of the mass of Comp B residues was in the top few centimeters. Water draining off the mudflat after flooding tides had detectable concentrations of RDX, TNT, and HMX in the water immediately adjacent to the low-order detonation sites. RDX was the only analyte detectable at the farthest downstream sample point within the tidal drainage gully (Walsh, M.E., et al. 2008).

9.2 Objective

The objective of this study was to evaluate the potential for migration of Comp B residues to groundwater using shallow monitoring wells installed in May 2009. This report documents the well installation procedure and discusses the results from water samples from the wells that were collected in July and September 2009 and in May and September 2010.

9.3 Materials and methods

The low-order detonation sites were located on either side of a drainage channel from the main river that bisects the salt marsh (Fig. 9-1). We installed a total of six wells, three wells each at two sites with Comp B residues. At both sites, one well was installed near the crater that contained the tail fin and part of the body of the partially detonated mortar projectile (Fig. 9-2). At the site designated LO2, the other two wells were placed downgradient of the crater and the area where the Comp B was scattered. At the site designated LO3, one well was placed in the middle of the Comp B scatter area and another was placed in an up-gradient location.

9.3.1 Shallow wells

The 51-mm (2-in.) ID (internal diameter) well casing had a pre-pak well screen made of 65-mesh stainless steel (Fig. 9-3a) and 20 × 40 silica sand over a 0.25-mm (0.01-in.) slotted schedule 40 PVC pipe¹. The screening length was 1.45 m of the 1.52 m casing. The down-hole end had a drive point cap, and the uphole end had a 0.762 m foam bridge (Fig. 9-3b) and a 0.762-m riser. The depth of each well was 2 m.

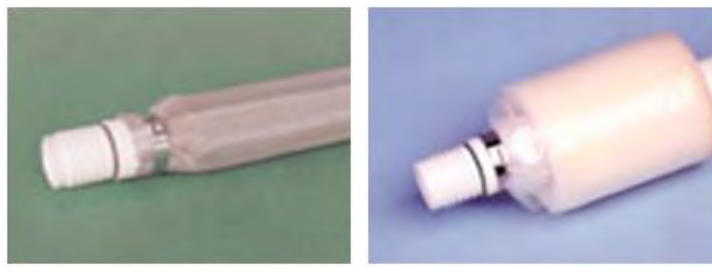
¹ Geolnsght, Las Cruces, NM 88005.



Figure 9-1. Aerial image (Aerometric, October 2010) showing the locations of six shallow groundwater monitoring wells (black dots) at two low-order detonations sites on a salt marsh impact area. The scatter area of the Comp B residues are outlined in black. The craters are located on the south boundary of each outline. Sites are designated LO2 (on the east of the distributary channel) and LO3 (on the west side).



Figure 9-2. Image showing the crater at LO3 in 2006. The red staining is from photo-transformation of TNT. A monitoring well was installed adjacent to the north edge of this crater in May 2009.



a. Well screen. b. Foam bridge.

Figure 9-3. Images of well screen and foam bridge used for construction of the monitoring well.¹

At each well site, the surface 15 cm of sediment was removed to prevent cross-contamination between the surface and subsurface (Fig. 9-4a). Then, a 76-mm (3-in.) stainless steel bucket auger² equipped with a mud bit was used to core a hole (Fig. 9-4b and 4c). As soon as the last lift was removed, the preassembled well casing was inserted into the augered hole. Sand³ was poured into the hole to fill any gaps between the sediment and the well casing. The wells were sealed with bentonite⁴, and the top of the well casing was protected with a PVC cap that had a vent hole (Fig. 9-4d).



a. Top 15 cm of sediment was removed to prevent cross-contamination between the surface sediments and the subsurface.

Figure 9-4. Well installation.

¹ <http://www.geoinsightonline.com/products/smdiam/intake.html>.

² AMS, Inc., American Falls, ID 83211.

³ Ogle Bay Norton® Industrial Sands, Inc. Colorado Silica Sand™, Colorado Springs, CO 80910.

⁴ Pure Gold TM Medium Bentonite Chips, Colloid Environmental Technologies Company, Arlington Heights, IL 60004.



b. Stainless steel bucket auger equipped with a mud bit.



c. Augering the hole for a well.

Figure 9-4 (cont'd). Well installation.



d. Finished well near the crater at LO3 (14 May 2009). The vented protective PVC cap was installed during the next site visit.

Figure 9-4 (cont'd). Well installation.

9.3.2 Water sampling

Water samples were recovered from the wells in July and September of 2009 and May and September of 2010 using 2-in. HYDRASleevesTM¹. Each 0.5-L water sample was preserved by acidification with 0.8 g of sodium bisulfate (Jenkins et al. 1995; Douglas et al. 2009) and stored at 4°C until analysis.

¹ GeolInsight Inc., Las Cruces, NM 88005.

9.3.3 Piezometer well

Subsurface water levels were monitored in a nearby piezometer well that was installed in June 2008 for another project. Depth of the piezometer well was 1.4 m. Water level within the well was monitored during the summers of 2009 and 2010 using a pressure transducer¹. Output from the pressure transducer was taken every 10 minutes, and the hourly and 24-hour averages recorded by a data logger². The data logger can be seen mounted inside a protective box on a tripod in Figure 9-5.

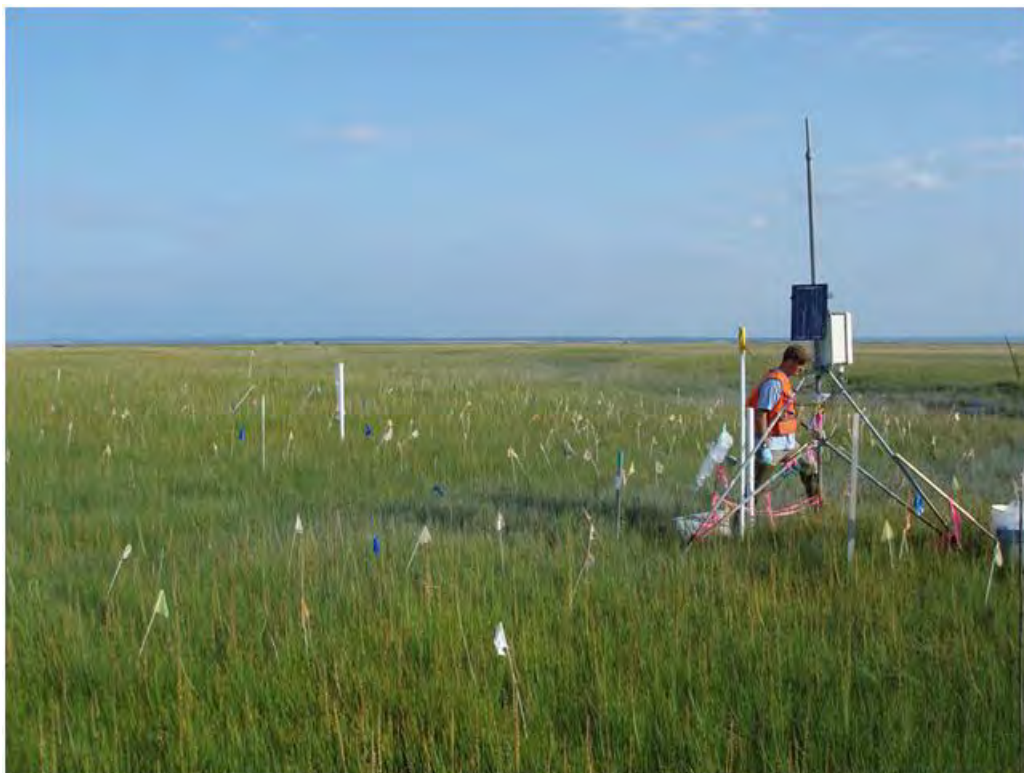


Figure 9-5. Instrumentation for collecting piezometer water depth readings.

9.3.4 Analysis of water samples

Samples were prepared for analysis by solid phase extraction. Cartridges filled with hydrophobic polymeric poly(divinylbenzene-vinylpyrrolidone) resin³ were preconditioned with 15 mL of acetonitrile (AcN) using gravity flow, then with 30 mL of reagent grade water⁴ at less than 10 mL/min. A

¹ Model PDCR 1830, GE Measurement and Control Solutions, Billerica, MA 01821-4111.

² Model CR10 Measurement and control module; SM716 Storage Module, Campbell Scientific, Logan, UT 84321.

³ PoraPak RDX Sep-Pak Vac cartridge, Waters Corporation, Milford, MA 01757.

⁴ Milli-Q Filtration System, Millipore, Billerica, MA 01821.

500-mL (or less) water sample was passed through each cartridge at less than 10 mL/min, then each cartridge dried under vacuum for at least 20 minutes to remove residual water. The dried cartridges were eluted with 5 mL of AcN. Generally, 4.5 mL were recovered, so the final volume was made up to 5.0 mL with AcN to yield a one-hundred-fold concentration factor.

Prior to HPLC analysis, a 1.00-mL aliquot of each AcN solid phase extract was mixed with 3.00 mL of reagent-grade water and filtered through a hydrophobic 0.45- μm filter unit¹. Determinations were made on a modular system² composed of a Spectra-SYSTEM Model P4000 pump, a Spectra-SYSTEM UV2000 dual wavelength ultraviolet/visible absorbance detector set at 210 nm (to detect NG) and 254 nm (cell path 1 cm), and a Finnegan SpectraSYSTEM AS3000 autosampler. Samples were introduced with a 100- μL sample loop. Separations were achieved on a 15 cm \times 3.9 mm (4- μm) NovaPak C8 column³ at 28°C and eluted with 1.4 mL/min of 15:85 isopropanol/water (v/v).

Calibration standards were prepared from commercially available analytical reference materials⁴, including an 8095 Calibration Mix A (HMX, RDX, TNT, 2,4-DNT, 2,6-DNT, 1,3-DNB, 1,3,5-TNB, 2-Am-4,6-DNT, 4-Am-2,6-DNT, and tetryl) and a single-component solution of NG. The concentration of each analyte was 1 mg/mL in AcN. Both 1- and 10-mg/L solutions were used to calibrate the HPLC-UV.

The solid phase extracts were also analyzed by GC- μ ECD, which provides lower detection limits. Autosampler vials with the solid phase extracts were placed into an HP 7683 Series autosampler tray continuously refrigerated by circulating 0°C glycol/water through the trays. A 1- μL aliquot of each extract was directly injected into the HP 6890 purged packed inlet port (250°C) containing a deactivated Restek Uniliner. Separation was conducted on a 6-m \times 0.53-mm-ID RTX-TNT fused-silica column that has a 1.5- μm thick film of a proprietary Crossbond® phase. The GC oven was temperature-programmed as follows: 100°C for 2 minutes, 10°C/minute ramp to 250°C. The carrier gas was hydrogen at 1.28 psi inlet pressure.

¹ Millex-FH, PTFE, Millipore, Billerica, MA 01821.

² Thermo Scientific Corporation, Waltham, MA 02451.

³ Waters Chromatography Division, Milford, MA 01757.

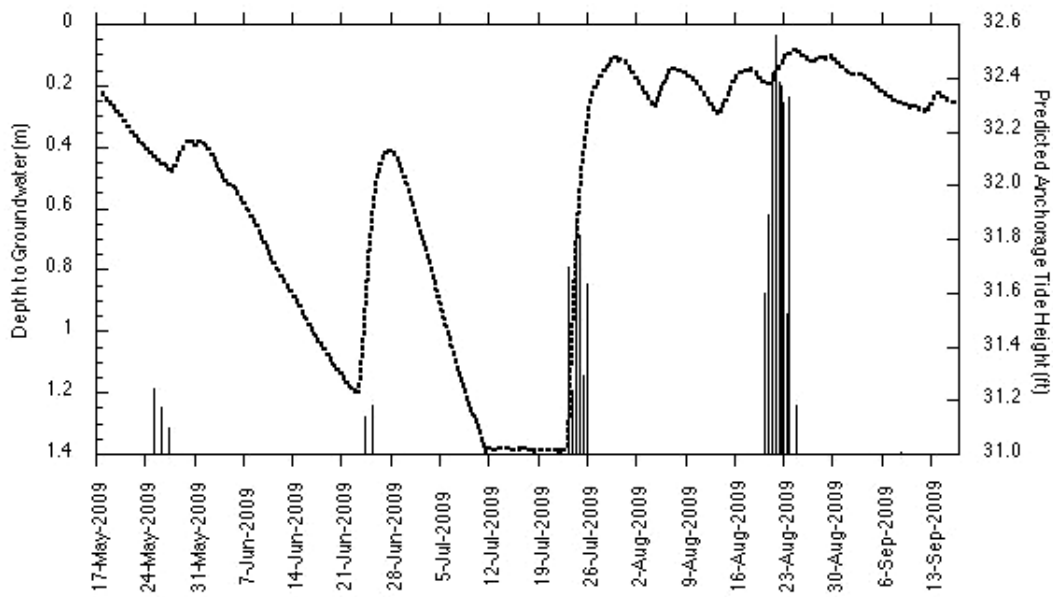
⁴ Restek Corporation, Bellefonte, PA 16823.

The μ ECD detector temperature was 280°C; the makeup gas was nitrogen at 45 mL/minute.

9.4 Results

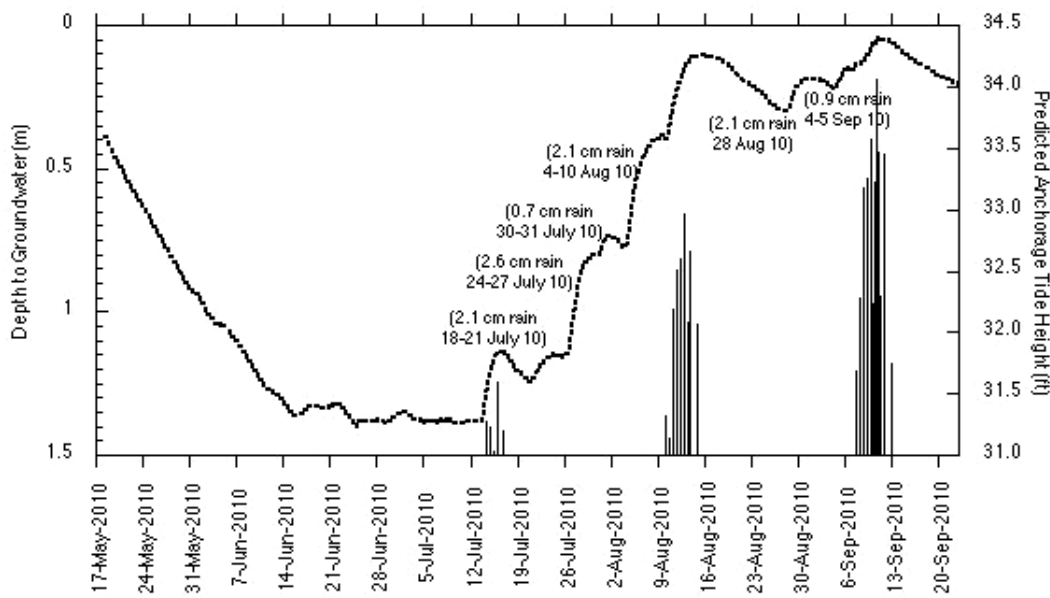
9.4.1 Water levels

Water level within the nearby piezometer well was affected primarily by the heights of the tides and to a lesser extent by rainfall (Fig. 9-6). During both 2009 and 2010, water levels generally declined through May and increased when the predicted tide for Anchorage exceeded 31 ft (Anchorage Tidal Datum), which corresponds to a mean sea level of 15 ft (4.6 m). The surface elevation at the wells at the low-order detonation sites is approximately 4.9 m, so the water level rise within the wells was from tide water seeping in from the nearby channel. Tides were sufficiently high to inundate the Comp B residues 12 times in 2009 and 18 times in 2010 between mid-May and mid-September (NOAA 2009, 2010). The flooding tidal water has the potential to transport Comp B residues by vertical flow into the underlying sediments (Fig. 9-7).



- a. In 2009, tides exceeded the 31 ft (Anchorage Tide Datum) 25–27 May, 24–25 June, 23–25 July, 20–24 August, and 8 September.

Figure 9-6. Water levels in 2009 and 2010 within a piezometer well near the water monitoring wells.



b. In 2010 tides exceeded 31 ft (Anchorage Tide Datum) 14–16 July, 10–14 August, 7–12 September.

Figure 9-6 (cont'd). Water levels in 2009 and 2010 within a piezometer well near the water monitoring wells.

9.4.2 Comp B residues

RDX and HMX were the only analytes detected at each sampling event (Table 9-1), and they were detected consistently in only one well. This well is located immediately adjacent (within 1 m) to a low-order detonation crater (Fig. 9-2).



a. View looking south across channel during a rising tide.

Figure 9-7. Views across the mouth of the drainage channel located between the two low-order detonation sites. Tides exceeding 31 ft (Anchorage Tide Datum) will fill the channel and flood the sediment that has Comp B residue. These photos were taken before the wells were installed at the site.



b. View looking northwest across channel at flood stage.

Figure 9-7 (cont'd). Views across the mouth of the drainage channel located between the two low-order detonation sites. Tides exceeding 31 ft (Anchorage Tide Datum) will fill the channel and flood the sediment that has Comp B residue. These photos were taken before the wells were installed at the site.

Table 9-1. Aqueous concentrations ($\mu\text{g}/\text{L}$) of RDX and HMX found in water samples collected from shallow monitoring wells. No other analytes were detected.

Well	RDX concentration ($\mu\text{g}/\text{L}$)				HMX concentration ($\mu\text{g}/\text{L}$)			
	2009		2010		2009		2010	
	18 July	17 Sept	24 May	23 Sept	18 July	17 Sept	24 May	23 Sept
L03 Crater	1.0	1.8	4.5	3.3	0.20	0.55	0.43	0.80
L03 North	<0.04	<0.04	0.04	<0.04	<0.05	<0.05	<0.05	<0.05
L03 South	0.1	<0.04	0.09	<0.04	<0.05	<0.05	<0.05	<0.05
L02 Crater	<0.04	0.02	<0.04	<0.04	<0.05	<0.05	<0.05	<0.05
L02 North	-- ¹	<0.04	<0.04	<0.04	<0.05	<0.05	<0.05	<0.05
L02 South	--	<0.04	<0.04	<0.04	<0.05	<0.05	<0.05	<0.05

¹ -- Not enough water in the well.

9.5 Discussion

Comp B is composed of RDX and TNT, with HMX present as an impurity in RDX. Once these energetic materials dissolve in water, they can migrate through the vadose zone to groundwater. Mobility is greatest for HMX and least for TNT; however, transformation by reduction of the nitro groups plays a major role in their fate. For example, TNT is readily transformed to 2-Amino-4,6-Dinitrotoluene and 4-Amino-2,6-Dinitrotoluene; both of these products are frequently detected with TNT in environmental samples. However, these transformation products are not stable and do not accumulate; the reduced products bind to the organic matter, thus TNT can be completely transformed as it migrates through sediment. Addition-

ally, an anoxic and iron-rich environment—such as that found in salt marsh sediments—provides ideal conditions for reduction of nitro-compounds (Larese-Casonova and Scherer 2008). RDX, which can persist in aerobic soils and has migrated to groundwater at some military installations, can be completely degraded under anaerobic conditions, forming compounds such as formaldehyde, nitrous oxide, and ammonia. Recent reviews of studies of the transformation of these energetic compounds are given by Monteil-Rivera et al. (2009) and Zheng et al. (2009).

The results obtained for the water samples from shallow wells in the salt marsh are consistent with the known fate processes for energetics in anaerobic sediment. Even though copious amounts of Comp B were scattered on the surface sediment, Comp B residues were generally not detectable in the groundwater. The nitramines (RDX and HMX) were consistently detected in the one well that was located immediately adjacent to a low-order detonation crater (Fig. 9-2) that contained an estimated hundreds of grams of Comp B within the surface sediment of the crater. The concentrations of RDX and HMX were low, and neither TNT, 2-Am-DNT, nor 4-Am-DNT, were detected, indicating that these compounds are not persisting in the subsurface pore water.

9.6 Conclusions

Water samples from six shallow ground water monitoring wells at two low-order detonation sites were collected twice yearly for 2 years. Only one well located proximal to a detonation crater had consistently detectable concentrations of RDX and HMX. TNT was not detected in any of the wells. The anaerobic and iron-rich sediments of a salt marsh impact area provide an ideal in-situ environment for reductive transformation of these compounds and decrease the likelihood of groundwater contamination.

10 Subsampling of Soils Containing Energetics Residues

Michael R. Walsh, Marianne E. Walsh, Alan D. Hewitt, Thomas F. Jenkins, and Kelsey Gagnon

10.1 Introduction and background

The collection of representative soil samples in the field is critical to obtaining valid data when characterizing a site contaminated with energetics. These compounds are generally found on military training ranges as widely dispersed particles. Their heterogeneous distribution makes representative sampling by most methods very difficult and even the best sampling methods will sometimes result in order-of-magnitude differences in the analytical results between samples.

What applies in the field also applies to the processing of the samples in the laboratory. Rasemann states in *The Encyclopedia of Analytical Chemistry* (2000) that the sources of error for site characterization can be approximated as up to 1000% for the acquisition of the samples in the field, between 100 and 300% for the sample preparation process, and between 2 and 20% for the analytical process. When a sample arrives at the analytical lab, the energetics residues mirror the composition and distribution of the residues in the field: they are dispersed nonuniformly throughout the sample and the particles of the soil and the energetics are not of uniform size. These two characteristics are called distribution heterogeneity (DH) and compositional heterogeneity (CH) and lead to grouping and segregation error (GSE) and fundamental error (FE), respectively. These errors can be minimized but not eliminated by proper sampling processing and subsampling. Grinding the sample to near-uniform size will minimize the FE. Previous studies have demonstrated that grinding using a puck mill minimizes the subsampling uncertainty for soil samples containing residues of explosives or propellants (Walsh, M.E., et al. 2002, 2007a; Hewitt et al. 2009). Other types of grinders (e.g., shaker ball mills, automated mortars, roller mills) have not been demonstrated to achieve a reduction in subsampling error for energetics (Penfold 2010).

Grinding will also help reduce the GSE but will not eliminate it. Samples with very low residues concentrations (<1 mg/kg) are especially susceptible to GSE because of the small amount of energetics in a comparatively large sample. Without the proper grinding of the field soil sample, obtaining a small (10 g) representative subsample is impossible. Even with grinding, it can be difficult. For this reason, we recommend using the *MULTI-INCREMENT[®]*¹ (MI) sampling technique for subsampling ground soil samples containing energetics, especially propellants, prior to final processing and analysis.

10.2 Objective

The objective of this study was to determine the effect of the number of subsampling increments on the recovery and reproducibility of analytes from soil samples containing moderate to low concentrations of energetic compounds.

10.3 Materials and methods

Field-contaminated soils containing either explosives or propellants were used in this study. The soils were collected during site characterization studies using MI sampling techniques to minimize field collection error. In the two phases of the study, samples that were previously ground with a ring and puck mill (LabTech ESSA Model LM2) were used. Total mass varied for each sample, with the larger samples requiring grinding in three batches (0.5- to 1.5-kg samples), while the smaller samples (<0.5 kg) required only one batch. The multiple batches had been recombined in a plastic bag after grinding. Because explosives and propellants are ground according to different protocols, we ran a two-component study to determine the results for the two classes of energetics. Soil samples containing explosives are ground in the ring and puck mill for one 60-second grind. For propellants, because of the fibrous nature of the nitrocellulose (NC) matrix, five 60-second grinds with 120 seconds between grinds are necessary to achieve a thorough grind and mix of the sample. Grinding in excess of 60 seconds and not allowing a cool-down period risks loss of the analytes through sublimation. Analytes of interest were 2,4,6-trinitrotoluene (TNT), octahydro-1,3,5,7-tetranitro-1,3,5,7-tetrazocine (HMX), and hex-

¹ *MULTI INCREMENT* is a registered trademark of EnviroStat, Inc. of Fort Collins, CO, for a comprehensive sampling methodology.

ahydro-1,3,5-trinitro-1,3,5-triazine (RDX) for explosives and nitroglycerine (NG) and 2,4-dinitrotoluene (DNT) for propellants.

The study was conducted in two phases to determine the effect of subsampling methods for different types of energetics at concentrations ranging from less than one to several hundred parts per million ($\mu\text{g/g}$). In both phases, replicate sampling was used to enable statistical evaluation of the results. For the first part of the study, soil samples of moderate to high concentrations that had been ground using Method 8330B (USEPA 2006) were subsampled either with a single grab sample or multiple increments. Seven repetitions were conducted for each subsampling method on each sample. For the second phase of the study, samples with known low residues concentrations that were processed in accordance with Method 8330B were used. Subsamples of the same mass (10 g) were built with various numbers of increments, ranging from 1 to 40.

The sample processing and analytical procedures will not be discussed in this chapter, other than the broad outlines given above and in the following sections. These procedures are detailed in EPA Method 8330B (USEPA 2006).

10.3.1 Phase I Study

The Phase I study was designed to determine if multiple increments are necessary to build a subsample from a properly ground sample. Three samples were collected at Fort Lewis, WA—two from firing points and one from an urban breaching training range. Concentrations of propellant residues at the firing points were known to be high ($>500 \mu\text{g/g}$) from previous analyses (Jenkins et al. 2007). The two air-dried firing point samples weighed 1128 and 338 g. The air-dried urban breaching range sample weighed 1330 g. The two samples with a mass over 1000 g were ground with the puck mill in multiple lifts (batches), the smaller sample in one batch. The ground soil from each batch for each sample was combined in a bag and then evenly spread over a piece of aluminum foil (Fig. 10-1a) before subsampling. Two sets of seven subsamples were collected from each ground sample, one set containing single grab samples of 10-g each and the other set containing subsamples consisting of 30 increments collected randomly throughout the original sample (Table 10-1). All subsamples were analyzed according to Method 8330B.

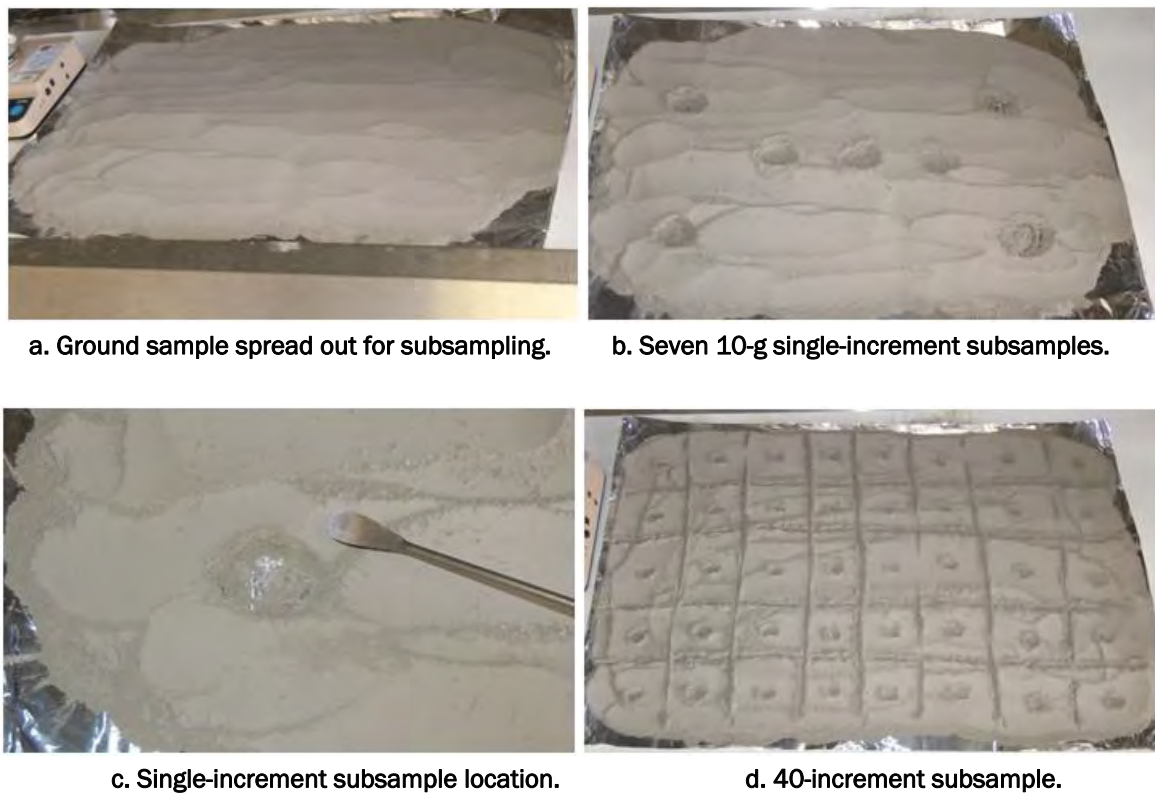


Figure 10-1. Subsampling of a ground large sample.

Table 10-1. Sample and subsample data for Phase I study.

Sample number and range type	Previous results	Sample mass (g)	Subsampling method	Number of subsamples	Increments per subsample	Subsample mass (g)
17: LAW/AT4 Firing Point	NG 728 µg/g	1128	Grab	7	1	10
			Multi-increment	7	30	10
35: Urban Breaching Range.	HMX 11.4 µg/g	1330	Grab	7	1	10
			Multi-increment	7	30	10
46: Small Caliber Firing Point	NG 522 µg/g	338	Grab	7	1	10
			Multi-increment	7	30	10

10.3.2 Phase II study

For the Phase II study, ground samples that were known to have low quantities of propellants or explosives were chosen from the soil archives at CRREL to determine the number of increments required to build a subsample for samples containing low analyte concentrations. The two samples chosen were originally obtained from a firing point (Lampkin Range,

Donnelly Training Area [DTA], Fort Wainwright, AK) and a site where 120-mm high-explosive mortar projectiles detonated low-order (LO2 on the Eagle River Flats impact range, Fort Richardson, AK). The samples, both ground on a ring and puck mill according to EPA Method 8330B, were collected in July 2009 and May 2010, respectively. The DTA sample was analyzed for the propellant compounds DNT and NG, and the LO2 sample analyzed for the explosive compounds HMX and RDX. Each sample was subsampled seven times with 1, 5, 10, 20, and 40 increments collected to build each subsample (Fig. 10-1 and Table 10-2). Method 8330B was used for both sets of analyses.

Table 10-2. Sample and subsample data for Phase II study.

Sample number and range	Previous results	Sample mass (g)	Sub-sampling method	Number of subsamples	Increments per subsample	Subsample mass (g)
09 DTA 34 FP Lampkin	2,4-DNT 0.5 µg/g NG 13 µg/g	1125	Grab	7	1	10
			Multi-increment	7	5, 10, 20, 40	10
10 FRA 61 ERF LO2	HMX 0.6 µg/g RDX 1.7 µg/g	2150	Grab	7	1	10
			Multi-increment	7	5, 10, 20, 40	10

10.4 Results

10.4.1 Phase I study

The results of the Phase I study are presented in Tables 10-3 through 10-6. Tables 10-3 and 10-4 contain the results for the large (>1 kg) firing point and urban training range samples, along with their duplicate and triplicate subsample worst-case analyses. Tables 10-5 and 10-6 contain the results for the small (<0.5 kg) firing point sample, and the worst-case analyses for duplicate and triplicate subsamples. For the worst case analyses, we used the extreme values of the analyte concentrations for statistical analyses of the results that would be derived if only two or three replicate subsamples were taken from the original sample mass. This would be the more typical practice in an analytical lab. Comparing these values to the average values of the seven subsamples will give one an indication of how close to the bulk averages these two forms of replicate subsampling will be. Note that

the ranges for the seven subsamples, the duplicate scenarios, and the triplicate scenarios are all the same.

Table 10-3. Results for Phase I study: large (>1 kg) firing point sample.

Analyte: NG ($\mu\text{g/g}$)				Worst-case analyses		
Increments:	One	Thirty	Means		One	Thirty
Sample FL17	740	740		Duplicates		
Aug-06	700	730		Range	150	90
Wt: 1128 g	800	760		Mean	720	750
Grind:	700	800		RPD	21%	12%
	660	740		Triplicates		
Multiple bowls	650	710		Range	150	90
	730	740		Mean	750	760
Max : Min	800 : 650	800 : 710		Std deviation	84	47
Mean	710	750	730	%RSD	11	6.2
Std Deviation	51	28	43			
%RSD	7.2	3.8	6.0			
Variance	2300	800				
Student's <i>t</i>	1.7					

Table 10-4. Results for Phase I study: large (>1 kg) urban range sample.

Analyte: HMX ($\mu\text{g/g}$)				Worst-case Analyses		
Increments:	One	Thirty	Means		One	Thirty
Sample 35	11.9	11.6		Duplicates		
Aug-06	11.4	11.6		Range	1.0	1.0
Wt 1330 g	11.3	11.5		Mean	12	12
Grind:	11.5	11.4		RPD	8.7	8.7
	10.5	11.5		Triplicates		
Multiple bowls	10.8	11.9		Range	1.0	1.0
	11.2	11.5		Mean	11	12
Max : Min	12 : 11	12 : 11		Std Deviation	0.58	0.58
Mean	11	12	12	%RSD	5.1	4.9
Std Deviation	0.45	0.18	0.51			
%RSD	4.0	1.3	4.4			
Variance	0.21	0.03				
Student's <i>t</i>	1.7					

Table 10-5. Results for Phase I study: small (<0.5 kg) firing point sample.

Description	Concentration ($\mu\text{g/g}$)					
	One Increment		Thirty Increments		Means	
	NG	DNT	NG	DNT	NG	DNT
Sample 46 Aug-06 Wt: 338 g Grind:	530	5.0	530	5.0		
	560	5.3	540	5.0		
	520	5.0	520	4.9		
	530	4.9	520	4.9		
	500	4.8	530	5.0		
Single bowl	530	5.1	540	5.0		
	530	4.9	540	5.0		
Max : Min	560 : 520	5.3 : 4.8	540 : 520	5.0 : 4.9		
Mean ¹	530	5.0	530	5.0		
Std Deviation	18	0.15	9.0	0.049	14	0.11
%RSD	3.3	3.1	1.7	0.98	2.6	2.2
Variance	310	0.027	81	0.0024		
¹ Comparison of the mean concentrations estimated from seven replicates of single and 30-increment subsamples yielded Student t-values of 0.38 and 0.44 for NG and 2,4-DNT, respectively.						

Table 10-6. Results for Phase II study: worst-case analyses for the small firing point sample.

Study Case	Triplicates		RPD (%)	Duplicates	
	NG	DNT		NG	DNT
One Increment	530	5.0		530	5.0
Mean ($\mu\text{g/g}$)	31	0.25		—	—
Std Deviation ($\mu\text{g/g}$)	5.8	5.0	11	9.6	
RSD (%)	530	2,4-DNT		NG	2,4-DNT
Thirty Increments	530	5.00		530	5.0
Mean ($\mu\text{g/g}$)	12	0.064		—	—
Std Deviation ($\mu\text{g/g}$)	2.2	1.3	RPD (%)	3.8	2.4
RSD (%)					

The percent relative standard deviations (RSDs) are all below 8% for the seven-replicate subsamples. This low RSD indicates a well ground sample with near-uniform dispersion of the explosives or propellants within the soil matrix. However, when the variances were compared using an F -test, significant differences were found for HMX and 2,4-DNT, where the 30-increment subsamples yielded lower variances. Both HMX and 2,4-DNT were present at much lower concentrations than NG, for which the va-

riances were not different. The mean concentration estimates obtained from each pair of seven subsamples were compared using a Student's *t*-test (using equal or unequal variances where appropriate) and no significant differences were found between the means obtained from single increment 10-g subsamples and 30-increment 10-g subsamples.

The analysis of seven replicate subsamples is not a common practice in analytical labs. Rather, duplicate subsamples may be taken and sometimes triplicates. The relative percent differences (RPDs) for the duplicate worst-case subsample pairs are 12% or below in all but one case (21%), averaging 13% for the single-increment subsamples and 6.7% for the 30-increment pairs. The average RPD for all six cases is 9.7%. The RSDs for the triplicate worst-case groupings are very low, averaging 5.2%, with average values of 6.7% for the single-increment subsamples and 3.7% for the 30-increment subsamples. This worst-case analysis indicates that a triplicate subsample will give a truer indication of the concentration of the sample than a duplicate subsample.

10.4.2 Phase II Study

The results of the Phase II study are presented in Tables 10-7 through 10-10. Tables 10-7 and 10-8 contain the results for the firing point and impact point samples. Two analytes were examined for each: DNT and NG for the firing point and HMX and RDX for the impact point. Analyte concentrations are an order of magnitude less than for the previous study. Tables 10-9 and 10-10 contain the worst-case replicate analyses for this study. The method for choosing the duplicate and triplicate worst cases are the same as in the Phase I study. The low concentrations in the gross sample are reflected in higher average RPDs and RSDs in the replicate subsamples.

The RSDs for the two sets of analyses (Tables 10-7 and 10-8) are generally quite close for all five subsample increment tests. The RSDs for the Phase II study are higher than those of the Phase I studies. They average over 12% compared to an average RSD of 5.2% for the higher-concentration samples in the Phase I study. The single-increment (grab) subsample results are a bit misleading as three of the seven subsamples were co-located (Fig. 10-1b). However, the five-increment subsamples generally have low RSDs as well.

Table 10-7. Results for Phase II study: firing point—low concentration sample.

	Analyte: 2,4-DNT ($\mu\text{g/g}$)					
Increments	One	Five	Ten	Twenty	Forty	Means
Sample 09DTA34 Jul-09	0.43	0.24	0.24	0.41	0.29	
	0.36	0.34	0.53	0.50	0.45	
	0.40	0.41	0.34	0.34	0.36	
	0.41	0.30	0.31	0.24	0.38	
Wt: 1125 g	0.39	0.36	0.50	0.37	0.34	
	0.34	0.27	0.38	0.28	0.34	
	0.40	0.35	0.40	0.36	0.37	
Max : Min	0.43 : 0.36	0.41 : 0.24	0.53 : 0.24	0.50 : 0.24	0.45 : 0.29	0.46 : 0.27
Mean	0.39	0.32	0.39	0.36	0.36	0.36
Std Deviation	0.031	0.058	0.10	0.085	0.049	0.070
%RSD	7.9	18	26	24	14	19
1-Way ANOVA						$F^1 = 0.99$
	Analyte: NG ($\mu\text{g/g}$)					
Increments	One	Five	Ten	Twenty	Forty	Means
Sample 09DTA34 Jul-09	11	11	11	11	10	
	12	11	11	11	11	
	11	12	11	11	12	
	11	11	11	10	11	
Wt: 1125 g	12	12	11	11	10	
	11	12	10	11	11	
	11	11	12	12	11	
Max : Min	12 : 11	12 : 11	12 : 10	12 : 10	12 : 10	12 : 10
Mean	11	11	11	11	11	11
Std Deviation	0.49	0.53	0.58	0.58	0.69	0.58
%RSD	4.5	4.8	5.3	5.3	6.3	5.3
1-Way ANOVA						$F = 1.3$

Table 10-8. Results for Phase II study: impact point—worst-case analyses for the low-concentration samples.

Increments:	Analyte: 2,4-DNT ($\mu\text{g/g}$)					
	One	Five	Ten	Twenty	Forty	Means
<i>Duplicates</i>						
Range	0.09	0.17	0.29	0.26	0.16	0.19
Mean	0.39	0.33	0.39	0.37	0.37	0.37
%RPD	23	52	74	70	43	52
<i>Triplicates</i>						
Range	0.09	0.17	0.29	0.26	0.16	0.19
Mean	0.38	0.31	0.42	0.34	0.36	0.36
Std Deviation	0.047	0.091	0.16	0.14	0.082	0.10
%RSD	12	29	38	41	23	29
Analyte: NG ($\mu\text{g/g}$)						
Increments:	One	Five	Ten	Twenty	Forty	Means
<i>Duplicates</i>						
Range	1.0	1.0	2.0	2.0	2.0	1.6
Mean	12	12	11	11	11	11
%RPD	8	8	18	18	18	14
<i>Triplicates</i>						
Range	1.0	1.0	2.0	2.0	2.0	1.6
Mean	11	11	11	11	11	11
Std Deviation	0.58	0.58	1.0	1.0	1.0	0.83
%RSD	5.3	5.3	9.1	9.1	9.1	8

The means of the concentration values for each analyte were compared using ANOVA; the calculated *F* values were all below the critical *F* (*p*=0.05); thus, the means were not significantly different. These results indicate that after grinding and recombining the ground soil, the analytes are widely dispersed in the soil matrix.

Table 10-9. Results for Phase II study: firing point—worst-case analyses for the low-concentration samples.

Increments:	Analyte: HMX ($\mu\text{g/g}$)					
	One	Five	Ten	Twenty	Forty	Means
<i>Duplicates</i>						
Range	0.15	0.25	0.13	0.15	0.25	0.19
Mean	0.43	0.51	0.41	0.40	0.48	0.45
%RPD	35	49	32	38	52	41
<i>Triplicates</i>						
Range	0.15	0.25	0.13	0.15	0.25	0.19
Mean	0.44	0.48	0.43	0.37	0.45	0.43
Std Deviation	0.081	0.13	0.075	0.087	0.13	0.10
%RSD	18	27	17	24	29	23
Analyte: RDX ($\mu\text{g/g}$)						
Increments:	One	Five	Ten	Twenty	Forty	Means
<i>Duplicates</i>						
Range	0.40	0.40	0.60	0.40	0.30	0.42
Mean	1.9	1.8	1.9	1.9	1.8	1.9
%RPD	21	22	32	21	17	23
<i>Triplicates</i>						
Range	0.40	0.40	0.60	0.40	0.30	0.42
Mean	1.8	1.8	2.0	1.8	1.8	1.8
Std Deviation	0.231	0.21	0.32	0.23	0.21	0.24
%RSD	13	12	16	13	12	13

The worst-case scenarios for the two sets of analyses (Tables 10-9 and 10-10) are much more descriptive of the difference between duplicate and triplicate subsampling than in the Phase I study. RPDs are high, averaging 33%, higher than the 30% value generally considered acceptable. For the lowest-concentration analytes (<1.0 $\mu\text{g/g}$), the average RPD is 39%. The triplicate RSDs are significantly lower, averaging 18%, with lowest-concentration RSDs averaging an acceptable 22%. RPDs were only consistently acceptable if the sample concentration was greater than 1.0 $\mu\text{g/g}$.

Only two RSDs exceeded 30%. The triplicate RSDs are consistently around half the duplicate RPDs, but the mean replicate concentrations are very close to the grand mean concentrations for the samples. Although RPDs and RSDs cannot be directly compared, they indicate the precision of the

methods in this application and point to the use of triplicate subsamples rather than duplicates. There is little difference between the explosives and the propellants results, indicating that both samples had been well ground and the analytes similarly dispersed throughout the soil matrixes.

10.5 Discussion

The proper subsampling of a field sample is a critical element in obtaining valid data for the characterization of an area for energetic compounds. Previous research demonstrated that the heterogeneous, dispersed nature of the contaminant of training ranges requires the proper grinding of the sample prior to subsampling for analysis. Replicate concentration estimates obtained by subsampling of unground samples were not reproducible, could range in value from below the reporting limit to several hundred parts per million, and typically underestimated the concentration in the bulk sample. By contrast, the replication among the MI subsamples of ground samples had a 1:1 correlation with the bulk sample extract analyses, which is an indication of the importance of both the MI subsampling protocol and the proper grinding of the sample prior to subsampling (Hewitt et al. 2009).

The Phase I study answers the question of whether MI sampling is necessary to build a subsample. The variances for the 30-increment subsamples were for the most part not significantly different from those of the single grab subsamples, nor were the mean concentrations significantly different. These results may be attributable to the compositing effect of the grab samples, returning a result similar to a multi-increment sample ($n=7$). The big difference occurs in the replicate subsamples, where the triplicate MI samples average 3.7% RSD, while the duplicate MI samples have an average RPD of 6.7% and the duplicate grab subsamples have an average RPD of 13%. The MI subsampling method is clearly the correct choice for this procedure, and if it is applicable for the replicate subsamples it must be used for the normal subsamples.

The Phase II study returned what are perhaps the most interesting results. Low concentrations are always problematic when sampling and analyzing for constituents that are very heterogeneously distributed. It is more difficult to overcome GSE and FE when a large (>1 kg) sample must be collected to ensure that a widely dispersed compound is recovered. Detection limits are approached and great care must be taken to properly grind the

sample without volatilizing the analytes. The very close RSD values for all five cases may indicate a well-ground sample, although the higher RSDs for the Phase I study than for the previous study also indicate a uniform dispersion of the compounds in the soil matrix. In the end, the number of increments needed to build a subsample was not clearly demonstrated in our study. The results for the worst-case duplicate and triplicate replicate subsampling follow these trends, with no one number of increments standing out as the best and no trends obvious. Co-locating three of the seven grab samples returned deceptively low RSDs for that case, which is what we were looking for when we designed that test. As in the Phase I study, triplicates are shown to be superior to duplicates when doing replicate subsampling of the bulk sample.

10.6 Conclusions

Error abounds in every step of the soil characterization process. From the choice of the decision unit size to the interpretation of the analytical chemistry results, the goal is to minimize that error to return the best possible results that are practically achievable. The possibility of introducing unnecessary error should be eliminated from every step in the process. This includes the subsampling of a sample. It is a rare occasion when a sampler or a lab tech has a solid indication of what the analyte concentrations or heterogeneity will be in the field or the sample. It is thus prudent to sub-sample with an eye towards the most consistent results. This study proves that multi-increment subsampling of a properly ground sample is the best approach for reducing subsampling error. It also shows that replicate subsampling should be done in triplicate rather than duplicate to return average results that are the best estimate of the true sample mean.

11 Report Summary

Michael R. Walsh

11.1 Introduction

This report documents the collective work for the final year of SERDP ER-1481. The previous 10 chapters cover much ground, from propellant residues resulting from live-fire training to disposal of propellants and the consequences of low-order detonations and unexploded ordnance on an active range. Although this project's main objective was to study the sources, deposition, accumulation, fate, and transport on military training ranges, these are not the only factors contributing to the environmental impact of training on military ranges. That is why we included the measurement of explosives residues from blow-in-place operations, explosives residues fate and transport at low-order sites, and the impact on unexploded ordnance from a detonating round. It is essential that all military activities be considered when determining the environmental impact of training on ranges.

This chapter summarizes the previous 10 chapters to give the reader a quick overview of our last year's research. It is organized in the order of the tasks originally outlined in the project's Scope of Work. The following chapter will tie this research with that covered in the interim report (Walsh, M.R., et al. 2010b) and with the work conducted under SERDP CP-11-55 and ER-1155. Taken together, these projects have given the sponsor and the wider range community a tremendous amount of information on the long- and short-term environmental impacts of training on military ranges.

11.2 Characterization of residues deposition and accumulation

11.2.1 Deposition rate studies

Two studies on firing point deposition rates were completed over this period. The first study was of residues from the firing of two types of 40-mm grenades from a grenade machine gun, the first look we have had at residues from a medium-caliber (12.7- to 60-mm) weapon system. Two muni-

tions were fired, each with a different propellant. The second study examined firing point residues from triple-base propellants. These rounds, 155-mm artillery high-explosive (HE) rounds, utilize a bagged charge system that can be customized on-site to fit the distance the projectile is to be fired by varying the number of bags used. Three charge loads were tested, with samples collected by two methods before firing and after each test.

11.2.1.1 Propellant residues deposition from firing of 40-mm grenades

The 40-mm firing point test proved to be more of a challenge than anticipated. Originally, we thought both types of rounds, a training-practice (TP) round and an HE round, utilized the same M2 double-base propellant ($19.5 \pm 1.0\%$ nitroglycerin [NG]). The TP rounds were fired first, followed the next day by the HE rounds at an adjacent location. When the samples were processed, it was obvious we were working with two different propellants as there was much more residue from the TP rounds than the HE rounds. We calculated that 420 mg/round of propellant was deposited in the first 5 m in front of the gun firing the HE rounds whereas 710 mg/round was deposited in an equivalent area in front of the gun firing the TP rounds. Analysis of the samples also indicated a wide difference between the two propellants, although in the opposite direction. The TP residues averaged an estimated 2.1 mg NG per round while the HE residues averaged an estimated 76 mg/round. Through additional research, we found that the TP rounds utilized an NG-impregnated nitrocellulose (NC)-based propellant designated F15080 that contains 9.1% NG, whereas M2 propellant contains 19% NG embedded in the NC matrix. The NG in the residues was calculated to be a rather high 8.4% of the original NG load for the HE rounds and a more moderate 0.59% for the NG-impregnated TP rounds. Over 90% of the residues were recovered in the first 5 m in front of both guns, with over 99.5% in the first 10 m. The implications are that both munitions will cause a dangerous accumulation of unburned propellant if fired from a fixed position or a vehicle mount, with the M2 propellant residues containing a large amount of NG.

11.2.1.2 Study of the propellant residues emitted by triple base ammunition live firing using a British 155-mm howitzer gun at CFB Suffield, Canada

The triple-base propellant tests were very interesting because this is the first research we know of on firing point residues from this type of propellant (NC, NG, and nitroguanadine [NQ]). Three charge loads were utilized in the following order: charge 5 (660 g NG / 1940 g NQ)—30 rounds,

charge 3 (260 g NG / 760 g NQ)—30 rounds, and charge 8 (2280 g NG / 6700 g NQ)—19 rounds. A breach explosion on the 155-mm self-propelled howitzer prevented the firing of the planned 20th charge 8 round. Tests were conducted in summer, and both soil and particle trap (tray) samples were taken. Background soil samples prior to our research did not contain detectable levels of the two analytes. None of the soil samples collected by either the Canadian or U.S. researchers following the three firing sequences contained detectable levels of the analytes. Tray samples contained very low masses of propellants. Analysis of the samples indicates that deposition rates for both NG and NQ are around 10⁻⁵%, with NQ percentages slightly higher than NG percentages. Differences in deposition rates are small and likely not significant between the different charges. Cross-contamination from soil kicked up by the muzzle blast may have influenced our results as the muzzle blast was quite violent at the higher charge levels. Overall, the residues rates were as expected based on past experience with artillery: 10⁻² for 105-mm howitzers, 10⁻³ for a 105-mm-gunned tank, and 10⁻⁴ for a 155-mm howitzer. The 39-cal. 155-mm self-propelled howitzer firing triple-base propellant is the cleanest-firing weapon system we have tested.

11.2.2 Fate and behavior of energetic material residues in the unsaturated zone: sand columns and dissolution tests

Three sets of large-diameter sand columns (60-cm ø × 60-cm high) were constructed to determine the fate and transport of firing point residues, impact point residues, and propellant burn site residues through soil. The top 1.5 cm of one of the sets of columns contained soil and residues from the anti-tank impact area (analytes trinitrotoluene [TNT] and HMX), one set of columns was topped with 1 cm of soil from an artillery firing position (analyte dinitrotoluene [DNT]), and the third set of columns had single-base propellant residue (analyte DNT) from a winter burning test spread on the sand on top of the column. The columns were set up in a controlled-temperature room and subjected to accelerated temperature and rainfall regimes that mimicked those found in the areas where the test material was obtained. Seven seasons were simulated over an 11-month period, starting with spring and ending with autumn. Tracers were used to determine hydraulic velocity in the column. Velocities were monitored with time-domain reflectometry probes and effluent was collected from the bottom of the columns through seven ports with wicks.

The artillery firing point propellants released a high dose of analyte (DNT) early in the process but rapidly stabilized, as expected. The insoluble NC matrix retains all but the readily available surface DNT on the particles. The run was thus terminated after 1 year's simulation. By contrast, the analytes in the explosives residues at the rocket impact point readily leached into the soil column, with TNT spiking the first spring before dropping to non-detectable levels in the effluent and the HMX attaining a plateau and continuing through to the end of the test. The implication is that the residues will continue leaching HMX past the period simulated in these tests. Less than 2% of the analytes had been recovered by the end of the tests. The propellant burn residues behaved similarly to the firing point propellant residues, with the exception that there was a decline in the leachate concentrations after the first spring rather than an abrupt drop to non-detectable levels. Although the reason for this difference in behavior is not known, it is postulated that the mass and shape of the particles may be the cause. At the end of the second simulated spring, only 3% of the original mass of DNT in the residues had been recovered in the effluent. The burn and impact point columns are still active at the time of this writing, supported by other funding sources. The firing point column tests are under evaluation and have not been restarted.

A parallel water drop dissolution study similar to that conducted by Taylor et al. (2009) was conducted using energetics residues from the three sites where the column residues were obtained. A fourth test was done using Comp B particles. The purposes of the study were to better define the energetic compound input to the columns from the simulated precipitation and to determine if a correlation between controlled drip tests and the column effluent data can be made. Water drop tests results suggest that the residence time of applied water in contact with the particles, the duration of the test, the compositional heterogeneity of the formulations, and the specific surface area of the compounds are the principal parameters that control energetics dissolution. At this time, the correlation between the two studies is not strong, but work has begun on a new study that will reduce the differences in physical attributes between the column and dissolution studies.

11.3 Characterization and optimization of open burning of excess propellants: Fixed and mobile burn pans

Disposal of excess propellant can take place either at the training site or at a central location. Each requires a different type of structure for optimum

use. At a central location, where very large (>500 kg) quantities of propellant must be burned, a large, rugged, permanent structure is needed. In the field, excess propellant generated during training exercises will be much less, and the burn structure needs to be portable so it can go where the troops train. Both systems are needed, so Canadian and U.S. researchers divided up the work, the Canadians developing a static burn pan and the Americans a portable burn pan.

The Canadian design is the product of several iterations. At present, it is constructed of aluminum and measures $3 \times 5 \times 0.1$ m. Removable perforated stainless steel shields are assembled along the sides of the pan after the propellant is loaded. Up to 370 kg of propellant has been burned in the fixed pan without any warping of the pan and little warping of the shields. Temperatures of the burn flames reached 650°C; the metal of the table did not exceed 100°C where the thermocouples were located. Residues ejected from the table during the burn were less than 0.01% of the total burned propellant mass. A standard operating procedure has been written for the use of the fixed burn structure and the system is now to be used at all Canadian central disposal facilities.

The U.S. design is not as complete as the Canadian design. An all-stainless mobile pan with a solid-sided bonnet was built and tested in Canada. The unit weighed a hefty 240 kg, but was movable by four personnel. The greatest propellant load burned during the tests was 120 kg. Temperatures of the metal parts of the pan did not exceed 130°C, and the ejected mass of propellant was estimated to be <0.01% of the total burned mass. The U.S. table will be modified using design and performance lessons learned from the tests and incorporating suggestions from the Canadians. The goal is to get the weight down to around 100 kg without sacrificing performance.

In all tests, significant quantities of lead particles were found both within and outside of the pans following burns. These particles as well as lead nanoparticles that may be lofted during disposal may constitute an immediate and long-term health hazard. This issue will need to be addressed by modifying either the burn protocols or the pan designs. Although the lead residues contamination will be higher at fixed burn locations, it should be addressed for both burn procedures.

11.4 Simulation of live-fire breaching of UXO

11.4.1 A simple device for initiating high-order detonations

Simulating a high-order detonation of a high explosive projectile is necessary to conduct research on the performance of munitions without actually firing them. For the close-proximity detonation tests to be carried out for SERDP ER-1481, it was critical to be able to detonate a round high-order to enable realistic research into the blast effects on a proximate unexploded round (UXO). A device was designed that can be substituted for a live fuze that contains the same mass of booster charge as a fuze and can be initiated with a standard military blasting cap. The initiation device was tested with a cap and booster load and performed as expected. The 81-mm HE mortar projectiles were then assembled with the initiation devices and detonated separately on snow. The residues surrounding the detonation points were sampled to determine if the rounds detonated high-order. Residues analysis yielded a deposition rate of <0.0018% on average for the three rounds, which is comparable to the residues rate previously found for live-fired, high-ordered 81-mm HE rounds, 0.0014%, and an order of magnitude lower than for similar rounds blown in place with an external donor charge, 0.014% (Hewitt et al. 2005; Walsh, M.R., 2007). The device worked well and was utilized for the close-proximity detonation tests.

11.4.2 Characteristics of the physical damage to UXO from a close-proximity high-order detonation

A series of 11 tests was conducted to determine the damage caused to an unexploded round (UXO) by a fully functioning round detonating high-order and in close-proximity. M374 high-explosive mortar rounds were used as both the detonating and “UXO” rounds. The detonating rounds were armed with the initiator device described above. The UXO had nose plugs installed to fully enclose the explosive load and were placed at pre-determined distances and orientations from the detonating round. All tests were conducted on a packed, clean snow surface. Following detonation of the armed round, the UXO remains were collected and measured. We observed a variety of damage to the UXO rounds, from shallow surface dings, pierced casings, and partial detonations to low-order and high-order detonations.

There was much variability in the fragmentation damage to the UXO. Arena tests carried out using mortar projectiles similar to the 81-mm

rounds used in these tests show that detonating rounds produce thousands of fragments, some up to 13 g in mass, and demonstrate that fragmentation of the round is a process with high intrinsic variability. The tests we conducted show that the pattern of damage is unique for each of the rounds even if the exact same setup was used. For tests where the detonating round is almost vertical, simulating a fired incoming round, exposure of the energetic material inside the “UXO” casing occurred for distances up to 1.2 m. When the detonating round was laid on the snow parallel to the “UXO,” the damage was more severe. Of the four replicates, one was breached, one detonated high-order, the third partially detonated, and the fourth was not recovered. Prior tests by Lewis et al. (2009) indicated that partial detonation occurred at distances below 0.15 m, whereas we had a partial detonation at 0.6 m. The difference is caused in part by the different detonation initiation methods, an external donor charge of an unfuzed round in Lewis’ case versus a functioning fuzed round in our tests. Of 23 UXO utilized in our tests, four had surface damage only (17%), 16 received damage extensive enough to expose the filler (70%), one detonated high-order (4%), and two were not recovered (8%). These tests indicate that a round detonating in close-proximity (<1.3 m) to a UXO is much more likely to breach the UXO and expose the explosive filler through physical damage or detonation of the UXO than previously hypothesized.

11.4.3 Particle mass distribution of high explosives from sympathetic partial detonations

The largest sources for explosives compounds contamination on impact areas are low-order detonations and UXO. Surface UXO are exposed to frag and shock from rounds detonating in close-proximity to them. We carried out a series of controlled close-proximity detonations with simulated UXO in various configurations to determine the damage to the rounds and the distribution of high explosives (HE) from breached, partially detonated, and low-ordered rounds. The explosives debris from four of the rounds with well-defined debris plumes were examined for this study with the objective of characterizing the particles in relation to previous research on blast-damaged munitions and the dissolution of HE particles.

The Comp B HE filler of the 81-mm rounds used in these tests fragmented into smaller particles with narrower mass distributions than partial detonations of Tritonal- or TNT-filled munitions. Distribution of energetics varied according to the reaction of the UXOs to the detonation, with pierced

rounds not disgorging any HE and cracked rounds spilling small amounts of filler locally. Partial detonations scattered particles over varying distances, depending on the severity of the reaction. The debris field from a partial detonation measured 25 × 50 m, with chunks as large as 20 g found up to 75 m away and the carcass of the body containing remnants of the filler found 150 m away. One round's low-order detonation scattered mostly small (<1 g) particles over an area of about 10 × 20 m. The majority of particles measured for the five detonation events studied measured 0.1 to 1.0 g. Previous research by Taylor et al. (2009, 2010) indicates that small particles of Comp B explosives quickly weather, dissolving out the TNT matrix during precipitation events, and leaving the small RDX crystals to slowly dissolve and percolate into the vadose zone.

11.5 Explosives residues deposition rates: Sampling for Comp B residues using shallow wells at two low-order detonation sites

Low-order detonations are the greatest source of readily available energetics residues on impact ranges. When a round detonates low-order, the projectile body splits open during detonation and unconsumed HE filler is ejected over an area that can be hundreds of square meters. Particles from microscopic to centimeter size are exposed to weathering, with the result that explosive compounds leach from the debris into the ground. This research looked into the groundwater impacts from two 120-mm HE low-order events on the Eagle River Flats impact range on Fort Richardson, AK.

Three small groundwater monitoring wells were installed at each of two low-order impact sites. The wells were sampled twice in 2009 and 2010 using 2-in HYDRASleeve™ water samplers. Groundwater levels were monitored with a 1.4-m deep piezometer sensor in a separate, nearby instrumented well. Only two energetics analytes were detected in the wells, RDX and HMX, both components of the common explosive munitions filler Comp B. Of the six wells, only one, located near the crater of one of the detonations, consistently contained explosives compounds. The results obtained for the water samples from the shallow wells in this salt marsh impact area are consistent with the known fate processes for energetics in anaerobic sediment. Even though copious amounts of Comp B were scattered on the surface sediment, Comp B residues were generally not detectable in the groundwater. The concentrations of RDX and HMX were low, and TNT, 2-Am-DNT, nor 4-Am-DNT were not detected, indicating that these compounds are not persisting in the subsurface pore water. The

anaerobic and iron-rich sediments of a salt marsh impact area provide an ideal in-situ environment for reductive transformation of these compounds and decrease the likelihood of groundwater contamination.

11.6 Dissemination, promotion, and demonstration of the multi-increment sampling strategy and EPA Method 8330B: Subsampling of soils containing energetics residues

The collection of representative soil samples in the field is critical to obtaining valid data when characterizing a site contaminated with energetics. These compounds are generally found on military training ranges as widely dispersed particles. Samples collected at these sites should closely resemble the characteristics of the site, with the compounds heterogeneously distributed within the sample. Proper preparation of the samples prior to sampling is critical to reduce subsampling error prior to analysis (Walsh, M.E. et al. 2002, 2007a; Hewitt et al. 2009). The purpose of this study was to determine the number of increments necessary to build a 10-g subsample that will properly represent the field sample.

The study was conducted in two phases. In the first phase, we examined if multiple increments were required to obtain a representative subsample of a soil samples containing moderate to high levels of energetics residues (propellants or explosives). Seven replicates of 1- and 30-increment subsamples were collected and analyzed. Statistical analyses indicated no statistical difference between the two subsampling methods. When collecting replicate samples, the data indicated that triplicate multiple increment subsamples are much more representative of the ground sample than duplicate grab samples ($RSD=3.7\%$ vs. $RPD=13\%$). Both numbers are acceptable for this well-ground and well-mixed sample.

The phase two study examined subsampling of soils with very low concentrations of energetics. Five tests were performed on each of two samples, one containing propellant residues, the other explosives residues. Again, the samples were well ground and well mixed. The number of increments taken for each of seven replicates varied from 1 to 40: 1, 5, 10, 20, and 40. As with the higher-concentration study, there was no clear trend or indication of how many increments are needed to build a representative subsample. However, once again, when doing replicate subsampling, we found that triplicate subsamples are much more representative of the sample than duplicates.

Our recommendation is that when doing replicate sampling, triplicate samples should be built from at least 20 increments. As replicates are taken at the same time as other subsamples, all subsamples should be taken using multiple increments. Because not all soil samples containing energetics will be as well ground and mixed as the ones used for our study, we advise taking multi-increment subsamples to reduce the potential of error in this step of the characterization process. This work will be presented to a NATO committee on the fate and transport of energetics on military ranges as part of the promulgation of EPA Method 8330B (USEPA 2006).

12 Project Summary

Michael R. Walsh

12.1 Introduction

This is the final report for the extension of SERDP project ER-1481, *Characterization and Fate of Gun and Rocket Propellant Residues on Testing and Training Ranges*. However, the research described in this and the interim report (Walsh, M.R., et al. 2010b) does not stand alone. It is a continuation of research conducted under SERDP and ESTCP that dates back to 2000, with SERDP CP-1155, *Distribution and Fate of Energetics on DoD Test and Training Ranges*. As we have moved forward, we have also moved backward, working our way from the impact point of high-explosive munitions to firing positions. This series of projects and this project in particular has required that we not only be flexible in our research, but that we keep an open eye (and an open mind) towards all range activities so that we can increase our knowledge of what are the important inputs for a comprehensive assessment of the impacts of training activities on ranges.

In this project summary, the environmental impacts of training with different weapon systems will be summarized and the implications of the results discussed. Some weapon systems will have more information than others, depending on their configuration or our ability to conduct research on different aspects of the training on these systems. For instance, small arms do not have detonating projectiles, so impact points were not investigated for these weapon systems. Unexploded 40-mm munitions are extremely dangerous, so we were unable to look into explosives residues for this weapon system. And the impact points for GMLRS rockets are many tens of kilometers away from the launch point, making access to these areas difficult.

In total and taken with previous research, a tremendous amount of very useful information has been generated by these projects over the last 11 years. This brief summary of significant findings wraps up this report. Suggested future research topics follow.

12.2 Research Summaries

12.2.1 Small arms

There are many ways to define small arms. For the purpose of this summary, we will use man-portable weapon systems that are 12.7 mm and below and that fire non-dudding munitions. Small arms thus cover such common weapon systems as pistols, rifles, and machine guns. As small arms projectiles are generally non-detonating, we looked only at firing points. And as munitions for these weapon systems are sealed cartridges, no research was done on propellant disposal. Both the Canadians and the U.S. conducted research on a wide range of weapons, from 5.56 to 12.7 mm. Both deposition and characterization research was conducted.

12.2.1.1 Deposition rates

Deposition rates for the various caliber arms are given in Table 12-1. It is interesting to note that the larger caliber weapon systems tend to be cleaner firing, and that shorter-barreled weapons tend to have higher deposition rates. Propellants work best under higher pressures and temperatures and over a longer confined period. Thus, a 155-mm howitzer will deposit less mass of residues per round than a 9-mm pistol, even though the howitzer may use almost 10,000 times as much propellant. Most residues from the U.S. tests were deposited within 20 m of the firing position, with the larger caliber weapon residues extending furthest. The exception is the 9-mm pistol. The short barrel of the pistol limits the gas pressure, thus propelling the residues a shorter distance than a higher barrel pressure system.

Constituents of interest for small arms, which utilize double-base propellants, are primarily nitroglycerin (NG) and 2,4-dinitrotoluene (DNT). Although nitrocellulose (NC) is the primary constituent to these and most other propellants, it is not a constituent of concern as it is not soluble and thus very persistent in the environment (Taylor et al. in prep), although this has implications as well as we will see later with the 40-mm and shoulder-fired rocket weapon systems. For small arms, NG is the primary energetic compound of concern as DNT is used in small quantities as a plasticizer or is present as an artifact from reworked propellant.

Another important factor to consider is that most training with small arms takes place on qualifying ranges. These ranges are heavily utilized and have fixed firing positions. This will result in high concentrations of ener-

getics residues near the firing position. Counteracting this is the regular maintenance conducted at most small arms firing ranges. The soils are regularly graded to remove vegetation and even out the topography of the firing lanes. This not only mixes the residues into the soils, diluting their concentration, it creates new surfaces on the residue particles, enabling renewed leaching of NG and DNT from the residues to groundwater.

Table 12-1. Small arms weapon systems firing points: propellant residues deposition rates.

Weapon system / ammunition type	Analyte	Initial NG mass in propellant load (mg/round)	Recovered NG residue mass (mg/round)	NG mass recovered/initial mass	Distance from firing position (m) ²	Reference report
9-mm Pistol						
Ball	NG	40	2.1	5.3%	10 / 4.5	Walsh, M.R., et al. 2007a
Ball		53	0.74	1.4%		Jenkins et al. 2008
Ball		52	2.9	3.9%		Jenkins et al. 2008
5.56 Rifle						
Ball	NG	190	1.8	0.95%	10 / 8.6	Walsh, M.R., et al. 2007a
Ball		170	1.1	0.62%		Jenkins et al. 2008
Ball		160	0.3	0.19%		Jenkins et al. 2008
Ball		170	0.07	0.04%		Jenkins et al. 2008
Blank		40	0.02	0.05%		Jenkins et al. 2008
Blank		40	0.02	0.06%		Jenkins et al. 2008
5.56-mm MG¹						
Ball	NG	180	1.3	0.71%	20 / 13	Walsh, M.R. et al. 2007a
Ball		170	0.05	0.03%		Jenkins et al. 2008
Blank		76	0.01	0.01%		Jenkins et al. 2008
.338-cal Rifle						
Ball	NG	170	0.03	0.002%		Jenkins et al. 2008
7.62-mm MG						
Ball	NG	267	1.5	0.56%	10 / 9.2	Walsh, M.R., et al. 2007a
	DNT	4	0.0018	0.048%		Walsh, M.R., et al. 2007a
Ball	NG	230*	0.98	0.43%		Jenkins et al. 2008
12.7-mm Rifle						
Ball	NG	1,400	0.27	0.02%		Jenkins et al. 2008
12.7-mm MG						
Ball	NG	1,500	11	0.73%	40 / 20	Walsh, M.R., et al. 2007a
Ball		1,300	0.25	0.02%		Jenkins et al. 2008

¹ Specification mass value used rather than experimental mass.

² Distance downrange residues were detected / Distance downrange over which >99% of residues were recovered.

Residues from the small arms propellants used by the U.S. team in this research were examined by Taylor (in Jenkins et al. 2008). The NG in the residues collected after firing contained less NG than the original propellant grains. These values are 74% for the 9-mm test residues, 71% for the 5.56-mm residues, 39% for the 7.62-mm residues, and 62% for the 12.7-mm residues. Particle size, surface volatilization of the analyte, and leaching losses from processing likely affect the analyte concentration of the residues. Airborne particles, examined by Faucher (in Jenkins et al. 2008), were composed mostly of lead and copper.

12.2.1.2 Characterization

Small arms firing points have been characterized by several researchers for both ESTCP and SERDP. For this project, most of the work occurred prior to the ER-1481 extension and is reported in Jenkins et al. (2007, 2008). Concentrations of NG ranged from less than 0.02 mg/kg to over 500 mg/kg. Table 12-2 summarizes this research.

Table 12-2. Small arms weapon systems firing points: propellant residues soil concentrations.

Range type	Location	Number of ranges	Concentration range (mg/kg)		Average high concentration of NG (mg/kg)
			2,4-DNT	NG	
Pistol	U.S.	1	<0.4	80–120	120
	Canada	3	<0.04–0.13	<0.1–40	28
Rifle	U.S.	3	<0.01–4.0	<0.02–500	200
	Canada	7	<0.05–2.2	<0.05–110	42
Machine Gun	U.S.	5	<0.01–17	0.24–580	200
	Canada	1	<0.05–0.1	1.0–7.4	7.4
Mounted Arms	U.S.	1	<0.01	0.07–2.0	2.0

Groundwater contamination at small arms ranges is an obvious concern. Accumulation of energetics residues at these heavily used, fixed firing position sites. Martel (in Jenkins et al. 2008) examined groundwater below a heavily used small arms range at the firing positions. The maximum soil concentration for NG at this 105-year-old site was 70 mg/kg. No NG was detected in the groundwater. However, his team did detect perchlorates in the groundwater (0.12 µg/L) from what they suspect were flares and simulators used during training. The absence of NG in the groundwater is not because of the absence of NG in the soils. Rather, the NC matrix of the

propellants is inhibiting the leaching of the NG from the residues, resulting in the presence of NG in the soil that can be released if the soils and residues are worked. NG transformation also occurs as the compound is transported through the soil column, attenuating the concentration of the NG before reaching groundwater.

12.2.2 Medium caliber weapon system

Only one medium caliber weapon system was tested, the 40-mm grenade machine gun (Walsh, M.R., et al. 2010c). Two types of munitions were fired: a training-practice cartridge that contained F15080 propellant and a high explosive (HE) cartridge that contained M2 propellant. Sampling down-range was prohibited because of the danger from the very sensitive 40-mm HE unexploded ordnance (UXO) on the snow-covered range. The munitions are not designed for variable propellant loads so no propellant was available for expedient burn tests.

The results from these tests are very interesting in that, although both propellants are double base, the results are quite different (Table 12-3). The F15080 propellant has the NG impregnated on the surfaces of the propellant grains whereas the M2 propellant has it diffused throughout the NC matrix of the grain, as is typical of most double base propellants. In addition, the propellant mass was weighed on the filters from the samples taken in the decision unit 0 to 5 m in front of the gun emplacement. The F15080 test yielded 12.5 mg/round, whereas the M2 test yielded 5.3 mg/round. Although the mass of propellant residues per round recovered for the TP rounds (7.9 mg/round) was about twice as high as for the HE rounds (4.5 mg/round), the analyte recovery rate was less than 10%. The surface deposition of the NG on the F15080 grains results in the more efficient consumption of the analyte but results in the reduced burn of the underlying NC matrix, which does not contain the more reactive NG.

Table 12-3. Medium Caliber weapon systems firing points: propellant residues deposition rates (Walsh, M.R., et al. 2010c).

Weapon system / ammunition type	Analyte	Initial NG mass in propellant load (mg/round)	Recovered NG residue mass (mg/round)	NG mass recovered/initial mass	Distance from firing position (m) ¹
40-mm MG					
Training/Practice	NG	370	2.2	0.59%	11.5 / 9
High Explosive	NG	900	76	8.4%	13.5 / 10

¹ Distance downrange residues were detected / Distance downrange over which >99% of residues were recovered.

12.2.3 Mortars and howitzers

Mortars and howitzers are artillery weapon systems that fire projectiles that have a variable propellant load. The munitions are issued with propellant charges that can be broken down into smaller charges designed to propel the projectile over a fixed range of distances. Excess propellant charges are typically disposed of at the firing point. With the mortars and howitzers, we were able to do a full suite of deposition studies, from propellant burns to blow-in-place disposal of UXO.

Howitzers differ from mortars in that they have a relatively long rifled barrel. Thus, they should consume the propellant charges more efficiently. The number of charges should also affect efficiency, but we were not able to fully test this theory. Howitzer propellant is generally single base, with 2,4-DNT the constituent of concern. However, recent propellant formulations are triple base, with NC, NG, and nitroguanadine (NQ) as the primary constituents. Mortar propellants can be either single or double base.

12.2.3.1 Propellant disposal

When troops train with artillery in the U.S. and Canada, the excess propellant is often burned on-site following the cessation of firing. This entails piling (mortar) or lining up (howitzer) the charges and igniting them, allowing them to burn down. Observations of several expedient field burns led us to hypothesize that these burns, especially smaller burns on wet soils or snow, may leave behind substantial residues. Small-scale tests with mortar propellants on snow in the U.S. and large burns of howitzer propellants on snow in Canada indicated that this was the case. Controlled studies in the U.S. using mortar propellant on snow, frozen ground, and a small pan were conducted as well as a test using howitzer propellant on dry and wet soil to determine the effect various environmental conditions have on burning efficiency (Walsh, M.R., et al. 2010a). Table 12-4 shows the results.

The results from these tests indicate that environmental factors will greatly affect the efficiency of an expedient propellant burn. This is especially true in winter. The one test in a burn pan demonstrates that burning within an open device will greatly enhance the efficiency of the burn. We, therefore, determined that the most effective way to reduce propellant residues from excess propellant disposal was to provide units and facilities with dedicated devices to burn propellants.

Table 12-4. Expedient propellant disposal: environmental influence tests.

Propellant type/ environmental condition	Analyte	Initial mass in propellant load (mg/round)	Recovered residue mass (mg/round)	Mass recovered/ initial mass (%)	Reference report
Double base (Mortar)	Snow surface	NG	5,300	870	1.7
	Pan on snow	NG	130,000	720	0.21
	Frozen ground*	NG	140,000	7,300	5.2
	Snow surface	NG	140,000	25,000	18
Single base (Howitzer)	Dry sand	DNT	330,000	3,000	0.94
	Wet sand	DNT	330,000	3,100	0.99
Triple base (Howitzer)	Dry sand - Charge 4	NG	660,000	16	0.002
		NQ	1,900,000	200	0.01
	Dry sand - Charge 7	NG	1,100,000	8.0	0.0007
		NQ	3,300,000	63	0.002

Excess propellants are burned in two general locations: at the training site (firing positions) and in a central disposal location. These two locations deal with different quantities: the site burns with propellants generated from a training mission and the central location with much larger accumulated quantities. Central locations will thus need a large structure capable of burning hundreds of kilograms of propellants at a time. This structure can be fixed or moveable by heavy equipment. The device for unit training locations must be small enough to be moved by hand but capable of burning up to 100 kg of excess propellant charges. These two devices will share some characteristics but will be of different design. The Canadians agreed to work on the larger structure while the U.S. concentrated on a mobile burn pan.

The Canadians developed a series of burn tables to test materials and design efficiencies. The final design, capable of burning over 350 kg of propellant at a time with less than a half hour cycle time, consists of an elevated aluminum table measuring 3- × 1.5- × 0.1-m high with 1-m-high removable, perforated stainless steel screens (0.635-cm \varnothing / 58% open area) surrounding the table. A static discharge device, which connects the loader's wrist to the table via a wire, an ignition channel, and an aluminum cover are part of the design. Testing demonstrated that the screens were necessary, reducing the ejected propellant from 0.1% of the pre-burn mass

to about 0.001%. The Canadian burn table has been integrated into their armed forces, with a standard operating procedure written for its use.

The development of the mobile burn pan by the U.S. has lagged a bit behind the Canadian efforts. We have taken advantage of this by integrating the Canadians' lessons learned into the mobile pan design. An all-stainless prototype was built and tested in Canada burning single base propellant. Up to 120 kg of propellant was burned in a shot, with a total of about 340 kg burned over the course of four tests. About 0.01% of the original mass of DNT was recovered outside the pan following the burn. A second prototype pan, incorporating the stainless steel screens and an aluminum pan, was built and tested in Alaska in 2011. A single burn of 65 kg of single base propellant was burned at a firing point following an artillery exercise. Preliminary results indicate that the DNT residues recovered from outside the pan totaled approximately 0.02%. The new design weighs 127 kg, about half the original design. We would like to get the final weight below 100 kg.

One interesting offshoot of this work occurred when the Canadians discovered furans and dioxins at their field burn sites. As a result of discussions among team members, the ignition source for the burns was examined. The standard procedure was to ignite the propellant with a highway flare, which contains perchlorates. Investigations by Poulin et al. (in Walsh, M.R., et al. 2010b) revealed that the flares were responsible for the deposition of these highly toxic compounds. The procedure has since been changed.

12.2.3.2 Firing point deposition

Firing point deposition tests were conducted for a full range of weapons systems. Three mortars and three howitzers were tested. All three types of propellants were utilized during these tests, including the first tests ever conducted with triple base propellants.

Table 12-5 depicts the results from our research. As could be anticipated, the larger caliber systems with their longer rifled barrels had significantly lower deposition rates than for the mortars. The results for the 60-mm mortar are misleading as only the ignition cartridge, integral with the tail of the round, was utilized during our tests. It is interesting to note that neither NG nor NQ residues were detected in the soil in front of the 155-mm self-propelled howitzer prior to and following the firing of the 79 rounds

for our triple-base propellant tests. Both the 155-mm howitzers were 39-caliber gun systems, so their results can be better compared to each other.

Table 12-5. Artillery systems firing points: propellant residues deposition rates.

Weapon system / caliber	Analyte	Initial mass in propellant load (mg/round)	Recovered residue mass (mg/round)	Residue recovered/ initial mass (%)	Distance from Firing Position (m) ³	Reference Report
Mortar						
60-mm ¹	NG	1,350	0.088	0.007	10 / 10	Walsh, M.R., et al. 2006b
81-mm	NG	30,000	1,000	3.5	50 / 15	Walsh, M.R., et al. 2006b
120-mm	NG	26,000	350	1.4	- / 15	Walsh, M.R., et al. 2005b
Howitzer						
105-mm	DNT	42,000	34	0.08	30 / 25	Walsh, M.E., et al. 2004
105-mm ²	DNT	Varied	190	0.2–0.4	-	Jenkins et al. 2008
155-mm	DNT	275,000	1.2	5×10 ⁻⁴	30 / 30	Walsh, M.R., et al. 2005b
155-mm	NG	Varied	≈ 0.08 (Avg)	0.6–4 × 10 ⁻⁵	10 / 5	Ampleman et al. 2010
	NQ	Varied	≈ 0.5 (Avg)	0.6–3 × 10 ⁻⁵	15 / 5	

1 Ignition cartridge only (firing at Charge 0).
 2 Rounds fired from an enclosed muffler using charge 4 and charge 6.
 3 Distance downrange residues were detected / Distance downrange over which >99% of residues were recovered.

12.2.3.3 Impact point deposition

Impact point deposition tests were conducted for the previous SERDP projects but are presented here as they are directly related to the research conducted for the ER-1481 extension. The same weapon systems tested for firing point energetics deposition (with the exception of the triple-base howitzer tests) were utilized for this series of tests. Most munitions contained the explosive filler Composition B (Comp B), which is composed of 60% RDX and 39% trinitrotoluene (TNT). TNT degrades rapidly in the environment so RDX and its related explosive compound HMX (up to 9% of RDX) were the analytes of interest. Detonation plumes for at least seven rounds for each weapon system were sampled and analyzed. Table 12-6 depicts the results. Once again, with the exception of the 60-mm mortar projectiles, the larger weapon systems tend to be cleaner than the smaller. The howitzer munitions are also much more efficient than the mortar munitions.

Table 12-6. Artillery systems impact points: high explosives residues deposition rates (Hewitt et al. 2005; Walsh, M.R., 2007).

Weapon system / caliber	Analyte	Initial mass in explosive load (mg/round)	Recovered Residue Mass (mg/round)	Residue recovered/initial mass (%)
Mortar				
60-mm	RDX	230,000	0.073	3.2×10^{-5}
81-mm	RDX	600,000	8.5	1.4×10^{-3}
120-mm	RDX	1,800,000	1.9	1.1×10^{-3}
Howitzer				
105-mm	RDX	1,300,000	0.095	7.3×10^{-6}
155-mm	RDX	4,200,000	0.30	7.1×10^{-6}
	TNT	6,600,000	<0.001	-

12.2.3.4 Low-order detonations

When fired into an impact area, a fuzed round can react in several ways upon impact. The most common is a high-order detonation, in which the round functions properly and >99.99% of the filler is consumed in the detonation. The rounds tested in the previous section all detonated high-order. Other end states are dudded rounds, sometimes called UXO, partially detonating rounds, where only the fuze and a small amount of filler function, and low-order detonations.

Low-order detonations occur when a fuzed round is fired into an impact area and the round functions incompletely. For this report, a low-order detonation occurs when the fuze functions on impact and most but not all of the HE filler is consumed in the ensuing detonation. The body of the round fragments and scatters, with some larger sections of the body remaining intact. Chunks of the filler scatter around the point of detonation. Low-order detonations can be the greatest source of HE contamination on a range.

A series of low-order detonation sites were investigated by CRREL under separate funding, with leverage provided by this SERDP project. Degradation of the Comp B HE chunks and particles at three low-order detonation sites were monitored over a 4-year period (Walsh, M.E., et al. 2010).

Smaller particles quickly degraded in the hydrologically active environment, where flooding brackish-water tides, rains, and snowmelt all contributed to the process. Larger chunks disaggregated, accelerating the disso-

lution process. The TNT component quickly photodegraded, adding to the disaggregation process. Little HE was detected in overland flow, so soil and groundwater concentrations were investigated.

Two soil profile samples were taken to analyze for soil concentrations of RDX, TNT, and HMX. One, taken below a 2.8 g chunk that was removed, was cored to a depth of 32 cm. RDX concentrations fell rapidly to about 1% of the surface levels (670 mg/kg) at 6–8 cm and then leveled off through the remainder of the soil column, averaging around 5 mg/kg. TNT concentration fell from 360 to 2 mg/kg in the first 2 cm, slowly decreasing after that with depth. HMX behaved as did RDX, with a drop from 79 mg/kg at the surface to 0.44 mg/kg at 6–8 cm, then leveling off at about 0.7 mg/kg through the remainder of the profile. The presence of energetics compounds at depth led us to hypothesize that contaminants were transported along the coring barrel, affecting concentrations.

The second profile was taken adjacent to a disaggregating Comp B chunk using a 40-cm deep pit rather than a corer to try to minimize cross contamination. Surface concentrations were 1300, 540, and 170 mg/kg for RDX, TNT, and HMX respectively. Again, the concentrations of the three compounds dropped to 1% at the 6-cm level. At the 20-cm level, no residues were detected. For both cases, the bulk of the residues was detected in the first 4 cm, tapering off quickly with depth. To determine if the contaminants were reaching groundwater, we needed to install monitoring wells.

In 2009, a piezometer well for monitoring groundwater levels and six groundwater monitoring wells at two low-order sites were installed to investigate energetics migration to groundwater. Only RDX and HMX were detected in the wells, and only one well contained consistent detectable quantities of these compounds. This well was located adjacent to a heavily contaminated (>100 g Comp B) detonation crater. Transformation processes reduced the TNT and the anoxic, iron-rich environment at the impact area reduced RDX to compounds such as ammonia and nitrous oxide. Only very small concentrations of RDX (<5 µg/L) and HMX (<1 µg/L) were detected in the wells.

This study demonstrated that, in the right environment, explosives compounds will degrade and transform through natural processes. Penetration into the soil column will occur, but there will be a rapid decrease in concentration with depth. Penetration to groundwater will also occur, but the

deeper the groundwater is the less likely concentrations of concern will be reached. Fate and transport in other environments will differ, and care must be taken to characterize any site accurately before making any predictions of these processes.

12.2.3.5 Blow-in-place operations

As stated above, not all rounds fired into an impact area detonate. There is a safety factor built into the arming of the fuzes of projectiles to reduce the probability of accidental initiation, and this results in a percentage of the rounds not functioning as designed. The result is dudded rounds, known as UXO.

UXO are the largest point source of legacy energetics contamination on impact ranges. A 155-mm HE projectile will hold 6.6 kg of TNT. Air force bombs can hold over 4.5 metric tons of explosive. This ordnance not only presents an environmental hazard but also poses a safety hazard to operations on a range. Thus, reported UXO are periodically blown in place to clear a range.

UXO clearance operations take on two forms: render safe and disposal. Render safe operations usually are used where a detonation is inappropriate, such as near populated areas or sensitive instrumentation. The ordnance is destroyed using shaped charges that destroy the ordnance body but do not effectively detonate the explosive filler, resulting in much contamination. The operation typically results in a breached round or a partial detonation of the round, similar to the low-order detonation described above but with much more residue. The second type of operation, disposal, requires an external donor charge, typically a block of C4 explosive. The detonation of the donor charge sends a shock wave into the UXO, setting off the filler. The round detonates, usually high-order, with little residues.

Blow-in-place (BIP) disposal of munitions research was conducted on three mortar cartridges and three howitzer projectiles. Seven rounds of each type of munition were detonated using a single block of C4 (520 g RDX) taped axially to the side of the body of the round. All rounds were fuzed. Results for these tests as well as for unconfined detonation of several C4 blocks are given in Table 12-7.

The larger rounds once again proved more efficient in the consumption of the high explosives. The donor charge adds a substantial amount of HE to most of the munitions tested, and as it is unconfined, it does not detonate as efficiently, adding to the residues from the operation. Adding a second donor charge or conducting the operation with an unfuzed round added to the residues, although orienting the round vertical rather than horizontal decreased the residues mass (Walsh, M.R. et al. 2006a,b).

Table 12-7. Artillery systems UXO BIP tests: High explosives residues deposition rates.

Weapon system / caliber	Analyte	Initial mass in explosive load (mg/round) ¹	Recovered residue mass (mg/round)	Residue recovered/initial mass (%)	Reference
Mortar					
60-mm	RDX	230,000	180	3×10^{-2}	Walsh, M.R., et al. 2008
	HMX ²		22		
81-mm	RDX	600,000	130	1×10^{-2}	Walsh, M.R., et al. 2007a
	HMX		23		
120-mm	RDX	1,800,000	22	1×10^{-3}	Walsh, M.R., et al. 2008
	HMX		3.0		
Howitzer					
105-mm	RDX	1,300,000	41	3×10^{-3}	Walsh, M.R., et al. 2007a
	HMX		8.7		
155-mm (TNT)	RDX	21,000	5.0	9×10^{-5}	Walsh, M.R., et al. 2007a
	HMX		0.21		
155-mm (Comp B)	RDX	4,200,000	15	3×10^{-4}	Walsh, M.R., et al. 2007a
	HMX		1.0		
Donor Charge					
M118 (C4)	RDX	520,000	12	4×10^{-3}	Walsh, M.R. et al., 2007a
	HMX		7		

1 520 g of RDX/HMX will be added to the tested mass with the application of the donor charge.
2 HMX is a manufacturing by-product of RDX and may constitute up to 9% of the RDX mass.

12.2.3.6 Close-proximity detonations

Close-proximity detonations occur when an incoming round detonates close to an unexploded ordnance item in the impact area. UXO can accumulate in great numbers near targets on impact areas, increasing the probability of a close-proximity detonation. UXO also contain the largest source of potential energetics contaminants on a range. No research had been previously done on the effects of a close-proximity detonation on a

UXO. Therefore, we proposed studying these effects in a controlled manner by detonating 81-mm HE projectiles in close-proximity to ordnance placed near the detonating round.

Work done by Lewis (2007) on leaching of explosives from breached ordnance indicated that unfuzed UXO will partially detonate only when in close-proximity (<0.5 m) to an unfuzed round detonated with a donor charge. We postulated that a round detonating in a manner for which it was designed, from the fuze end of a complete round, would give more realistic results than were observed during Lewis' test. The proximate rounds would also have to have the fuze well plugged to better simulate an impact range UXO. An initiation device was designed and tested that successfully initiated a high-order detonation in the mortar cartridge. Rounds armed with this device were then detonated among unarmed rounds placed at fixed distances and orientations to the detonating round. Damage to the UXO was cataloged and, where possible, the mass and distribution of residues ejected from the damaged rounds recorded.

Table 12-8 contains the damage assessment for each of the proximate rounds involved in the tests. Categorizing the damage is difficult, as the terminology is not well defined and the assessment is open to interpretation. In this summary, we will use the following categories and definitions:

- High-order detonation: Fully detonating round with total fragmentation of the projectile body and >99.99% consumption of HE filler.
- Low-order detonation—functioning round: Round functions inefficiently. Body fragments (frag) with some large pieces that may have HE adhesion. Most HE filler (>75%) consumed.
- Low-order detonation—UXO: Same as above except initiation comes from shock or frag penetration or impact from a close-proximity detonation.
- Partial detonation—functioning round: Detonation of only a small amount of HE at the nose of the round with partial fragmentation of the projectile body.
- Partial detonation—UXO: Same as above but the detonation can occur anywhere along the round from frag penetration.
- Breached or pierced round: Damage to the body of the UXO from frag that penetrates the round.

When a UXO is damaged, the HE filler becomes available to the environment. Partial detonations were found to generate the largest mass of external particles, with breached rounds spilling small amounts. Low-order detonations also were responsible for scattering HE debris, with some HE still adhered to large segments of fragmented body sections and at the base near the tail assembly. This distribution pattern has been observed in the field with 120-mm HE mortar projectile low-order detonations.

Table 12-8. Close-proximity detonation tests: damage assessment.

Test round	Detonation configuration	UXO distance from detonation (cm)	Damage assessment
1	Vertical	50	Pierced—Two locations
2	Vertical	50	Dings
3a	Vertical	50	Pierced—Two locations. Partial detonation at nose
3b	Vertical	50	Deep dings
4a	Vertical	30	Round not recovered
4b	Vertical	30	Partial detonation approaching Low-order detonation
5a	Vertical	50	Pierced – One location
5b	Vertical	50	Deep dings
6a	Vertical	50	Pierced—One location
6b	Vertical	50	Pierced—One location
7a	Vertical	50	Pierced—One location. Partial detonation
7b	Vertical	50	Low-order detonation
8a	Vertical	50	Low-order detonation
8b	Vertical	50	Partial detonation
9a	Horizontal	50	Partial detonation
9b	Horizontal	50	Round not recovered
10a	Horizontal	50	Low-order detonation
10b	Horizontal	50	High-order detonation
11a	Vertical	40	Low-order detonation
11b	Vertical	60	Partial to low-order detonation*
11c	Vertical	80	Shallow dings
11d	Vertical	100	Pierced—One location
11e	Vertical	120	Pierced—One location
* Section of body near tail badly distorted, but intact			

Table 12-9 tabulates the recovered HE from each of the tests. Not all HE was collected from each detonation as it was difficult to find the smaller particles on the roughened snow surface. It is difficult to make a correlation between largest particle size and total ejected mass with the type of detonation because the damage to the partially damaged round will vary. Much of the HE filler may remain internal to the carcass of the round, but this material is now exposed to the environment and disaggregation and dissolution will commence. Where an intact UXO is a latent point source, a breached round becomes an active point source.

Table 12-9. Close-proximity detonation tests: mass of high-explosive debris collected outside damaged rounds.

Test round	Detonation type	Largest chunk (g)	Total mass collected (g)	Debris area (m ²)
4b	Partial	9.3	221	600
8a	Low-order	3.1	26	Not measured
8b	Partial	3.6	22	2
9a	Partial	1.6	12	Not measured
10a	Low-order	11.7	60	140

12.2.4 Tanks

Tanks are direct-fire weapon systems that utilize cartridge-type munitions. There is no adjustment that can be made to the propellant load. The most common type of munition used in modern tank warfare is the penetrating round, essentially a very strong, dense bullet with no HE component. The muzzle blast from a tank is tremendous, making sampling a firing position almost impossible in the summer and difficult on snow-covered ground. One successful firing point sampling exercise was conducted in Canada with a 105-mm rifled cannon equipped heavy tank firing practice munitions utilizing single-base propellant (Ampleman et al. 2009b). No impact point samples were obtained.

Firing point samples were collected following two protocols: weighted particle traps distributed in rows in front of the firing position and post-firing snow samples collected from areas demarcated based on visual residues densities. The muzzle blast caused problems for both methods. Several particle traps were displaced downrange but none were overturned. Snow kicked up by the muzzle blast was deposited in the nearer traps. The final location of the traps was used in calculating the residues mass for the rows

they were nearest, and the snow in the traps was collected and the residues contained therein counted towards the trap total. Snow samples containing residues were taken in parallel with the particle trap collections. Samples were taken in accordance with the protocol established by Walsh, M.R., et al. (2007b). The main residues plume downrange was visually demarcated and a triplicate multi-increment surface sample taken to a depth of 2.5 cm. A subsurface sample composed of increments taken from the middle of the surface increment locations was collected in the highly disturbed main plume area. A 3-m annulus surrounding the lateral sides outside of the main plume (OTP) and a down slope area and OTP were also taken to determine if the site was correctly characterized. The results (Table 12-10) show very close agreement between the two methods, especially considering the violence of the muzzle blast. Extrapolating the subsurface residues for the snow samples to a depth of 75 cm will result in a deposition rate that matches that of the particle traps.

Table 12-10. Tank firing point test: DNT mass deposition.

Unit	Area (m ²)	Analyte	Initial mass in propellant load (mg/round)	Recovered residue mass (mg/round)	Residue recovered/initial mass (%)	Percent of total recovered mass
Particle Traps						
Main plume (Traps)	930	2,4-DNT	710	7.9	0.0026	100
Snow Sampling						
Main plume - Surface	430	2,4-DNT	390	4.3	0.0014	65
		2,6-DNT	4.1	0.05	2×10 ⁻⁵	
Main plume - Subsurface	430	2,4-DNT	160	1.8	6×10 ⁻⁴	27
		2,6-DNT	1.8	0.02	1×10 ⁻⁵	
Main plume - OTP	170	2,4-DNT	9.1	0.1	3×10 ⁻⁵	1.5
		2,6-DNT	ND ¹	-	-	
Down slope plume	490	2,4-DNT	36	0.4	1×10 ⁻⁴	6.1
		2,6-DNT	0.28	0.003	1×10 ⁻⁶	
Down slope - OTP	210	2,4-DNT	1.0	0.01	3×10 ⁻⁶	0.2
		2,6-DNT	ND	-	-	
Total - Snow samples	1,300	Both	610	6.8	0.0023	100

12.2.5 Rockets

Two types of rockets were studied for this project, the large guided rockets that are launched from a dedicated vehicle and those that are man-portable. For this project, we concentrated on the portable weapon systems. Testing of these systems was much easier to coordinate and more practical from a funding standpoint. They are also much more commonly used in training.

12.2.5.1 Deposition rates

Deposition rate studies were conducted on three shoulder-fired rocket systems. In Canada, the 84-mm Carl Gustav and M72 66-mm systems were tested (Thiboutot et al. 2007b). In the U.S., the 84-mm AT4 rocket was tested. Samples were collected in particle traps in Canada and on snow in the U.S. Past characterizations of rocket ranges indicated that most of the residues are deposited behind the firing line. This was the area we concentrated on in our studies.

All three weapon systems utilized double-base propellant. Nitroglycerin is thus the analyte of concern. The M7 double-base propellant of the M72 rocket contains a small concentration (7.8%) of perchlorate. The AKB 204 propellant of the 84-mm rockets contains no perchlorate. Down-range impact areas were generally off limits and no substantive deposition studies were conducted at impact points. The results of our firing point deposition rate investigations are presented in Table 12-11.

It is interesting to note from these results the difference the propellant formulation makes in the consumption efficiency. The M7 propellant of the M72 LAW rocket contains perchlorate and burns two orders of magnitude cleaner than the AKB double-base propellants used with the 84-mm rockets. From these results, residues accumulation may be a problem at heavily used rocket ranges.

12.2.5.2 Characterization

Site characterizations conducted at several rocket ranges confirmed our concerns about residues accumulation at rocket ranges in the U.S. and Canada. Table 12-12 summarizes some of the results. The Petawawa ranges had been closed for over 25 years when they were characterized. The results signify the persistence and stability of the NC-based propellant

residues in the environment. The Ft. Richardson range firing position was not located where these weapons are normally fired. Thus, the results may be for just the six rockets fired in our tests.

Table 12-11. Shoulder-fired rockets firing points: propellant residues deposition rates.

Weapon system / caliber	Analyte	Initial mass in propellant load (mg/round)	Recovered residue mass (mg/round)	Residue recovered/initial mass (%)	>90% Residue deposition ¹	Reference
M72 LAW						
66-mm	NG	43,000	42	0.097	-10 m	Jenkins et al. 2007
M136 / AT4						
84-mm	NG	130,000	95,000	73	-18 m	Walsh, M.R., et al. 2009b
M3 / Carl Gustav						
84-mm	NG	140,000	20,000	14	-15 m	Thiboutot et al. 2007b

1 90% or more of total estimated analyte residues were recovered within this distance. Negative numbers indicate distance behind firing position.

Table 12-12. Shoulder-fired rockets firing points: firing point characterizations (NG and potassium perchlorate).

Range	Analyte	Surface soil		Soil profile		Groundwater concentration ($\mu\text{g/L}$)	Reference
		Maximum concentration (mg/kg)	>90% Range ¹	Maximum concentration (mg/kg)	>90% Range		
CFB Petawawa						Jenkins et al. 2008	
Alpha Range	NG	3100	-7.5 m	4500	20 cm	ND ²	
	KClO ₄	-	-	-	-	0.41	
Area 8	NG	2200	-10 m	-	-	ND	
	KClO ₄	-	-	-	-	0.46	
CFB Valcartier						Jenkins et al. 2008	
Carpiquet Range	NG	2700		4800	12 cm	ND	
CFB Gagetown						Jenkins et al. 2008	
Wellington Range	NG	5700					
CFB Wainwright							
AT Range	NG			70	60 cm		
Ft. Richardson						Walsh, M.R., et al. 2009b	
40-AT4 Range	NG	13	-30 m	-	-		

1 90% or more of total estimated analyte residues were recovered within this distance. Negative numbers indicate distance behind firing position. KClO₄ from single wells.

2 ND: Not detected (<3 $\mu\text{g/L}$)

12.2.5.3 Fate and transport

High depositional rates of propellant residues and the high concentrations of NG in the soils resulting from the firing of portable rockets indicated that rocket firing positions may be a significant source of contamination for groundwater. Dissolution tests similar to those conducted on explosives residues (Taylor et al. 2009) and large column physical model tests were thus conducted on residues and soils containing residues from shoulder-fired rocket firing positions.

Following firing point deposition tests conducted in March of 2011, propellant residues were allowed to weather naturally for 60 days, through a spring snowmelt and early summer rains. Two segments of propellant contained 66% of their original NG content when compared to six segments collected immediately after the firing exercise. Photomicrographs showed that the NG was leached from the edges, where the pieces were translucent compared to the central portions. Drip dissolution tests on rocket residues from CFB Gagetown by researchers at the University of Quebec, INRS-ETE, showed a 20% loss in NG mass, mostly during the first spring simulation. Both tests show a rapid leaching of a portion of the NG in the propellant. The INRS tests further indicated that the residues stabilized for at least 1.5 years following the initial leaching.

Column studies, also conducted by INRS, modeled leaching and percolation to groundwater of actual range residues through soils typical of the area, mostly coarse to fine sand (82–87% of mass, $D_{50}=0.38\text{--}0.28\text{ mm}$). The soil/residues samples were collected from behind firing lines at two Canadian bases. Two years of temperature and precipitation cycles were simulated. Effluent from the pre-wetted columns was collected from the base of the setup. NG and NG-related compounds spiked quickly, as was seen with the drip tests. After the first spring, the concentration of nitrates and nitrites rapidly fell, indicating both a slowdown in leaching and that its transport is not retarded. The NG transformed to DNGs and MNGs, decreasing the concentration and mass of NG reaching the base of the column. Recovery was around 23% of the original NG mass, similar to what was found with the naturally weathered propellants and the drip tests.

12.2.6 EPA 8330B Dissemination

Dissemination of EPA Method 8330B, *Nitroaromatics, nitramines, and nitrate esters by high performance liquid chromatography* (USEPA

2006) was added to the project by SERDP to promulgate the sample collection methods outlined in Appendix A of the method through outreach, demonstrations, and presentations (Hewitt et al. 2009). Alan Hewitt worked diligently on this segment of the project until his untimely death in January of 2010. Since then, we have continued his work through conference presentations, workshops, and participation in NATO technical groups. We have been able to leverage this effort with other projects and have also provided limited support to others, such as the Federal Facilities Forum and Envirostat, a company that provides courses on multi-increment sampling to industry and state and federal government agencies.

Work continues with the refinement of this method. Past research has demonstrated that grinding of soil samples is required to reduce the very large variance found when taking replicate laboratory subsmples of the sample (Walsh, M.E., et al. 2002, 2007a). We looked at the next step, developing a subsampling strategy for the ground soil samples. Ground samples containing moderate and low concentrations of either explosives or propellant residues were subsampled using a range of increments to build the subsample. Duplicate and replicate subsample worst case analyses were performed with the resulting data. We found that with well-ground soils containing energetics, there was no significant difference in results among subsamples built from 1, 5, 10, 20, and 40 increments. To better match the bulk concentration of the sample, replicate sampling is much better when done in triplicate than in duplicate. As samples are not always well ground prior to subsampling, we also recommend the subsample be built from at least 20 increments.

The strong resistance to the multi-increment sampling methodology and the sample preparation protocols developed by CRREL through the ESTCP and SERDP programs has attenuated as more and more entities are adopting the methods every day. We are now working with researchers from NATO countries to educate them on the strengths and capabilities of this important environmental sampling method.

12.3 Future work

SERDP Projects CP-1155, ER-1155, ER-1481, and the ER-1481 Extension have generated a tremendous amount of significant literature on the causes, impacts, fate, and transport of energetics residues on U.S. and Canadian military ranges. This information has filled many data gaps, provid-

ing the military with valuable information on the environmental impacts resulting from training with energetics. Not all weapon systems and munitions were tested, an impossibly large task and not necessarily a research function. We recommend that these tests be carried out by the ammunition and test communities.

New types of munitions are arriving to both the American and Canadian armed forces. Both green munitions and insensitive munitions have been developed and are being readied for introduction into the ammunition pipeline. These munitions are designed to have less of an impact on the environment and to be safer to transport, store, and use. The same data gaps exist for these new munitions as existed for the current standard munitions prior to our research. These data gaps should be addressed prior to full implementation of these munitions.

Our NATO work continues. Our Exploratory Team has been transitioned to a Research Technical Group, focusing on the fate and transport of energetics on military training lands. We will be holding workshops on preparation of soil samples containing energetics at our next meeting, followed by water sampling and analysis of samples for energetics. Our first workshop on sampling was very well received, and Envirostat will be conducting a 4-day workshop this summer in Europe.

We are still developing the mobile propellant burn pan for use by units training in the field. In March 2011, we tried a burn test using an updated, lighter weight burn pan with a field artillery unit in Alaska (Fig. 12–1). We will be discussing implementation of the pan with training units on ranges in Alaska with environmental and range officials from U.S. Army Alaska in April. This will be a great opportunity to get a trial unit into the system and determine how well it will work with field units.



Figure 12-1. Propellant burn test, FP Neibar, Ft. Richardson, AK, March 2011.

References

- Ampleman, G., S. Thiboutot, S. Désilets, A. Gagnon, and A. Marois. 2000. *Evaluation of the soils contamination by explosives at CFB Chilliwack and CFAD Rocky Point*. DREV Report TR-2000-103.
- Ampleman, G., S. Thiboutot, J. Lewis, A. Marois, A. Gagnon, M. Bouchard, R. Martel, R. Lefebvre, C. Gauthier, J.M. Ballard, T. Jenkins, T. Ranney, and J. Pennington. 2003. *Evaluation of the impacts of live-fire training at CFB Shilo (Final Report)*. DRDC Valcartier TR 2003-066.
- Ampleman, G., S. Thiboutot, J. Lewis, A. Marois, A. Gagnon, M. Bouchard, T.F. Jenkins, T.A. Ranney, and J.C. Pennington. 2004. *Evaluation of the contamination by explosives and metals in soils, vegetation, surface water and sediment at Cold Lake Air Weapons Range (CLAWR), Alberta, Phase II, Final report*. DRDC Valcartier TR 2004-204.
- Ampleman, G., S. Thiboutot, A. Marois, A. Gagnon, and D. Gilbert. 2007. *Evaluation of the propellant residues emitted during 105-mm Leopard tank live firing and sampling of demolition ranges at CFB Gagetown, Canada*. DRDC Valcartier TR 2007-515.
- Ampleman, G., S. Thiboutot, A. Marois, T. Gamache, I. Poulin, B. Quémérais, and L. Melanson. 2008. *Analysis of propellant residues emitted during 105-mm howitzer live firing at the muffler installation in Nicolet, Lac St-Pierre, Canada*. DRDC Valcartier TR 2007-514.
- Ampleman, G., S. Thiboutot, A. Marois, A. Gagnon, D. Gilbert, M.R. Walsh, M.E. Walsh, and P. Woods. 2009a. *Evaluation of the propellant residues emitted during 105-mm Leopard tank live firing at CFB Valcartier, Canada*. DRDC Valcartier TR 2009-420.
- Ampleman, G., S. Thiboutot, A. Marois, A. Gagnon, M.R. Walsh, and M.E. Walsh. 2009b. Study of the propellant residues deposited by the live firing of 105-mm Leopard tank. Poster: *SERDP & ESTCP's Partners in Environmental Technology Technical Symposium & Workshop, Washington DC, USA, 1–3 December 2009*.
- Ampleman, G., S. Thiboutot, A. Marois, and A. Gagnon. 2009c. *Surface soil characterization of explosives and metals at the Land Force Central Area Training Centre (LFCA TC) Meaford, Ontario (Phase II) Final report*. DRDC Valcartier TR 2009-218. Val-Bélair, QC: DRDC-Valcartier.
- Ampleman, G., S. Thiboutot, A. Marois, A. Gagnon, P. Woods, M.R. Walsh, M.E. Walsh, C.A. Ramsey, and P. Archambault. 2010. *Evaluation of the propellant residues emitted during the live firing of triple base ammunition using a British 155-mm howitzer gun at CFB Suffield, Canada*. DRDC Valcartier TR 2010-269. Val Belair, Quebec: Defence Research and Development, Canada.

- Ampleman, G., S. Thiboutot, A. Marois, A. Gagnon, P. Woods, M.R. Walsh, M.E Walsh, C.A. Ramsey, and P. Archambeault. In prep. *Study of the propellant residues emitted by triple-base ammunition live firing using British 155-mm Howitzer gun at CFB Suffield, Canada*. Defence Research and Development Canada (DRDC)-Valcartier.
- Bellavance-Godin, A. 2009. Devenir environnemental des résidus de propulsif aux positions de tir anti-char à travers la zone non saturée. M.Sc. mémoire, Université du Québec, INRS-Eau, Terre et Environnement.
- Bordeleau, B., R. Martel, G. Ampleman, and S. Thiboutot. 2008. Environmental impacts of training activities at an air weapons range. *Journal of Environmental Quality*, 37: 308–317.
- Bosch, L., and J. Perena. 1988. Deflagration to detonation transition of small arms propellants and nitroglycerine/solvent mixtures. In: *Proceedings of the 19th International Annual Conference of ICT, Paper 79*.
- Boulay, R.J. 2007. *ASSB engineering assessment 02-11 open burning of propellant design requirement for a propellant burning tray*. Report 1150-2-2 (DAVPM9). Ottawa, ON: Directorate Armoured Vehicle Project Management.
- Brochu, S., E. Diaz, S., Thiboutot, G. Ampleman, A. Marois, A. Gagnon, A.D. Hewitt, S.R. Bigl, M.E. Walsh, M.R. Walsh, K. Bjella, C. Ramsey, S. Taylor, H. Wingfors, U. Qvarfort, R.-M. Karlsson, M. Ahlberg, A. Creemers, and N. van Ham. 2008. *Environmental assessment of 100 years of military training at Canadian Force Base Petawawa. Phase 1—Study of the presence of munitions-related residues in soils and biomass of main ranges and training areas*. Technical Report DRDC TR 2008-118. Val-Bélair, QC: RDC-Valcartier.
- Brochu, S., I. Poulin, D. Faucher, E. Diaz, and M.R. Walsh. 2009. Environmental assessment of small arms live firing: Study of gaseous and particulate residues. *Poster presentation, 237th ACS National Meeting, Salt Lake City, UT. 22–26 March 2009*.
- Clausen, J., J. Robb, D. Curry, and N. Korte. 2004. A case study of contaminants on military ranges: Camp Edwards, Massachusetts, USA. *Environmental Pollution*, 129:13–21.
- Coburn, D.R., J.B. DeWitt, J.V. Derby, Jr., and E. Ediger. 1950. Phosphorus poisoning in waterfowl. *Journal of the American Pharmaceutical Association*, 39: 151–158.
- Department of National Defence Canada. 1974. Canadian Forces Technical Order, *Description and maintenance instruction, fusee, warning, railroad*. C-74-370-GAA/TA-000.
- Department of National Defence Canada. 2004. *Ammunition and explosives technical information: ammunition for 105 mm howitzer*. C-74-315-H00/TA-000.
- Department of National Defence Canada. 2005. *Ammunition and explosives procedural manual: Destruction of duds and misfired ammunition on CF ranges and training areas*. C-09-008-002/FP-000.

- Department of National Defence Canada. 2006. *Technical information. Ammunition and explosives: Ammunition for 155 mm howitzer.* C-74-320-BA0/TA-0.
- Diaz, E., S. Brochu, S. Thiboutot, G. Ampleman, A. Marois, and A. Gagnon. 2007. *Energetic materials and metals contamination at CFB/ASU Wainwright, Alberta. Phase I.* DRDC Valcartier TR 2007-385. Val-Bélair, QC: DRDC-Valcartier.
- Diaz, E., D. Gilbert, D. Faucher, A. Marois, and A. Gagnon. 2008. *Gun propellant residues dispersed from static artillery firings of LG1 Mark II and C3 105-mm howitzers.* Technical Report DRDC Valcartier TR 2007-282. Val-Bélair, QC: DRDC-Valcartier.
- Diaz, E., S. Brochu, I. Poulin, D. Faucher, A. Marois, A. Gagnon. In press. *Residual dinitrotoluenes from open burning of gun propellant.* Technical Report DRDC Valcartier (number pending). Val-Bélair, QC: Defence Research and Development Canada (DRDC)-Valcartier.
- Douglas, T.A., L. Johnson, M.E. Walsh, and C.M. Collins. 2009 A time series investigation of the stability of nitramine and nitroaromatic explosives in surface water samples at ambient temperature. *Chemosphere*, 76: 1–8.
- Dubé, P., S. Thiboutot, G. Ampleman, A. Marois, and M. Bouchard. 2006. *Preliminary assessment of the dispersion of propellant residues from the static live firing of 105-mm howitzer.* DRDC Valcartier TM 2005-284.
- Elmasri, B., H. Shimm, K. Moran, and B. Vogelsanger. 2008. Enhanced ammunition performance with ECL® technology. Presented at *43rd U.S. Department of Defense, Defense Technical Information Center, Annual Armament Systems Gun and Missile Systems Conference and Exhibition, New Orleans, LA, 21–24 April 2008.*
- ExproTech D&T Department. 2005. *Study on critical height properties of propellants.* Valleyfield, Canada.
- Fortier, C. 2007. Artillery/mortar lethality simulation with focus on safe distance estimation. *Presentation to RCAS Gagetown, 11 October 2007.*
- Fortier, C. 2009. Personal communication, January 2009, fragmentation tables from Robert Durocher (DRDC Valcartier).
- Gilman, H., and A.H. Blatt. 1941. Nitroguanidine and guanidine nitrate. In: *Organic Syntheses Collective.* Volume 1, pp. 399-400 and pp. 302-304.
- Goliger, J., and J.P. Lucotte. 1981. *Détonabilité des Poudres.* In Sciences et Techniques de l'Armement. Mémorial de l'Artillerie Francaise 1er fascicule.
- Grossman, R.B., and T.G. Reinsch. 2002. The solid phase. Bulk density and linear extensibility. In: *Methods of Soil Analysis. Part 4—Physical Methods* (J.H. Dane and G.C. Topp, eds.). Madison, WI: Soil Science Society of America, Inc., pp. 201–228.

- Haeselich, D., R. Kelly, and R.M.Miller. 2006. Results of investigations conducted to improve the insensitive munitions properties of the 40mm MK281 target practice cartridge. In *Proceedings of IMEMTS 2006, Bristol, UK. Report No. 210/15459/96.*
- Hewitt, A.D., T.F. Jenkins, T.A. Ranney, J.A. Stark, M.E. Walsh, S. Taylor, M.R. Walsh, D.J. Lambert, N.M. Perron, N.H. Collins, and R. Kern. 2003. *Estimates for explosives residues from the detonation of army munitions.* ERDC/ CRREL TR-03-16.
- Hewitt, A.D., T.F. Jenkins, M.E. Walsh, M.R. Walsh, and S. Taylor. 2005. RDX and TNT residues from live-fire and blow-in-place detonations. *Chemosphere*, 61: 888–894.
- Hewitt, A.D., T.F. Jenkins, and M.E. Walsh. 2009. *Validation of sampling protocol and the promulgation of method modifications for the characterization of energetic residues on military testing and training ranges.* ERDC/CRREL TR-09-6.
- Hooker, D.E., 1990. Modeling of compaction wave behavior. In *Confined granular energetic material.* Technical Report BRL-TR-3138. Aberdeen Proving Ground, MD: U.S. Army Ballistic Research Lab.
- http://www.sitecsrl.com/PagineRolledAlloys/ra310alloy_rolledalloys.htm
- IARC. 1997. International Agency for Research on Cancer—*Summaries & Evaluations—2,4- and 2,6-Dinitrotoluenes (Group 2B), 3,5-Dinitrotoluene (Group 3): Summary of data reported and evaluation.* International Programme on Chemical Safety, Canadian Centre for Occupational Health and Safety, Hamilton, ON, CA. <http://www.inchem.org/documents/iarc/vol65/dinitrotoluene.html>
- Jeenigs, B. 2004. Alternative pan liners for OB of propellants.
http://p2library.nfesc.navy.mil/P2/Opportunity_Handbook/15_2.html
- Jenkins, T.F., P.G. Thorne, E.F. McCormick and K.F. Myers. 1995. Preservation of water samples containing nitroaromatics and nitramines. CRREL Special Report 95-16.
- Jenkins, T.J., T.A. Ranney, P.H. Miyares, N.H. Collins, and A.D. Hewitt. 2000a. Use of surface snow sampling to estimate the quantity of explosives residues resulting from land mine detonations. ERDC/CRREL TR-00-12.
- Jenkins, T.J., T.A. Ranney, M.E. Walsh, P.H. Miyares, A.D. Hewitt, and N.H. Collins. 2000b. Evaluating the use of snow-covered ranges to estimate the explosives residues that result from detonation of army munitions. ERDC/CRREL TR-00-15.
- Jenkins, T.F., J.C. Pennington, T.A. Ranney, T.E. Berry, Jr., P.H. Miyares, M.E. Walsh, A.D. Hewitt, N. Perron, L.V. Parker, C.A. Hayes, and E. Wahlgren. 2001. Characterization of explosives contamination at military firing ranges. ERDC TR-01-05.
- Jenkins, T.J., M.E. Walsh, P.H. Miyares, A.D. Hewitt, N.H. Collins, and T.A. Ranney. 2002. Use of snow-covered ranges to estimate explosives residues from high-order detonations of army munitions. *Thermochimica Acta*, 384: 173–185.

- Jenkins, T.F., S. Thiboutot, G. Ampleman, A.D. Hewitt, M.E. Walsh, T.A. Ranney, C.A. Ramsey, C.L. Grant, C.M. Collins, S. Brochu, S.R. Bigl, and J.C. Pennington. 2005a. Identity and distribution of residues of energetic compounds at military live-fire training ranges. ERDC TR-05-10.
- Jenkins, T.J., A.D. Hewitt, M.E. Walsh, T.A. Ranney, C.A. Ramsey, C.L. Grant, and K.L. Bjella. 2005b. Representative sampling for energetic compounds at military training ranges. *Environmental Forensics*, 6: 25–55.
- Jenkins, T.F., A.D. Hewitt, C.L. Grant, S. Thiboutot, G. Ampleman, M.E. Walsh, T.A. Ranney, C.A. Ramsey, A.J. Palazzo, and J.C. Pennington. 2006a. Identity and distribution of residues of energetic compounds at army live-fire training ranges. *Chemosphere*, 63: 1280–1290.
- Jenkins, T.F., S. Thiboutot, G. Ampleman, A.D. Hewitt, M.E. Walsh, S. Taylor, J. Clausen, T.A. Ranney, C.A. Ramsey, C.L. Grant, C.M. Collins, S. Brochu, E. Diaz, S.R. Bigl, and J.C. Pennington. 2006b. Identity and distribution of residues of energetic compounds at military live-fire training ranges. Chapter 2. In *Distribution and fate of energetics on DoD test and training ranges: Final report*. ERDC TR-06-13.
- Jenkins, T.F., J. Pennington, G. Ampleman, S. Thiboutot, M.R. Walsh, K. Dontsova, E. Diaz, S. Bigl, A. Hewitt, J. Clausen, D. Lambert, N. Perron, S. Yost, J. Brannon, M.C. Lapointe, S. Brochu, M. Bassard, M. Stowe, R. Fainaccio, A. Gagon, A. Moris, T. Gamche, G. Gilbert, D. Faucher, M.E. Walsh, C. Ramsey, R. Rachow, J. Zufelt, C. Collins, A. Gelvein, and S. Sarri. 2007. *Characterization and fate of gun and rocket propellant residues on testing and training ranges: Interim report 1*. ERDC TR-07-1.
- Jenkins, T.F., G. Ampleman, S. Thiboutot, S.R. Bigl, S. Taylor, M.R. Walsh, D. Faucher, R. Martel, I. Poulin, K.M. Dontsova, M.E. Walsh, S. Brochu, A.D. Hewitt, G. Comeau, E. Diaz, M.A. Chappell, J.L. Fadden, A. Marois, R. Fifield, B. Quemerais, J. Simunek, N.M. Perron, A. Gagnon, T. Gamache, J.C. Pennington, V. Moors, D.J. Lambert, D. Gilbert, R.N. Bailey, V. Tanguay, C.A. Ramsey, L. Melanson, and M.-C. Lapointe. 2008. *Characterization and fate of gun and rocket propellant residues on testing and training ranges: Final report*. ERDC TR-08-1.
- Johnson, C.H. 1977. Explosive tests for establishing hazard classification for M1SP propellant in automated single-base finishing operations. Technical Report 5020. Dover, NJ: Picatinny Arsenal.
- Kovero, E., and J. Tervo. 2002. Open burning of gun propellants. Specific methods and environmental analysis. In *Proceedings of the Finex 2002 Seminar. Levi, Kittilä, Finland*.
- Lahaye, C., and I. Abi-Zeid. 1994. *Fragmentation and lethality evaluation of the 81-mm C70A1 mortar cartridge (Protected A)*. Defence Research Establishment Valcartier, DREV Report 4763/94.
- Larese-Casanova, P. and M.M. Scherer. 2008. Abiotic transformation of hexahydro-1,3,5-trinitro-1,3,5-triazine (RDX) by green rusts. *Environmental Science and Technology*, 42: 3975–3981.

- Lever J., Taylor S., L. Perovich, K. Bjella, and B. Packer. 2005. Dissolution of Composition B residuals. *Environmental Science and Technology*, 39: 8803–8811.
- Lewis, J. 2006. The transport and fate of detonation residues originating from cracked unexploded ordnance in the vadose zone. PhD. Thesis, Université du Québec, INRS-Eau, Terre et Environnement.
- Lewis, J. 2010. Personal communication by email, April 30.
- Lewis, J. 2007. The transport and fate of detonation residues originating from cracked unexploded ordnance in the vadose zone. Ph.D. thesis, Université du Québec INRS-Eau, terre et environnement.
- Lewis, J., R. Martel, L. Trepanier, G. Ampleman, and S. Thiboutot. 2009. Quantifying the transport of energetic materials in unsaturated sediments from cracked unexploded ordnance. *Journal of Environmental Quality*, 38: 2229–2236.
- Lynch, J.C., K.F. Myers, J.M. Brannon, and J.J. Delfino. 2001. Effects of pH and temperature on the aqueous solubility and dissolution rate of 2,4,6-Trinitrotoluene (TNT), Hexahydro-1,3,5-trinitro-1,3,5-triazine (RDX), and Octahydro-1,3,5,7-tetranitro-1,3,5,7-tetrazocine (HMX). *J. Chem. Eng. Data*, 46 (6): 1549–1555.
- Lynch, J.C., J.M. Brannon, and J.J. Delfino. 2002. Effects of component interactions on the aqueous solubilities and dissolution rates of the explosive formulations Octol, Composition B, and LX-14. *J. Chem. Eng. Data*, 47: 542–549.
- Marois, A., A. Gagnon, S. Thiboutot, G. Ampleman, G. and M. Bouchard. 2004. *Caractérisation des sols de surface et de la biomasse dans les secteurs d'entraînement*. Base des Forces Canadiennes, Valcartier. DRDC Valcartier TR 2004-206.
- Martel, R., G., Comeau, S. Brochu, and A.D. Hewitt. 2008. Propellant residues in surface soils and groundwater at firing positions at Canadian force base Petawawa, Ontario. In: *Characterization and fate of gun and rocket propellant residues on testing and training ranges: Final report*. ERDC TR-08-1.
- Martel, R., A. Bellavance-Godin; R. Levesque; and S. Cote. 2010. Determination of nitroglycerin and its metabolites by solid-phase extraction and HPLC-UV. *Chromatographia*, 71: 285–289.
- Martel, R., S. Lange, S. Côté, G. Ampleman, and S. Thiboutot. 2011. Fate and behaviour of energetic material residues in the unsaturated zone: sand columns and dissolution tests. Institut National de la Recherche Scientifique, Quebec, Quebec, Canada, INRS-ETE, SERDP ER-1481 annual report, chapter 5, March 2011.
- McBride, W., R.A. Henry, J. Cohen, and S. Skolnik. 1951. Solubility of nitroguanidine in water. *J. Am. Chem. Soc.*, 73 (1): 485–486.

- Ministere du developpement durable, de l'environnement et des parcs, Quebec. 2002. Politique de protection des sols et de rehabilitation des terrains contamines. Gouvernement du Quebec. http://www.mddep.gouv.qc.ca/sol/terrains/politique/annexe_2_grille_eaux.htm Chap 5
- Monteil-Rivera, F., A. Halasz, C. Groom, J.S. Zao, S. Thiboutot, G. Ampleman, and J. Hawari. 2009. Fate and transport of explosives in the environment: A chemist's view. In *Ecotoxicology of Explosives* (G.I Sunahara, G. Lotufo, R.G. Kuperman and J Hawari eds.). New York: CRC Press,
- Moor, R. 2006. *European community safety data sheet for F 15080 (P-Code 6900)*. European Commision Enterprise and Industry DG, Communication and Information Unit R4, Brussels, BE.
- Morris, M.W., and L. Fallin. 2008. Effects of reducing conditions on the fate and transport of RDX in groundwater: A multivariate approach. In *Proceedings of the Annual International Conference on Soils, Sediments, Water and Energy*. Amherst, MA, University of Massachusetts, Vol. 13, Article 13.
- Napadensky, H.S., R. Joyce, R. Rindner, and D. Satriana. 1978. *Development of hazards classification data on propellants and explosives*. ADA064138. Chicago, IL: ITT Research Institute.
- Napadensky, H.S., R. Pape, R. Rindner, and D. Satriana. 1980. *Development of a hazard classification procedure for inprocess propellant and explosive materials*. ADA094741. Chicago, IL: ITT Research Institute.
- NATO Standardization Agency. 2009. STANAG 4439 JAIS (Edition 2)—*Policy for assessment of insensitive munitions*, NSAI0128(2009)-JAIS/4439.
- NOAA (National Oceanic and Atmospheric Administration). Undated. National Ocean Service Center for Operational Oceanographic Products and Services. Tide Predictions Anchorage, Alaska. <http://tidesandcurrents.noaa.gov/noaatidepredictions/NOAATidesFacade.jsp?Stationid=9455920>
- Ontario ministry of the environment. 2004. Soil, ground water and sediment standards for use under part XV.1 of the environmental protection act. Government of Ontario. <http://www.ene.gov.on.ca/envision/gp/4697e.pdf> Chap 5
- Penfold, L. 2010. Personal communication.
- Pennington, J., T. Jenkins, G. Ampleman, S. Thiboutot, J. Brannon, J. Lynch, T. Ranney, J. Stark, M.E. Walsh, J. Lewis, C. Hayes, J. Mirecki, A. Hewitt, N. Perron, D. Lambert, J. Clausen, and J. Delfino. 2001. *Distribution and fate of energetics on DoD Test and training ranges: Interim report 1*. ERDC TR-01-13.
- Pennington, J. C., T.F. Jenkins, G. Ampleman, S. Thiboutot, J.M. Brannon, J. Lynch, T.A. Ranney, J. A. Stark, M.E. Walsh, J. Lewis, C.A. Hayes, J.E. Mirecki, A.D. Hewitt, N. Perron, D. Lambert, J. Clausen, and J.J. Delfino. 2002. *Distribution and fate of energetics on DoD test and training ranges: Interim report 2*. ERDC TR-02-8.

- Pennington, J., T. Jenkins, G. Ampleman, S. Thiboutot, J. Brannon, J. Lewis, J. DeLaney, J. Clausen, A. Hewitt, M. Hollander, C. Hayes, J. Stark, A. Marois, S. Brochu, H. Dinh, D. Lambert, A. Gagnon, M. Bouchard, R. Martel, P. Brousseau, N. Perron, R. Lefebvre, W. Davis, T.A. Ranney, C. Gauthier, S. Taylor, and J.M. Ballard. 2003. *Distribution and fate of energetics on DoD test and training ranges: Interim report 3.* ERDC TR-03-2.
- Pennington, J.C., T.F. Jenkins, G. Ampleman, S. Thiboutot, J. Brannon, J. Clausen, A.D. Hewitt, S. Brochu, P. Dubé, J. Lewis, T.A. Ranney, D. Faucher, A. Gagnon, J.A. Stark, P. Brousseau, C.B. Price, D. Lambert, A. Marois, M. Bouchard, M.E. Walsh, S.L. Yost, N.M. Perron, R. Martel, S. Jean, S. Taylor, C.A. Hayes, J.M. Ballard, M.R. Walsh, J.E. Mirecki, S. Downe, N.H. Collins, B. Porter, and R. Karn. 2004. *Distribution and fate of energetics on DoD test and training ranges: Interim report 4.* ERDC TR-04-4.
- Pennington, J. C., T.F. Jenkins, S. Thiboutot, G. Ampleman, J. Clausen, A.D. Hewitt, J. Lewis, M.R. Walsh, T.A. Ranney, B. Silverblatt, A. Marois, A. Gagnon, P. Brousseau, J.E. Zufelt, K. Poe, M. Bouchard, R. Martel, D.D. Walker, C.A. Ramsey, C. A. Hayes, S. Yost, K.L. Bjella, L. Trepanier, T.E. Berry, D.J. Lambert, P. Dubé, and N.M. Perron. 2005. *Distribution and fate of energetics on DoD test and training ranges: Report 5.* ERDC TR-05-02.
- Pennington, J.C., T.F. Jenkins, G. Ampleman, S. Thiboutot, A.D. Hewitt, S. Brochu, J. Robb, E. Diaz, J. Lewis, H. Colby, R. Martel, K. Poe, K. Groff, K.L. Bjella, C.A. Ramsey, C.A. Hayes, S. Yost, A. Marois, A. Gagnon, B. Silverblatt, T. Crutcher, K. Harriz, K. Heisen, S.R. Bigl, T.E. Berry, Jr., J. Muzzin, D.J. Lambert, M.J. Bishop, B. Rice, M. Wojtas, M.E. Walsh, M.R. Walsh, and S. Taylor. 2006a. *Distribution and fate of energetics on DoD test and training ranges: Interim report 6.* ERDC TR-06-12.
- Pennington, J.C., T.F. Jenkins, G. Ampleman, S. Thiboutot, J.M. Brannon, A.D. Hewitt, J. Lewis, S. Brochu, E. Diaz, M.R. Walsh, M.E. Walsh, S. Taylor, J.C. Lynch, J. Clausen, T.A. Ranney, C.A. Ramsey, C.A. Hayes, C.L. Grant, C.M. Collins, S.R. Bigl, S. Yost, S. and K. Dontsova. 2006b. *Distribution and fate of energetics on DoD test and training ranges: Final report.* ERDC TR-06-13.
- Pennington, J. C., T.F. Jenkins, S. Thiboutot, G. Ampleman, and A.D. Hewitt. 2006c. Conclusions. In *Distribution and fate of energetics on DoD test and training ranges: Final report.* ERDC TR-06-13.
- Poulin, I., S. Thiboutot, and S. Brochu. 2009. *Production of dioxins and furans from the burning of excess gun propellant.* DRDC-Valcartier TR 2009-365. Val Belair, Quebec: DRDC-Valcartier.
- Racine, C.H., M.E. Walsh, B.D. Roebuck, C.M. Collins, D.J. Calkins, L.R. Reitsma, P.J. Buchli, and G. Goldfarb. 1992a. White phosphorus poisoning of waterfowl in an Alaskan saltmarsh. *Journal of Wildlife Diseases*, 28(4):669–673.
- Racine, C.H., M.E. Walsh, C.M. Collins, D.J. Calkins, B.D. Roebuck, and L. Reitsma. 1992b. *Waterfowl mortality in Eagle River Flats, Alaska: The role of munitions residues.* CRREL Report 92-5
- Rasemann, W. 2000. Industrial waste dumps, sampling and analysis. In *Encyclopedia of Analytical Chemistry* (R.A. Meyers, ed.). John Wiley and Sons, Ltd.

- Robidoux, P.Y., B. Lachance, L. Didillon, F.O. Dion, and G.I. Sunahara. 2006. *Development of ecological and human health preliminary soil quality guidelines for energetic materials to ensure training sustainability of the Canadian Forces.* NRC report # 45936. Montreal, QC: National Research Council.
- Savard, S., and M.J. Hardy. 2010. *Émissions gazeuse à la bouche d'un canon, rapport d'étape phase II, essai 5, table de brûlage.* Report # 640-PE35480. Contract # W7701-7-1924/A. Quebec, QC : Centre de Recherche Industrielle du Québec.
- Stiefel, L., and M. Summerfield, eds. 1988. Gun propulsion technology. *Progress in Astronautics and Aeronautics*, 109: 121–123.
- Strecker, A. 1861. Untersuchungen über die chemischen Beziehungen zwischen Guanin, Xanthin, Theobromin, Caffein und Kreatinin. *Annalen der Chemie und Pharmacie* 118: 151–177.
- Taylor S., A. Hewitt, J. Lever, C. Hayes, L. Perovich, P. Thorne and C. Daghlian. 2004a. TNT particle size distributions from detonated 155-mm howitzer rounds. *Chemosphere*, 55: 357–367.
- Taylor S., J.H. Lever, B. Bostick, M.R. Walsh, M.E. Walsh, and B. Packer. 2004b. *Underground UXO: Are they a significant source of explosives in soil compared to military training on ranges?* ERDC/CRREL Technical Report TR-04-23.
- Taylor S., E. Campbell, L. Perovich, J. Lever and J. Pennington. 2006. Characteristics of Composition B Particles from blow-in-place detonations. *Chemosphere* 65: 1405–1413.
- Taylor, S., J.H. Lever, J. Fadden, N. Perron, and B. Packer. 2009. Simulated rainfall-driven dissolution of TNT, Tritonal, Comp B and Octol particles. *Chemosphere*, 75: 1074–1081.
- Taylor, S., J.H. Lever, M.E. Walsh, J. Fadden, N. Perron, S. Bigl, R. Spanggord, M. Curnow. and B. Packer. 2010. *Dissolution rate, weathering mechanics and friability of TNT, Comp B, Tritonal, and Octol.* ERDC/CRREL TR-10-2.
- Taylor, S., C. Richardson, J.H. Lever, N.M. Perron, and M. Chappell. In prep. *Dissolution of nitroglycerin from small arms propellants and their residues.*
- Tetratech Inc. 2002. *Draft final OB/OD permitting guidelines.* http://www.epa.gov/reg3wcmr/OBOD_guidelines.pdf
- Thiboutot, S., G. Ampleman, A. Gagnon, A. Marois, T.F. Jenkins, M.E. Walsh, P.G. Thorne, and T.A. Ranney. 1998. *Characterization of antitank firing ranges at CFB Valcartier, WATC Wainwright, and CFAD Dundurn.* DREV-R-9809. Val-Bélair, QC: DRDC-Valcartier.
- Thiboutot, S., G. Ampleman, A. Gagnon, and A. Marois. 2000. *Characterization of an unexploded ordnance contaminated range (Tracadie Range) for potential contamination by energetic materials.* DREV Report TR-2000-102.

- Thiboutot, S., G. Ampleman, G., A. Marois, A. Gagnon, M. Bouchard, A.D. Hewitt, T.F. Jenkins, M.E. Walsh, K. Bjella, C. Ramsey, and T.A. Ranney. 2004. *Environmental conditions of surface soils, CFB Gagetown Training Area: Delineation of the presence of munitions related residues (Phase III, Final Report)*. DRDC Valcartier TR 2004-205.
- Thiboutot, S., A. Marois, A. Gagnon, T. Gamache, N. Roy, C. Tremblay, and G. Ampleman. 2007a. *Caractérisation de la dispersion de résidus de munitions dans les sols de surface d'un secteur d'essai*. DRDC Valcartier TR 2007-110. Val-Bélair, QC: DRDC-Valcartier.
- Thiboutot, S., G. Ampleman, A. Marois, A. Gagnon, D. Gilbert, V. Tanguay, and I. Poulin. 2007b. *Deposition of gun propellant residues from 84-mm Carl Gustav rocket firing*. DRDC Valcartier TR 2007-408. Val Belair, Quebec: DRDC-Valcartier.
- Thiboutot, S., G. Ampleman, A. Marois, A. Gagnon, D. Gilbert, V. Tanguay, and I. Poulin. 2008a. Energetic residues deposition from 84-mm Carl Gustav antitank live-firing. In *Characterization and fate of gun and rocket propellant residues on testing and training ranges: Final report* (T.F. Jenkins and S.R. Bigl, eds.). ERDC TR-08-1.
- Thiboutot, S., G. Ampleman, A. Marois, A. Gagnon, and D. Gilbert. 2008b. Deposition of nitroglycerin from the live firing of M72 A5 66-mm rockets. In *Proceedings of the 2008 SERDP & ESCP Partners in Environmental Technology Technical Symposium and Workshop, Washington, DC, 2–4 December 2008*.
- Thiboutot, S., G. Ampleman, A. Marois, and A. Gagnon. 2008c. *Caractérisation des sols de surface du champ de tir et secteurs d'entraînement de la garnison Valcartier*. Technical Report DRDC Valcartier TR 2008-190. Val-Bélair, QC: DRDC-Valcartier.
- Thiboutot, S., G. Ampleman, M.C. Lapointe, S. Brochu, M. Brassard, R. Stowe, R. Farinaccio, A. Gagnon, A. Marois, and T. Gamache. 2008d. *Study of the dispersion of ammonium perchlorate following the static firing of MK-58 rocket motors*. Technical Report DRDC Valcartier TR 2008-240. Val-Bélair, QC: DRDC-Valcartier.
- Thiboutot, S., G. Ampleman, A. Marois, A. Gagnon, and D. Gilbert. 2009. *Nitroglycerine deposition from M72 rocket firing*. DRDC-Valcartier TR 2009-003. Val Belair, Quebec: DRDC-Valcartier.
- Thiboutot, S., G. Ampleman, A. Gagnon, A. Marois, R. Martel, and G. Bordeleau. 2010. *Persistence and fate of nitroglycerine in legacy antitank ranges*. DRDC-Valcartier TR 2010-059. Val Belair, Quebec: DRDC-Valcartier.
- Topp, G.C., and P.A. Ferré. 2002. Water content. In *Methods of Soil Analysis. Part 4—Physical Methods* (J.H. Dane and G.C. Topp, eds.). Madison, WI: Soil Science Society of America, Inc., pp. 417–546.
- Towndrow, D. 2007. UK MoD munitions disposal. In Proceedings of the NATO – AVT 115 Meeting, Sofia, Bulgaria.
- U.S. Army. 1976. *Propellant, M2, for M5 subsystem ammunition*. Military specification, Mil Spec MIL-P-60989A. Washington, D.C: U.S. Government Printing Office.

- U.S. Army. 1984. *Military explosives*. Technical Manual TM 9-1300-214. Washington, D.C: U.S. Government Printing Office.
- U.S. Army. 1994. *Army ammunition data sheets: Artillery ammunition (FSC 1310, 1315, 1320, 1390)*. Technical Manual TM 43-0001-28. Washington, DC: U.S. Government Printing Office.
- U.S. Army. 2005. *Propellants: A guide to recognizing and identifying specific types of nitrocellulose-based propellants*. McAlester, OK: U.S. Army Defense Ammunition Center.
- U.S. Department of Health and Human Services. 1998. *Toxicological Profile, 2,4- and 2,6-Dinitrotoluene*. Agency for Toxic Substances and Disease Registry.
- USEPA. 2006. Nitroaromatics, nitramines, nitrate esters by high performance liquid chromatography (HPLC). Washington, DC: U. S. Environmental Protection Agency. SW-846 Method 8330B.
- USEPA. 2009. *Edition of the drinking water standards and health advisories*. EPA 822-R-09-11 Office of Water, U.S. Environmental Protection Agency, Washington, DC, USA.
- Vandebeek, R.R. 1988. *Deflagration to detonation transition of gun and small propellant: a study and review*. Contract no. 07SQ.23440-7-9157. Kingston, ON: Mining Resource Engineering Ltd (MREL).
- Vaselinovica, J. 2004. *SALW ammunition destruction: Environmental Releases from open burning (OB) and open detonation (OD) events*. Belgrade, Serbia and Montenegro: South Eastern Europe Clearinghouse for the Control of Small Arms and Light Weapons (SEESAC).
- Walsh, M. E. 1989. Analytical methods for determining nitroguanidine in soil and water. CRREL Special Report 89-35.
- Walsh, M.E., and T.A. Ranney. 1998. Determination of nitroaromatic, nitramine, and nitrate ester explosives in water using solid-phase extraction and GC-ECD. CRREL Special Report 98-2.
- Walsh, M.E., C.M. Collins, C.H. Racine, T.F. Jenkins, A.B. Gelvin, and T.A. Ranney. 2001. *Sampling for explosives residues at Fort Greely, Alaska: Reconnaissance visit July 2000*. ERDC/CRREL TR-01-15.
- Walsh, M.E., C.A. Ramsey, and T.F. Jenkins. 2002. The effect of particle size reduction by grinding on subsample variance for explosive residues in soil. *Chemosphere*, 49 (10): 1267–1273.
- Walsh, M.E., C.M. Collins, A.D. Hewitt, M.R. Walsh, T.F. Jenkins, J. Stark, A. Gelvin, T.S. Douglas, N. Perron, D. Lambert, R. Bailey, and K. Meyers. 2004. *Range characterization studies at Donnelly Training Area, Alaska: 2001 and 2002*. ERDC/CRREL TR-04-3.

- Walsh, M.E., C.A. Ramsey, C.M. Collins, A.D. Hewitt, M.R. Walsh, K. Bjella, D. Lambert, and N. Perron. 2005. *Collection methods and laboratory processing of samples from Donnelly Training Area firing points, Alaska: 2003*. ERDC/CRREL TR-05-6.
- Walsh, M.E., C.A. Ramsey, S. Taylor, A.D. Hewitt, K. Bjella, and C.M. Collins. 2007a. Subsampling variance for 2, 4-DNT in firing point soils. *Soil and Sediment Contamination: An International Journal*, 16 (5): 459–72.
- Walsh, M.E., C.M. Collins, C.A. Ramsey, T.A. Douglas, R.N. Bailey, M.R. Walsh, A.D. Hewitt, and J.L. Clausen. 2007b. *Energetic residues on Alaskan training ranges*. ERDC/CRREL TR-07-9.
- Walsh, M.E., C.M. Collins, M.R. Walsh, C.A. Ramsey, S. Taylor, S.R. Bigl, R.N. Bailey, A.D. Hewitt, and M. Prieksat. 2008. Energetic residues and crater geometries from the firing of 120-mm high-explosive mortar projectiles into Eagle River Flats, June 2007. ERDC/CRREL TR-08-10.
- Walsh, M.E., S. Taylor, A.D. Hewitt, M.R. Walsh, C.A. Ramsey, and C.M. Collins. 2010. Field observations of the persistence of Comp B explosives residues in a salt marsh impact area. *Chemosphere*, 78 (10): 467–473.
- Walsh, M.R. 2007. Explosives residues resulting from the detonation of common military munitions: 2002–2006. ERDC/CRREL TR-07-2.
- Walsh, M.R., M.E. Walsh, and C.A. Ramsey. 2005a. An examination of protocols for the collection of munitions-derived explosives residues on snow-covered ice. ERDC/CRREL TR-05-8.
- Walsh, M.R., S. Taylor, M.E. Walsh, S. Bigl, K. Bjella, T. Douglas, A.B. Gelvin, D. Lambert, N.M. Perron, and S.P. Saari. 2005b. *Residues from live-fire detonation of 155 mm howitzer rounds*. ERDC/CRREL TR 05-14.
- Walsh, M.R., M.E. Walsh, C.M. Collins, S.P. Saari, J.E. Zufelt, A.B. Gelvin, and J.W. Hug. 2005c. *Energetic residues from live-fire detonations of 120-mm mortar rounds*. ERDC/CRREL TR-05-15.
- Walsh, M.R., M.E. Walsh, C.A. Ramsey, R.J. Rachow, J.E. Zufelt, C.M. Collins, A.B. Gelvin, N.M. Perron, and S.P. Saari. 2006a. *Energetic residues deposition from 60-mm and 81-mm mortars*. ERDC/CRREL TR-06-10.
- Walsh, M.R., M.E. Walsh, G. Ampleman, S. Thiboutot, and D.D. Walker. 2006b. *Comparison of explosives residues from the blow-in-place detonation of 155-mm high-explosive projectiles*. ERDC/CRREL TR-06-13.
- Walsh, M.R., M.E. Walsh, S.R. Bigl, N.M. Perron, D.J. Lambert, and A.D. Hewitt. 2007a. *Propellant residues deposition from small arms munitions*. ERDC/CRREL TR-07-17.
- Walsh, M.R., M.E. Walsh, and C.A. Ramsey. 2007b. *Measuring energetics residues on snow*. ERDC/CRREL TR-07-19.

- Walsh, M.R., M.E. Walsh, and A.D. Hewitt. 2008. Energetic residues from blow-in-place detonation of 60-mm and 120-mm fuzed high-explosive mortar cartridges. ERDC/CRREL TR-08-19.
- Walsh, M.R., M.E. Walsh, and A.D. Hewitt. 2009a. Energetic residues from the expedient disposal of artillery propellants. ERDC/CRREL TR-09-8.
- Walsh, M.R., M.E. Walsh, S. Thiboutot, G. Ampleman, and J. Bryant. 2009b. *Propellant residues deposition from firing of AT4 rockets*. ERDC/CRREL TR-09-13.
- Walsh, M.R., M.E. Walsh, and A.D. Hewitt. 2010a. Energetic residues from field disposal of gun propellants. *Journal of Hazardous Materials*, 173: 115–122.
- Walsh, M.R., G. Ampleman, S. Thiboutot, M.E. Walsh, I. Poulin, A. Bellavance-Godin, R. Martel, G. Bordeleau, S. Brochu, A.D. Hewitt, A. Marois, A Gagnon, C.M. Collins, D. Gilbert, P. Woods, J.N. Bryant, S.R. Bigl, and K. Gagnon. 2010b. *Characterization and fate of gun and rocket propellant residues on testing and training ranges: Interim Report 2*. ERDC/CRREL TR-10-13.
- Walsh, M.R., M.E. Walsh, J.W. Hug, S.R. Bigl, K.L. Foley, A.B. Gelvin, and N.M. Perron. 2010c. *Propellant residues deposition from firing of 40-mm grenades*. ERDC/CRREL TR-10-10.
- Walsh, M.R., M.E. Walsh, and Hug, J.W. (in this report) A simple device for initiating high-order detonations. Chapter 6 in *Characterization and Fate of Gun and Rocket Propellant Residues on Testing and Training Ranges: Final Report*. ERDC/CRREL TR-11-XX.
- Wang, Q.J. 1991. The POT model described by the generalized Pareto distribution with Poisson arrival rate. *J. of Hydrology*, 129: 263–280.
- Wingfors, H., C. Edlund, L. Hägglund, A. Waleij, J. Sjöström, R.-M. Karlsson, P. Leffler, U Qvarfort, M. Ahlberg, S. Thiboutot, G. Ampleman, R. Martel, W. Duvalois, A. Creemers, and N. van Ham. 2006. *Evaluation of the contamination by explosives and metals in soils at the Alvdalen Shooting Range—Part II: Results and discussion*. Scientific Report FOI-R-1877-SE. Stockholm, Sweden: FOI/Swedish Defence Research Agency.
- Zheng, W., J. Lichwa, M. D'Alessio, and R. Chittaranjan. 2009. Fate and transport of TNT, RDX, and HMX in streambed sediments: Implications for riverbank filtration. *Chemosphere*, 76: 1167–1177.

Appendix A: Munitions Data

Table A-1 contains information relevant to the munitions used during the test covered in this report. Images of the ammunition cans from the tests are shown in Figures A-1 and A-2. Information displayed on the cans includes national stock number (NSN) Department of Defense Identification Code (DODIC), military designation, and lot number. Propellant loads for the analytes of concern are given in Table 2-1 (of the main text). Table A-2 gives more detailed information on the propellants for each type of munition.

Table A-1. Munitions data.

NSN	DODIC	Nomenclature	Lot No.	Drawn for tests
1310-01-472-9871	BA12	Cartridge, 40 Millimeter: Practice, Mk281 Mod 0	NPG08L003-055	128
1310-01-159-8043	B542	Cartridge, 40 Millimeter: HEDP, M430	MA-88G023Y033F	144

Note: Munitions were drawn from inventory, Ammunition Supply Point, Ft. Richardson, AK.
Source.: U.S. Army (1994).

Table A-2. Propellant data.

DODIC	Propellant	Mass of propellant (g)	Mass (mg) / percentage NG	Other major constituents
BA12	F15080	4.04	370 / 9.1%	NC: 88% Akardit II: 1.2% Ethyl Centralite: 0.2% KSO ₄ : 0.65%
B542	M2	4.64	900 / 19.44%	NC: 77.5% K Nitrate, 0.75% Ba Nitrate: 1.4% Ethyl Centralite: 0.60% C (Graphite): 0.30%

Sources: F15080 (BA12): Moore (2006), B. Vogelsanger (e-mail communication); M2 (B542): U.S. Army (2005).



Figure A-1. Ammunition box for TP rounds used during test.

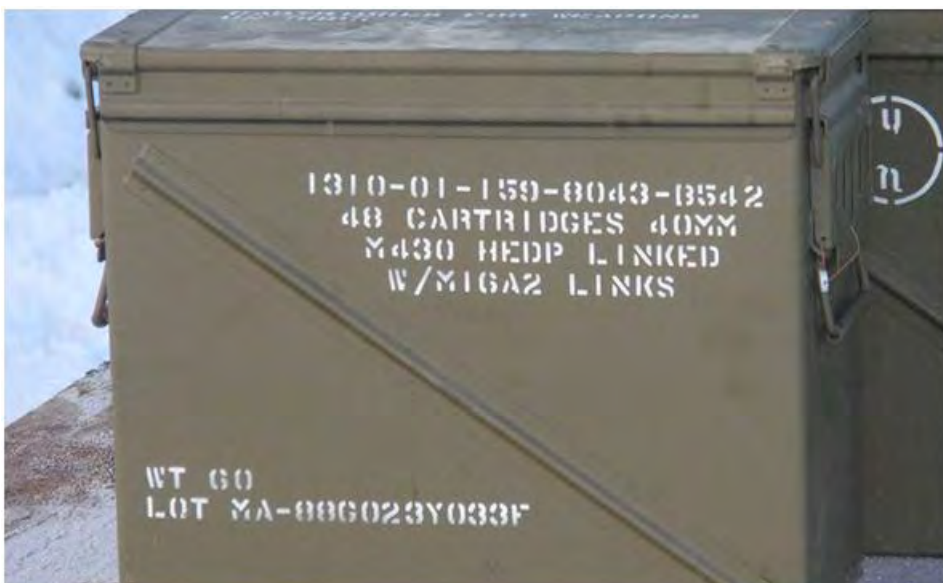


Figure A-2. Ammunition box for HE rounds used during test.

Appendix B: Analytical Results

Table B-1 contains sampling data for the test conducted on snow at the 40 mm/AT4 (40/90) Range at Fort Richardson on 22–23 February 2010.

Tables B-2 and B-3 contain the results of the analyses.

Table B-1. 40-mm firing point sampling data.

Sample ID number	Scoop size (cm × cm)	Sample description	Number of increments	Samplers	Sampled Area (m ²)	Notes
FRA10-01	10 × 10	Background Sample	30	SB/KLF	0.30	Entrance road
FRA10-02	10 × 10	Pad 1 (TP) 9 to 11.5 m	40	SB/JH	0.40	
FRA10-03	10 × 10	Pad 1 (TP) 9 to 11.5 m	40	SB/JH	0.40	
FRA10-04	10 × 10	Pad 1 (TP) 9 to 11.5 m	40	SB/JH	0.40	
FRA10-05	10 × 10	Pad 1 (TP) 5 to 9 m	40	MRW/AG	0.40	
FRA10-06	10 × 10	Pad 1 (TP) 5 to 9 m	40	MRW/AG	0.40	
FRA10-07	10 × 10	Pad 1 (TP) 5 to 9 m	40	MRW/AG	0.40	
FRA10-08	10 × 10	Pad 1 (TP) 0 to 5 m	40	MEW/KLF	0.40	
FRA10-09	10 × 10	Pad 1 (TP) 0 to 5 m	40	MEW/KLF	0.40	
FRA10-10	10 × 10	Pad 1 (TP) 0 to 5 m	40	MEW/KLF	0.40	
FRA10-11		Lab Filtration Blank				
FRA10-12	20 × 20	Pad 1 (TP) 0 to 5 m	38	MRW/AG	1.52	Larger scoop
FRA10-13	15 × 15	Baseline—Pad 2 mine	20	MEW	0.45	
FRA10-14	15 × 15	Baseline—Pad 2 mine	20	MEW	0.45	
FRA10-15	15 × 15	Background—Near FP	20	MEW	0.45	
FRA10-16	15 × 15	Background—End of lot	20	MEW	0.45	
FRA10-17	10 × 10	Pad 2 (HE) 10 to 13.5 m	40	SRB/JH	0.40	
FRA10-18	10 × 10	Pad 2 (HE) 10 to 13.5 m	40	SRB/JH	0.40	TriPLICATE SPE
FRA10-19	10 × 10	Pad 2 (HE) 10 to 13.5 m	40	SRB/JH	0.40	
FRA10-20	10 X 10	Pad 2 (HE) 5 to 10 m	48	MRW/AG	0.48	TriPLICATE SPE
FRA10-21	10 × 10	Pad 2 (HE) 5 to 10 m	48	MRW/AG	0.48	
FRA10-22		Lab Filtration Blank				
FRA10-23	10 × 10	Pad 2 (HE) 5 to 10 m	48	MRW/AG	0.48	
FRA10-24	10 × 10	Pad 2 (HE) 0 to 5 m	41	MEW/KLF	0.41	
FRA10-25	10 × 10	Pad 2 (HE) 0 to 5 m	42	MEW/KLF	0.42	
FRA10-26	10 × 10	Pad 2 (HE) 0 to 5 m	40	MEW/KLF	0.40	TriPLICATE SPE
FRA10-27	20 × 20	Pad 2 (HE) 0 to 5 m	48	MRW/AG	1.92	Larger scoop
FRA10-28		Lab Filtration Blank				

Table B-2. Sample analytical results (NG) for 40-mm firing positions.

Sample	NG Mass in Sample					NG mass in test areas	
	Filtrate portion		Filter portion				
ID Number	Total (mg/L)	Total (mg)	Calculated (mg/m ²)	Total (mg)	Calculated (mg/m ²)	Total (mg)	Average (mg)
FRA10-01	-ND-	-	-	-	-	-	-
FRA10-02	-ND-	-	-	0.0020	0.005	0.11	
FRA10-03	-ND-	-	-	0.0050	0.013	0.26	
FRA10-04	-ND-	-	-	0.0020	0.005	0.11	0.16
FRA10-05	0.0024	0.0067	0.017	0.30	0.75	22	
FRA10-06	0.0014	0.0046	0.011	0.29	0.73	21	
FRA10-07	0.0017	0.0061	0.015	0.30	0.75	22	22
FRA10-08	0.021	0.0549	0.14	2.8	7.0	260	
FRA10-09	0.021	0.0525	0.13	2.7	6.7	250	
FRA10-10	0.025	0.0582	0.15	2.7	6.7	250	250
FRA10-11	-ND-	-	-	-	-	-	-
FRA10-12	0.017	0.21	0.14	12	7.8	290	290
FRA10-13	-ND-	-	-	-	-	-	-
FRA10-14	-ND-	-	-	-	-	-	-
FRA10-15	-ND-	-	-	-	-	-	-
FRA10-16	-ND-	-	-	-	-	-	-
FRA10-17	0.0025	0.0091	0.023	0.049	0.12	4.6	
FRA10-18	0.0017	0.0061	0.015	0.036	0.091	3.4	
(Triplicate)	0.0016	0.0056	-	-	-	-	-
(Triplicate)	0.0017	0.0062	-	-	-	-	-
FRA10-19	0.0033	0.011	0.028	0.039	0.10	4.1	4.0
FRA10-20	0.0044	0.021	0.043	1.9	3.9	160	
(Triplicate)	0.0044	0.020	-	-	-	-	-
(Triplicate)	0.0044	0.020	-	-	-	-	-
FRA10-21	0.0037	0.016	0.033	1.2	2.4	100	
FRA10-22	-ND-	-	-	-	-	-	-
FRA10-23	0.0051	0.023	0.047	3.0	6.2	250	170
FRA10-24	0.60	1.4	3.4	120	290	11000	
FRA10-25	0.58	1.4	3.2	110	260	10000	
FRA10-26	0.68	1.4	3.6	120	300	11000	11000
(Triplicate)	0.66	1.4	-	-	-	-	-
(Triplicate)	0.69	1.5	-	-	-	-	-
FRA10-27	0.24	3.2	1.7	350	180	7000	7000
FRA10-28	-ND-	-	-	-	-	-	-

Table B-3. Sample analytical results (Akaradite II®) for 40-mm firing positions.

Sample	Akaradite II mass in sample					Akaradite II mass in test Area	
	Filtrate Portion			Filter Portion			
ID number	Total (mg/L)	Total (mg)	Calculated (mg/m ²)	Total (mg)	Calculated (mg/m ²)	Total (mg)	Average (mg)
FRA10-01	-ND-	-	-	-ND-	-	-	-
FRA10-02	-ND-	-	-	-ND-			
FRA10-03	-ND-	-	-	-ND-			
FRA10-04	-ND-	-	-	-ND-			
FRA10-05	0.06	0.2	0.4	1.0	2.6	87	
FRA10-06	0.04	0.1	0.3	0.85	2.1	70	
FRA10-07	0.04	0.1	0.4	1.0	2.5	83	80
FRA10-08	0.51	1.3	3.3	9.4	24	978	
FRA10-09	0.52	1.3	3.2	8.8	22	913	
FRA10-10	0.58	1.4	3.4	9.0	23	948	946
FRA10-11	-ND-	-	-	-	-	-	-
FRA10-12	0.43	5.3	3.5	35	23	955	

Appendix C: DRDC Soil Samples and Results

Table C-1. DRDC soil samples and results.

Lab no	Description	Number of incr.	Series	Concentration (ppm)												
				HMX	1,3,5-TNB	RDX	1,3-DNB	TNT	TETRYL	NG	2,4-DNT	2,6-DNT	2-ADNT	4-ADNT	2 et 3-NT	4-NT
S-Suff-1	0-30 m Blank 1	60 inc.		n.d.	n.d.	n.d.	n.d.	n.d.	n.d.	n.d.	n.d.	n.d.	n.d.	n.d.	n.d.	n.d.
S-Suff-2	0-30 m Blank Duplicate	60 inc.		n.d.	n.d.	n.d.	n.d.	n.d.	n.d.	n.d.	n.d.	n.d.	n.d.	n.d.	n.d.	n.d.
S-Suff-3	30-60 m Blank 1			n.d.	n.d.	n.d.	n.d.	n.d.	n.d.	n.d.	n.d.	n.d.	n.d.	n.d.	n.d.	n.d.
S-Suff-4	30-60 m Blank 1 Dup			n.d.	n.d.	n.d.	n.d.	n.d.	n.d.	n.d.	n.d.	n.d.	n.d.	n.d.	n.d.	n.d.
S-Suff-5	0-30 m after firing series 1	51 inc.	Charge 5	n.d.	n.d.	n.d.	n.d.	n.d.	n.d.	n.d.	n.d.	n.d.	n.d.	n.d.	n.d.	n.d.
S-Suff-6	0-30 m after firing series 1 dup	51 inc.	Charge 5	n.d.	n.d.	n.d.	n.d.	n.d.	n.d.	n.d.	n.d.	n.d.	n.d.	n.d.	n.d.	n.d.
S-Suff-7	30-60 m after firing series 1	53 inc.	Charge 5	n.d.	n.d.	n.d.	n.d.	n.d.	n.d.	n.d.	n.d.	n.d.	n.d.	n.d.	n.d.	n.d.
S-Suff-8	30-60 m after firing series 1 dup	53 inc.	Charge 5	n.d.	n.d.	n.d.	n.d.	n.d.	n.d.	n.d.	n.d.	n.d.	n.d.	n.d.	n.d.	n.d.
S-Suff-9	0-30 m after firing series 2	76 inc.	Charge 3	n.d.	n.d.	n.d.	n.d.	n.d.	n.d.	n.d.	n.d.	n.d.	n.d.	n.d.	n.d.	n.d.
S-Suff-10	0-30 m after firing series 2 dup	76 inc.	Charge 3	n.d.	n.d.	n.d.	n.d.	n.d.	n.d.	n.d.	n.d.	n.d.	n.d.	n.d.	n.d.	n.d.
S-Suff-11	30-60 m after firing series 2	65 inc.	Charge 3	n.d.	n.d.	n.d.	n.d.	n.d.	n.d.	n.d.	n.d.	n.d.	n.d.	n.d.	n.d.	n.d.
S-Suff-12	30-60 m after firing series 2 dup		Charge 3	n.d.	n.d.	n.d.	n.d.	n.d.	n.d.	n.d.	n.d.	n.d.	n.d.	n.d.	n.d.	n.d.
S-Suff-13	30-60 m after firing series 2 tripl		Charge 3	n.d.	n.d.	n.d.	n.d.	n.d.	n.d.	n.d.	n.d.	n.d.	n.d.	n.d.	n.d.	n.d.
S-Suff-14	30-60 m after firing series 3		Charge 8	n.d.	n.d.	n.d.	n.d.	n.d.	n.d.	n.d.	n.d.	n.d.	n.d.	n.d.	n.d.	n.d.
S-Suff-15	30-60 m after firing series 3 dup		Charge 8	n.d.	n.d.	n.d.	n.d.	n.d.	n.d.	n.d.	n.d.	n.d.	n.d.	n.d.	n.d.	n.d.
S-Suff-16	30-60 m after firing series 3 tripl		Charge 8	n.d.	n.d.	n.d.	n.d.	n.d.	n.d.	n.d.	n.d.	n.d.	n.d.	n.d.	n.d.	n.d.

Notes: Series 1: 30 x Charge 5; Series 2: 30 x Charge 3; Series 3: 19 x Charge 8.

Appendix D: Data Processing for the Dissolution Tests.

Table D-1. Theoretical mass of residues for water drop tests in accordance to large sand column tests.

Type of residues	Large sand column test			Fritted glass funnel test		
	Radius (cm)	Surface (cm ²)	Mass of contaminated soil or particles (g)	Radius (cm)	Surface (cm ²)	Mass of contaminated soil or particles (g)
Propellant in soil from anti tank range firing position (Range Wellington at CFB Gagetown) ¹	29.8	2,800	5,000	0.60	1.1	2.0 ¹
Composition B particles sampled on snow after 81-mm mortar sympathetic detonation ²	29.8	2,800	45	0.75	1.8	0.028 ²
Propellant in soil from anti tank range firing position (Range A at CFB Petawawa) ¹	29.8	2,800	5,000	0.60	1.1	2.0 ¹
Octol in powder ² or in flakes ²			nd			nd
Soil sample from the artillery firing position Hotel Tower at CFB Petawawa [†]	29.8	2,800	9,500 ¹	0.60	1.1	3.9
Residues from artillery gun powder bag burning test on snow at CFB Valcartier ²	29.8	2,800	150 ²	0.60	1.1	0.061
Soils samples from the Wellington anti-tank impact area at CFB Gagetown ¹	29.8	2,800	7,000 ¹	0.60	1.1	2.8

1 Contaminated soil.
 2 Particles only.
 3 nd: No correspondence between the large sand column test and dissolution test.

Table D-2. Theoretical mass of residues for water drop tests in accordance to large sand column tests.

Flow rates of	Large sand column test		Fritted glass funnel test				
	Spring precipitation (8 hr/day)	Autumn precipitation (24 hr/day)	Spring Volume (mL)	Spring flow rates and duration	Autumn Volume (mL)	Calculated Autumn flow rates and duration	Applied Autumn flow rates and time ¹
CFB Valcartier	250 mm in 30 days	120 mm in 61 days	29	0.12 mL/hr for 240 hr	13.1	0.009 mL/hr for 1464 hr	0.074 mL/hr for 177h
CFB Petawawa	160 mm in 30 days	75 mm in 61 days	18	0.076 mL/hr for 240 hr	8.50	0.006 mL/hr for 1464 hr	0.074 mL/hr for 115h

1 Due to the minimum pump flow rate of 0.074 mL/hr.

Table D-3. Example of data processing for propellant residue in soil at firing positions of Wellington anti-tank ranges from range CFB-Gagetown.

Sample	Eluted water volume (mL)	Cumulative eluted water (mL)	EM concentration in the effluent					Mass lost ¹			% of cumulative NG mass lost in relation to initial content ²	% cumulative NG mass lost ²
			2-Nitro	1-Nitro	1,3-Dinitro	1,2-Dinitro	NG	NG	1,2-Dinitro	1,3-Dinitro		
			(mg/L)	(mg/L)	(mg/L)	(mg/L)	(mg/L)	(mg)	(mg)	(mg)		
	0.00		0	0	0.00	0.00	0	0	0.00	0.00	0.00	0.00
1-d	8.1	8.1	0	0	0.050	0.20	85	± 0.40	0.66	0.002	0.00	11
2-d	8.5	17	0	0	0.15	0	16	± 0.09	0.14	0.00	0.001	2.3
3-d	8.5	25	0	0	0.080	0	6.3	± 0.05	0.073	0.00	0.001	1.2
4-d	8.9	34	0	0	0	0	4.3	± 0.05	0.047	0.00	0.00	0.77
5-d	8.5	42	0	0	0	0	2.8	± 0.05	0.00	0.00	0.00	15

1 (EM concentration in the effluent/ Cumulative eluted water)/1000.

2 Calculated with initial NG content presented in Table 5-11.

Table D-4. Example of data processing for Composition B particles sampled on snow after 81-mm mortar sympathetic detonation (Lewis 2006).

Sample	Eluted water volume (mL)	Cumulative eluted water (mL)	EM concentration in the effluent			EM mass lost ¹			Sum of cumulative EM mass lost (mg)	Cumulative mass lost in relation to initial EM mass ²			Cumulative EM mass lost ² %
			RDX	HMX	TNT	RDX	HMX	TNT		RDX	HMX	TNT	
			(mg/L)	(mg/L)	(mg/L)	(mg)	(mg)	(mg)		(%)	(%)	(%)	
		0.00							0.0000	0.00	0.00	0.00	0.00
1-g	8.0	8.0	0.59	0.086	0.31	0.0056	0.0008	0.0029	0.0093	0.05	0.13	0.04	0.05
2-g	7.7	16	0.73	0.077	0.29	0.0065	0.0007	0.0026	0.019	0.11	0.23	0.08	0.10
3-g	9.1	25	0.33	0.021	0.14	0.0055	0.0003	0.0023	0.027	0.16	0.29	0.11	0.15
4-g	8.7	33	0.34	0.049	0.30	0.0042	0.0006	0.0037	0.036	0.20	0.38	0.16	0.19
5-g	8.8	42	0.028	0.000	0.033	0.0005	0.0000	0.0006	0.037	0.21	0.38	0.17	0.20
6-g	3.6	46	0.022	0.000	0.033	0.0004	0.0000	0.0006	0.038	0.21	0.38	0.17	0.20
7-g	3.6	49	0.27	0.013	0.13	0.0017	0.0001	0.0008	0.040	0.23	0.39	0.19	0.22
8-g	3.3	53	0.12	0.003	0.090	0.0013	0.0000	0.0010	0.043	0.24	0.40	0.20	0.23
9-g	3.4	56	0.29	0.012	0.25	0.0028	0.0001	0.0025	0.048	0.27	0.42	0.23	0.26
10-g	3.5	60	0.24	0.013	0.36	0.0016	0.0001	0.0025	0.052	0.28	0.43	0.27	0.28
11-g	0.91	61	0.044	0.000	0.14	0.0004	0.0000	0.0012	0.054	0.29	0.43	0.28	0.29
12-g	8.3	69	1.4	0.051	3.6	0.0086	0.0003	0.023	0.085	0.37	0.48	0.60	0.46
13-g	9.0	78	3.3	0.16	11	0.030	0.0014	0.094	0.21	0.65	0.70	1.90	1.14
14-g	8.5	86	2.9	0.13	8.3	0.032	0.0014	0.091	0.33	0.94	0.92	3.16	1.81

1 (EM concentration in the effluent/ Cumulative eluted water)/1000

2 [mass lost / initial mass (see Table 5-11)]×100

Appendix E: Munitions Data

Below is an image of the ordnance used for the initiator tests.



Figure E-1. Mortar rounds, C4 blocks, and blasting caps used for tests.

The following data describe the specific munitions used during our tests. They were taken from the ordnance or the packaging for the munitions:

Mortar cartridges

On rounds:

81mm Comp B
CRTG M374A2
AMM Lot LS-67-68A6-73

On crating:

NSN 1315 00143 7184 C236
3 Cartridge 81 mm w/o Fuze for HE
M374A2
Mortars M1 and M25
Comp B
Lot LS-67-68A

Demolition charges

NSN 1375 01389 3854 M023
Charge Demolition M112
With Taggant (1-1/4 lbs Comp C-4)
MA-03L028-01

Appendix F: Analytical Data and Results

Table F-1 contains sample and analytical data and the results of the analyses on the samples. Sample mass is divided by the sampled area (m^2) to derive the mass per unit area ($\mu\text{g}/m^2$). This number is multiplied by the plume area (m^2) to obtain the estimated total residue masses reported in the report. We use two significant digits for all calculated or derived values in this report.

Table F-1. Mass of energetics recovered from plumes.

Sample ID Number	Plume Number and Replicate	Number of Increments	Sampled Area (m ²)	Filtrate Vol. (L)	AcN Volume (L)	Mass (µg) in Snowmelt			Mass (µg) in Soot			Total Mass in Sample (µg)			Mass per Unit Area (µg/m ²)			
						HMX	RDX	TNT	HMX	RDX	TNT	HMX	RDX	TNT	HMX	RDX	TNT	
10FRA30	1-1	62	0.62	5.0	0.02	1.2	1.1	ND ¹	ND	3.0	ND	1.2	4.1	ND	1.9	6.6	ND	260
10FRA31	1-2	62	0.62	4.8	0.02	8.5	130	130	2.8	41	ND	11	170	130	18	280	200	260
10FRA32	1-3	62	0.62	4.7	0.02	2.5	3.3	0.88	ND	1.2	ND	2.5	4.5	0.88	4.0	7.2	1.4	260
10FRA33	2-1	71	0.71	4.6	0.02	ND	4.7	1.84	ND	0.74	ND	ND	5.5	1.8	ND	7.7	2.6	220
10FRA34	2-2	71	0.71	4.4	0.02	0.84	8.5	4.80	ND	0.88	ND	0.84	9.3	4.8	1.2	13	6.8	220
10FRA35	2-3	71	0.71	4.5	0.02	ND	ND	ND	ND	ND	ND	ND	ND	ND	ND	ND	ND	220
10FRA36	3-1	73	0.73	4.0	0.02	ND	3.3	6.30	1.1	2.4	ND	1.1	5.6	6.3	1.5	7.7	8.6	200
10FRA37	3-2	73	0.73	3.7	0.02	ND	ND	ND	ND	ND	ND	ND	ND	ND	ND	ND	ND	200
10FRA38	3-3	73	0.73	3.5	0.02	ND	ND	ND	ND	0.67	ND	ND	0.67	ND	ND	0.9	ND	200
10FRA41	Annulus of Plume 1	50	0.5	1.5	0.01	ND	ND	ND	ND	ND	ND	0.16	ND	ND	0.3	ND	67	
10FRA42	Baseline	30	1.2	2.3	0.01	ND	ND	ND	ND	ND	ND	ND	ND	ND	ND	ND	ND	

1 ND = Not detected.

Detection limit was 0.02 mg/L for HMX, RDX, and TNT in the acetonitrile extract obtained by solid phase extraction of the melted snow or from solvent extraction of the soot fraction.

Appendix G: Results of prior Canadian study

Table G-1. Experimental conditions used by Lewis et al. (2009). The Mk 7 is a shaped charge.

Trial no.	Detonator	Position	C-4 used (g)	Condition of UXO
1	Mk 7 Mod 1	Longitudinal, 0 stand-off	15.1	No effect
2	Mk 7 Mod 1 + C4 ball	Longitudinal, 0 stand-off	16.3 + 5.7*	Groove blasted into projectile casing
3	Mk 7 Mod 2 + C4 ball	Longitudinal, 0.5-cm stand-off	15.4 + 7.7*	Thick groove blasted into projectile casing
4	Mk 7 Mod 3 + C4 ball	Longitudinal, 0 stand-off	24.7 + 5.0*	Long thick groove blasted into projectile casing
5	Mk 7 Mod 2 + C4 ball	Perpendicular, 2.9-cm stand-off	16.0 + 7.0*	Thin groove blasted into projectile casing
6	Mk 7 Mod 4 cut in half	Perpendicular, 1.5-cm stand-off	27.1 + 6.0*	Thick groove blasted into projectile casing
7	Mk 7 Mod 8 cut in half	Perpendicular, 9.5-cm stand-off	71.0	Thick groove, casing opened, Comp. B exposed
8	C4 ball	In fuze well	20.0	Detonation
9	C4 ball	In fuze well, 2.5 cm stand-off	10.0	Exposed Comp. B in the fuze well
10	C4 block	On nose	72.3	Cracked, exposed Comp. B
11	C4 block	On nose	72.0	Cracked, exposed Comp. B
12	C4 block	On nose	72.0	Cracked, exposed Comp. B
13	C4 block	On nose + plug fuze	70.2	Partial Crack at the nose and plug fuze
14	C4 block	On nose	72.1	Cracked, exposed Comp. B
15	C4 block	On nose	90.0	Detonation
16	C4 block	On nose	80.0	Cracked, exposed Comp. B
17	C4 hemisphere	On nose	80.0	Cracked, exposed Comp. B
18	C4 hemisphere	On nose	80.0	Cracked, exposed Comp. B
19	C4 hemisphere on cracked shell	On nose	80.0	Cracked, exposed Comp. B
20	C4 hemisphere	On nose	80.0	Cracked, exposed Comp. B
21	C4 hemisphere on cracked shell	On nose	80.0	Cracked, exposed Comp. B
22	C4 hemisphere on cracked shell	Outside, at the nose	63.2	Cracked, exposed Comp. B
23	C4 hemisphere on cracked shell	Outside, at the nose	64.0	Cracked, exposed Comp. B

* Amounts refer to mass of C4 in shaped charge + mass of C4 ball required to seat detonator on shaped charge.

Table G-2. Experimental conditions used in method 2 Lewis et al. (2009).

Trial	Distance between projectiles (cm)	Material under "UXO"	Material above "UXO"	Resulting condition of UXO projectile
1	0	Metal plate	Air	HODetonation
2	20	Metal plate	Air	Casing cracked (110 x 20 mm), explosives scattered
3	15	Metal plate	Air	Casing ruptured end to end, explosives scattered
4	10	Metal plate	Air	Detonation
5	13	Metal plate	Air	Detonation
6	15	Metal plate	Air	Casing ruptured end to end, crack 30 mm wide
7	15	Metal plate	Air	Casing ruptured end to end, crack 25 mm wide
8	25	Metal plate	Air	Casing cracked (100 x 20 mm)
9	45	Metal plate	Air	Casing cracked (50 x 10 mm)
10	100	Metal plate	Air	Pierced (10 cm ²)
11	157	Metal plate	Air	Pierced (1 cm ²)
12	15	Sand	Sand flush with top surface of UXO	Casing deformed
13	15	Sand	Sand 10 cm	Casing cracked (85 x 15 mm)
14	15	Sand	Proj. planted at 45° in sand, but not covered	Casing cracked (50 x 20 mm) in the unburied part
15	15	Sand	Water	Casing cracked (80 x 10 mm)
16	15	Snow	Air	Casing ruptured end to end, crack 30 mm wide
17	15	Snow	Sand 2.5 cm	Casing cracked (125 x 20 mm)

Appendix H: STANAG Definitions of Sympathetic Detonation Reactions

The following are STANAG (i.e., Standard NATO agreement) definitions of sympathetic detonation reactions.

Type I Response (Detonation)

The most violent type of explosive event. A supersonic decomposition reaction (detonation) propagates through the energetic material to produce an intense shock in the surrounding medium (e.g., air or water) and a very rapid plastic deformation of metallic cases followed by extensive fragmentation. All energetic materials will be consumed. The effects will include large ground craters for munitions on or close to the ground, perforation, plastic deformation or fragmentation of adjacent metal plates, and blast overpressure damage to nearby structures.

(This reaction was referred to as high-order detonation in this work.)

Type II Response (Partial Detonation)

The second most violent type of explosive event. Some but not all the energetic material reacts as in a Type I Response. An intense shock occurs; a part of the case is broken into small fragments; a ground crater can be produced, the adjacent metal plates can be damaged as in a Type I Response and there will be blast overpressure damage to nearby structures. A Type II Response can also produce large case fragments as in a violent pressure rupture (brittle fracture). The amount of damage, relative to a Type I Response, depends on the portion of material that detonates.

(This reaction was not observed in this work.)

Type III Response (Explosion)

The third most violent type of explosive event. Ignition and rapid burning of the confined energetic material build up high local pressures leading to violent pressure rupture of the confining structure. Metal cases are fragmented (brittle fracture) into large pieces that are often thrown long distances. The unreacted or burning energetic material is also scattered

about. Air shocks are produced that can cause damage to nearby structures. Fire and smoke hazards will exist. The blast and high velocity fragments can cause minor ground craters and damage (break-up, tearing, gouging) to adjacent metal plates. Blast pressures are lower than for Type I or Type II Responses.

(This reaction was referred to as partial detonation in this work.)

Type IV Response (Deflagration)

The fourth most violent type of explosive event. Ignition and burning of the confined energetic materials lead to non-violent pressure release as a result of a low strength case or venting through the case walls (outlet gap, initiation capsule, etc.). The case may rupture but does not fragment; orifice covers may be expelled and unburnt or burning energetic material may be scattered about and spread the fire. Pressure releases may propel an unsecured test item causing an additional hazard. No blast effect or significant fragmentation damage to the surroundings, only heat and smoke damage from the burning energetic material.

(This reaction was not observed in this work.)

Type V Response (Burning)

The least violent type of explosive event. The energetic material ignites and burns non-propulsively. The case may split up non-violently; it may melt or weaken sufficiently to allow slow release of combustion gases; the case covers may be dislodged by the internal pressure.

Debris stays mainly within the area of the fire. This debris is not expected to cause fatal wounds to personnel or be a hazardous fragment beyond 15 m (49 ft).

(This reaction was not observed in this work.)

No Reaction

A non-explosive event in which there is no externally perceptible reaction of the energetic material to the applied stimulus.

(This reaction was referred to as surfaces damage, including dings, holes and cracks.)

Bibliography

The following is a bibliography of published work on the project that has been compiled since the beginning of the SERDP ER-1481 Extension in January 2008. All publications are unclassified.

Journal articles

Martel, R., A. Bellavance-Godin, R. Levesque, and S. Côté. 2010. Determination of nitroglycerin and its metabolites by solid-phase extraction and HPLC-UV. *Chromatographia*, 71(3/4): 285–289.

Walsh, M.E., S. Taylor, A.D. Hewitt, M.R. Walsh, C.A. Ramsey, and C.M. Collins. 2010. Field observations of the persistence of Comp B explosives residues in a salt marsh impact area. *Chemosphere*, 78: 467–473.

Walsh, M.R., M.E. Walsh, and A.D. Hewitt. 2010. Energetic residues from the field disposal of gun propellants. *Journal of Hazardous Materials*, 173: 115–122.

Submitted book chapters

Diaz, E., S. Brochu, I. Poulin, D. Faucher, A. Marois, and A. Gagnon. 2011. *Residual dinitrotoluenes from open burning of gun propellant*. Submitted to the American Chemical Society, November 2010.

Walsh, M.E., A.D. Hewitt, T.F. Jenkins, C.A. Ramsey, M.R. Walsh, S.R. Bigl, C.M. Collins, and M.A. Chappell. 2011. *Assessing sample processing and sampling uncertainty for energetic residues on military training ranges: Method 8330B*. Submitted to the American Chemical Society, November 2010.

Technical reports

Ampleman, G., S. Thiboutot, A. Marois, A. Gagnon, and D. Gilbert. 2008. *Evaluation of the propellant residues emitted during 105-mm Leopard tank live firing and sampling of demolition ranges at CFB Gagetown, Canada*. DRDC Valcartier TR-2007-515. Val Belair, Quebec: Defence Research and Development Canada.

Ampleman, G., S. Thiboutot, A. Marois, A. Gagnon, P. Woods, M. R. Walsh, M. E. Walsh, C. A. Ramsey, and P. Archambault. 2010. *Evaluation of the propellant residues emitted during the live firing of triple base ammunition using a British 155mm howitzer gun at CFB Suffield, Canada*. DRDC Valcartier TR-2010-269. Val Belair, Quebec: Defence Research and Development Canada.

AVT-115. 2010. *Environmental impact of munition and propellant disposal, final report of task group*. RTO Technical Report TR-AVT-115. Research and Technology Organisation (NATO) BP 25, F-92201 Neuilly-sur-Seine Cedex, France.

- Diaz, E., D. Gilbert, D. Faucher, A Marois, and A. Gagnon. 2008. *Gun propellant residues dispersed from static artillery firings of LG1 Mark II and C3 105-mm howitzers.* DRDC Valcartier TR 2007-282. Val Belair, Quebec: Defence Research and Development Canada.
- Jenkins, T.F., G. Ampleman, S. Thiboutot, S.R. Bigl, S. Taylor, M.R. Walsh, D. Faucher, R. Martel, I. Poulin, K.M. Dontsova, M.E. Walsh, S. Brochu, A.D. Hewitt, G. Comeau, E. Diaz, M.A. Chappell, J.L. Fadden, A. Marois, R. Fifield, B. Quemerais, J. Simunek, N.M. Perron, A. Gagnon, T. Gamache, J.C. Pennington, V. Moors, D.J. Lambert, D. Gilbert, R.N. Bailey, V. Tanguay, C.A. Ramsey, L. Melanson, and M.-C. Lapointe. 2008. *Characterization and fate of gun and rocket propellant residues on testing and training ranges: Final report.* ERDC TR-08-1.
- Poulin, I., S. Thiboutot, and S. Brochu. 2009. *Production of dioxins and furans from the burning of excess gun propellant.* DRDC Valcartier TR-2009-365. Val Belair, Quebec: Defence Research and Development Canada.
- Thiboutot, S., G. Ampleman, A. Marois, A. Gagnon, and D. Gilbert. 2009. *Nitroglycerine deposition from M-72 antitank rocket firing.* DRDC Valcartier TR-2009-003. Val Belair, Quebec: Defence Research and Development Canada.
- Thiboutot, S., G. Ampleman, A. Gagnon, A. Marois, R. Martel, and G. Bordeleau. 2010. *Persistence and fate of nitroglycerine in legacy antitank ranges.* DRDC Valcartier TR-2010-059. Val Belair, Quebec: Defence Research and Development Canada.
- Thiboutot, S., G. Ampleman, M. Kervarec, A. Cinq-Mars, A. Gagnon, A. Marois, I. Poulin, F. Boucher, R. Lajoie, K. Legault, S. Withwell, T. Sparks, J. Eng, M. Cartier, and P. Archambault. 2011. *Development of a table for the safe burning of excess artillery propellant charge bags.* DRDC Valcartier TR 2010-254. Val Belair, Quebec: Defence Research and Development Canada.
- Walsh, M.R., M.E. Walsh, and A.D. Hewitt. 2008. *Energetic residues from blow-in-place detonation of 60-mm and 120-mm fuzed high-explosive mortar cartridges.* ERDC/CRREL TR-08-19.
- Walsh, M.R. 2009. *User's manual for the CRREL multi-increment sampling tool.* ERDC/CRREL SR-09-2.
- Walsh, M.R., M.E. Walsh, and A.D. Hewitt. 2009. *Energetic residues from the expedient disposal of propellants.* ERDC/CRREL TR-09-8.
- Walsh, M.R., M.E. Walsh, S. Thiboutot, G. Ampleman, and J.N. Bryant. 2009. *Propellant residues deposition from firing of AT4 rockets.* ERDC/CRREL TR-09-13.
- Walsh, M.R., M.E. Walsh, J.W. Hug, S.R. Bigl, K.L. Foley, A.B. Gelvin, and N.M. Perron. 2010. *Propellant residues deposition from firing of 40-mm grenades.* ERDC/CRREL TR-10-10.
- Walsh, M.R., G. Ampleman, S. Thiboutot, M.E. Walsh, I. Poulin, A. Bellavance-Godin, R. Martel, G. Bordeleau, S. Brochu, A.D. Hewitt, A. Marois, A. Gagnon, C.M. Collins, D. Gilbert, P. Woods, J.N. Bryant, S.R. Bigl, and K. Gagnon. 2010. *Characterization and fate of gun and rocket propellant residues on testing and training ranges: Interim Report 2.* ERDC/CRREL TR-10-13.

Conference presentations

- Ampleman, G., S. Thiboutot, A. Marois, A. Gagnon, M.R. Walsh, and M.E. Walsh. 2009. Study of the propellant residues deposited by the live firing of 105-mm Leopard tank. Poster: *SERDP & ESTCP's Partners in Environmental Technology Technical Symposium & Workshop, 1–3 December 2009, Washington, DC.*
- Ampleman, G. and S. Thiboutot. 2010. DRDC environmental findings. *Land Force Central Environment Seminar, May 2010, Halifax, NS, Canada.*
- Ampleman, G. 2010. Sustainable range and training areas. *Research and Technology Agency (RTA) Sustainment Forum, June 2010, Ottawa, ON, Canada.*
- Ampleman, G. 2010. Sampling strategies and objectives. Presentation: *NATO AVT-ET-108. 6–8 October 2010. Bucharest, Romania.*
- Ampleman, G., S. Thiboutot, A. Marois, A. Gagnon, P. Woods, M.R. Walsh, M.E. Walsh, C.A. Ramsey, and P. Archambault. 2010. Evaluation of the propellant residues emitted during the live firing of triple base ammunition using a British 155-mm howitzer gun at CFB Suffield, Canada. Poster: *SERDP & ESTCP's Partners in Environmental Technology Technical Symposium & Workshop, December, 2010, Washington, DC.*
- Brochu, S., I. Poulin, D. Faucher, and M.R. Walsh. 2008. Assessment of gaseous and particulate propellant residues resulting from small arms live firing. Poster: *SERDP & ESTCP's Partners in Environmental Technology Technical Symposium & Workshop, 2–4 December 2008, Washington, DC.*
- Brochu, S., I. Poulin, D. Faucher, E. Diaz, and M.R. Walsh. 2009. Environmental assessment of small arms live firing: study of gaseous and particulate residues. Poster: *237th ACS National Meeting, March 2009, Salt Lake City, UT.*
- Diaz, E., I. Poulin, S. Brochu, A. Marois, and A. Gagnon. 2009. Residues from the open burning of gun propellant. Poster: *237th ACS National Meeting, March 2009, Salt Lake City, UT.*
- Hewitt, A.D., M.E. Walsh, M.R. Walsh, S. Bigl, and M Chappell. 2009. Assessing sample processing uncertainty for energetic residues on military training ranges: Method 8330B. *237th ACS National Meeting, March 2009, Salt Lake City, UT.*
- Hewitt, A.D., M.E. Walsh, M.R. Walsh, S.R. Bigl, S. Brochu, M.A. Chappell, and C.A. Ramsey. 2009. Method 8330B and multi-increment sampling (2009 Project of the Year Award). Poster: *SERDP & ESTCP's Partners in Environmental Technology Technical Symposium & Workshop, 1–3 December 2009, Washington, DC.*
- Hewitt, A.D. 2009. Estimating the surface loading of munitions constituents on military training ranges. Invited Speaker: *SERDP & ESTCP's Partners in Environmental Technology Technical Symposium & Workshop, 1–3 December 2009, Washington, DC.*

- Martel, R., A. Bellavance-Godin, G. Ampleman, S. Thiboutot, and L. Trépanier. 2009. Fate and behavior of propellant residues in water of the unsaturated zone under an anti-tank firing position. Presentation: *8th ISICP, 2–6 November 2009, Cape Town, South Africa.*
- Martel, R., A. Bellavance-Godin, S. Thiboutot, and G. Ampleman. 2009. Behavior of nitroglycerine and its metabolites in the unsaturated zone under an antitank firing position: Sand column test. Poster: *SERDP & ESTCP's Partners in Environmental Technology Technical Symposium & Workshop, 1–3 December 2009, Washington, DC.*
- Poulin, I., S. Thiboutot, and S. Brochu. 2009. Open burning of excess gun propellant: Investigation of the production of dioxins and furans as combustion by-products. Poster: *SERDP & ESTCP's Partners in Environmental Technology Technical Symposium & Workshop, 1–3 December 2009, Washington, DC.*
- Poulin, I. 2010. Un entraînement militaire "vert", est-ce réaliste? ("Green" military training, is it realistic?). *14th Colloque Annuel du Chapitre St-Laurent. May 2010, Quebec, QC, Canada.*
- Poulin, I., S. Taylor, M.R. Walsh, S.R. Bigl, M.E. Walsh, A.M. Wagner, and J.W. Hug. 2010. Effect of close-proximity munitions detonations on surface unexploded ordnance. Poster: *SERDP & ESTCP's Partners in Environmental Technology Technical Symposium & Workshop, 1–2 December 2010, Washington, DC.*
- Taylor, S., I. Poulin, S.R. Bigl, M.R. Walsh, M.E. Walsh, A. Wagner, and J.W. Hug. 2010. Particle size distribution from a partial detonation. Poster: *SERDP & ESTCP's Partners in Environmental Technology Technical Symposium & Workshop, 1–2 December 2010, Washington, DC.*
- Thiboutot, S., G. Ampleman, A. Marois, A. Gagnon, and D. Gilbert. 2008. Deposition of nitroglycerine from the live firing of M72 A5 66-mm rockets. Poster: *SERDP & ESTCP's Partners in Environmental Technology Technical Symposium & Workshop, 2–4 December 2008, Washington, DC.*
- Thiboutot, S., G. Ampleman, S. Brochu, E. Diaz, I. Poulin, T.F. Jenkins, M.R. Walsh, M.E. Walsh, S. Taylor, A.H. Hewitt, R. Martel, J. Hawari, G. Sunahara, P.Y. Robidoux, F. Monteil-Rivera, B. Lachance, S. Rocheleau, R.G. Kuperman, R.T. Checkai, M. Simini, R. Lajoie, and K. Legault. 2009. Canadian perspectives on risk-based contaminant management on active army training ranges. Invited Speaker: *SERDP & ESTCP's Partners in Environmental Technology Technical Symposium & Workshop, 1–3 December 2009, Washington, DC.*
- Thiboutot, S., G. Ampleman, A. Marois, A. Gagnon, and G. Bordeleau. 2009. Long-term fate of propellant residues in the soil surface and subsurface. Poster: *SERDP & ESTCP's Partners in Environmental Technology Technical Symposium & Workshop, 1–3 December 2009, Washington, DC.*
- Thiboutot, S., G. Ampleman, I. Poulin, M. Kervarec, A. Gagnon, A. Marois, and F. Boucher. 2009. Prototype table for the burning of excess artillery propellant bags. Poster: *SERDP & ESTCP's Partners in Environmental Technology Technical Symposium & Workshop, 1–3 December 2009, Washington, DC.*

- Thiboutot, S. 2010. Burn table as a tool for effective burning of excess artillery propelling charges. *Land Force Central Environment Seminar, May 2010, Halifax, NS, Canada.*
- Thiboutot, S. 2010. Burn table for implementation by the Canadian forces. *Research and Technology Agency (RTA) Sustainment Forum, June 2010, Ottawa, ON, Canada.*
- Thiboutot, S., G. Ampleman, M. Kervarec, A. Gagnon, A. Marois, F. Boucher, and M.R. Walsh. 2010. Fix and mobile burn pans for the burning of excess artillery propellant charge bags. Poster: *SERDP & ESTCP's Partners in Environmental Technology Technical Symposium & Workshop, 1–2 December 2010, Washington, DC.*
- Walsh, M.E., A.D. Hewitt, M.R. Walsh, S. Taylor, C.M. Collins, S.R. Bigl, M.A. Chappell, and C.A. Ramsey. 2008. Surface water and sediment sampling adjacent to a low-ordered 120-mm mortar projectile. Poster: *SERDP and ESTCP's Partners in Environmental Technology Technical Symposium and Workshop, 2–4 December 2008, Washington, DC.*
- Walsh, M.E., C.A. Ramsey, C.M. Collins, A.D. Hewitt, M.R. Walsh, and T.A. Douglas. 2009. Multi-increment sampling to estimate the accumulation of propellant residues at firing points. Poster: *SERDP and ESTCP's Partners in Environmental Technology Technical Symposium and Workshop, 1–3 December 2009, Washington, DC.*
- Walsh, M.E., M.R. Walsh, S.R. Bigl, K.L. Foley, A.B. Gelvin, N.M. Perron, and J.W. Hug. 2010. Propellant residues from the live-fire of Mk-19 40-mm grenade machine gun. Poster: *SERDP & ESTCP's Partners in Environmental Technology Technical Symposium & Workshop, 1–2 December 2010, Washington, DC.*
- Walsh, M.R., M.E. Walsh, A.D. Hewitt, and C.M. Collins. 2008. Field-expedient disposal of excess artillery propellants. Poster: *SERDP & ESTCP's Partners in Environmental Technology Technical Symposium & Workshop, 2–4 December 2008, Washington, DC.*
- Walsh, M.R., M.E. Walsh, S. Thiboutot, and G. Ampleman. 2009. Propellant residues resulting from training with shoulder-fired rockets. Poster: *SERDP & ESTCP's Partners in Environmental Technology Technical Symposium & Workshop, 1–3 December 2009, Washington, DC.*
- Walsh, M.R., S. Thiboutot, G. Ampleman, I. Poulin, M.E. Walsh, S. Taylor, R. Martel, and C.A. Ramsey. 2010. A holistic view of the impacts from training with energetic compounds on military ranges. Poster: *SERDP & ESTCP's Partners in Environmental Technology Technical Symposium & Workshop, 1–2 December 2010, Washington, DC.*

Short courses

- Hewitt, A.D., M.E. Walsh, M.R. Walsh, and C.A. Ramsey. 2009. Multi-increment sampling (MIS) applications for environmental remediation. Short course: *SERDP and ESTCP's Partners in Environmental Technology Technical Symposium and Workshop, 3 December 2009. Washington, DC.*

Ramsey, C.A., M.E. Walsh, and M.R. Walsh. 2010. Multi-increment sampling development for military training ranges. Short course: *NATO AVT-ET-108*. 6-8 October 2010. Bucharest, Romania.

REPORT DOCUMENTATION PAGE

*Form Approved
OMB No. 0704-0188*

Public reporting burden for this collection of information is estimated to average 1 hour per response, including the time for reviewing instructions, searching existing data sources, gathering and maintaining the data needed, and completing and reviewing this collection of information. Send comments regarding this burden estimate or any other aspect of this collection of information, including suggestions for reducing this burden to Department of Defense, Washington Headquarters Services, Directorate for Information Operations and Reports (0704-0188), 1215 Jefferson Davis Highway, Suite 1204, Arlington, VA 22202-4302. Respondents should be aware that notwithstanding any other provision of law, no person shall be subject to any penalty for failing to comply with a collection of information if it does not display a currently valid OMB control number. **PLEASE DO NOT RETURN YOUR FORM TO THE ABOVE ADDRESS.**

1. REPORT DATE (DD-MM-YYYY) August 2011		2. REPORT TYPE Final		3. DATES COVERED (From - To)	
4. TITLE AND SUBTITLE Characterization and Fate of Gun and Rocket Propellant Residues on Testing and Training Ranges				5a. CONTRACT NUMBER	
				5b. GRANT NUMBER	
				5c. PROGRAM ELEMENT NUMBER	
6. AUTHOR(S) Michael R. Walsh, Sonia Thiboutot, Marianne E. Walsh, Guy Ampleman, Richard Martel, Isabelle Poulin, and Susan Taylor				5d. PROJECT NUMBER	
				5e. TASK NUMBER	
				5f. WORK UNIT NUMBER	
7. PERFORMING ORGANIZATION NAME(S) AND ADDRESS(ES) Cold Regions Research and Engineering Laboratory U.S. Army Engineer Research and Development Center 72 Lyme Road Hanover, NH 03755				8. PERFORMING ORGANIZATION REPORT NUMBER ERDC/CRREL TR-11-13	
9. SPONSORING / MONITORING AGENCY NAME(S) AND ADDRESS(ES) Strategic Environmental Research and Development Program Arlington, Virginia 22203				10. SPONSOR/MONITOR'S ACRONYM(S)	
				11. SPONSOR/MONITOR'S REPORT NUMBER(S)	
12. DISTRIBUTION / AVAILABILITY STATEMENT Approved for public release; distribution is unlimited.					
13. SUPPLEMENTARY NOTES					
14. ABSTRACT The Cold Regions Research and Engineering Laboratory and the Defence Research and Development Canada—Valcartier have partnered to improve the understanding of the distribution and fate of propellant residues on military training ranges. Field studies were conducted to estimate the propellant residue mass deposited per round fired from various munitions as well as residues from the field disposal of excess propellants. Experiments were conducted to measure the rate of release of energetic compounds after deposition. Training ranges were examined to determine the mass and distribution of residue accumulation. Profile sampling was conducted to document the depth to which these residues had penetrated the ground. Column studies were conducted with propellants to document transport rates for solution-phase propellant constituents and to develop process descriptors for use in models to enable prediction of fate and transport for constituents of concern. Gaps were filled in other areas of energetics residues impacts in an effort to describe all aspects of energetics impacts on range environments. Testing of propellant burn structures was begun, and we continue to promote and refine the multi-increment sampling protocol for energetics. Major accomplishments are presented for the final year and the total of Environmental Restoration Project 1481, Phase II.					
15. SUBJECT TERMS Characterization Damaged UXO		Deposition Disposal Fate and Transport		Low-order Detonations Military Munitions Multi-increment Sampling	
16. SECURITY CLASSIFICATION OF:			17. LIMITATION OF ABSTRACT U	18. NUMBER OF PAGES 381	19a. NAME OF RESPONSIBLE PERSON
a. REPORT U	b. ABSTRACT U	c. THIS PAGE U			19b. TELEPHONE NUMBER (include area code)

15. SUBJECT TERMS (cont'd)

Propellants

Sympathetic Detonations

Unexploded Ordnance